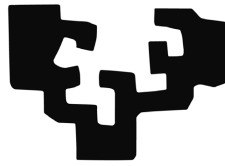eman ta zabal zazu

Universidad del País Vasco   Euskal Herriko Unibertsitatea

Department of Systems Engineering and Automation

Doctoral Program in Control Engineering, Automation and Robotics

DOCTORAL THESIS

Optimized energy management strategies and sizing of hybrid storage systems for transport applications

presented by:

Víctor Isaac Herrera Pérez

Supervised by:

Prof. Haritza Camblong Ruiz (UPV-EHU)

Dr. Aitor Milo Urquiola (IK4-IKERLAN)

2017

Hay una fuerza motriz más poderosa que el vapor,
la electricidad y la energía atómica.
Esa fuerza es la voluntad

— Albert Einstein

To my wife and parents. . .

Acknowledgements

I really consider that this part, from the personal point of view, becomes in the most important one along this thesis. I will try to summarize in short paragraphs the deep gratitude I feel for all the people that have contributed by supporting and helping me during these almost four years to reach this objective.

I would like to do a special mention to my supervisor Aitor and my boss Haizea who always were there to support me in the technical part, but more important for me, you have been there as my friends. I have learned a lot from both during these years and this thesis is the result of our join work. Thank you for always believe in my skills and encourage me to be a better person and researcher. Thanks a lot to my bosses Unai and Igor for their support and for believing in my potential as person and professional to continue contributing in the Ikerlan's project. In the same way, thanks so much to my thesis director Haritza for his help and support in each stage of this PhD and for his interest on the development of my personal and professional skills.

I want to thank God for taken care of me at every step I have taken and every challenge I have undertaken. Thanks a lot to my lovely wife for her support in this objective and, over all, during those long months when we were apart on different continents. Thanks for enduring my good and bad moods, have you with me has made this long way easier to walk. Many thanks to my parents, grandparents and brother for believing in me and make the efforts to support every challenge that I have proposed myself.

Thanks a lot to the first group from Ikerlan who contact me. To Ander, Ion and Aitor who gave me this wonderful opportunity to form part of this family called Ikerlan. Thank you also for selecting me for the Marie Curie Scholarship, I did my best to fulfill your expectations on the EMVeM project. I still remember that email confirming not only I was selected for the PhD student position but also that my whole life would change opening me the way to new personal experiences and cultures. Couple months later, me and two bag crossed the Atlantic and arrived in the small town of Mondragón in the beautiful region of Euskadi. A place of people speaking a strange (and not easy to understand) language but full of hospitality and kindness who adopted me, becoming in my second home.

Thanks so much to all the people from the AEP department in Olandixo for being friendly people and welcome me as one of you into your team. Thanks to the amazing

Acknowledgements

group of PhD student (some of them doctors now): Maitane, Andoni, Gustavo, Damián, Ugaitz, Aitor, Ander, Joannes and Fernando with who I shared not only technical but also funny moments along these years. It was an enriching experience from personal and professional point of view to have shared this stage with all of you.

Thanks to all the people in my new department, Storage and Energy Management, for all the knowledge and personal experiences shared up to today and all the ones we will share in the future. Regarding the new group of PhD student I met in Galarreta: Egoitz, Maitane, Leire, Amaia, Mattin and Iñigo, all the best for you guys. Also my gratitude to the group of researchers, but over all exceptional people, in this area; specially to Eli, Nerea, Gustavo, Iñigo and Andrés for their support and help. How not mention this crazy (but always ready to help me) friend who has been close to me, Andoni, this thesis would not have been the same without your support.

Finally but not least, a grateful acknowledgement the European Commission for its support of the Marie Curie program through the ITN EMVeM project, which has allowed me to live a unique experience of personal and professional training in the research field. In the same way, to all the fellow and researchers involved in this project. Thank you for all the amazing moments, meetings and travels we shared along these three years.

All of you have contributed to this thesis. All of you form part of my life and have collaborated from different aspects to become who I am now, the human being and the researcher.

Eskerrik asko danori,
Muchas gracias a todos,
Many thanks to all,
Victor

Summary

Title: Optimized Energy Management Strategies and Sizing of Hybrid Storage Systems for Transport Applications.

Currently with the massive demand of mobility and an increasing concern about the sustainable use of energy resources, more-efficient, best-performed and cost competitive mobility solutions are required. In this topic, the hybrid energy storage systems (HESS) are shown as interesting solutions by combining storage technologies with different power and energy characteristics, where batteries (BTs) and supercapacitors (SCs) stand out as the most important ones.

However, with several energy sources on-board the vehicle, the optimal management to supply the power/energy demand during operation from them (for a better harnessing of the HESS) becomes in a complex problem. This aspect increases its relevance since the degradation process of the HESS (BTs and/or SCs) is mainly related with their behavior during the vehicle operation. Hence, the selected energy management strategy (EMS) and the proper HESS sizing represent a key factor to ensure the correct and efficient system operation while offering a competitive operating cost for the vehicle manufacturer and end users. Therefore, both technical as well as economic issues must be considered, especially for on-board HESS systems where the implementation and replacement costs are highly important.

This PhD thesis deals with the topic of the optimal sizing and operation of HESS (combining BTs and SCs) in order to be integrated in vehicles for public mobility in urban scenarios. Thus on the one hand, a novel adaptive EMS is proposed to deal with the proper split of the power demand among the available energy sources on-board the vehicle. This adaptive EMS is based on fuzzy logic in order to define (in a more intelligent and intuitive way) the desired vehicle operation and to face the management of multiple energy sources and operating conditions in a hybrid electric system. This EMS considers, in addition to the instantaneous power demanded for the vehicle operation and energetic conditions of the HESS, the future energy demand (related to the BTs and SCs) by applying a sliding forward window to estimate their possible energetic behaviors. Thus, the proposed adaptive EMS evaluates the current and future estimated energy information to adapt, in an optimized and efficient way, the HESS operation in order to improve the energy harnessing of the sources on-board the vehicle.

On the other hand, a methodology for the co-optimization of the EMS and HESS

sizing has been proposed. This optimization methodology includes, firstly, the technical evaluation of the operating performance either of the vehicle and on-board energy sources when the EMS is applied. The second phase is in charge of evaluating the economic performance resulting from the vehicle operation and defined HESS sizing, with the aim of determining the most suitable solution (HESS sizing and EMS operating performance) which offers the lowest operating cost for the vehicle. For this purpose, a multi-objective problem has been proposed based on an economic model which considers both initial investment as well as replacement costs of the HESS to estimate the daily operating cost of the vehicle. To determine the replacement cost, ageing and lifetime estimation models for the HESS (BT and SC) have been applied and the whole vehicle lifetime has been considered. The targets' values obtained from the optimization process are used to configure the adaptive fuzzy-based EMS. This way, allowing the EMS operation toward the most efficient and best performed values to assure the fulfillment of the techno-economic objectives.

With the aim of validating the proposal of this PhD thesis: *adaptive EMS for a HESS* and *methodology for the co-optimization of EMS and HESS sizing*, two relevant case studies from the public transportation have been selected: Hybrid Electric Tramway (HET) and Hybrid Electric Bus (HEB).

In the first case (HET), a real scenario based on the tramway of Seville has been chosen. In this case, the vehicle operates in zones with and without catenary. In the second case (HEB), an urban scenario including zones with free-emissions requirement (full-electric operation) has been considered. The adaptive EMS proposed in this thesis has been modified to accomplish the operating requirements in each case study, as well as to include the suitable operation of the third energy source to propel the vehicles: catenary (HET) and Internal combustion engine (HEB). The optimization results have been compared in technical, economic, and efficiency terms with base scenarios considering rule-based EMSs in order to determine the improvements that can be obtained with the approach proposed in this thesis. The results confirm that the co-optimization methodology together with the adaptive EMS allow obtaining significant cost savings in the operating costs of the vehicles (HET and HEB), ensuring the fulfillment of the operation requirements in each scenario while improving the energy efficiency of these systems.

Key words: Battery, energy management strategy, fuzzy logic, supercapacitor, hybrid electric bus, hybrid electric tramway, hybrid energy storage system, multi-objective optimization, sizing.

Resumen

Título: Estrategias Optimizadas de Gestión Energética y Dimensionamiento de Sistemas Híbridos de Almacenamiento para Aplicaciones de Transporte.

En la actualidad, con la masiva demanda de movilidad y la creciente preocupación con respecto al uso sostenible de los recursos energéticos, se requieren soluciones de transporte cada vez más eficientes, con mejores prestaciones y que ofrezcan un costo competitivo. En este tema, los sistemas híbridos de almacenamiento de energía (HESS) se presentan como soluciones interesantes combinando tecnologías de almacenamiento con diferentes características de potencia y energía, donde baterías (BTs) y supercapacitores (SCs) destacan como los más importantes.

Sin embargo, con varias fuentes de energía a bordo del vehículo, la óptima gestión para suministrar la demanda potencia/energía durante la operación desde dichas fuentes (para lograr un mejor aprovechamiento del HESS) se convierte en un problema complejo. La relevancia de este aspecto se incrementa debido a que el proceso de degradación del HESS (BTs y/o SCs) está relacionado principalmente con su operación durante el funcionamiento del vehículo. Por lo tanto, la estrategia de gestión energética (EMS) seleccionada y el adecuado dimensionamiento del HESS representa un factor clave para asegurar la adecuada y eficiente operación del sistema, y al mismo tiempo resulte en un costo de operación competitivo para el fabricante del vehículo y los usuarios finales. De esta manera, tanto aspectos técnicos como económicos deben ser considerados, especialmente para sistemas HESS a bordo del vehículo donde los costos relacionados a la implementación y sustitución son muy importantes.

Esta tesis doctoral aborda la temática acerca del óptimo dimensionamiento y operación de HESS (combinando BTs y SCs) con el objetivo de ser integrados en vehículos para movilidad pública en entornos urbanos. Por una parte, se propone una innovadora estrategia energética para gestionar la división de la demanda de potencia entre las fuentes de energía disponibles a bordo del vehículo. Esta EMS adaptativa está basada en lógica difusa para definir (de una forma más inteligente e intuitiva) la operación deseada del vehículo y abordar la gestión de múltiples fuentes de energía y condiciones de operación en un sistema eléctrico híbrido. Esta nueva EMS considera, además de la potencia instantánea requerida para la operación del vehículo y las condiciones energéticas del HESS, la futura demanda de energía (en las BTs y SCs) por medio de una ventana deslizante que permite estimar sus posibles comportamientos energéticos. La EMS adaptativa que

Resumen

se propone evalúa la información energética actual y futura (estimada) para adaptar, de una forma optimizada y eficiente, la operación del HESS con el objetivo de mejorar el aprovechamiento de la energía almacenada en los recursos a bordo del vehículo.

Por otro lado, se ha propuesto una metodología para la co-optimización de la EMS y dimensionamiento del HESS. Esta metodología de optimización incluye, primeramente, la evaluación técnica de la operación del vehículo y de las fuentes de energía a bordo como resultado de la gestión realizada por la EMS. La segunda fase se encarga de evaluar el desempeño económico resultante de la operación del vehículo y del dimensionamiento definido para el HESS, con el objetivo de determinar la solución más adecuada (dimensionamiento del HESS y operación de la EMS) que ofrece el costo más bajo de operación para el vehículo. Para este propósito, se ha planteado un problema multi-objetivo basado en un modelo económico que considera tanto los costos de inversión inicial y de reemplazo del HESS para estimar el costo diario de operación del vehículo. Para determinar el costo de reemplazo han sido aplicados modelo de envejecimiento y estimación de vida para el HESS (BT y SC) y se ha considerado la vida útil del vehículo. Los valores de las consignas obtenidas del proceso de optimización se emplean para configurar la estrategia adaptativa basada en lógica difusa. De esta manera, permitiendo la operación de la EMS en torno a sus valores más eficientes y con mejor desempeño, asegurando así el cumplimiento de los objetivos tecno-económicos planteados.

Con el objetivo de validar la propuesta de esta tesis doctoral: *estrategia de gestión energética adaptativa* y *metodología para la co-optimización de dimensionamiento de HESS y operación de la EMS*, dos casos de estudio relevantes en la transportación pública han sido seleccionados: Tranvía Eléctrico Híbrido (HET) y Autobús Eléctrico Híbrido (HEB).

En el primer caso (HET), se ha seleccionado un caso real basado en el tranvía de Sevilla. En este caso, el vehículo opera en zonas con y sin catenaria. En el segundo caso (HEB), se ha considerado un escenario urbano que incluye zonas libre de emisiones (operación puramente eléctrica). La EMS adaptativa que se propone en esta tesis ha sido modificado para cumplir los requerimientos de operación en cada caso de estudio, así como para incluir la adecuada operación de la tercera fuente de energía con que cuentan los vehículos: catenaria (HET) y motor de combustión interna (HEB). En ambos casos de estudio, los resultados de la optimización han sido comparados en términos técnicos, económicos y de eficiencia con escenarios base considerando EMSs basadas en reglas con el objetivo de determinar las mejoras obtenidas con el enfoque propuesto en esta tesis. Los resultados confirman que la metodología de co-optimización junto con la EMS adaptativa permiten obtener ahorros significativos en el costo de operación de los vehículos (HET y HEB), asegurando el cumplimiento de los requerimiento de operación en cada escenario, y al mismo tiempo, mejorando la eficiencia energética de estos sistemas.

Palabras clave: Batería, estrategia de gestión energética, lógica difusa, supercapacitor, autobús eléctrico híbrido, tranvía eléctrico híbrido, sistema de almacenamiento de energía híbrido, optimización multi-objetivo, dimensionamiento.

Laburpena

Izenburua: energia kudeaketarako estrategia optimizatuak eta biltegiratze sistema hibridoen dimentsionamendua garraio aplikazioetarako.

Gaur egun, mugikortasun eskari handien eta baliabide energetikoen erabilpen iraunkorrarekiko dagoen goranzko kezkarekin, garraio aldetik geroz eta konponbide eraginkorragoak, prestazio hobeekin eta kostu lehiakorragoak eskatzen ari dira. Gai honetan, energia biltegiratze sistema hibridoak (HESS) konponbide interesgarri bezala agertzen ari dira potentzi eta energia ezaugarri desberdinez osatutako teknologiak nahastuz, non bateriak (BT) eta superkondentsadoreak (SC) nabarmentzen diren garrantzitsuenen artean.

Hala ere, ibilgailuaren barruan hainbat energi iturri izanda, potentzia eta energia eskaerak elikatzeko, kudeaketa optimoa (HESSaren erabilpen hobea lortzeko) arazo konplexua bihurtzen da. Gai honen garrantzia geroz eta handiagoa da HESSan (bai BTetan eta baita SCetan ere) degradazio prozesuak berauen erabilpenaren araberakoa dela jakinda, ibilgailuaren operazioaren funtzionamenduan. Beraz, aukeratutako energia kudea keta estrategia (EMS) eta HESSaren dimentsionamendu egokiak faktore erabakigarriak direla argi dago sistemaren operazio egoki eta efizientea ziurtatzeko eta aldi berean, ibilgailuaren fabrikatzailearentzat eta baita azken erabiltzaileentzat operazio kostu lehiakor bat izateko. Hala, aspektu teknikoak eta nahiz ekonomikoak kontuan hartu behar dira, bereziki ibilgailuaren barnean doazen HESS sistementzat non inplementazio eta aldatze kosteak oso garrantzizkoak diren.

Tesi honek HESSaren dimentsionamendu optimoa eta bere operazio bateratuaren (BTs eta SCs) gaiak jorratzen ditu, hiriguneetako mugikortasun publikoko ibilgailuetan integratzeko helburuarekin. Alde batetik, estrategia energetiko berritzaile bat proposatzen da ibilgailuaren barruan erabilgarri dauden iturrien artean potentzi eskaeraren bereizketa egiteko. EMS moldakor honek logika difusoan oinarrituta dago ibilgailuaren operazioa definitzeko (era adimentsu eta intuitiboagoan), hainbat energi iturrien kudeaketa eta sistema elektriko hibrido batek hainbat funtzionamendu baldintzetan lan egin dezan. EMS berri honek, ibilgailua mugitzeko momentu horretan bertan behar den potentziaz eta HESSaren egoera energetikoaz aparte, etorkizuneko energia beharrak (baterietan eta superkondentsadoretan) kontsideratzen ditu, leiho mugikor baten bidez, bere portaera energetikoak estimatzeko gai dena. Proposatzen den EMS moldakor honek momentuko informazio energetikoa eta etorkizunekoa (estimatua) ebaluatzen ditu, era efiziente eta

optimizatu batean HESSaren operazioa moldatzeko ibilgailuak biltegiratuta daukan baliabide energetikoen aprobetxamendua hobetzeko helburuarekin.

Beste alde batetik, ko-optimizazio metodologia bat proposatu da bai EMSa eta baita HESSaren dimentsionamendua elkarrekin optimizatzeko. Metodologia honek, lehenik eta behin ibilgailuaren operazioaren eta barneko energi iturrien ebaluaketa tekniko bat egiten du EMSak emaitza moduan ematen duen kudeaketa energetikoa aplikatuz. Bigarren pausu batek, ibilgailuaren operazioa eta bere biltegiratze sistemaren analisi ekonomikoa kalkulatzen du, ibilgailuaren operazioaren kosturik txikiena ematen duen soluziorik aproposena helburu izanik (bai HESSaren dimentsionamendua eta baita EMSaren operazioa). Helburu hau betetzeko, HESSaren inbertsio iniziala eta aldaketak kontutan hartzen dituen modelo ekonomiko batean oinarrituriko problema helburuanitz bat planteatu da ibilgailuaren eguneko operazio kostea kalkulatzeko. Aldaketa kostua kalkulatzeko, bai zahartze ereduak eta bizitza estimazio ereduak aplikatu dira HESSrako eta ibilgailuaren bizitza bera ere kontsideratu da. Optimizazio prozesuan lortu diren kontsignen balioak logika difusoan oinarrituta dagoen estrategia moldakorra konfiguratzeko erabili dira. Era honetan, EMSaren operazioa bere puntu efiziente eta egokienetan landuz gero, helburu teknoekonomikoen betetzea bermatuz.

Energia kudeaketarako estrategia moldakorra eta HESSaren dimentsionamendu eta EMSaren operazioaren ko-optimizazioaren metodologia. Doktore-tesi proposamen honen helburua balioztatzeko bi hiri garraio kasu aipagarri aukeratuak izan dira: Tranbia Elektriko Hibridoa (HET) eta Autobus Elektriko Hibridoa (HEB).

Lehen kasuan (HET), Sevillako tranbian oinarritutako kasu erreal bat aukeratu da. Kasu honetan, ibilgailuak bai katenaria duen eta katenaria gabeko tarte desberdinetan operatzen du. Bigarren kasu gisa, hiri ibilbide bat aukeratu da emisiorik gabeko tarteak dituena (operazio guztiz elektrikoa).Tesi honetan proposatzen den EMS aldakorra, bai kasu bakoitzaren operazio baldintzen arabera, bai ibilgailuek daukaten hirugarren energi iturria gehitzeko moldatu da: katenaria (HET) eta barne-errekuntzako motorra (HEB). Bi kasutan lortutako emaitzak termino teknikotan, ekonomikotan eta efizientzian alderatuak izan dira oinarrizko kasu batzuekiko, arauetan oinarritutako EMSak kontsideratuz eta tesi honetan proposatutako ikuspuntuarekin lortutako hobekuntzak zehazteko helburuarekin. Lortutako emaitzek ko-optimizazioaren metodologia EMS aldakorrarekin batera aukera ematen dute aurrezpen nabaria lortzeko ibilgailuen kostu operazioan (HET eta HEB), kasu bakoitzaren operazio beharren betetzea bermatuz, eta aldi berean, sistema hauen efizientzia energetikoa hobetuz.

Hitz gakoak: bateria, kudeaketa energetikoko estrategia, logika difusoa, superkondentsadorea, autobus elektriko hibridoa, tranbia elektriko hibridoa, biltegiratze sistema hibridoa, optimizazio helburuanitza, dimentsionamendua.

Glosary of terms

Ageing

Process which affect the electrochemical cells over time, causing a reduction in their capacity to provide energy and power.

Battery pack

One or more electrochemical cells connected in series or parallel to fulfill the specifications required in a certain application. The battery pack often includes the BMS and other elements which integrate the final component.

Battery Management System (BMS)

It includes the hardware and software used for ensuring the proper operation of the battery, optimizing its life and performance, by monitoring and controlling each cell.

C-rate

Speed of charge or discharge rate of the battery. This parameter is related to the capacity of the cell. A charge or discharge of nC rate means that the capacity of the battery will be charged or discharged in 1/n hours (when the capacity is measured in Ah). For example, a 10 Ah battery which is being discharged at 1C rate implies a 10A current and a 1 h discharge time.

Calendar ageing

Degradation suffered by the battery even when it is stored.

Capacity

It is the amount of energy that can be stored in the battery, measured in Ah. This value can be calculated performing a discharge of the battery, starting completely charged. If the discharge is done under different conditions the measured value can differ.

Cell

Basic unit of electrochemical energy storage, composed of anode, cathode and electrolyte.

Glosary

It transforms electric energy in chemical energy and vice versa by means of electrochemical reactions.

Charge

Process which stores the electric energy supplied to the battery converting it in chemical energy.

Coulomb Counting

Technique used for determining the SOC of a battery, based on the integration of the current through the battery. Also named Ah-Counting.

Cycle

Process that produces one charge and one discharge of a battery.

Cycle ageing

Degradation of the battery performance caused by working cycles.

Depth of Discharge (DOD)

Relationship between the energy extracted and the entire capacity of a battery. It is opposed to the State of Charge.

Discharge

Process which extracts the chemical energy stored in a battery as electrical energy.

Efficiency

Relationship between the extracted energy during the discharge and the energy required to charge the battery to the initial State of Charge.

End of life (EOL)

Point in the battery lifetime when the battery cannot fulfil the energy and power requirements from the application. In some applications, the EOL of a battery is established when the capacity is reduced to 80% compared to the capacity of a new battery.

Energy density

Available energy in a battery per unit of volume. It is measured in Wh/l.

Full Equivalent Cycles (FEC)

Equivalent number of cycles of 100% DOD which produce the same Ah throughout than a number of cycles with less depth of cycle discharge.

Fuzzy set

Fuzzy set is an extension of the classical set. In classical crisp set theory, the membership of elements complies with a binary logic, either the element belongs to the crisp set or the element does not belong to the set. While in fuzzy set theory, it can contain elements with degree of membership between completely belonging to the set and completely not belonging to the set. This is because a fuzzy set does not have a crisp, clearly defined boundary, and its fuzzy boundary is described by membership functions which make the degree of membership of elements.

Internal resistance

The opposition or resistance to the flow of an electric current within a cell or battery; the sum of the ionic and electronic resistances of the cell components.

Membership function (MF)

A membership function is a curve that defines the feature of fuzzy set by assigning to each element the corresponding membership value, or degree of membership range from 0 to 1.

Memory effect

Temporal loss of the battery capacity, produced when it is repeatedly and incompletely discharged.

Nominal voltage

The characteristic operating voltage or rather typical voltage of the battery given by the manufacturer.

Open circuit voltage (OCV)

Difference of electrical potential between the cell terminals when the load is disconnected and the cell is relaxed, which means that the dynamics processes which occur inside it are stopped. The OCV value depends on several factors as the State of Charge, the temperature or the previous history of the cell.

Glosary

Parallel

Term used to describe the interconnection of cells or batteries in which all of the like terminals are connected together. Parallel connection increase the capacity of the resultan battery pack according to the number of cells connected.

Power density

Available power in a battery per unit of volume. It is expressed in W/l.

Root mean square error (RMSE)

It is a frequently used measure of the differences between values (sample and population values) predicted by a model or an estimator and the values actually observed.

Sample time

Time between two consecutive samples of a continuous signal to obtain a discrete signal.

Self-discharge

It is a phenomenon which reduces the charge of a battery when it is stored. This loss of energy depends on the temperature, the initial state of charge and the storage time. This reduction of charge is expressed as a percentage of the battery capacity.

Series

The interconnection of cells or batteries in such a manner that the positive terminal of the first is connected to the negative terminal of the second and so on. Series connections increase the voltage of the resultant battery pack according to the number of cells connected.

Specific energy

Available energy in a battery per unit of mass. It is measured in Wh/kg.

Specific power

Available power in a battery per unit of mass. It is expressed in W/Kg.

State of Charge (SOC)

Amount of energy stored in the battery. It is expressed as a percentage of the capacity of the battery.

State of health (SOH)

Ageing level of the battery which is reflected in the ability of supplying energy and power in comparison with a new battery.

Supercapacitor pack

One or more supercapacitor cells connected in series or parallel to fulfill the specifications required in a certain application.

Scientific contributions

Within this research project, several scientific contributions to the literature were published. These are listed below.

JOURNAL ARTICLES:

a. **V. I. Herrera**, A. Milo, H. Gaztañaga, I. Etxeberria-Otadui, I. Villarreal, H. Camblong, *Adaptive energy management strategy and optimal sizing applied on a battery-supercapacitor based tramway*, Applied Energy, vol. 169, May 2016, pp. 831-845.
DOI: 10.1016/j.apenergy.2016.02.079

b. **V. I. Herrera**, H. Gaztañaga, A. Milo, A. Saez-de-Ibarra, I. Etxeberria-Otadui, T. Nieva, *Optimal Energy Management and Sizing of a Battery-Supercapacitor based Light Rail Vehicle with Multi-objective approach*, in IEEE Transactions on Industry Applications, vol. 52, no. 4, pp. 3367-3377, July-Aug. 2016.
DOI: 10.1109/TIA.2016.2555790

c. A. Saez–de–Ibarra, **V. I. Herrera**, A. Milo, H. Gaztañaga, I. Etxeberria-Otadui, S. Bacha, A. Padrós, *Management Strategy for Market Participation of Photovoltaic Power Plants including Storage Systems*, in IEEE Transactions on Industry Applications, vol. 52, no. 5, pp. 4292-4303, Sept.-Oct. 2016.
DOI: 10.1109/TIA.2016.2585090

d. **V. I. Herrera**, A. Milo, H. Gaztañaga, H. Camblong, *Adaptive and non-adaptive strategies for optimal energy management of a dual energy storage system in a hybrid electric bus*, submitted to Applied Energy, Feb. 2017.

CONFERENCE ARTICLES:

e. **V. I. Herrera**, A. Saez–de–Ibarra, A. Milo, H. Gaztañaga, H. Camblong, *Optimal energy management of a hybrid electric bus with a battery-supercapacitor storage system using genetic algorithm*, in: IEEE International Conference on Electrical Systems for Aircraft, Railway, Ship Propulsion and Road Vehicles (ESARS), Aachen, 2015, pp. 1-6.
DOI: 10.1109/ESARS.2015.7101452

Scientific contributions

f. **V. I. Herrera**, H. Gaztañaga, A. Milo, A. Saez–de–Ibarra, I. Etxeberria–Otadui, T. Nieva, *Optimal energy management of a battery-supercapacitor based light rail vehicle using genetic algorithms*, in: IEEE Energy Conversion Congress and Exposition (ECCE), Montreal, 2015, pp. 1359-1366.
DOI: 10.1109/ECCE.2015.7309851

g. A. Saez–de–Ibarra, A. Milo, H. Gaztañaga, **V. I. Herrera**, I. Etxeberria-Otadui, A. Padrós, *Intelligent photovoltaic power plants management strategy for market participation*, in: IEEE Energy Conversion Congress and Exposition (ECCE), Montreal, 2015, pp. 35-42.
DOI: 10.1109/ECCE.2015.7309666

h. **V. I. Herrera**, H. Gaztañaga, A. Milo, T. Nieva, I. Etxeberria–Otadui, *Optimal Operation Mode Control and Sizing of a Battery-Supercapacitor Based Tramway*, in: IEEE Vehicle Power and Propulsion Conference (VPPC), Montreal, 2015, pp. 1-6.
DOI: 10.1109/VPPC.2015.7352988

i. E. Martinez–Laserna, **V. I. Herrera**, E. Sarasketa–Zabala, A. Milo, I. Villarreal, *Techno–Economic Impact of Li–ion Battery Lifetime Modelling on Energy Storage System Sizing*, in: 29th Electric Vehicles Symposium & Exhibition (EVS), Montreal, 2016, pp. 1-12.

j. **V.I. Herrera**, A. Milo, H. Gaztañaga, H. Camblong, *Multi-objective Optimization of Energy Management and Sizing for a Hybrid Bus with dual Energy Storage System*, in: IEEE Vehicle Power and Propulsion Conference (VPPC), Hangzhou, 2016, pp. 1-6.
DOI: 10.1109/VPPC.2016.7791731

k. I. Prasad, P.N. Borza, **V. I. Herrera**, A. Milo, *Energy management of hybrid energy storage system for e-bike application*, in IEEE Conférence Internationale en Sciences et Technologies Electriques au Maghreb (CISTEM), Morocco, 2016, pp. 1-7.
DOI: pending

BOOK CHAPTER:

l. **V. I. Herrera**, A. Milo, H. Gaztañaga, H. Camblong, I. Isasa, *Energy Management for Hybrid Storage Systems in Transport Applications*, in: "EMVeM" Energy efficiency Management for Vehicles and Machines, A European Commission FP7 Marie Sklodowska-Curie, Initial Training Network (ITN), Ed. KU Leuven: Academic Press, Chapter 10, 2016, pp. 191-224.
ISBN 9789073802964

Contents

Contents

Contents

Notations

Abbreviations

AC	Alternating Current
A-EMS	Adaptive Energy Management Strategy
AM	Autonomous Mode
BT	Batteries
CB	Crowbar
CD	Charge Depleting
CM	Charing Mode
CS	Charge Sustaining
CSM	Catenary Support Mode
DC	Direct Current
DM	Depleting Mode
DOD	Depth-of-Discharge
DP	Dynamic Programming
DPSO	Dynamic-neighborhood Particle Swarm Optimization
ECMS	Equivalent Consumption Minimization
ECM	Energy Charging Mode
EDLC	Electrochemical Double Layer Capacitors
EG	Electric Generator
EM	Electric Motor
EMS	Energy Management Strategy
EOL	End-of-Life

ESS	Energy Storage System
FC	Fuel Cell
FEC	Full Equivalent Cycle
FEV	Full-Electric Vehicle
FIS	Fuzzy Inference System
FLC	Fuzzy Logic Control
FW	Forward Window
GA	Genetic Algorithm
GHG	Greenhouse Gas
GPS	Global Positioning System
HDCD	Hybrid Driving Charge Depleting
HDCS	Hybrid Driving Charge Sustaining
HEB	Hybrid Electric Bus
HESS	Hybrid Energy Storage System
HET	Hybrid Electric Tramway
HEV	Hybrid Electric Vehicle
HIL	Hardware-in-the-Loop
IEA	International Energy Agency
ICE	Internal Combustion Engine
Li-ion	Lithium-ion
LRV	Light Rail Vehicle
MO	Multi-Objective
MPC	Model Predictive Control
NN	Neural Networks
NiCd	Nickel Cadmium
NiMH	Nickel Metal Hydride
PED	Pure Electric Driving

PES	Power Electronic System
PHEV	Parallel Hybrid Electric Vehicle
PMP	Pontryagin's Minimum Principle
PO	Permanent Operation
PSO	Particle Swarm Optimization
PV	Photovoltaic
RB-EMS	Rule-Based Energy Management Strategy
REDOX	Reversible Electrochemical Reduction/Oxidation
RMSE	Root-Mean-Square Error
RTP	Real time Pricing
SA	Simulated Anneling
SC	Supercapacitors
SDP	Stochastic Dynamic Programming
SHEV	Series Hybrid Electric Vehicle
SM	Sustaining Mode
SOC	State-of-Charge
SOH	State-of-Health
SORT	Standardized On-Road Test Cycle
USO	Unscheduled-Stop Operation
VDC	Voltage of Direct Current

Abbreviations Fuzzy logic

H	High
HC	High Charging
HD	High Discharging
HR	High Regenerative
HT	High Traction

L	Low
LC	Low Charging
LD	Low Discharging
LR	Low Regenerative
LT	Low Traction
M	Medium
MH	Medium High
ML	Medium Low
N	Negative
P	Positive

Symbols

A_f	Frontal area of the vehicle	$[m^2]$
a_{veh}	Vehicle acceleration	$\left[\frac{m}{s^2}\right]$
α	Slope angle of the road	$[\measuredangle]$
α_1	Fitting coefficient on Semi-empirical model	
α_2	Fitting coefficient on Semi-empirical model	
α_3	Constant fitting coefficient on Semi-empirical model	
α_4	Constant fitting coefficient on Semi-empirical model	
BT_{Ca_y}	Annualized capital (initial investment) cost of the BT pack	$\left[\frac{euros}{year}\right]$
BT_{M_y}	Average annual cost of maintenance of the BT pack	$\left[\frac{euros}{year}\right]$
BT_{Re_y}	Annualized replacement cost (cycling cost)	$\left[\frac{euros}{year}\right]$
BT_{Tcost}	Total operating cost of the BT pack	$\left[\frac{euros}{day}\right]$
β_1	Fitting coefficient on Semi-empirical model	
β_2	Fitting coefficient on Semi-empirical model	

β_3	Constant fitting coefficient on Semi-empirical model	
β_4	Constant fitting coefficient on Semi-empirical model	
C_{nom_BTcell}	Nominal capacity of the BT cell	$[Ah]$
Ca_{BT}	Nominal energy capacity of the installed BT pack	$[kWh]$
Ca_{SC}	Nominal energy capacity of the installed SC pack	$[kWh]$
$Cat_{EN}(k)$	Catenary enable (*true* or *false*)	
Cat_{Tcost}	Total cost of the energy absorbed from the catenary	$\left[\frac{euros}{day}\right]$
C_{BT}	Nominal capacity of the BT pack	$[Ah]$
c_d	Aerodynamic drag coefficient	$[-]$
$ceil(x)$	Mathematical function which returns the higher integer value of its argument x	
$CH_{ST}(k)$	Charging station enable (*true* or *false*)	
C_{kWh_BT}	Referential cost of the BT technology	$\left[\frac{euros}{kWh}\right]$
C_{kW_dcdc}	Referential cost of the DC/DC converter	$\left[\frac{euros}{kW}\right]$
C_{kwh_g}	Referential cost of the grid energy	$\left[\frac{euros}{kWh}\right]$
C_{kWh_SC}	Referential cost of the SC technology	$\left[\frac{euros}{kWh}\right]$
$C_{L\_fuel)}$	Referential cost of the liter of fuel (diesel)	$\left[\frac{euros}{liter}\right]$
c_r	Rolling friction coefficient of the wheels	$[-]$
C_{rate}	C-rate limitation for the BT cell	$[-]$
CRF	Capital recovery factor	$\left[\frac{1}{year}\right]$
C_{SC}	Equivalent capacitance of the SC pack	$[F]$
C_{SCcell}	Capacitance of the SC cell	$[F]$
$DeltaE_{BT}(k)$	Energy variation in FW_k for the BT pack calculated at the discrete step k	$[kWh]$
$DeltaE_{SC}(k)$	Energy variation in FW_k for the SC pack calculated at the discrete step k	$[kWh]$

Notations

$dw_{wh}(k)$	Wheel rotational acceleration	$\left[\frac{m}{s^2}\right]$
Δt	Time step	$[s]$
$E_{BT\_rg,k}$	Estimation of energy absorbed in the BT pack in FW_k	$[kWh]$
$E_{BT\_tr,k}$	Estimation of energy supplied by the BT pack in FW_k	$[kWh]$
$E_{Cat,k}$	Estimation of energy provided by the catenary in FW_k	$[kWh]$
$E_{CB,k}$	Estimation of energy absorbed by the crowbar resistance in FW_k	$[kWh]$
$E_{genset,k}$	Estimation of energy provided by the genset in FW_k	$[kWh]$
$E_{SC}(k)$	Energy stored in the SC pack	$[J]$
$E_{SC\_rg,k}$	Estimation of energy absorbed in the SC pack in FW_k	$[kWh]$
$E_{SC\_tr,k}$	Estimation of energy supplied by the SC pack in FW_k	$[kWh]$
$E_{u\_max\_n}$	Maximum negative value of energy variation reached in the vector $DeltaE_u$ ($u \in [BT, SC]$)	$[kWh]$
$E_{u\_max\_p}$	Maximum positive value of energy variation reached in the vector $DeltaE_u$ ($u \in [BT, SC]$)	$[kWh]$
F_a	Aerodynamic drag force	$[N]$
F_g	Gravitational force	$[N]$
F_i	Inertial force	$[N]$
F_r	Rolling friction force	$[N]$
$F_t(k)$	Required traction force	$[N]$
$Fuel_{Tcost}$	Total cost of fuel consumption	$\left[\frac{euros}{day}\right]$
FW_k	Forward window corresponding to the discrete step k	
g	Gravitational acceleration constant	$\left[\frac{m}{s^2}\right]$
I	Interest rate	$[\%]$

$I_{BT}(k)$	BT pack current	$[A]$
i_{evt}	Type of event that can occur during the lifetime of a BT cell until it reaches its EOL	
$I_{SC}(k)$	SC pack current	$[A]$
I_{1C_BTcell}	Nominal current of the BT cell at 1C of discharge rate	$[A]$
k	Discrete step	
k_{cs}	Global factor to cold starts	$[-]$
LC_{BTj}	Specific amount of available life cycles at the DOD range j	$[cycles]$
$Life_{BT}$	Lifespan estimation for the BT pack	$[years]$
$Life_{BT\_cal}$	Floating lifetime of the BT pack (calendar)	$[years]$
$Life_{BT\_r}$	Remaining lifetime of the BT pack at iteration r	$[years]$
$Life_{SC}$	Lifespan estimation for the SC pack	$[years]$
$Life_{SC\_cal}$	Floating lifetime of the SC pack (calendar)	$[years]$
$Life_{SC\_0}$	Remaining lifetime of the SC pack at first iteration 0	$[years]$
LL	Total loss of lifetime in the BT considering the whole range of events that could happen (whole range of DODs)	
$LL_{i_{evt}}$	BT Lifetime lost caused by the occurrence of a certain number of i_{evt} events (certain DOD)	
m	Iteration index when the EOL of the BT has been reached	
$mass_{BT}$	Weight of the BT pack	$[kg]$
$mass_{SC}$	Weight of the SC pack	$[kg]$
m_{BT}	Number of branches (strings) in parallel in the BT pack	
$mf_{ICE}(k)$	ICE fuel mass flow	$\left[\frac{kg}{s}\right]$
m_{it}	Total inertial mass in vehicle	$[kg]$

Notations

m_{obj}	Number of objective function in a MO problem	
m_{pas}	Average weight per person	$[kg]$
m_{SC}	Number of branches (strings) in parallel in the SC pack	
m_{tot}	Total vehicle mass	$[kg]$
m_{veh}	Empty bus weight	$[kg]$
n_{BT}	Number of BT cells in series (string) in the BT pack	
N_{BT_dj}	Number of cycles/day counted (by Rainflow algorithm) in the DOD range j done in the BT pack	$\left[\frac{cycles}{day}\right]$
n_{cstr}	Number of constraints in a MO problem	
n_d	Time frame considered to update the SOH calculation	$[days]$
$NE_{i_{evt}}$	Number of i_{evt} type events accounted	
$NE_{i_{evt}}^{max}$	Maximum number of events i_{evt} type (certain DOD) that the BT can withstand	
n_{FW}	Number of discrete steps taken for the FW (window size)	
n_{ICE}	Number of discrete ICE rotational speeds in which the available range of speed has been split	
n_{pas}	Number of passengers	
n_{SC}	Number of SC cells in series (string) in the SC pack	
N_{SC_dj}	Number of cycles/day counted (by Rainflow algorithm) in the DOD range j done in the SC pack	$\left[\frac{cycles}{day}\right]$
η_{conv}	Efficiency for DC/DC converter	$[\%]$
$\eta_{EG}(k)$	EG operating efficiency	$[\%]$
$\eta_{EM}(k)$	EM operating efficiency	$[\%]$
$\eta_{ICE}(k)$	ICE operating efficiency	$[\%]$

η_{inv}	Efficiency for AC/DC inverter	$[\%]$
OP^*	Intermediate ICE operating points	
OP_{Tcost}	Total daily operating cost for the vehicle	$\left[\frac{euros}{day}\right]$
Ω	Feasible solution space	
p	Number of discrete steps in the daily profile	
P_{aux}	Power consumption from auxiliary loads	$[kW]$
$P_{BT\_AM\_tr}$	Power target during traction in *AM* for BT pack	$[kW]$
P_{BT_ch}	Power target for charging the BT pack related to the C-rate limitation	$[kW]$
$P_{BT\_CSM\_tr}$	Power targets during traction in *CSM* for BT pack	$[kW]$
P_{BT_dch}	Power target for discharging the BT pack related to the C-rate limitation	$[kW]$
P'_{BT}	Provisional power target for the BT pack	$[kW]$
$P_{BT}(k)$	Power target for the BT pack	$[kW]$
$P_{BT\_max\_ch}$	Maximum allowable power target for charging the BT pack	$[kW]$
$P_{BT\_max\_dch}$	Maximum allowable power target for discharging the BT pack	$[kW]$
$P_{CAT}(k)$	Power absorbed from catenary at the discrete step k	$[kWh]$
$P_{CB}(k)$	Power absorbed in crowbar resistance	$[kW]$
p_{ch}	Power split ratio for charging the BT pack	$[-]$
P_{dcdc_BT}	Power of the DC/DC converter linked to the BT pack	$[kW]$
P_{dcdc_SC}	Power of the DC/DC converter linked to the SC pack	$[kW]$
p_{dch}	Power split ratio for discharging the BT pack	$[-]$
$P_{DEM}(k)$	Total power demand during vehicle operation	$[kW]$
$P_{genset(k)}$	Genset power target	$[kW]$

Notations

P_{genset_max}	Maximum power output of the genset	$[kW]$
P_{genset_min}	Minimum power output of the genset	$[kW]$
$P_{genset\_max\_i}$	Maximum power output from the genset at the discrete ICE rotational speed w_{ICE_i}	$[kW]$
$P_{genset\_min\_i}$	Minimum power output from the genset at the discrete ICE rotational speed w_{ICE_i}	$[kW]$
$P_{genset\_range\_i}$	Power range at ICE rotational speed w_{ICE_i}	$[kW]$
P_{genset_1}	Power target limit 1 for genset operation	$[kW]$
P_{genset_2}	Power target limit 2 for genset operation	$[kW]$
P_{max_rg}	Power peak demand during regenerative braking phase	$[kW]$
P_{max_tr}	Power peak demand during traction	$[kW]$
P_{rg_1}	Average power value of the low power demands during regenerative braking phase	$[kW]$
P_{rg_2}	Average power value of the medium-low power demands during regenerative braking phase	$[kW]$
$P_{SC\_CSM\_tr}$	Power targets during traction in CSM for SC pack	$[kW]$
P_{SC_ECM}	Power target during regenerative braking phase ECM for SC pack	$[kW]$
$P_{SC}(k)$	Power target for the SC pack	$[kW]$
$P_{SC\_max\_ch}$	Maximum allowable power target for charging the SC pack	$[kW]$
$P_{SC\_max\_dch}$	Maximum allowable power target for discharging the SC pack	$[kW]$
P_{tr_1}	Average power value of the low power demands during traction	$[kW]$
P_{tr_2}	Average power value of the medium-low power demands during traction	$[kW]$
ρ_a	Density of air	$\left[\frac{kg}{m^3}\right]$
ρ_{BT}	Energy density of the BT cell technology	$\left[\frac{kg}{kWh}\right]$

ρ_{fuel}	Volumetric density of the fuel	$\left[\frac{kg}{liter}\right]$
ρ_{SC}	Energy density of the SC cell technology	$\left[\frac{kg}{kWh}\right]$
$Q_{BT}(k)$	Available electric charge of the BT pack	$[C]$
Q_{BT_0}	Nominal charge of the BT pack	$[C]$
Q_{loss}	Total capacity loss in BT	$[\%]$
Q_{loss_cal}	Capacity loss due to calendar life in BT	$[\%]$
Q_{loss_cyc}	Equivalent capacity fade caused by cycling in BT	$[\%]$
$Q_{SC}(k)$	Available electric charge of the SC pack	$[C]$
r	Index of iteration for Rainflow algorithm	
r_BT	Number of BT pack replacements during the lifetime of the system T	
R_{BT}	Equivalent internal resistance of the BT pack	$[Ohm]$
R_{int_BTcell}	Internal resistance of the BT cell	$[Ohm]$
R_{int_SCcell}	Internal resistance of the SC cell	$[Ohm]$
r_SC	Number of SC pack replacements during the lifetime of the system T	
R_{SC}	Equivalent internal resistance of the SC pack	$[Ohm]$
r_{wh}	Wheel radius	$[m]$
SC_{Ca_y}	Annualized capital (initial investment) cost of the SC pack	$\left[\frac{euros}{year}\right]$
SC_{M_y}	Average annual cost of maintenance of the SC pack	$\left[\frac{euros}{year}\right]$
SC_{Re_y}	Annualized replacement cost (cycling cost)	$\left[\frac{euros}{year}\right]$
SC_{Tcost}	Total operating cost of the SC pack	$\left[\frac{euros}{day}\right]$
$sgn(X)$	Sign function (returns sign of its argument)	
SOC_{BTcell}	SOC of the BT cell	$[\%]$
$SOC_{BT}(k)$	SOC of the BT pack	$[\%]$
SOC_{BT_max}	Maximum allowable SOC for the BT pack	$[\%]$
SOC_{BT_min}	Minimum allowable SOC for the BT pack	$[\%]$

Notations

SOC_{l_ctrl}	SOC lower control level for the BT pack	$[\%]$
$SOC_{SC}(k)$	State of charge of the SC pack	$[\%]$
SOC_{SC_max}	Maximum allowable SOC for the SC pack	$[\%]$
SOC_{SC_min}	Minimum allowable SOC for the SC pack	$[\%]$
SOC_{u_ctrl}	SOC upper control level for the BT pack	$[\%]$
SOH_{EOL}	SOH value when the life BT cell is considered exhausted (EOL)	$[\%]$
SOH_r	SOH corresponding to the remaining lifetime $Life_{BT\_r}$	$[\%]$
t	Time elapsed on storage	$[s]$
T	Lifetime of the system (vehicle)	$[years]$
$T_{EM}(k)$	EM mechanical torque	$[Nm]$
$Temp$	Ambient temperature	$[°C]$
$T_{ICE}(k)$	ICE torque target	$[Nm]$
$T_{ICE\_max\_i}$	Maximum allowable torque at ICE rotational speed w_{ICE_i}	$[Nm]$
$T_{ICE\_min\_i}$	Minimum allowable torque at ICE rotational speed w_{ICE_i}	$[Nm]$
$T_{wh}(k)$	Required torque in wheels	$[Nm]$
U_{oc_BT}	Equivalent open circuit voltage of the BT pack	$[V]$
$U_{SC}(k)$	Voltage of the SC pack	$[V]$
U_{SC_nom}	Nominal voltage of the SC pack	$[V]$
$\mu A(z)$	Membership function of the aggregated fuzzy set A with respect to z	
$\mu(x)$	Degree of membership of the input variable x	
V_{oc_BTcell}	Open circuit voltage of the BT cell	$[V]$
V_{nom_BTcell}	Nominal voltage of the BT cell	$[V]$
$v_{veh}(k)$	Vehicle speed at the discrete state k	$\left[\frac{m}{s}\right]$
$w_{EM}(k)$	EM rotational speed	$\left[\frac{rad}{s}\right]$

w_{ICE_i}	Discrete ICE rotational speed	$[rpm]$
$w_{ICE}(k)$	ICE rotational speed target	$[rpm]$
$w_{wh}(k)$	Wheel rotational speed	$\left[\frac{rad}{s}\right]$
X	Vector of variables in a real N-dimensional space	
X^s	Alternative optimal solution	
γ_1	Constant fitting coefficient on Semi-empirical model	
γ_2	Constant fitting coefficient on Semi-empirical model	
γ_3	Constant fitting coefficient on Semi-empirical model	

General introduction

In the last years, problems derived from the CO2 emissions such as climate change, urban air pollution and fossil fuels dependence have received significant interest due the increasing concern about the future environmental state of the world. In this issue Industry, Energy Generation and Transport are the most relevant agents that contribute to the pollutant emissions. Transport sector, which generates a high percent of emissions, has been the focus of efforts to conserve energy by reducing the fossil fuel consumption and developing alternative propulsive system. However, the International Energy Agency (IEA) projects an average annual increase in global transport energy demand of 1.6% between 2007 and 2030.

Therefore, in order to sustain the current level of mobility while at the same time being able to reduce the corresponding CO2 emissions, more efficient means of transportation are required. Vehicle manufacturers have focused their efforts on developing greener propulsion solutions in order to meet the market demand and ecological need for clean transportation.

One of the main aspects where the current researches and developments have been addressed is the topic of the energy storage systems (ESS). Thanks to the wide development of the energy storage technologies, and mainly the electric one, the vehicle manufacturers are able to offer more and more competitive solutions based on ESS. In the current market a wide offer of this kind of solutions can be found from electric bikes and motorbikes, through passenger cars and buses up to tramways and trains. In all the aforementioned solutions the aim is to be able to recover energy from the drivetrain, in the regenerative braking process, as well as to propel the vehicle to reduce or even avoid the energy consumption from fossil fuels.

An important topic on mobility issues corresponds to the public transportation. Despite the impact of public mobility might be considered smaller than the individual one, the public transport is an important candidate for ESS applications showing advantages on two main issues. As technical advantage, public transport normally operate on fixed routes with several starts/stops phases, low speeds, they have more physical space for energy storage units and possibility of implementing recharging points throughout the route. As environmental advantage, the increasing concern of the governments promotes research and implementation of more environmental friendly solutions for urban mobility, both to meet the rigorous current emission standards and to offer a greener image of their

cities and countries. Indeed, a big number of cities are already focused on cleaner public transport solutions by renewing their vehicle fleets, while many vehicle manufacturers and operators currently offer low or zero-emissions power-trains.

Therefore, focusing on the public mobility can be mention two important case studies: urban buses and light rail vehicles (LRV). These have to be analyzed separately to define their requirements, challenges and possible solutions.

For urban buses case, one of the viable policies to reduce emissions is the use of pure electric traction. Full electric buses (or normally known as battery electric buses) have the advantage of not producing any pollutant emissions directly from their operation. Their emissions are entirely "upstream" related to fuel production of electricity. This is especially advantageous in city centers where there is typically heavy traffic and air quality can be poor. Battery electric buses are also interesting because their energy consumption is very low when idling comparing to conventional diesel buses. However, the future development of full electric buses is slowed mainly for technical factors. Full electric buses require too large, heavy and expensive ESSs (mainly batteries) to achieve an acceptable degree of autonomy. To find satisfactory solutions to these problems, hybrid electric buses (HEB) are shown in the medium term as the most viable alternative.

A HEB can be defined as one that combines at least two power machines linked to two sets of different energy storages, where at least one of these is electric storage. With the broad development of internal combustion engines (ICE), it is usually to begin from this point to define the HEB as one that combines an ICE and electric motor powered from an ESS.

Hybrid electric city buses are becoming more popular all around the world but, despite their relative technological maturity, these buses have not been able to replace the conventional diesel buses in a large scale. The fuel economy of diesel buses has not significantly improved during the last decade, and the stricter emission regulations lay out more challenges that can even increase the fuel consumption and maintenance needs.

In HEBs the reduction on fuel consumption is related to a high use of the ESS. Therefore, this leads to a higher number of charge/discharge cycles and an early degradation of the ESS. Mainly in BT this approach has a strong impact due to the limited number of cycles in their lifespan. Considering the entire system, an early degradation of the ESS leads to the need of replacing it more times along the lifetime of the system, increasing the total cost.

On the other hand, for LRV case, it is worth noting that in the last years they have staged an impressive comeback, thanks to the environmental, economic and social advantages they offer. Most of these urban tramway systems are powered by an overhead catenary line, which implies some negative consequences as full overhead cables in city centers, peak power injected/absorbed variations in the grid, low energy efficiency cause the limited energy recovered to the catenary in the regenerative braking phase and high

cost of overhead catenary infrastructure. Efficient ways of overcoming these problems are removing partially the overhead cables (catenary-free zones) and implementing on-board ESS to supply energy during the travel (hybrid electric tramway, HET).

Currently in these kind of vehicles (HEB and HET) the main ESSs are based on electrochemical storage solutions, mainly batteries (BT) and supercapacitors (SC). From this point of view, both technologies present different features to be considered for transport applications. Thus, BTs have high energy density and they are charged/discharged (generally during minutes or hours) at lower power rates than comparing with SCs. The aim of this operation is to avoid frequent and high power charge/discharge phases due to the limited number of cycles in their lifespan. On the other hand, SCs have high power density and they are rapidly (generally seconds) and frequently charged/discharged with a limited amount of energy. The BTs define the autonomy in full electric operation while SCs deal with the power peaks in the regenerative braking or acceleration phases, respectively.

Based on the previously mentioned features a hybrid ESS (HESS) combining BTs with SCs could be interesting on applications where high energy and power densities are required, which is the case of the HEB and HET. In both scenarios the vehicles have to overcome several start/stop phases with power peak requests during their operation. Furthermore, due to stricter emission regulations (Euro VI) which limit ICE operation or lack of catenary (catenary-free operation) both, hybrid bus and tramway will require to fulfill the energy demand from an alternative source.

When two storage systems work simultaneously with and another energy source (ICE or catenary), the power split ratio among these ones during the operation will have a strong influence mainly in the ESS degradation reducing the lifetime and having directly impact on the acquisition and operating cost of the hybrid system. Besides, the optimal sizing problem is closely coupled with the energy management and the application constraints, especially for on-board ESS where weight, space and investment costs are critical factors.

Therefore the main challenge for the combination of these two energy storage technologies in a hybrid vehicle is:

To obtain and integrated optimal sizing and management, from the efficient and economic point of view, which fulfills the vehicle services requirements while ensuring the minimum acquisition and operating cost for the vehicle during the whole lifetime.

In this framework, the development of advanced energy management strategies (EMS) as well as the implementation of methodologies to obtain the optimal sizing for the HESS taking into account the economic and ageing approach is shown as a very promising field essential to ensure the close future implementations of more-efficient, best-performed and cost-competitive mobility solutions.

To face the identified challenge, the objective of this PhD is:

To develop an optimized process for sizing and energy management of hybrid ESS,

combining BT and SC, based on adaptive EMS and applied on urban mobility vehicles.

Besides the main objective of this thesis, other secondary objectives proposed in the present study are:

- To develop the **methodology for selecting the optimal sizing and energy management of a hybrid ESS** considering the impact of the ESS ageing on the operating cost during the lifetime of the vehicle.

- To develop **optimized and on-line adapted energy management strategies** for operating and cost efficiency improvement in hybrid urban vehicles.

- To **validate the developed adaptive energy management approach by comparing with a non-adaptive one** in terms of **operating cost reduction**, **energy efficiency** and **system performance**.

The solutions to these objectives are presented along this thesis. Therefore, the document has been organized in six chapters:

The first chapter presents the state-of-the-art related to the main aspects that compose this PhD work. Firstly the topic of the hybrid and electric vehicles is reviewed, analyzing the current and forecast scenarios. Then the main energy storage technologies applied on hybrid vehicles are presented. Furthermore, the classification of hybrid vehicles taking into account the power-train architecture and hybridization level is described. Moreover, the scenario of hybrid vehicles in public mobility is described, focusing on two case studies: hybrid urban bus and tramway. In each one the main advantages and challenges are defined and the major commercial solutions are briefly described. Finally, the topic of the energy management applied in hybrid vehicles is addressed and the most relevant trends applied in literature are analyzed.

In the second chapter, the scenarios of hybrid urban bus and tramway are presented. Firstly the electrical modeling of the main power-train elements in a series hybrid vehicle is detailed. After that the economic model, which considers both initial investment and replacement costs of the ESS as well as the operating cost during the vehicle lifetime, is presented. Additionally the topic of the energy storage ageing, mainly focused on batteries, is introduced and two lifetime estimation methods are presented. Then the multi-objective optimization approach based on genetic algorithms (GA) is introduced for the vehicle scenario and the fitness function is described. Finally, the methodology for co-optimization of sizing and energy management in a vehicle with an on-board hybrid ESS is presented. This methodology is one of the main contributions of this PhD thesis.

The third chapter corresponds to the tramway scenario. Firstly, a rule-based EMS is presented taking into account the current operation in catenary and catenary-free zones.

Then, a novel adaptive EMS based on fuzzy logic for a hybrid ESS (combining batteries and supercapacitors) is introduced and the design of the fuzzy system is described. This adaptive approach considers, in addition of the instantaneous system conditions (available energy in the ESS, vehicle power demand), information about the future energy consumption of the vehicle by applying a sliding forward window strategy. This way, the operation targets for the ESS are adapted to fully supply the instantaneous and estimated energy demand (increasing/decreasing the instantaneous consumption from the BT and/or SC pack). Finally the optimization methodology, previously introduced in chapter 2, is applied and simulation tests are carried out for both rule-based and adaptive fuzzy-based EMSs. This optimized and adaptive EMS is the major contribution of this PhD thesis. Here the technical, economic and efficiency performance of the alternative optimal solutions are analyzed under normal and unscheduled-stops operation (mainly in the catenary-free zone) and the most suitable one is selected.

In the fourth chapter, the case study of the urban bus is analyzed and the hybrid and free-emission operation scenario is stated. Here the methodology for selecting the most efficient operating points in the whole power output range of the ICE is described. Then, similarly to the third chapter, a rule-based and the novel adaptive fuzzy-based EMSs are introduced and adapted to the urban bus scenario. Finally the multi-objective optimization approach is applied and the alternative optimal solutions, from rule-based and adaptive fuzzy-based EMSs, are compared in terms of fuel economy, operating cost, autonomy and energy efficiency for selecting the most performed solution.

The fifth chapter presents a sensitivity analysis on the factor of lifetime estimation accuracy impact in the proposed optimization methodology. The two ageing models previously introduced in chapter 2 are applied in parallel with the same methodology to determine the influence of the accuracy in lifespan forecast on the ESS sizing and energy management. This analysis is carried out in both case studies (hybrid urban bus and tramway) ir order to determine the hysteresis range from the optimal selected solution when the aforementioned factor is modified and the techno-economic impact of the lifetime estimation deviation from its expected value.

In the sixth and last chapter the general conclusions and contributions extracted in this PhD thesis are presented. Furthermore, some possible future lines related to the topic addressed in this thesis are presented. A diagram to present the chapters organization is depicted in figure 1.
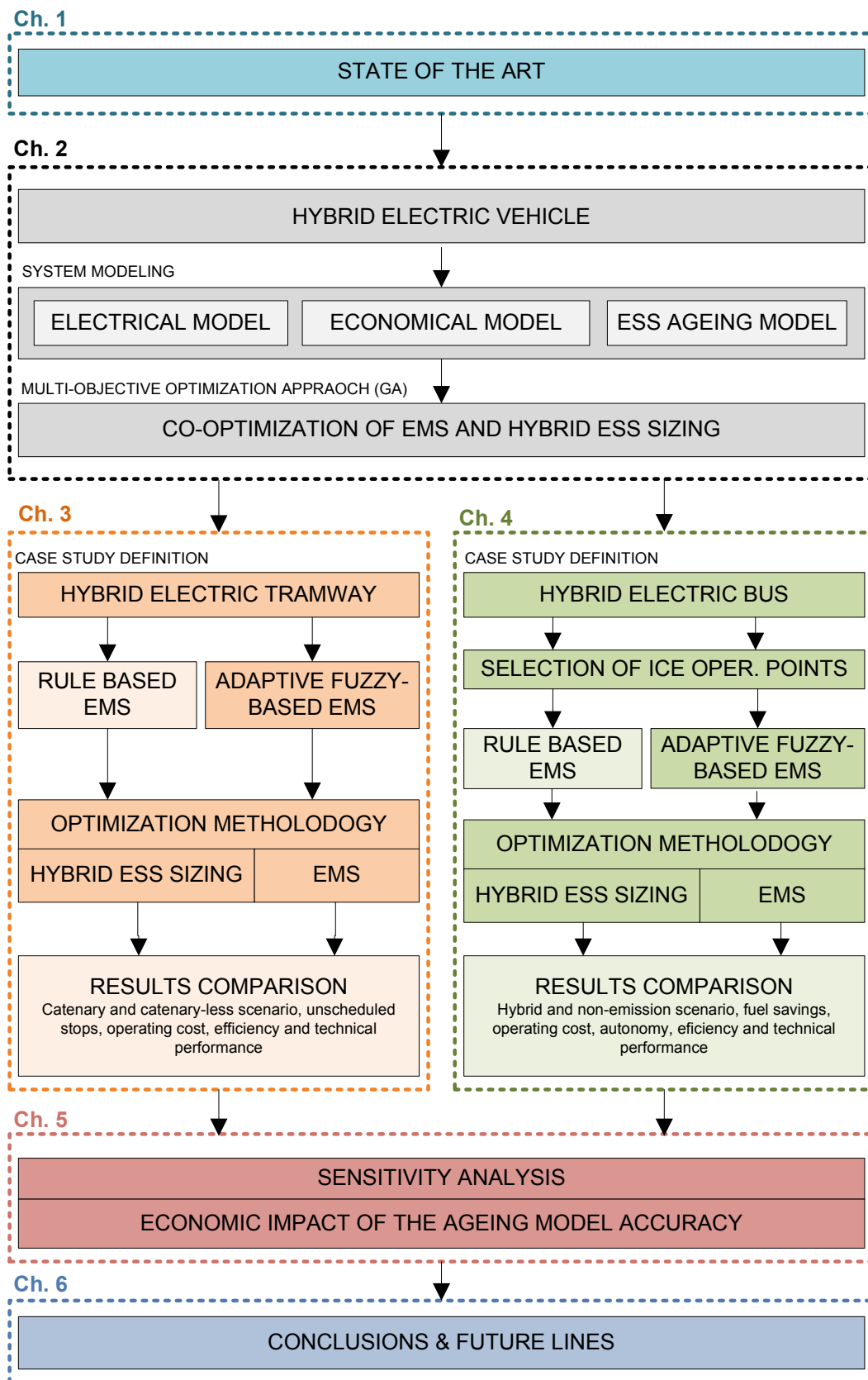
Figure 1: Chapters organization diagram.

1
State-of-art

1.1 State-of-art

Nowadays, the massive demand of energy and an increasing concern about the sustainable use of energy resources define the need of the development of alternative, more efficient and economic energy storage solutions [1,2]. Transport is one of the main sources of pollutant emissions, being responsible for 23% of CO_2 emissions associated with mobility (2010 levels, see figure 1.1a) [3]. For this reason the European Union is committed to significantly reduce its emissions – by at least 80% (from 1990's levels) by 2050 [1].

To fulfill this challenge, the public policies in the different countries are addressed both to establish stricter emission standards (currently Euro VI) [3] as well as to promote the transport electrification and use of energy coming mainly from renewable resources. As shown in figure 1.1b in the current world transport scenario most of the vehicles use fossil fuels as main energy source while the use of electrical sources is still less significant. Thus, the current and future focus is on the energy and fuel efficiency in search of solutions to reduce vehicle emissions while reducing consumption of fossil fuels [2]. Therefore, the collaboration among governments, academia and industrial institutions will play a key role to achieve the proposed objectives [1,3].
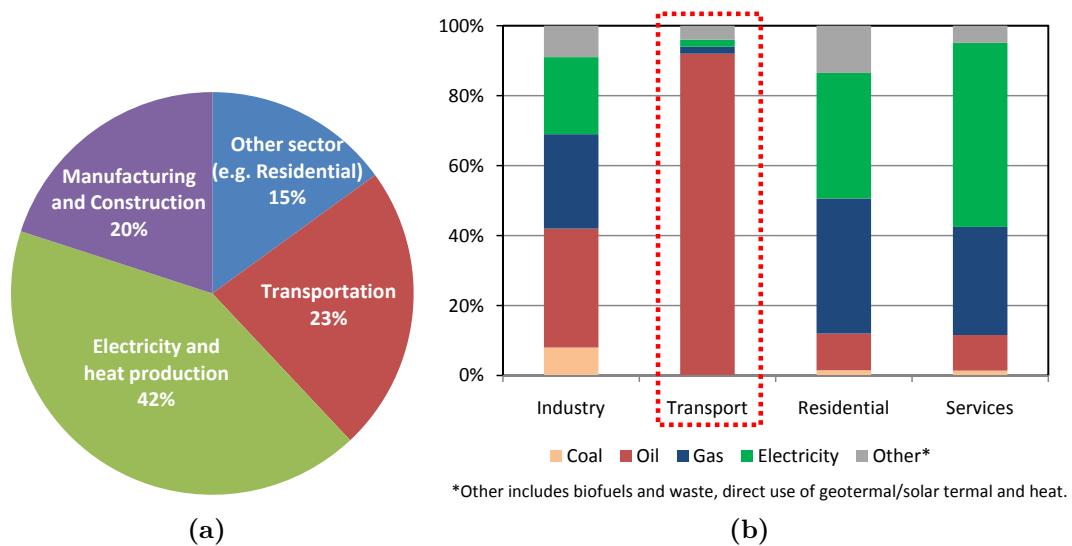
Figure 1.1: Pollution emission and energy consumption. (a) Global CO_2 emissions by sector [1]. (b) Global consumption by energy source [2].

In the last decade, successive development in vehicular electrification brought back the electrified vehicles in competition with ICE-based vehicles in terms of performance and globally emerged as sustainable alternative for conventional ICE-based vehicles. In addition, automobile industries are shifting towards more fuel efficient, improved performance, higher degree of reliability, durability, safety and added comforts for the new age of vehicles [4].

In recent years, hybrid electric vehicles (HEVs) have thrived as a feasible solution to

the aforementioned problems with their intermediate approach to achieve superior mileage and low emissions compared to conventional ICE vehicles [5]. HEV is a term used to describe vehicles that use ICEs in combination with one or more electric motors (EMs) connected to an ESS providing propulsion to the wheels either together or separately [6].

An extensive life-cycle cost analysis indicates that HEVs still are not fully competitive with ICE vehicles mainly due to the initial acquisition cost and the uncertainly of the ESS lifespan which may increase the cost of the vehicle during its lifetime with the ESS replacements [3, 5]. On the other hand, the full-electric vehicles (FEV), which are fully propelled by an ESS (without ICE), are less widespread in the automobile market due to similar cost reasons as the HEVs but mainly concerned on their driving autonomy. This kind of vehicles require very expensive and heavy ESS to achieve reasonable ranges of autonomy and the recharging infrastructure is still insufficient to guarantee the energy needed for long distance applications [6]. For this reason the FEVs are mostly used in urban applications while the HEVs are applied for longer distances combining urban and interurban scenarios.

However in recent years, with the rapid technological development of electric power-trains and improved ESS solutions, it has greatly increased interest in alternative power-train technologies for vehicle applications. Therefore, as depicted in figure 1.2, the sales forecasting expects an increasing market penetration of HEVs and FEVs in the upcoming years while the fossil fuel-based vehicles will be dramatically reduced.
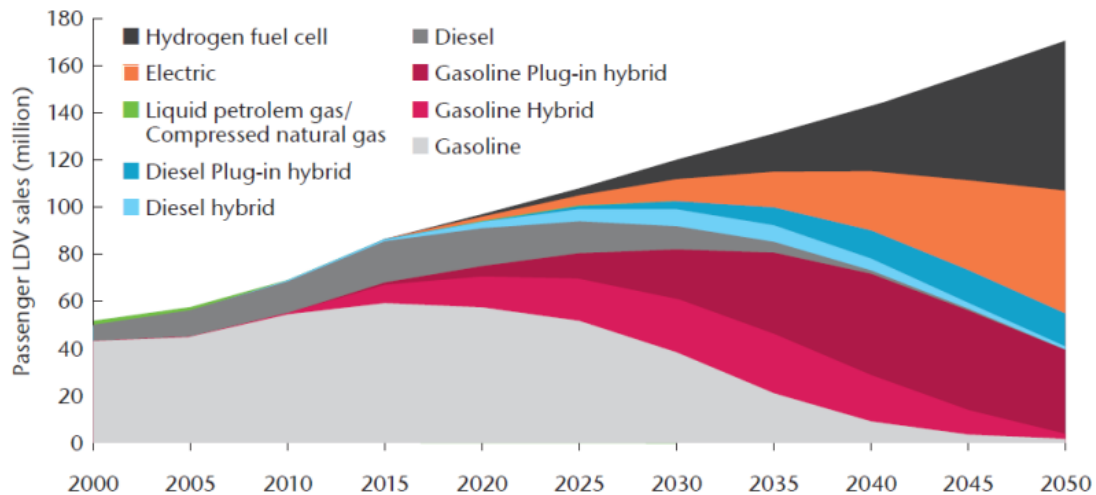
Figure 1.2: Sales forecasting of light vehicles [7].

Under this scenario is clear the importance of the current developments in hybrid and electric vehicles both to fulfill the emission reduction challenge as well as to guarantee the market penetration of this kind of vehicles in the upcoming years [5]. Nevertheless, as mention before, the ESS is the main core of the hybrid and electric vehicles and it defines most of their fuel savings, efficiency and autonomy during operation. Hence, special efforts should be addressed on the improvement of the ESS applications. On the one

hand, with the technology itself to improve the characteristics of the ESS: energy/power density, safety, cost, etc. On the other hand, related to the integration and operation of the ESS on-board the vehicle: ESS technology selection, proper sizing, management and control during operation, monitoring; in order to obtain the best performed operation while ensuring a competitive cost in the acquisition stage as well as during its entire lifetime.

1.2 Energy Storage Systems

Appropriate energy storage devices are core elements for more efficient, environmentally friendly and reliable solutions for mobile applications. The choice of each ESS is intrinsically related with the considered application and the desired operational characteristics, such as power and energy ratings (see figure 1.3), weight and volume, cost, response time and operating temperature [8].
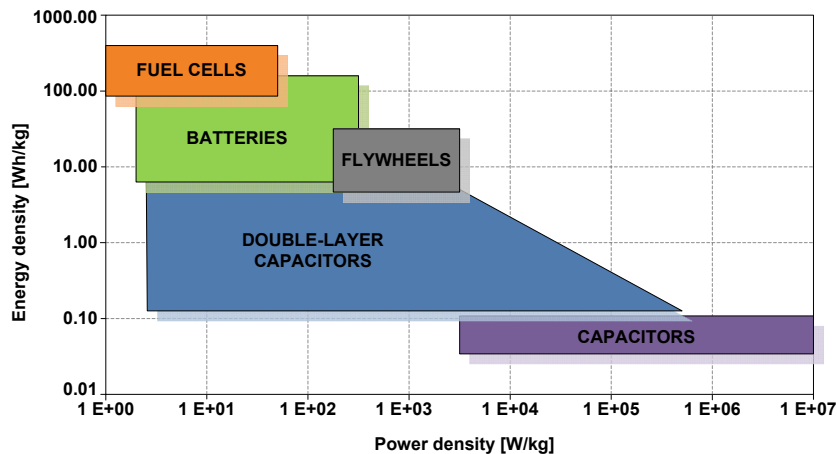
Figure 1.3: Power and energy density in different storage system technologies [9].

For mobile applications, hybrid and electric vehicles can be considered as the most relevant, where the ESS must be placed on-board the vehicle. Furthermore, can be considered other kind of vehicles such as trains or tramways and small personal mobility solutions (*e.g.* electric bikes [10]), where the ESS can be placed either on-board the vehicle or in the supplying substation [8].

As shown in figure 1.4, in terms of ESSs technology, the following categories can be considered: electrical, electrochemical, mechanical, chemical and thermal. This section is intended to cover the main technological solutions in the first four categories, which include supercapacitors, along with mature and emerging batteries, flywheel and fuel cells systems [8].

10
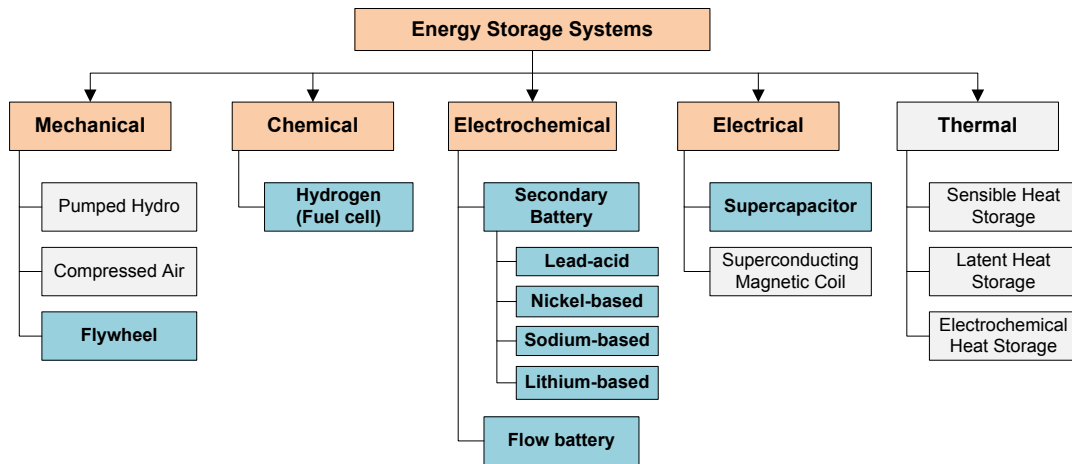
Figure 1.4: Classification of Energy Storage Systems [9].

1.2.1 Supercapacitors

Supercapacitors (SCs), also known as electrochemical double layer capacitors (EDLC), achieve a very high capacitance through the use of an electrochemical double layer and high surface area carbon electrodes [8]. Since there are no chemical changes, EDLCs present a very long life cycle (10,000–1,000.000 cycles) [11]. They also provide very high efficiency (90–98%) due to the fact that they only present ohmic resistance in the electrical connections. EDLCs have very high specific power (500–5000 W/kg), but low specific energy (2.5–15 Wh/kg) along with some self-discharging effects (20–40%Energy/day) [8].

Characteristics of SCs make them a very suitable option for energy storage in both HEVs and stationary power applications. Due to their rapid response they may be effectively used for supplying power peak demands and for voltage regularization purposes [9]. Current SCs researches primarily target on reducing material and device cost and increasing energy density without sacrificing power and lifespan [9].

1.2.2 Batteries

Rechargeable batteries, also known as secondary batteries, are the oldest form of electricity storage. The electricity is stored in the form of chemical energy and the energy conversion process is based on reversible electrochemical reduction/oxidation (REDOX) reactions. A battery is basically constituted by an electrolyte, an anode (positive electrode) and a cathode (negative electrode). Internal chemical reactions initiate an electron flux through the external circuit, being this flux reversible (charge and discharge) [8,9].

High energy/power density (see figure 1.5), modularity, flexibility and cost are the factors that guide the battery technology on the roadmap of vehicle electrification [4]. Therefore, several kinds of batteries can be found as commercial solutions, which can be classified depending on the technology applied to built up the battery cell.
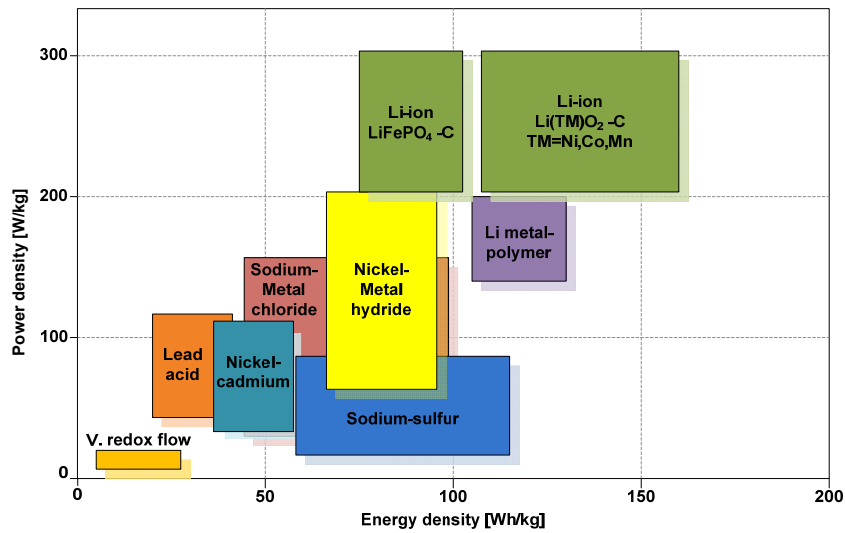
Figure 1.5: Power and energy density for different battery technologies [8].

A wide variety of battery technologies can be found in the market, such as lead-acid, Nickel Cadmium, Nickel metal hydride, Sodium Sulfur or Lithium ion batteries, each one with different battery composition and characteristics. Parameters like energy density, power density, specific energy and power, nominal voltage, lifetime or other factors are variable depending on the technology used to built-up the cell. For example, Lead-acid batteries have the most reduced costs, but they present a low energy density and specific energy. Among the nickel-based batteries, the nickel cadmium battery (NiCd) has higher energy and power density than lead-acid batteries, but their production costs are higher and furthermore, the cadmium is a very toxic element. Consequently, nickel metal hydride (NiMH) batteries have appeared to overcome this problem, providing some improvements as an increase in the energy and power density simultaneously with a long lifetime. Their main drawbacks are the high self-discharge rate and the presence of memory effect. Finally, the lithium-ion (Li-ion) technology provides some improvements over the previously commented chemistries in terms of energy and power density, although their main limitations are their cost and their more strict operating requirements [12].

Hence, according to the application performance requirements and the admissible costs, different solutions can be employed in each scenario. Compared to the other main chemistries, lithium based batteries have a higher energy and power density, in addition to a higher cell voltage. Moreover, lithium batteries do not present memory effect and they have very reduced self-discharge [13]. All these characteristics make lithium batteries the most suitable option in many applications. Because of this reason, jointly with the decrease in the manufacturing costs, the use of Li-ion batteries is experiencing a significant increment in the last decade.

1.2.3   Flywheels

Flywheel is a storage device which stores/maintains kinetic energy through a rotor/fly-wheel rotation. Flywheel systems are characterized by being able to provide very high peak power. In fact, the input/output peak power is limited only by the power converter. Modern flywheels can store more energy and power than existing metal hydride or lead-acid batteries of similar weight and volume [4]. Furthermore flywheels, unlike the BT and SC, are independent of depth-of-discharge (DOD) which improves its lifespan with vir-tually infinite number of charge–discharge cycles. Therefore, they are typically employed in transportation and power quality applications that require a long life system [14]. Unfortunately, the safety issues and gyroscopic force are their main disadvantages in transportation usage [13].

Table1.1 summarizes the main characteristics of the major ESSs technologies previ-ously described.

Table 1.1: Main features of major ESS technologies for hybrid vehicles [4, 15–17].

Technology	Energy and power density		Discharge time	Efficiency (%)
	Wh/kg	W/kg		
EDLC	2.5-15	500-5000	msec-min	90-98
Lead-acid	20-50	25-300	sec - hours	70-90
Ni-Cd	30-75	50-300	sec - hours	60-80
NiMH	60-80	200-250	sec - hours	65-70
NaS	120-240	120-230	sec - hours	75-90
Li-ion	75-200	100-350	sec-hours	90-100
Li-poly	100-200	150-350	sec -hours	90 - 100
Flywheel	5-100	1000-5000	msec - min	90 - 95

Technology	Self-discharge (daily %)	Lifespan (cycles)	Av. capitalcost	
			euros/kWh	euros/kW
EDLC	20-40	$<10^6$	300-2000	200-300
Lead-acid	0.05-0.3	200-2000	50-400	300-600
Ni-Cd	0.2-0.6	1500-3000	400-2400	500-1500
NiMH	1-2	1500-3000	300-500	-
NaS	20	2000-3000	300-500	1000-3000
Li-ion	0.1-0.3	1000-10.000	500-2500	1200-4000
Li-poly	0.15	600-1500	900-1300	-
Flywheel	100	$<10^7$	1000-5000	250-350

1.2.4   Fuel cells

A fuel cell (FC) is an energy conversion device where chemical energy (hydrogen) is converted into electric energy via an electrolysis process. The by-product of an FC is heat and water. Significant advantages of a FC are eco-friendly, simplicity, continuous

power supply, durability and silent operation along with strict conformation to emission norms of vehicular systems [4]. In fact, a FC combines the best features of IC engines (they can operate as long as fuel is supplied) and batteries (they can produce electricity directly from fuel, without combustion) thereby reducing emissions and noise increases the efficiency [4].

The specific energy of FC is as good as gasoline; however, its specific power is much less; therefore the starting performances of FC vehicles are very poor. Consequently, to improve the power density as well as starting performance, BTs or SCs can be used in conjunction with the FC for vehicular application [4]. The dedicated efforts are given on infrastructure for hydrogen production, storage and refilling station which are major issues in fuel cell technology [13].

1.2.5 Hybrid energy storage systems

As explained in the previous sections, each ESS technology offer different strengths and operational characteristics for applications of mobility. An ESS including a single power source has significant limitations, and cannot meet the requirements of energy density and power density simultaneously [18]. Thus, the concept of hybrid ESS can be introduced in order to combine the characteristics of different technologies to fulfill the technical requirements of the application.

Taking into account the current developments in energy storage technologies and the maturity of some of them, there are several combinations that can be possible to integrate a hybrid system. However, the selection of the technologies involved in the ESS is intended to complement at each other. It means, combining technologies that offer energy and power characteristics with the aim of cover the whole range of traction requirements during vehicle operation. Other important criteria for technology selection can address the considerations of weight, volume and especially the implementation cost and expected lifetime of them [19, 20]. These kind of considerations are highly relevant in onboard ESS where the economic and space factors can be strong limitations for the development of more-electric vehicles.

In the last years, considering the wide development that have had the electrochemical storage solutions the most widespread hybrid ESS combine batteries and supercapacitors. In general, batteries are intended to provide energy during long time at low power rates in order to avoid the continuous charging/discharging process and prevent the power peaks during operation, respectively, which could early degrade the battery pack [21]. Both in literature [20–25] as well as practical applications [26–29] there are many different types of hybrid ESS which are formed by batteries and supercapacitors. Supercapacitors can be paralleled directly connected to the DC bus with battery connected through a DC/DC converter [30, 31], battery directly connected to the DC bus with supercapacitors connected through a DC/DC converter [32, 33] and both battery and supercapacitors

through DC/DC converters [24, 25, 34, 35].

Other kind of hybrid ESS can include FC combining with batteries [36–38] and supercapacitors [39, 40]. In this case, due to the slow dynamic response from the FC, the ESS is intended to meet the pulse power requirements and supply the energy during the FC's transients. In the literature, more advanced solutions integrating both supercapacitors and batteries as hybrid ESS and combined with FCs have been analyzed. Thus, the role of FC and the battery is to supply mean power to the load, whereas supercapacitors are used to satisfy acceleration and regenerative braking requirements. In this case, scenarios with battery directly connected to the DC bus and supercapacitors through a DC/DC converter [41–43] as well as with both (batteries and supercapcitors) connected through DC/DC converters [44, 45] have been reported.

Finally, some researches have been addressed to combine flywheel storage systems with batteries in hybrid vehicles [46–48]. In these hybrid ESS the aim of the battery is to extend autonomy range of the vehicle, operating the battery at low power rates while the advantages of fast power response and relatively long life from flywheels are used to compensate the power peaks. Similarly, some solutions include the combination of FCs and flywheels [49–51] to overcome the energy and power needs during operation, respectively.

Several simulation and experimental test results show that hybrid ESS can take advantage of each involved technology to yield with both high power density and high energy density [18]. Consequently, many current commercial and future under-research vehicle solutions are moving toward the hybrid ESS for better operating performance and energy efficiency improvement.

1.3 Hybrid Electric Vehicle: Classification

Hybrid electric vehicles can be classified from two points of view. On the one hand, it can be considered the physical architecture of the power-train. On the other hand, focusing on the degree of hybridization in the vehicle. Both kinds of classifications are detailed in the sections below.

1.3.1 Powertrain architecture

This kind of classification is defined as the way how the elements (converters, inverters, electric motor, internal combustion engine, energy storage system, auxiliary loads) are arranged and connected among them in the power-train (mechanically or electrically). Thus, three main topologies can be found:

1.3.1.1 Series configuration

Series hybrid electric vehicles (SHEVs) involve an ICE, electric generator (EG), ESS, inverter, converters and electric motor (EM) as shown in figure 1.6 [52]. The ICE in a serial power-train does not have mechanical contact with the drive wheels and all the energy produced by the ICE is converted to electric power by the EG that supplies energy to propel the vehicle and to feed the ESS. All the elements in the power-train are electrically connected to de DC bus through the power electronic devices (converters, inverters) [53]. Figure 1.6 depicts the main operating modes that are available in the series hybrid power-train. This kind of configuration is also adopted in most of the tramway vehicles where the ICE+EG is replaced by the main grid (catenary) which directly supply energy to the DC bus.
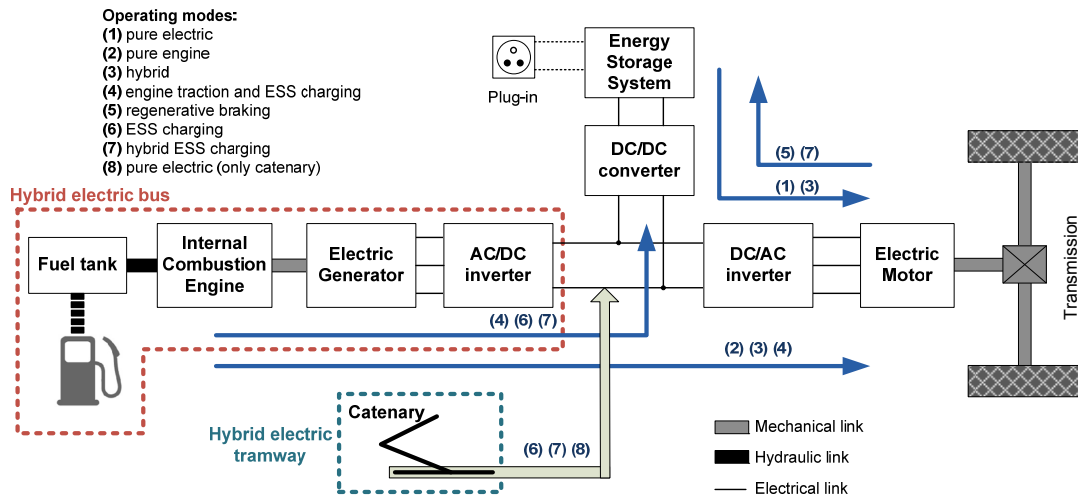
Figure 1.6: Series Hybrid configuration.

Series configuration allows regenerative braking energy recovery where this energy is stored in the ESS, leading to reduced consumption from the main energy sources (ICE or main grid) and increase the system efficiency. In ICE-based vehicles, one of the main advantages of a series configuration is that the engine and vehicle speeds are decoupled. Because of this, the engine can run at its optimum speed almost all the time and thereby reduce fuel consumption. This system is most efficient during the start/stop of city driving. In addition, the ICE+EG or catenary (in tramway case) of the SHEV can be replaced by a fuel cell and a DC-DC converter, thus converting it into a pure electric vehicle [36, 54].

The disadvantage of a SHEV is mainly related to the highway driving operation due the energy losses in the conversion process in addition to the lower torque output of the EM at high rotational speeds contributing to the overall lower efficiency of the system [54]. This makes the series configuration more adapted to urban scenarios where the most important application are heavy vehicles for massive transportation such as buses and

tramways [52]. Table 1.2 show some examples of hybrid vehicles for urban mobility with series configuration.

Table 1.2: Examples of Serial hybrid vehicles [27, 55].

Hybrid vehicle	MAN Lion's City Hybrid	SIEMENS Sitras HES
Type of Hybrid drive	Serial hybrid	Serial hybrid
Main energy source	Engine: MAN D0836 LOH CR, EEV, 6.9 litre, 191 kW/260 hp	Catenary line, 750 VDC
Energy Storage	Supercapacitors	Lithium-ion battery and Supercapacitors
Main characteristics	Up to 30 percent lower fuel consumption and CO2 emission	Energy saving up to 30 % of the supplied energy and 2500 m of catenary-less operation

1.3.1.2 Parallel configuration

In Parallel hybrid electric vehicles (PHEVs), both the mechanical power output (from ICE) and the electrical power output (from the ESS and EM) are mechanically connected in parallel to drive the transmission (see figure 1.7) [52]. Due to the parallel system, both the EM and ICE can provide power during acceleration. Therefore the ICE can be downsized compared to the one in a series power-train (and conventional diesel engines). Figure 1.7 illustrates the main operating modes in a parallel configuration.

Since both the ICE and EM can be utilized to propel the vehicle, a parallel configuration enables more power compared to a series one during most of driving conditions [53]. The advantage of a parallel configuration is that the system has the ability to offer higher efficiency during highway driving conditions. During highway driving, the vehicle speed does not vary significantly and therefore it is more efficient to drive the wheels directly from the ICE. On the other hand, the electric motor can be used solely during city driving to prevent the ICE operation in its low-efficiency zone, thus providing higher overall efficiency [54]. The main disadvantages with this topology are the complexity due to the mechanical coupling between the ICE and EM (which increase the system cost), and the need of a more sophisticated control algorithm to obtain the best performance of the whole system. Table 1.3 show some commercial solutions of hybrid buses with parallel configuration.
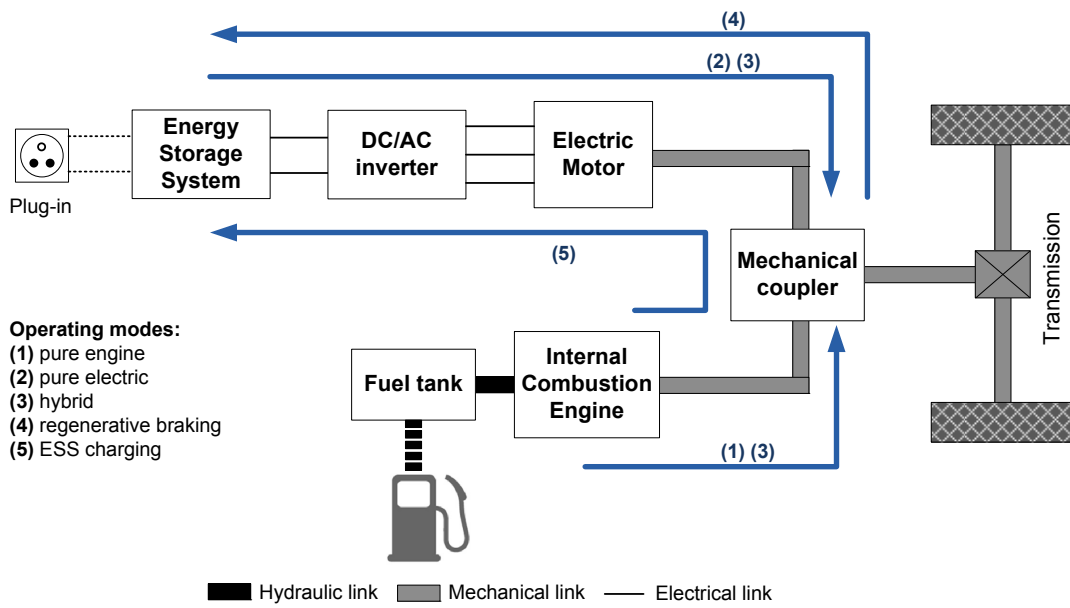
Figure 1.7: Parallel Hybrid configuration.

Table 1.3: Examples of Parallel hybrid vehicles [55].

Hybrid bus	VOLVO 7700 Hybrid	SOLARIS Urbino 18 Hybrid
Type of Hybrid drive	Integrated Starter Alternator Motor (I-SAM), Parallel hybrid	Voith DIWAhybrid, Parallel hybrid
Engine	New Volvo DSE, 505 litre capacity, rated at 210hp	Cummins ISB6.7 250H engine, 181kW (246hp), 6.7 litre capacity
Electric motor / generator	AC permanent magnet motor, power rating of 160hp and a continuous rating of 90hp	The motor provides 85kW of power continually with a maximum output of 150kW
Energy Storage	Lithium-ion battery	Ultra capacitors
Bus characteristics	Fuel savings uo to 35% Lower exhaust emissions	Average fuel savings up to 16%

1.3.1.3 Series-Parallel configuration

Combination of parallel and series configurations into a single package is quickly becoming the standard in passenger vehicle hybridization [6]. They conjugate with power

split devices (planetary gear set) and mechanical coupler the torque from ICE and EM allowing power paths from ICE to wheels and EG [52]. Figure 1.8 shows the essential of the combination architecture.

As advantage can be highlighted the possibility of multiple operating modes due to the different electrical and mechanical connections among the power-train elements. However, this kind of configuration results in a very expensive system mainly due to the several elements involved in the power-train as well as the complexity for the space packing. Furthermore this kind of architecture requires a more complex control algorithm to consider the several operating modes and energy flows to obtain the best performance and system efficiency [6]. Commercial examples of series-parallel vehicles are: Toyota Prius, Toyota Auris, Ford Escape and Nissan Tino.
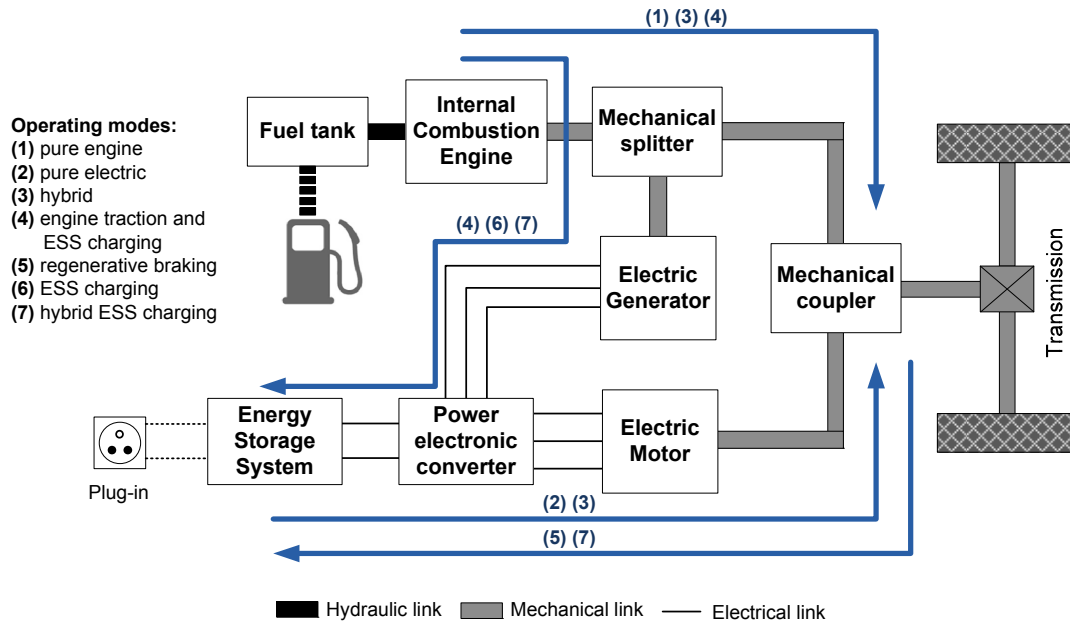
Figure 1.8: Series-Parallel Hybrid configuration.

1.3.2 Hybridization level

In HEVs the level of hybridization can be defined as the ratio between the energy coming from the ESS and the total energy demanded from the vehicle in different operation stages. In other words, the hybridization level defined how fuel-depended of electrical-depended is the vehicle. As can be seen in figure 1.9 four main categories can be highlighted [56]:

- *Micro hybrid*
A micro HEV is a vehicle with an integrated alternator/starter that uses start/stop technology which allows that the vehicle shuts down the ICE at a complete stop and then restarts when the driver releases the brake pedal. During cruising, the vehicle is propelled
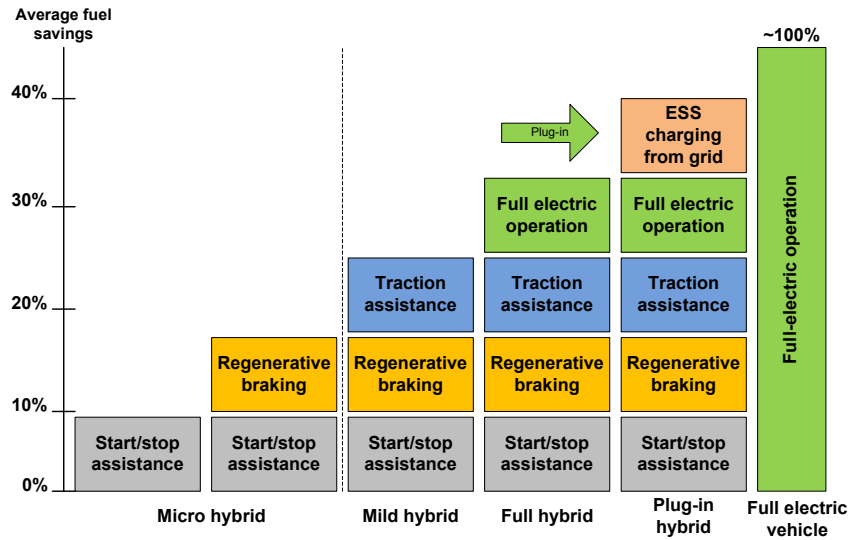
Figure 1.9: Degrees of hybridization in vehicles.

only by the ICE. In some cases, the system integrates regenerative braking facility but the amount of recovered energy is not significant due to the low ESS capacity.

- Mild hybrid

A mild HEV is similar to a micro HEV with the exception that the integrated alternator/starter is upgraded with stronger electric components that assist in vehicle propulsion. Compared to a micro HEV, the EM, alternator, and ESS are larger and play a greater role in the vehicle operation. In this kind of vehicles the recovered energy during braking phase is also larger than the one in micro hybrid systems.

- Full hybrid

The most relevant aspect of a full HEV are: full HEV typically uses a smaller ICE, it has the ability to propel the vehicle solely with the EM (powered from the ESS), and it utilizes a more sophisticated control system to optimize efficiency [56].

- Plug-in hybrid

A Plug-in HEV is essentially the same configuration as a full HEV, but it uses a more downsized ICE and even larger electrical components such as the EM, alternator, and ESS capable of charging from the electrical grid through a plug. Plug-in HEVs may run solely on electric power from the ESS and while the ICE operates, fuel efficiency is similar to a full HEV. Plug-in HEVs are ideal in urban routes where trips are short, but they are also equipped for long trips [56].

At the end of this hybridization chain can be placed the full-electric vehicles with complete independence from fuel consumption. It is worth mentioning that in full-electric vehicles the fuel savings are not completely avoided since there is an indirect upstream consumption related to vehicle and ESS manufacturing.

Figure 1.10 depicts the correlation between the two kinds of classifications for HEVs

¹ZEV: Zero Emission Vehicle
²ZEV supervisor mode: system selects operation mode
³ZEV user mode: driver selects operation mode
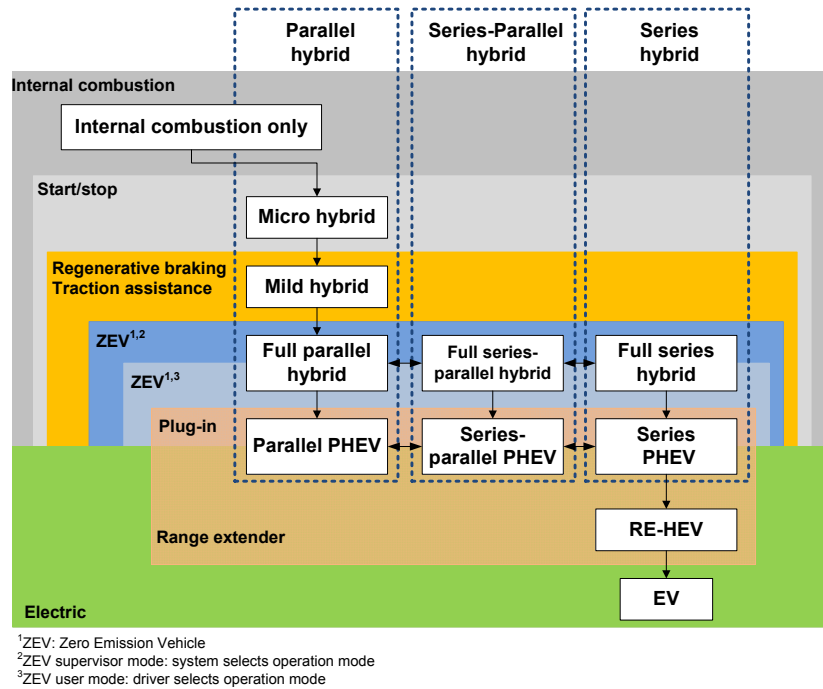
Figure 1.10: Powertrain architecture and degrees of hybridization in vehicles.

previously detailed in section 1.3.1 and section 1.3.2.

1.4 Public Mobility

Transport is currently one of the most energy-consuming and polluting sectors in both developing and developed countries [7]. In the European Union, for instance, it causes approximately 31% of total greenhouse gas (GHG) emissions. Within this sector, metropolitan transportation is responsible for about 25% of the total CO2 emissions [3]. Additionally, high levels of air pollution and congestion are major issues related to transport in urban areas. Therefore, in a worldwide context of growing urbanization, the implementation of efficient, reliable and environmentally friendly transport systems becomes imperative not only to meet the international agreements on GHG emissions reduction, but to guarantee livable conditions in urban areas [57].

Despite the impact of public mobility might be considered smaller than the individual one, the public transportation is an important candidate for ESS applications showing advantages on two main issues. As technical advantage, the public transports normally operate on fixed routes with several starts/stops phases, low speeds, they have more physical space for energy storage units and the possibility of implementing recharging points throughout the route [3, 55]. As environmental advantage, the increasing concern of the governments promotes research and implementation of more friendly environmental solutions for urban mobility, both to meet the rigorous current emission standards as well as to offer a greener image of their cities and countries [1]. Indeed, several cities are

currently focused on cleaner public transport solutions, while many vehicle manufacturers and operators are renewing their fleets or deploying low-emission power-trains [2, 3].

Focusing on public mobility, it can be mention two important case studies, urban buses and light-rail-vehicles (tramways). As shown in figure 1.11 of the total public transport journeys in Europe, buses account for a major share of 56% or an average of 32 billion travels followed by tramways (corresponding to about 14%) [29]. Although both scenarios are considered as massive transport solutions, these have to be analyzed separately to define their requirements, challenges and possible solutions.
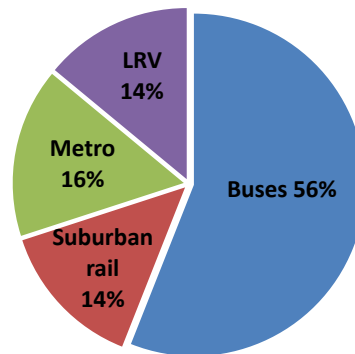
Figure 1.11: Breakdown of public transport journeys in Europe by means of transport [29].

1.4.1 Hybrid Electric Buses

For urban buses case, one of the viable policies to reduce emissions is the use of pure electric traction [3]. Full electric buses (or normally known as battery electric buses) have the advantage of not producing any pollutant emissions directly from their operation. This is especially advantageous in city centers where there is typically heavy traffic and air quality can be poor. Battery electric buses are also interesting because their energy consumption is very low when idling comparing to conventional diesel buses [5].

However, the future development of full electric buses is slowed mainly for technical factors. Full electric buses require too large, heavy and expensive ESS (mainly batteries) to achieve an acceptable degree of autonomy [3]. To find satisfactory solutions to these problems, hybrid electric buses (HEB) are shown in the medium term as the most viable alternative [58].

Hybrid electric buses are becoming more popular all around the world but, despite their technological maturity, these buses have not been able to replace the conventional diesel buses in a large scale mainly due to the ownership costs to renew the fleets [1]. However, the fuel economy of diesel buses has not significantly improved during the last decade, and the stricter emission regulations (currently Euro VI, see figure 1.12) lay out more challenges that promote the implementation of environmental friendly solutions [53]. Thus, different projects have been implemented in order to introduce in the urban mobility

the concept of HEBs [3, 53, 55].
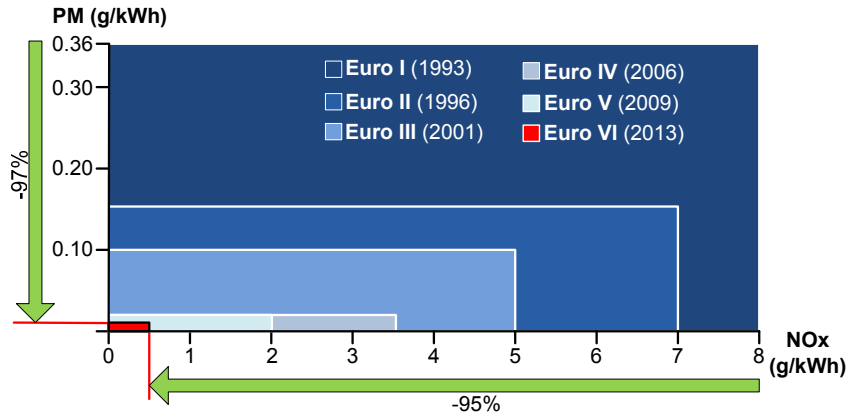
Figure 1.12: European emission standards [2].

On the other hand, and depending on the vehicle autonomy, can be considered as important factor the charging facilities installed along the route. Therefore, there are two main concepts of ESS charging available for urban buses that can be highlighted, overnight charging and opportunity charging [3, 55]. Full or hybrid electric buses today tend to be designed towards one of these characteristics; either larger battery packs with focus on overnight charging and limited or no charging during the day, or smaller battery packs that are frequently charged during the day at bus stops and/or end stations [53].

Overnight charged buses have significantly larger ESS capacity (>200 kWh) than opportunity charged buses [53]. The driving range is limited by ESS capacity on-board the vehicle and a typical driving range for overnight buses is 100-250 km. A challenge for overnight buses is the weight and price of the ESS which impacts the passenger capacity and purchase cost, respectively [53, 55].

For opportunity buses, due to the several charges of the ESS along route (normally at end or intermediate stops), the ESS capacity can be reduced. The driving range is relatively short compared to overnight charged buses with a range around 7-20 km after 2-8 minutes of opportunity charging [53]. The range can be extended with longer charging times and/or higher charging power. Opportunity charging is carried out either by inductive or conductive technologies. In this case the challenge is the charging infrastructure and the deployment of it across the city [55].

1.4.1.1 Driving phases

The vehicle operation through the route has to overcome different phases that define the power and energy requirements. These phases are normally repeated several times depending on the type of route (urban sub-urban, highway) where the vehicle is operating. Furthermore, the duration of each phase could be decreased or increased depending on the vehicle dynamics and the route's characteristics [29].

When considering a hybrid vehicle for urban mobility, the driving profile is characterized for continuous start-stop phases, followed of low speed and relatively low power stages. Taking into account the specific location of the stops, the speed limitations related to the massive transport vehicles and the average traffic conditions results easier to determine in general way the function of the power-train's elements during vehicle operation.

For HEB case when a genset (ICE+EG) and ESS are considered, the driving phases are depicted on figure 1.13. Some remarks in each phase are detailed below.
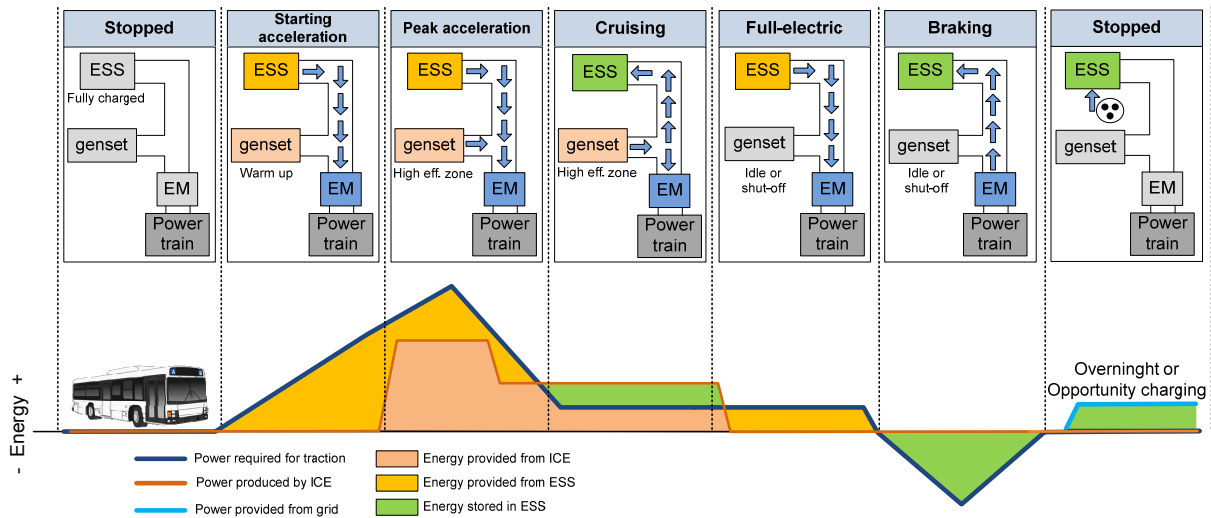
Figure 1.13: main driving phases in a HEB.

- When the vehicle is started, ICE warms up. In the initial phase, and depending on the hybridization level on the vehicle (see section 1.3.2), the ESS will provide the energy needed either to fulfill the power demand during acceleration (starting acceleration) or to start the ICE.

- During power peaks in acceleration or high power demands for traction both ICE and ESS are in charge of fully supply the energy demand. In this case, the aim of the ESS is to cover the power peaks and energy variations due to its fast dynamic response. The ICE is operated in its high efficient region (where the best performance is obtained), trying to maintain a constant power rate and avoiding the continuous changes between operating points [59, 60]. It is worth mentioning that the high efficient zone of a ICE is reached at high power rates [61].

- When the vehicle is in cruising phase and the traction demand decrease the objective is to continue operating the ICE, at a lower power rate than comparing with the peak acceleration demand, but still in a zone which offers a good efficiency. In this zone is important to denote that the ESS can be recharged from the ICE in order to increase its power rate and allowing its operation close to the nominal power (where the most efficient points are located [62]). This recharging process can be considered also with the aim of

increasing the vehicle autonomy in case of full-electric operation requirement or to reduce the ESS sizing. Other factor that have influence on this behavior is the recharging points facility. Depending on the concept considered in route, the hybrid bus could be charged in intermediate stops or at final depot.

- In case of full-electric operation requirement, the ESS must fulfill the power and energy needs for traction. During this phase the ICE could be turn-off or set at idle operation where it is not injecting power for traction but still remains switched on in order to avoid continuous on/off process. This behavior is mainly related with the duration of full-electric operation, the route characteristics (non-emissions or low-emission) as well as the the ICE' system (limitation in the number of on/off process).

- During braking phase, the regenerated energy is absorbed in the ESS. At this stage, the ICE can be maintained either in idle or turn-off for low consumption or fuel-cut, respectively.

- Finally, a recharging stage can be considered depending on the route conditions. As mention before this recharging can be defined at intermediate or end stops.

At this point, it worth mentioning that in case of a conventional bus (without ESS and only propelled by fuel), both high and low power demands are covered by the ICE. It causes low efficiencies during operating which finally lay on more pollutant emissions and increase in fuel consumption. Furthermore, the energy recovered during regeneration is lost as heat in the mechanical braking or crowbar system, this way, decreasing the energy efficiency of the vehicle.

1.4.1.2 Main Bus manufacturers

Currently, the major bus manufacturers have developed several commercial solutions of HEBs for urban applications. Thus, table 1.4 summarizes the main characteristics of commercial hybrid and electric buses.

1.4.2 Light Rail Vehicles

Light rail vehicles (LRV) have staged an impressive comeback in the last years thanks to the environmental, economic and social advantages they offer [72]. A LRV, also known as a tramway, is a rail vehicle that runs on tracks along public urban streets [9]. The tramways have been traditionally powered by electrical energy supplied by an overhead contact line (around 750 VDC) and captured by a sliding pantograph on the top of the vehicle [57]. The most common vehicles have 4–6 axes, a typical length of 13–21 m, a width of 2.3–2.8 m, a capacity of 150–250 passengers with 20%–40% of the seats, and a maximum speed of 60 km/h [73].

This kind of rail vehicles show some advantages as: low operating costs due to the low energy consumption (low rolling resistance), the absence of polluting emissions, medium-

Table 1.4: Main bus manufacturers and commercial solutions for HEBs.

Manufacturer / Bus model	Energy Storage Systems	Type of vehicle
MAN [63] Lion's City Hybrid	SCs ,Energy content: 0,5 kWh, Max. Charging/discharging power: 200 kW, Voltage: 400-750 V	
MERCEDES-BENZ [64] Citaro G Bluetec Hybrid	Lithium-ion BT, Energy content: 19,4 kWh, Max. Power output: 240 kW, Charging time: around 4 h at 5 kW	
VECTIA [65] Veris.12 Hybrid+	Lithium titanate BT, Energy content: 24 kWh, Max. Power output 210 kW, Charging time: 3-5 min at 150 kW	
VOLVO [66] 7900 Hybrid	Lithium-ion BT, Energy content: 19 kWh, Autonomy: around 10 km, Opportunity charging: 300 kW (400 A at 750 V), Recharging time: aroun 6 min at end station	Hybrid Bus (ICE + ESS)
SCANIA [67] Ethanol Hybrid Bus	SCs, Energy content: 400 Wh, 4x125 V modules, Design life: 10-15 years	
SCANIA [67] Citywide LE Hybrid	Lithium-ion BT, Energy content: 1,2 kWh	
SOLARIS [68] Urbino 18 DIWA Hybrid	SCs, Energy content: 0,5 kWh	
IVECO [69] Urbanaway bus	Lithium-ion, Nano-Phosphate BT, Energy content: 11 kWh, Max. Power/voltage output: 200 kW / 635 V	
ORION VII Hybrid Electric Bus	Lithium-ion BT, Energy content: 32 kWh, Weight 364 kg, 6 years design life	
MERCEDES-BENZ [64] Citaro Fuel Cell Hybrid Bus	Lithium-ion BT, Energy content: 26 kWh, Max. Power output: 250 kW	
VAN HOOL [55] Fuel Cell Hybrid Bus	Lithium-ion BT, Energy content: 17.4 kWh, Rated power: 76 - 125 kW	Fuel cell Bus (FC + ESS)
VAN HOOL [55] Fuel Cell Hybrid (UTC power)	NaNiCl (ZEBRA) BT, Energy content: 53 kWh	
NEW FLYER [53] Fuel cell Bus	Lithium-ion BT, Energy content: 47 kWh	
OPTARE [55] Solo EV battery Electric Bus	Lithium-ion BT, Energy content: 80 kWh	
SOLARIS [68] Urbino Electric Bus	Lithium-ion BT, Energy content: 120 kWh, Rated voltage: 600 V	
BYD [70] Battery Electric Bus eBUS-12	Lithium Iron-Phosphate BT, Energy content: 324 kWh, Autonomy: 300 km on a single charge	Battery Electric Bus (only ESS)
IRIZAR [71] i2e	Sodium Nickel BT and SCs, Energy content: 376 kWh, Autonomy: 200 - 250 km or 16 h on a single charge	

high passenger capacity, and considerably lower investment costs than those of a metro system [57]. On the other hand, these vehicles present some disadvantages due to their operation as: full overhead cables in city centers, voltage variations in the grid (by the power peaks during operation) and low energy efficiency due to the limited braking energy recovered in the catenary or lost in the crowbar (see figure1.14) [9, 72]. Efficient ways of overcoming these problems are removing the overhead cables (catenary-free zones) and implementing on-board ESS to supply energy during the travel (partially or entirely). On-board ESS in LRV can considerably contribute to the following advantages [15]:

- Shaving of peak power demanded during acceleration, which leads to reduce the power requested to the catenary.

- Limitation of voltage drops in the main grid, which might allow a higher traffic density without further modification in the existing infrastructure.

- Certain driving autonomy, in emergency situations (*e.g.* unscheduled stops), or in catenary-less zones (*e.g.* city centers) with visual impact restrictions.
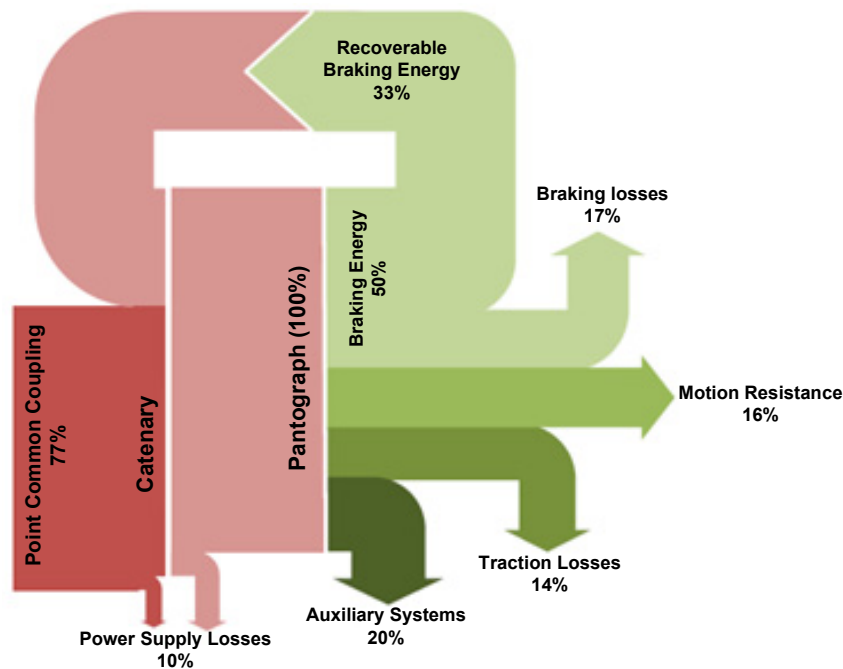
Figure 1.14: Illustrative traction energy flow diagram for urban rail systems [57].

Nevertheless, in a very competitive context where other transportation modes are considerably improving their environmental performance (in particular the automotive sector) and the energy costs are steadily increasing, it is crucial that urban rail vehicles reduce their energy use while maintaining or enhancing its service quality and capacity [57].

Therefore, the current efforts in Hybrid Electric Tramways (HETs) are focused on the operating efficiency improvement of the power-train's elements and full recovery of the regenerative energy. On the other hand, and due to the requirements for urban

infrastructure implementation, some city areas need to minimize the visual impact on their historical buildings, pedestrian sections, bridges and tunnels where the tramways running without an overhead line are shown as a feasible solution [57]. Thus, the ongoing developments also face the challenge about offering enough autonomy to fully supply the energy demand during ever longer distance and adapted for different conditions in urban areas.

1.4.2.1 Driving phases

In the scope of HETs (powered by catenary and on-board ESS) similar phases, as the ones previously explained for the hybrid bus (see section 1.4.1.1), are identified. Figure 1.13 illustrates this driving concept. However, due to the characteristics of the scenario, some operating modifications can be highlighted as follows:
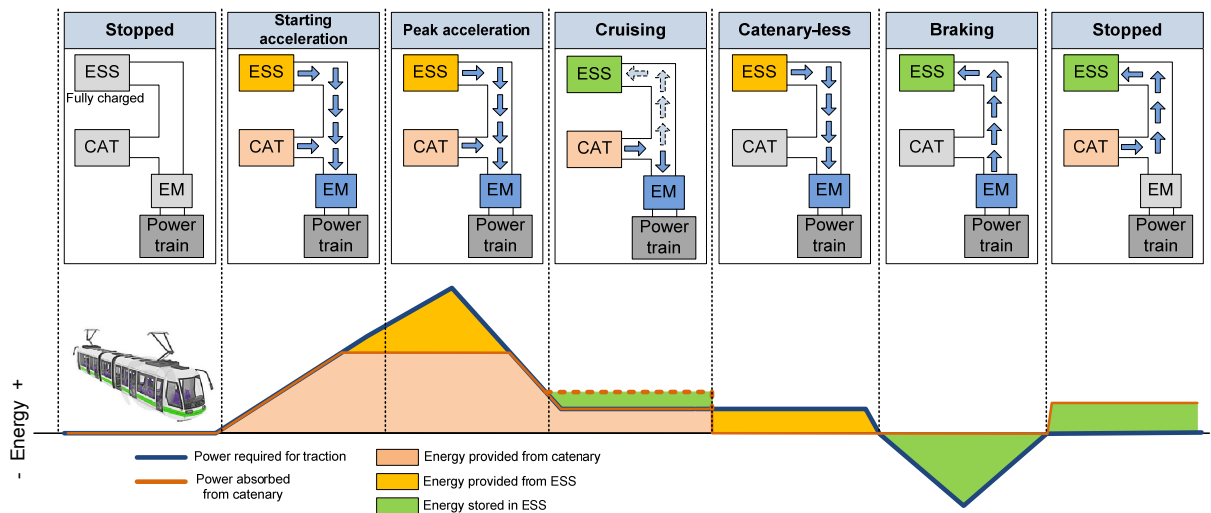
Figure 1.15: Driving phases in a hybrid electric tramway.

- During the starting acceleration and high power demand phases, the aim of the ESS is to provide the power peaks, reducing them from the catenary line.

- At cruising phase (with low power demands), the catenary is in charge of providing the energy for traction. However, in this stage can be considered the possibility of recharging the ESS from the catenary. This will be determined by the route characteristics, mainly if catenary-less operation (autonomy for longer distance) is required or if high power peaks are widespread along the route (where the ESS energy may be required).

- When catenary-free operation is required the ESS must fulfill the energy and power needs (as in the case of full-electric operation in hybrid bus). The concept of full-electric operation can be also applied in emergency situations as in case of catenary failure.

- During braking phase, the ESS is aimed to absorb the regenerated energy. This is intended for two main aspects: 1)avoid dissipating this energy as heat in crowbar or

mechanical braking and 2)avoid injecting power peaks to the main grid, which may cause voltage variations and relatively low efficiency.

- Finally, the ESS can be recharged from catenary during stops along the route.

1.4.2.2 Main tramway manufacturers

In the current market there are several urban rail applications including ESS, in this issue the major companies dedicated to the railway business have developed their own solutions. Table 1.5 summarizes the most relevant manufacturers and characteristics of the available LRVs.

1.5 Energy Management in hybrid vehicles

In this section, different approaches of energy management strategies (EMS) will be reviewed. The most relevant optimization methods or techniques that can be implemented in order to get an optimal behavior of the EMS will be reviewed as well. A control strategy is defined as an algorithm, which is a set of instructions or laws regulating the overall operation and power flow of the system. As shown in figure 1.16, the control and management of a power electronic system (PES) can be represented hierarchically [13,77].
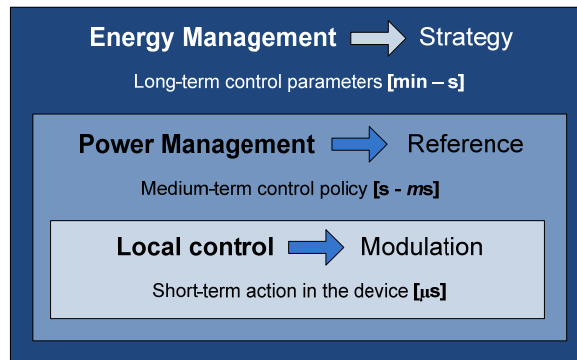
Figure 1.16: Representation of the hierarchical management and control of a power electronic system [77].

The *energy management* is in the outermost level of this hierarchy and its objective is to define the long-term behavior of the system, *i.e.*, to define the strategy. That is the reason why this management loop has the lowest dynamic (in the order of few seconds in forward). This management level sets the control parameters for the next inner level, such as operation modes, operating targets and constraints. In the HEV case, the energy management level considers the vehicle behavior with a long term view to have a wider scope of the energy that will be demanded. Thus, the aim will be to find out the proper way to manage the on-board energy for a better harnessing of it during the journey, fully ensuring the power/energy demand fulfillment.

Table 1.5: Main tramway manufacturers and commercial solutions for HETs.

Manufacturer	Energy Storage Systems	Main characteristics
BOMBARDIER [74] MITRAC Energy Saver	SCs, Energy content: 1 kWh, Max. output power: 300 kW, 2 boxes for 30 m long LRV	- Reduction of 50% in line current peak and voltage drop - Reduction of 30% in traction energy consumption - Run 500 m without catenary
SIEMENS [75] Sitras MES	SCs, Energy content: 0.85 kWh, 2x144 kW, Rated voltage: 190-480 V	- Energy saving up to 30% of the supplied energy - Stabilizing the line voltage
CAF [72, 76] ACR evoDRIVE	SCs (modular integration adapted to the scenario)	- 20% in energy savings and up to 100 m in catenary-free - Plug-in system, independent of the traction converter, enabling it to be incorporated in existing trams
ALSTOM [73] STEEM	SCs, Energy content:1.6 kWh fast charge at arrival station	- Reduce the average daily energy consumption by 13%, - Up to 300 m of autonomy in catenary-free
KAWASAKI [9] SWIMO	NiMH BT, Energy content: 120 kWh Rated power: 250 kW Rated voltage: 576 V	- Maximum speed of 40 km/h - Catenary free operation of 37.5 km
KINKI SHARYO [57] LFX-300	Lithium-ion BT	- Around 8 km with BT operation - Absorb regenerative braking energy - ESS mainly recharged during stops
ALSTOM [73] Citadis	NiMH BT, Energy content: 80 kWh, Rated voltage: 576 V	- 11 km of catenary-free operation - Up to 25% reduction in energy consumption - Maximun speed of 70 km/h
SIEMENS [26, 75] Sitras HES	NiMH BT, Energy content: 18 kWh SCs, Energy content: 2x0.425 kWh Rated power: 85 kW (BT), 2x144 (SC) Rated voltage: 528 V (BT), 190-480 V (SC)	- Catenary free operation of 2.5 km Battery supplies: - Catenary free operation - Pantograph failure - Fault in substation or maintenance
CAF [76] ACR freeDRIVE	Lithium-ion BT and SCs (modular integration adapted to the scenario)	- More than 1400 m of catenary-free operation - 30% energy savings - Ultra-fast charging (20 seconds) - Compatible both new installations or on already existing infrastructures

Then in the middle, it is the *power management level* and its objective is to define the medium-term evolution of the system. In this case, this control loops has a faster dynamic compared to the previous one, the order of few milliseconds up to seconds. This level sets the power references to the next lower level, such as power targets for power sources and ESS in HEV, in order to apply the defined EMS [77].

Finally, the *local control* is the innermost level of this hierarchy and its objective is to directly manipulate the interface of the power electronic devices. These control loops are the fastest ones, in the order of microseconds. This level implements the control loops from the power reference to the modulation of the power electronic devices by controlling the electrical variables of the system (voltage, current) [77].

Therefore, it is clear that the selected EMS plays a key factor to ensure the correct system performance, fulfilling the application requirements and operations constraints cause the other levels are highly dependent of it. Furthermore, the EMS will allow a deeper analysis to evaluate not only technical factors for the correct vehicle operation but also economic issues that are important during the vehicle design. This way, the techno-economic analysis can be carried out to improve the EMS with long term scope and, consequently, to obtain a more efficient operation in short term and instantaneous stages.

In the transportation scope, several strategies have been proposed to manage the energy in hybrid and electric vehicles. These EMSs can be divided into the two main topics as shown in figure 1.17: Rule Based methods and Optimization Based methods [4, 13, 52], both are detailed in the next sections.
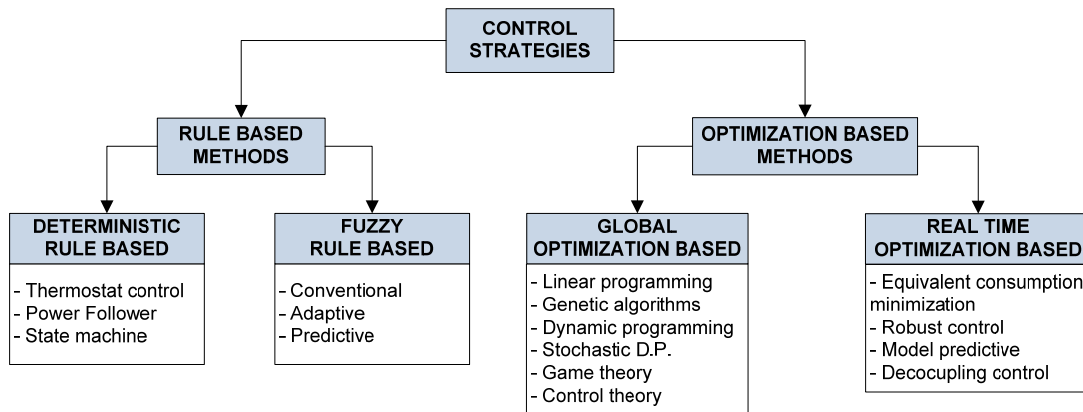
Figure 1.17: Energy management approaches for HEV [13].

1.5.1 Rule-based methods

The main aspect involved in rule-based energy management strategies (RB-EMS) is their effectiveness in real time supervisory control of power flow in a hybrid power-train [24, 78]. The rules are designed based on heuristics, intuition, human expertise

and even mathematical models and generally, without a priori knowledge of a predefined driving cycle.

The main idea of rule based strategies is commonly based on the concept of load-leveling. The idea behind load-leveling is to move the actual operating point as close as possible to some predetermined value for every time instant during vehicle operation [6]. For example, if the best efficiency is needed, all the elements (or at least the most relevant) in the power-train will be forced close the vicinity of their best operating region [52]. If other objective were determined such us low energy consumption (*e.g.* fuel consumption) or specific operation profile for some element (*e.g.* reducing power peaks from BTs) the rules will be addresses to fulfill these requirements. Rule-based methods can be classified into deterministic and fuzzy rule-based methods [13].

1.5.1.1 Deterministic rule-based methods

These kind of methods are based on the human experiences and knowledge on the application to design deterministic rules (generally implemented via lookup tables) to split the energy demand among the elements in the power-train (see figure 1.18). The most common deterministic rule based methods are: Thermostat (on/off) Strategy, Power Follower (Baseline) Control Strategy, Modified Power Follower (Baseline) Strategy and State Machine Based Strategy [52].
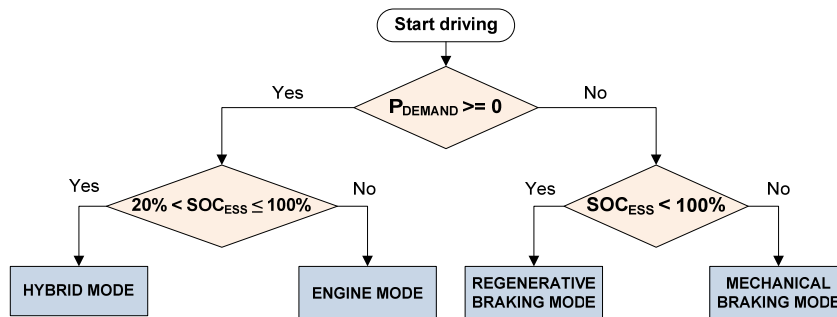
Figure 1.18: Example of deterministic rule based strategy for operating mode selection in a hybrid vehicle.

These energy management strategies require a low computational cost, and in consequence, they are suitable for an on-line implementation. They can also be developed and implemented relatively fast. In contrast, they require a wide knowledge of the application to determine the operating conditions and adequate manner to control the system. Besides, they are highly appropriate for a large number of control parameters due to the set of conditions can be increased hugely considering all possible combinations. However, concerning to the robustness, these strategies are subject to the model of the application and in the case of system's modifications the EMS could not work correctly. Moreover the self learning ability is totally dismissed [77].

In [44], an EMS for a real tramway, in Zaragoza (Spain) was presented. In this scenario the current propulsion system is replaced by a hybrid system based on FC as primary energy source and BTs and SCs as secondary energy sources. The authors analyze the dynamic response of the FC to apply the ESS to harness the regenerative energy generated during braking and decelerations. The proposed EMS is based on: 1) an operation mode control, which generates the FC reference power, 2) and cascade controls, which define the BT and SC reference power in order to achieve a proper control of the DC bus voltage and state-of-charge of BT and SC. The proposed approach (FC and hybrid ESS) allows the autonomous tramway operation without connecting to the electrical grid with good performed and efficient results. However, the operating target for the EMS remain fixed during the whole operation, which could limit the possibility of finding the optimal operation for the vehicle. Besides, any discussion about the sizing of the ESS or influence of its operation on the BT and SC lifetime is carried out, which could cause an early ESS degradation if a non-suitable operation is defined.

In [79], three different operating modes for a plug-in HEB are proposed: 1) pure electric driving (PED), 2) hybrid driving charge depleting (HDCD) and hybrid driving charge sustaining (HDCS) which operate depending on energy and power control thresholds. Different EMSs are developed based on the combination of the aforementioned operating modes and several simulation tests are carried out to determine the best performed one based on a fuel economy analysis. The authors propose the implementation of this RB approach, instead of using complex algorithms, due to the resulting heavy computational burden that these last need. Similarly to [44], the BT sizing approach is not addressed and the predefined energy and power thresholds are limited to the designer expertise, which can not be optimal for the vehicle behavior under different or non-considered conditions. Furthermore, the EMS fulfills to the instantaneous vehicle power demand without considering the future energy requirements for a better harnessing of the on-board ESS.

1.5.1.2 Fuzzy based methods

Looking into a hybrid power-train as a multi-domain, nonlinear and time varying plant, fuzzy logic seems to be the most logical approach to the problem [52, 80]. In fact, instead of using deterministic rules, the decision making of fuzzy logic can be adopted to realize a real time and suboptimal power split based on reasoning and human language for interpreting the system operation. In other words, the fuzzy logic controller is an extension of the conventional rule-based controller with the improvement of being able to deal with more complex problems and system's models avoiding the mathematical stiffness and representing the desired system's behavior in a more practical and user-language oriented way (linguistic terms) [80, 81].

These energy management strategies can be executed on-line and require a low computational cost to carry out the three steps of this algorithm (see figure 1.19). These three steps can be summarized as follows [77, 80]:

- First the subjective information is extracted in the fuzzification process from measurable variables.

- Then, this subjective information is compared to heuristic rules implemented with IF-CONDITION-THEN sentences.

- Finally, the defuzzification process is carried out, setting the control parameters from the obtained result in the heuristic rules.

These algorithms are appropriate for applications where the model is complex to obtain, or plainly, the system cannot be modeled. In contrast, it is required a wide knowledge of the application to defined the fuzzy sets and membership functions' thresholds as well as to set heuristic rules due to the decisions are adopted taking into account subjective information. Besides, this strategy is able to manage several control parameters but the heuristic rules are increased exponentially. Main advantage of the fuzzy algorithm is its robustness and tolerance to disturbances, because its response depends on the evaluation of several rules (if the system changes the strategy still controls it). Finally these algorithms are highly intuitive and have optionally the self learning ability if are combined with Neural Networks (NN) or other mathematical techniques for learning [77].
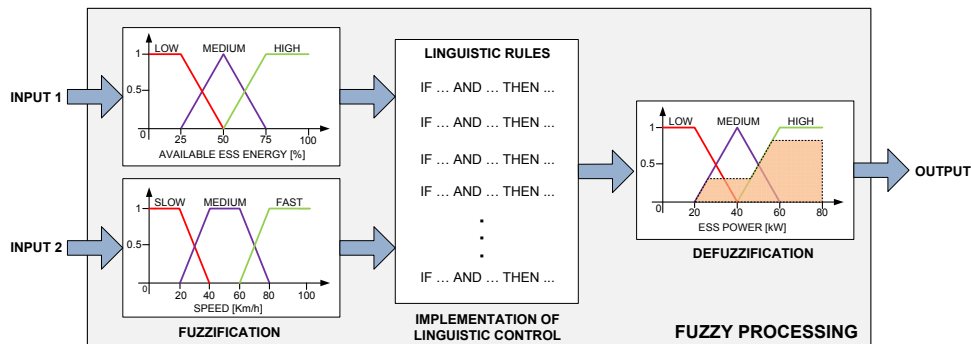
Figure 1.19: Example of fuzzy based strategy for battery power control in a hybrid vehicle.

Fuzzy rule based methods can be classified as: Conventional Fuzzy Strategies [43, 82, 83], Fuzzy Adaptive Strategies [25, 35, 37, 84, 85] and Fuzzy Predictive Strategies [86–88].

The *conventional fuzzy* strategies have been extensively used in HEVs where the energy storage system is composed by different technologies (ICE, FC, SCs, BTs) and the application requirements and suitable system operation that, from an electrical point of view, are difficult to define exactly. In these cases the objective of the EMS is to define the control parameters according to the operation modes, State-of-Charge (SOC) of the ESS and trying to achieve the maximum efficiency and performance of whole system [77].

For instance in [43], in order to enhance the fuel economy in a hybrid vehicle, a fuzzy logic control (FLC) was proposed to design the EMS for a FC/BT and FC/BT/SC hybrid vehicle. The authors used ADVISOR to develop the vehicle model based on a backward-/forward approach. The FC/BT fuzzy-based EMS considered as inputs the SOC of BT and

vehicle power demand to determine the required power for the FC system. In FC/BT/SC approach the fuzzy-based EMS considered, additionally, the SOC of the SC. In both cases, three driving modes were defined: Starting, FC individual, FC/BT, FC/BT/SC modes. Simulation tests were carried out under four driving cycles and compared with a deterministic power follower strategy. The results show that the FLC with hybrid ESS (BT+SC) had the lowest fuel consumption and better performance than comparing with single ESS (only BT) and power follower approach. Despite the power split strategy for a hybrid ESS is addressed in this work and the FLC shows an improvement over the deterministic approach, the ESS sizing and lifespan analysis is disregarded. Moreover, the fuzzy sets are defined by predefined parameters and, despite the fact that FLC offers a non-linear and variable output, the non-optimal definition of these membership functions ranges addresses the FLC output to a non-feasible values limited to the programmer's knowledge on the application.

Another interesting analysis is carried out in [82], where BT, SC and FC were combined in a HEV. The FLC was developed using the human expertise. To do so, a survey was conducted among experts in HEVs using linguistic labels. As each expert has defined different fuzzy sets and rules, the authors use a type-2 fuzzy sets, that permit to combine the knowledge from the experts handling the uncertainly associated with the meaning of the words. The strategy considers the vehicle speed to find a dynamic reference for the BT-SC ESS. However, the good performed solution is based in the expert's knowledge which could limit its utilization on a different scenario or system with unknown characteristics. However, by applying optimization techniques, the performance for different scenarios and operating constraints could be improved avoiding the need of depth application's knowledge and even allowing to evaluate multiple cases that otherwise would be disregarded by the human interpretation.

In the case of *Fuzzy adaptive* strategies, these are based on weight the fuzzy-sets' parameters. This weight defines the relative importance of the parameter (or variable) in order to modify the output value close to a desired range which improve the behavior of a specific variable in the system. Therefore, this weight has to be related to some input variable(s) allowing changing its value depending on the defined external/internal system's conditions. Some authors derive fuzzy adaptive controller on the basis of the driving environment awareness. This control technique uses driving environment information (expert knowledge that consist of roadway type, driving situation and energy flow in the drive train) to determine the effective distribution energy during operation [13, 35, 85].

Thus, in [85], an intelligent control strategy optimized by Genetic Algorithms (GA) was proposed for a PHEV. In this work only a BT-based ESS was considered, where the SOC is one of the inputs to the fuzzy control. Other considered input is the ratio between the motor target torque and the total demand torque. The aim of the FLC is to find the torque distribution coefficient between the ICE and the EM. In the fuzzy sets, the division of the membership function were defined as optimization variables. Thus

the most performed range to obtain the best system results can be defined. In fact, the optimization results showed that the proposed adaptive fuzzy strategy can maintain a smoothed charging/discharging BT process. Furthermore, the fuzzy strategy allows EM and ICE operation around their high efficiency zone (avoiding power peaks during operation) together with reduction in fuel consumption. The limitation of this study comes from the lack of ESS sizing analysis and, more important, the long term evaluation of the BT operation on its lifespan. This mainly because the fuel consumption reduction from the engine could address to an increase in the power demanded to the BT, which may early degrade the ESS.

Another case of adaptive fuzzy logic EMS is the one presented in [25]. Here the authors propose a fuzzy-based EMS to determine the power split between BT and SC pack in an electric vehicle. For designing the EMS three underlying principles were followed: 1) the power demand of the driving cycle should be satisfied consistently, 2) BT lifetime, efficiency and state-of-health (SOH) are largely dependent current dynamics and 3) the energy demand should be supplied only by BT, and SC should be used as energy buffer. As in [85], the distribution of the membership functions in the fuzzy set are off-line optimized and on-line adapted based on an iterative procedure and pattern recognition, respectively. Hardware-in-the-loop (HIL) simulation results showed that the proposed FLC leads to better comprehensive control performances that similar EMSs while it does not need the driving cycle information in advance. In this work the EMS was improved by optimization and some BT's operating constraints were considered for lifetime extension. However, still there is the lack of a proper BT and SC sizing methodology (in this work determined only by average energy required for system operation) that considers technical but also economic issues for an optimal performance with minimum operating costs for the end-client. It is worth mentioning that the concept of BT health care was introduced but any degradation model was applied to evaluate that the BT behavior guarantee the optimal lifespan (in short and long term view), instead of that, only general current limitations were defined.

Finally, *Fuzzy predictive* strategies are based on the driving history to decide the future state through a look-ahead window along a planned route. The drawback is that it is unable to perform real-time control task for example along a planned route; since the system unknows the obstacles (heavy traffic, steep grade, downhill, etc.) that will be faced in near future [13]. However, this kind of methods can be combined with optimization techniques and additional information coming from global positioning system (GPS) to improve the prediction of the demand in future stages of the travel [89].

For instance in [59], a predictive optimized EMS based on FLC and considering traffic condition was developed for a HEV which includes an ICE and BT ESS. The objective was to minimize fuel consumption and emissions. For this purpose, initially traffic condition is predicted by utilizing driving cycle classification based on its specifications. Then, the EMS is developed for various driving conditions where their membership function

parameters and rules are tuned by applying GA. In the next step, by recognition and prediction of upcoming traffic condition, control strategy is switched between optimized FLCs to enhance the optimal power split between energy sources and manage the ICE to work in the vicinity of its optimal condition.

In [90], authors present a novel predictive EMS for plug-in SHEV incorporating an on-line correction algorithm. A dynamic cost function is used to describe the energy consumption as the optimization objective, and a Dynamic-neighborhood particle swarm optimization (DPSO) algorithm is applied to optimize the power allocation during each 50 s interval based on the driving cycle prediction. The situation of imprecise prediction is considered in this study, and an on-line correction FLC is proposed to decrease the sensitivity to the prediction accuracy influenced by the BT SOC. Simulation results indicated that the DPSO-based predictive EMS could considerably reduce the fuel consumption compared with a common Charge-depleting/Charge-sustaining (CD-CS) EMS if the prediction of future driving cycle is precise. On the other hand, even for situation of imprecise predictions, the proposed predictive EMS could lessen the error deviation.

In both aforementioned works the use of predictive FLC, taking into account past, current and future driving information, could increase the fuel efficiency and improve the vehicle performance. Furthermore, the use of FLCs allows the implementation of more complex management strategies by minimizing the design and solving time effort. The approach is reinforced when optimization techniques are applied both to improve predictions and optimal power split purposes. However, still there is the lack of a methodology to address the development of the EMS based on a long term analysis where the sizing and ageing of the ESS as well as the cost-optimization approaches are taken into account in order to tune the FLC for better harnessing of the instantaneous and future energy demand while ensuring a minimum operating cost during the whole lifetime of the vehicle.

1.5.2 Optimization-based methods

These methods are based on the minimization/maximization of a cost function in order to obtain the best performance and efficiency of the power-train while minimizing the losses [52]. If this optimization is performed over a fixed driving cycle, a global optimum solution can be found [91]. In fact, the global optimal solution finds the minimum fuel (or energy) consumption using knowledge of future and past power demands [13, 52]. The optimization-based methods are composed of three elements, being these the followings [77]:

-*Objective or cost function:* It is a measure element and its aim is to be able to quantify the results, *i.e.*, to get a value from the system's behavior, according to the values of the function's variables. Then, the family of possible solutions are compared between themselves, trying to minimize or maximize this cost function in order to define the solution for the optimization problem.

- *Variables:* They are the elements of the system which can be modified by the optimization process in order to obtain a family of potential solutions.

- *Constraints*: They are the restrictions or bounds of these system's variables. The limits are represented as inequations or equations, delimiting operating regions.

Based on the fully knowledge of the driving profile or the forecasting of it, the optimization-based methods can be classified as follows:

1.5.2.1 Global optimization methods

Global optimization is based on knowledge of future and past power demands to minimize a cost function and obtain the optimal component operation at each instant over a fixed driving cycle. The drawback of such approach is that it cannot be used directly for real-time power management mainly because the need of the fully knowledge of the driving cycle as well as the time for solving the problem. However, it can be used as a basis for designing rules for on-line implementation [20] or comparison for evaluating other control strategies [13]. Global optimization control strategies can be divided into Linear programming, Control theory approach, Dynamic programming (DP), Stochastic DP, Game theory and Genetic algorithm [52].

Dynamic programming is a cost function based on Bellman's principle of optimization described by recursive equations and prior knowledge of future driving condition [13, 92]. The principle is to brake the sequential problem into subproblems, and then, each subproblem is solved with a backward approach (see figure 1.20). The aim is to reduce the problem complexity because each subproblem is solved once, and the global solution, it is the union of subproblem solutions [33, 93, 94]. In contrast, the memory requirement and computational cost are increased. DP can handle complicated rules, but calculation is time intensive. For this reason, in order to reduce the solving time, the system's model have to be reduced avoiding modeling complex and detailed structures [91].

In the case of stochastic systems, the Dynamic Programming can also be implemented. These problems are known as Stochastic Dynamic Programming (SDP) [92]. It is solved similar to Deterministic Dynamic Programming, incorporating the statistical description of the system or introducing a Markov decision process of the application. SDP is also a cost function, based on optimal algorithm.

For instance in [94], the authors presented a global optimal EMS for a plug-in HEB with parallel configuration. Here the torque and speed of the ICE and EM were selected as control variables and BT SOC was defined as state variable. DP was applied to find all possible control variables at every sample state in detail. Due to the high computational effort, the appropriate SOC increment for one single cycle was determined and then applied for complete driving distance. However, the main drawback is that the problem is addressed to minimize fuel consumption and the BT sizing and lifespan problem is not included. Other disadvantage could be that, in order to minimize the heavy computational
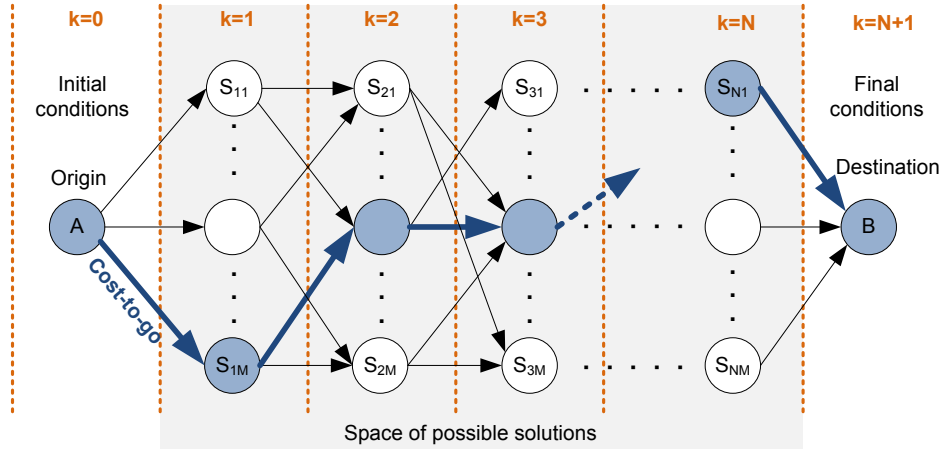
Figure 1.20: Example of possible state space and cost-to-go for global optimization process.

burden, the system's model has to be simplified which may limit either the analysis of more complex characteristics (such as ESS sizing and degradation) as well as to carried out long term analysis.

When the optimization problem is strongly complex and nonlinear, the best option is to use GA [13]. They belong to the evolutionary algorithms (stochastic methods of optimization), solving the problem inspired by natural evolution [23, 54, 84, 95]. Genetic Algorithms are capable to find as much the optimal solution, or a very good approximation for different problems. These techniques require a high computational cost, however compared with DP, it can be considered that this solving time is shorter [77]. Other important advantage of optimization methods based on evolutionary algorithms is the ability of obtaining a solution at any instant of the optimization process (*e.g.* at any generation during GA optimization) because they do not need the fully backward computation of the states variables as in case of DP. Nevertheless, the proximity to the optimal solutions will be determined based on how much have evolved the population at the breakdown instant.

In [95], a HET system with a SC-based ESS was presented. Here the design of the EMS is seen as a multi-objective optimization problem where the objectives are "minimize line peak power"and "minimize energy consumption". The EMS controls the SC SOC to be able of supplying the peaks during acceleration and fully absorb the energy during braking phase. An analysis about the correct selection of the proper solution from the set of alternative optimal solutions is carried out taking into account the priority of the objectives defined in the fitness function. Furthermore, a prior SC sizing is done but it is also considered as optimization parameter. Besides, the authors define that the optimization process is based on a prior knowledge of the driving cycle and the instantaneous power demand of the vehicle. However, they state that a controller with future forecasting of energy consumption, to react on parameter variations and deviations

from the driving cycle, could improve the system performance. Furthermore, the fitness function only considers the fulfillment of power and energy demand, it does not include economic term which allows the analysis of the system operating cost and the influence of the EMS on it.

Related to the topic of HEB, in [23] a simultaneous sizing optimization of a BT-SC ESS was presented. In this case, a multi-objective optimization based on GA was applied, where the objectives were the cost of the hybrid ESS and the capacity loss of a LiFePO4 BT. Here the problem of selecting the optimal number of BT and SC cells in series and parallel was analyzed. Furthermore, a degradation semi-empirical model was applied integrating both experimental as well as mathematical approximations to determine loss of capacity in the BT cell depending on the Ampere-hour cycled during operation. The optimal Pareto front allows selecting the best performed solution depending on the priority of a specific objective. During sizing analysis, authors considered only the influence of the SC sizing during the optimization while the number of BT cells allows a limited number of combinations. Despite the fact that using a more accurate degradation model could increase the effectiveness in the lifetime estimation, these kind of models require several experimental tests and mathematical modeling which increase both costs and time on developing the aforementioned model. Besides, another drawback that could be identified is the lack of analysis on the EMS which may allow both a better definition of the operation targets to fulfill the cost and lifespan requirements as well as the improvement of the EMS itself, in order to have a better harnessing of the instantaneous and estimated future energy (which is disregarded).

1.5.2.2 Real-time optimization methods

Real-time techniques are based on the system's variables and current data which are instantaneously optimized applying a cost function [13, 32]. The problem solutions are considered as sub-optimal due the fact that the complete driving cycle is unknown in advance. However, considering the stochastic driving trend in most of the individual vehicle in real applications, the use of real-time optimization techniques may improve the system efficiency and a well performed operation may be obtained. During cost function development, in addition to past and current energy consumption measurements, variation of the system variables are taken into account to guarantee electrical self sustainability where future information forecast can be included (see figure 1.21) [52]. Compared with global optimization method the real-time ones required much less computational effort, however their effectiveness is mainly related to the accuracy in the variables' forecasting or techniques to estimate the future states of them.

In the literature, different optimization approaches for real-time applications have been applied such as: Equivalent Consumption Minimization (ECMS) [96], Pontryagin's Minimum Principle (PMP) [22], Simulated Anneling (SA) [24], Model Predictive Control (MPC) [97], Particle Swarm optimization (PSO) [98] and evolutionary algorithm-based

optimization [99].
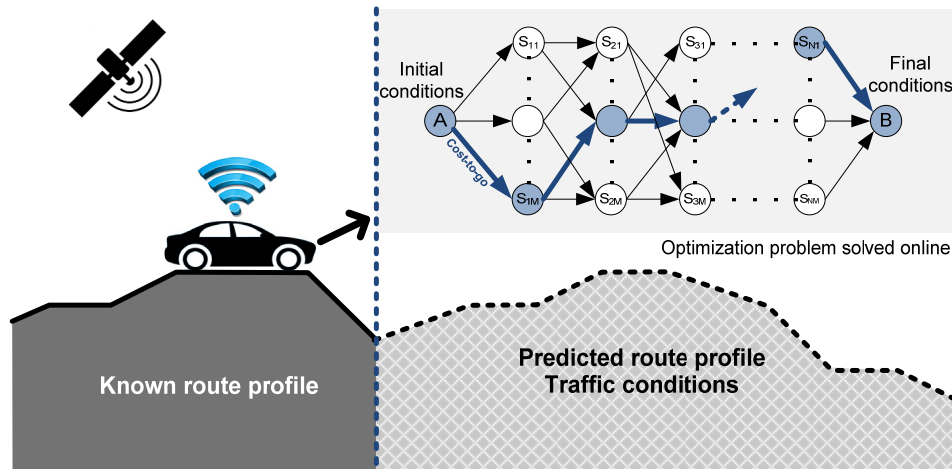
Figure 1.21: Example of look-ahead window for real time optimization.

In [96], an updating method for the equivalent factor in ECMS was presented to prolong the lifetime of BT in a FC HEV. The authors proposed a comparison between using a constant or adaptive weighting factor to track the desired SOC trajectory with the small variation in order to prevent the rapid decrease of the BT capacity. In this case, a loss of lifetime of the BT is determined by the well known Rainflow-counting method to count the cycles in different DODs. The proposed approach firstly calculates the constant equivalent factor for the Hamiltonian function off-line considering three different driving cycles. After that, during on-line operation, an instantaneous minimization problem is defined to compare the predicted and desired BT operation trend in order to maintain or determine the equivalent factor variation which will reduce the low and high DODs in the BT. However, the problem of the proper sizing for the BT pack and an economic long term evaluation for the whole vehicle operation (considering the other elements involved in the power-train) are not detailed in the analysis or included neither in the off-line and on-line minimization function.

In [97], a MPC approach for the energy management of a FC-BT-SC based tramway was presented. This work analyzes the hybrid power-train, by including the FC and BT, as possible solution for the catenary-less zones in an urban route. The proposed predictive controller generates the fuel cell and BT power references, while the SC deals with the power peaks during acceleration and braking. The objective of the controller is to hold the system's output at the reference value by adjusting the control variables. In this case, the MPC uses past and current information recorded from the application to estimate the future states over a finite horizon. Then, in order to make an intelligent sequences of moves the setpoints, measured disturbances, and constraints are evaluated and optimized to find out the best trajectory in the predictive horizon. Despite the fact that several constraints were defined in order to keep the BT operation in a safe range to prolong its

lifetime, additional implications of the BT operation on its lifespan were not analyzed in detail. Furthermore, the setpoints for the output variables are defined empirically, where the long term evaluation is disregarded and, therefore, they do not respond to optimal values that may guarantee a more efficient and economically feasible solutions.

1.6 Conclusions

The aim of the presented State-of-art has been to summarize the background knowledge in the topic of HEVs. Thus, the conclusions are intended to determine the challenges in the field of urban transportation as well as to highlight the main lacks and possible improvements over the current researches on the topic of sizing and efficient operation of on-board hybrid ESS, which will serve as basis for the developments proposed in this PhD thesis.

Regarding the first section, the current and future trend for vehicles development is focused on the electrification of their main energy source including ESS in order to minimize or even avoid the consumption from fossil fuels. The electrochemical storage solutions such as BTs and SCs have shown the most feasible energy and power characteristics, respectively. Mainly in BTs due to the electrical, economic and lifespan issues, lithium-ion technology is shown as the most promising one for mobility applications. However, the implementation of a single ESS is aimed to fulfill only one kind of need during operation, it means energy or power with BTs and SCs, respectively. Furthermore, considering the limited BTs lifespan (charging/discharging cycles) and their sensitivity to high currents and to demanding regimes (which may cause an accelerated cell degradation), the operation of BT-based ESS in applications with high power peaks is not recommended. Therefore, this PhD thesis has been addressed toward the study of hybrid ESS (BTs + SCs) for public urban vehicles which present both high power and energy requirements and the need of solutions with a high degree of electrification are currently greatly demanded.

Analyzing the second section, currently in the market there are several kinds of vehicles with different power-train's topologies and degrees of hybridization. On the one hand, series topology offers a better performance for urban routes and heavy vehicles. On the other hand, the parallel and series-parallel topologies seem to be better adapted to combined urban-interurban-highway scenarios and focused on light vehicles. Considering the HEB and HET as case studies for urban scenarios and that the vehicles' configuration are based on commercial solutions, the series topology has been determined as the basis for the study in this PhD thesis.

Regarding the topic of public transportation, many cities and governments have started a fleet renewal betting for more electrical solutions with reduced or even zero-emission features. However, the investment and operating costs of a HEV are still high comparing with conventional fuel-based one. The economic aspect becomes more important for on-board ESS where the unsuitable operation (mainly in BTs) may early-degrade the

system, this way, increasing the cost due to the pack replacements during the lifetime of the vehicle. Therefore, on the suitable sizing and operation of the vehicle will depend the improvements in energy savings and efficiency during operation as well as the competitive cost both for manufacturers and end-clients.

Analyzing the fourth section, the importance of the energy management was highlighted as supervisory level which determines the system's behavior with a long-term view and defines the instantaneous operation for the downstream control levels. In the literature, several approaches for energy management in HEVs were analyzed. On the one hand, the adaptive fuzzy-based methods are shown as the most feasible option to improve the simple rule-based approach and still keep the simplicity and fast response for on-line operation. This adaptive fuzzy-based EMS allows to obtain a nonlinear response to modify the system's behavior depending on the instantaneous/future route information and system's conditions as well as to take advantage of fuzzy approach to deal with complex control problems for systems with multiple energy sources and input conditions translating it into linguistics labels which make easier the interpretation of the desired operation. However, these strategies still need a depth application's knowledge from the programmer to design the rules and fuzzy sets. On the other hand, the optimization-based methods allow finding either global or on-line sub-optimal solutions for the vehicle operation. Nevertheless, the global optimization methods (such us DP) increase the computational effort during implementation and processing requiring sometimes the simplification of the system's model due to the complexity in the optimization problem formulation and solving time. To counteract this issue optimization methods based on the evolutionary theory (such us GA) can be applied to obtain sub-optimal but still well performed solutions while maintaining most of the complexity in the system's model.

Taking into account the scope of urban transportation, where the daily route is known in advance, the development of the novel energy management proposed in this PhD thesis will be addressed toward the adaptive fuzzy-based strategies combined with optimization methods based on evolutionary theory (GA) as main contribution of this PhD thesis. This way, the EMS will guarantee both an improved system's behavior taking into account the current and future energy/power demand conditions as well as the operation of the energy sources (hybrid ESS, ICE, catenary) toward their optimal values in order to meet the defined techno-economic objectives.

As defined in the previous paragraphs, the improvement on energy management in a HEV requires a more intelligent EMS but there are other factors that have to be taken into account such as the sizing, implementation and operating costs and ageing of the HESS. Thus, the main problem found out in the current literature is the lack of a methodology for the proper sizing and operation of the HEV based on the long-term assessment of the aforementioned factors and applied on the EMS to obtain efficiency and economic improvements. Therefore, additionally to the development of an adaptive EMS, a methodology for the proper sizing and operation of the HESS taking into account the

technical, economic and ESS degradation factors will be proposed as contribution of this PhD thesis.

2

System modeling and optimization methodology definition

2.1 System modeling and optimization methodology definition

This second chapter is intended to detail the scenario's modeling. As it has been identified in the previous chapter, the EMS strategy is the key factor for the energy efficiency improvement in HEVs. Therefore, the optimal vehicle operation is related both with technical but also economic factors that ensure the proper vehicle performance as well as the desired energy/fuel/cost saving for a minimum operating cost.

Thus, in the first part, the electrical models of the power-train's components are presented. Taking into account that in this thesis two case studies have been selected, the models will be presented in a generic way and will be particularized for the HEB and HET scenarios in the chapter 3 and chapter 4 respectively.

In the second part, the economic model applied for determining the vehicle operating cost is described. Here the cost functions are focused on the operation of the main energy sources on-board the vehicle: Hybrid ESS, genset (HEB) and catenary (HET). It is worth to mention that in case of the HESS, both initial investment, operation and replacement costs for BT and SC pack will be considered.

In the third part, the ESS ageing (mainly focused on BTs) during operation will be addressed. Thus, the main ageing factors will be highlighted and two different models for lifetime estimation will be presented: 1) a model based on Whöler curves and Rain-flow Counting method and 2) a semi-empirical model based on both mathematical and experimental tests carried out on a BT cell.

Finally, the multi-objective formulation of the problem will be introduced and the optimization methodology will be presented. This methodology, which constitutes one of the contributions of this PhD thesis, gather both the techno-economic models as well as the ESS degradation approach to determine the optimal sizing of a HESS and operation in a HEV.

2.2 Electrical model

In order to evaluate the vehicle performance with the proposed approach, including a HESS based on BTs and SCs, an electrical model of a generic SHEV has been developed. The model of the components is of quasi-static nature, where during the discrete time step k the variable values are considered constants [62]. The model of the power-train's elements is based on the backward or "effect-cause" approach. It calculates the power consumed by the vehicle at each discrete step following a predefined speed profile by going upstream through the vehicle components [35, 100].

The vehicle modeling has been implemented in a MATLAB/Simulink environment. For this purpose, a simulation tool has been developed in order to facilitate the configu-

ration of the techno-economic parameters as well as to gather all the electrical, economic and ageing models regarding the vehicle scenario (HET or HEB) and its HESS. Figure 2.1 depicts some windows of this simulation tool.
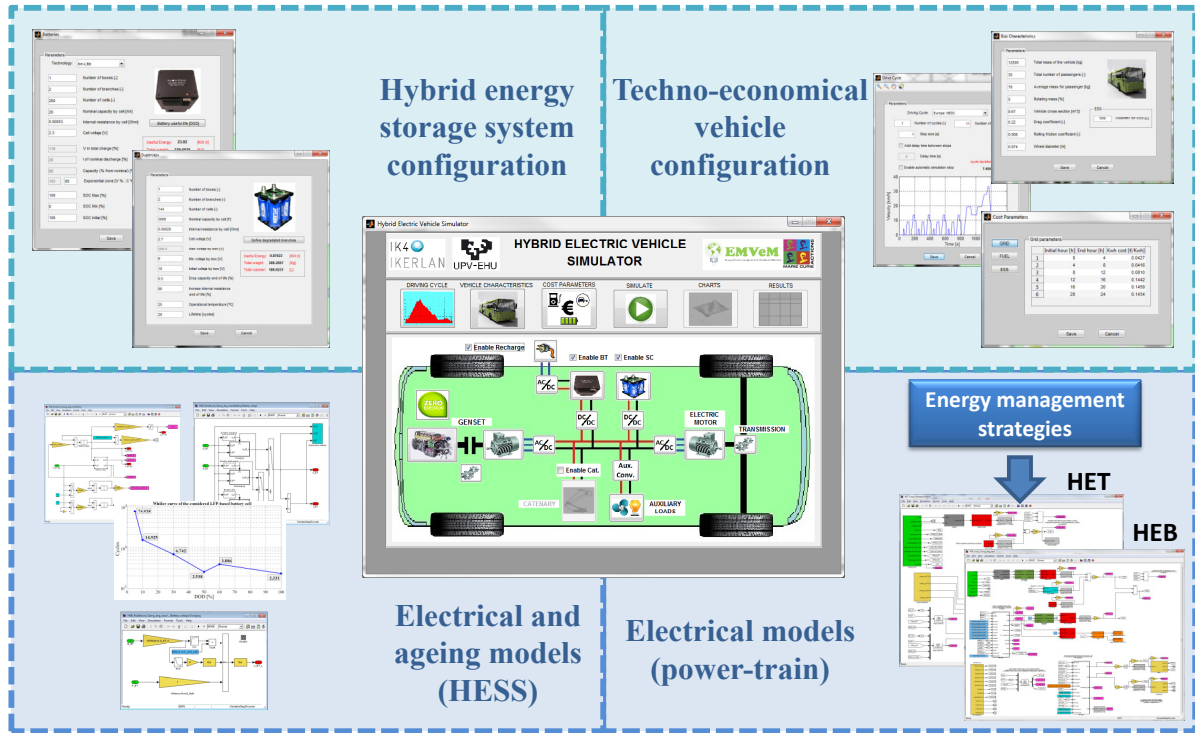
Figure 2.1: Simulation tool for hybrid electric vehicles.

Due to the fact that the analysis proposed in this work is focused on the energy management analysis by providing the power targets for the operation of the power-train elements and, in order to obtain a compromise with the computational cost during the optimization [33], a time step of 1 s has been selected [20, 92]. The local control on the devices (DC/DC converters and DC/AC inverters) could require a shorter time step [83] in order to evaluate the voltage and current transients. However, the DC/DC commutation and control issues are not addressed in this thesis because, as mention before, the aim of this work is focused in the outer layer of operation management which deals with the long-term control parameters (toward minutes or second).

Considering that the general topology adopted for the power-train is a series configuration (for both HEB and HET), all the elements are linked to a DC bus through power electronic devices and they will be controlled by power targets during operation. Therefore, in order to standardize the power flow direction, when and element is injecting power to the DC bus a positive value is considered otherwise (when it is absorbing power) a negative value is defined.

2.2.1 Vehicle Dynamics

In a quasi-static simulation, the inputs to the vehicle model are the speed profile and the slope angle α [°] of the road. Thus, the basic equation to evaluate the required torque in wheels $T_{wh}(k)$ [Nm] at each discrete state k can be defined as follows [62, 100]:

$$T_{wh}(k) = (F_t(k)) \cdot r_{wh} \; [Nm] \tag{2.1}$$

where the required traction force $F_t(k)$ [Nm] induced by the driving cycle is given by:

$$F_t(k) = F_i(k) + F_r(k) + F_a(k) + F_g(k) \; [N] \tag{2.2}$$

being r_{wh} [m] the wheel radius. The inertial force F_i [N], rolling friction force F_r [N], aerodynamic drag force F_a [N] and gravitational force F_g [N] at the discrete state k are defined as follows:

$$F_i(k) = (m_{tot} + m_{it}) \cdot a_{veh}(k) \; [N] \tag{2.3}$$

$$F_r(k) = c_r \cdot m_{tot} \cdot g \cdot cos(\alpha(k)) \; [N] \tag{2.4}$$

$$F_a(k) = 0.5 \cdot \rho_a \cdot A_f \cdot c_d \cdot v_{veh}^2(k) \; [N] \tag{2.5}$$

$$F_g(k) = m_{tot} \cdot g \cdot sin(\alpha(k)) \; [N] \tag{2.6}$$

being m_{tot} [kg] and m_{it} [kg] the total vehicle mass and total inertial mass respectively, a_{veh} $[\frac{m}{s^2}]$ the vehicle acceleration, c_r [-] the rolling friction coefficient of the wheels, g $[\frac{m}{s^2}]$ the gravitational acceleration constant, ρ_a $[\frac{kg}{m^3}]$ the density of air, A_f $[m^2]$ the frontal area of the vehicle, c_d [-] the aerodynamic drag coefficient and $v_{veh}(k)$ $[\frac{m}{s}]$ the vehicle speed at the discrete state k. Figure 2.2 shows the forces that act on the vehicle body during driving.
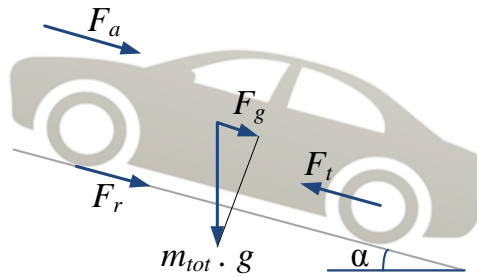
Figure 2.2: Forces acting on the vehicle body during driving.

The total mass of the vehicle m_{tot} [kg] can be defined as:

$$m_{tot} = m_{veh} + n_{pas} \cdot m_{pas} + mass_{BT} + mass_{SC} \; [kg] \tag{2.7}$$

where m_{veh} [kg] is the empty bus weight, n_{pas} is the number of passengers, m_{pas} [kg] is the average weight per person (assumed to be 75 kg), $mass_{BT}$ [kg] and $mass_{SC}$ [kg] are the BT and SC pack weight respectively.

The outputs of the vehicle model are the wheel rotational speed $w_{wh}(k)$ $[\frac{rad}{s}]$ (2.8), the wheel rotational acceleration $dw_{wh}(k)$ $[\frac{rad}{s^2}]$ (2.9), and the required torque in wheel $T_{wh}(k)$ [Nm].

$$w_{wh}(k) = \frac{v_{veh}(k)}{r_{wh}} \; \left[\frac{rad}{s}\right] \tag{2.8}$$

$$dw_{wh}(k) = \frac{a_{veh}(k)}{r_{wh}} \; \left[\frac{rad}{s^2}\right] \tag{2.9}$$

2.2.2 Electric Motor

By means of the transmission ratio (see figure 1.7) $w_{wh}(k)$ $[\frac{rad}{s}]$ and $T_{wh}(k)$ [Nm] are transformed in the EM rotational speed $w_{EM}(k)$ $[\frac{rad}{s}]$ and EM mechanical torque $T_{EM}(k)$ [Nm] respectively, which are the EM model inputs. As depicted in figure 2.3 the EM's operating efficiency $\eta_{EM}(k)$ [%] is function of both parameters (w_{EM}, T_{EM}). This efficiency map corresponds to a EM applied in road transport applications in projects where IK4-IKERLAN has formed part. The EM model output is the required electric power defined as follows [62, 100]:

When $w_{EM}(k) > 0$ and $T_{EM}(k) > 0$, (traction mode):

$$P_{EM}(k) = \frac{w_{EM}(k) \cdot T_{EM}(k)}{10^3 \cdot \eta_{EM}(k)(w_{EM}(k), \; T_{EM}(k))} \; [kW] \tag{2.10}$$

When $w_{EM}(k) > 0$ and $T_{EM}(k) < 0$, (regenerative mode):

$$P_{EM}(k) = \frac{w_{EM}(k) \cdot T_{EM}(k) \cdot \eta_{EM}(k) \left(w_{EM}(k), \; T_{EM}(k)\right)}{10^3} \; [kW] \tag{2.11}$$

2.2.3 Power Electronic devices

Since this study is intended to simulate the power flow throughout the power-train elements, the power electronic devices (DC/DC converters and DC/AC inverters) have not been modeled in detail. As in [33] and [101], the efficiencies for DC/DC converter (η_{conv}
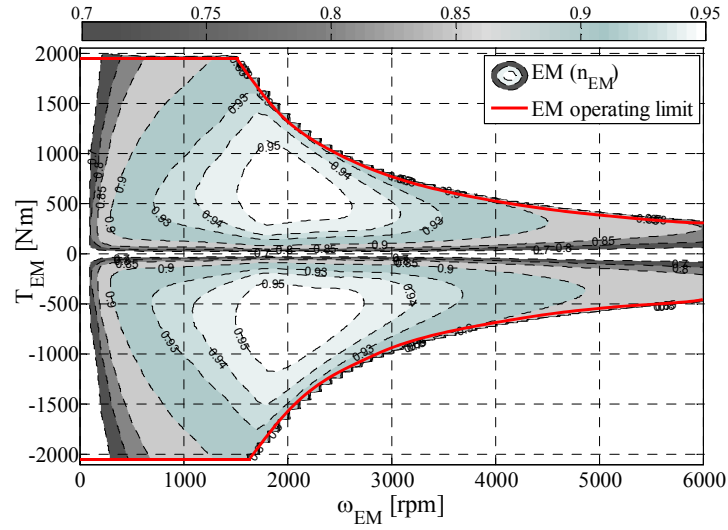
Figure 2.3: Efficiency map of an Electric Motor for road transport applications.

[%]) and DC/AC inverter (η_{inv} [%]) have been considered as fixed values by taking an average one from their operating ranges. It is worth to mention that the efficiency depends on the voltage and current during the converter operation. Therefore, some constraints (detailed in chapter 3 and chapter 4 for tramway and bus scenario respectively) have been considered about the minimum energy stored in the BT and SC pack allowing the DC/DC converter operation and avoiding the poor energy conversion (low efficiency).

2.2.4 Power demand from vehicle

The total power demand $P_{DEM}(k)$ (in the DC bus) during vehicle operation considers both the demand for traction as well as the power consumption by the auxiliary loads as follows:

$$P_{DEM}(k) = P_{EM}(k) \cdot \eta_{inv}^{-sgn(P_{EM}(k))} + P_{aux} \; [kW] \tag{2.12}$$

where the $sgn(X)$ function returns the sign of its argument.

2.2.5 Genset

The genset is made up by an ICE and an EG. Both are mechanically connected through a clutch, which is used during the starting process of the engine, but the dynamics related to this approach are not addressed in this thesis. The genset model input is the power target $P_{genset(k)}$ [kW] requested by the EMS. This power target can be obtained from different combinations of ICE rotational speed (w_{ICE} [$\frac{rad}{s}$]) and torque (T_{ICE} [Nm]). The optimal selection of these operating points is explained later in chapter 4. Therefore, the instantaneous fuel mass flow mf_{ICE} [$\frac{kg}{s}$] consumed at each discrete state k can be defined
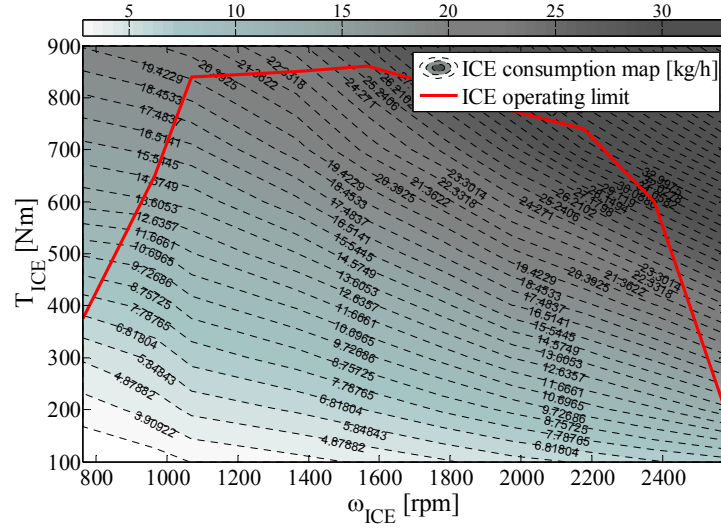
Figure 2.4: ICE fuel consumption map.

as follows [62, 100]:

$$mf_{ICE}(k) = f\left(w_{ICE}(k),\, T_{ICE}(k)\right) \left[\frac{kg}{s}\right] \tag{2.13}$$

The instantaneous fuel mass flow consumed from the ICE is obtained by interpolating the ICE speed and torque value in the fuel consumption map depicted on figure 2.4. In this case, the data of a commercial diesel motor of VOLVO used in hybrid buses applications has been considered for the vehicle modeling. The power generated by the ICE can be approximated by equation 2.14.

$$P_{ICE}(k) = \frac{P_{genset}(k)}{\eta_{EG}(k) \cdot \eta_{ICE}(k) \cdot \eta_{inv}} \, [kW] \tag{2.14}$$

where $\eta_{ICE}(k)$ [%] is the ICE efficiency (deducted from the fuel consumption map depicted on figure 2.4). η_{inv} [%] is the average efficiency of the inverter linked to the genset. $\eta_{EG}(k)$ [%] is the EG efficiency, obtained from the efficiency map depicted on figure 2.5 which corresponds to a commercial EG for transport applications.

2.2.6 Battery model

Considering that the aim of this study is the power and energy analysis for the optimal vehicle operation a basic electric model for the BT cell, known as steady-state battery equivalent circuit model, has been applied on this scenario [62]. In this model the major factor which limits the charging and discharging capability in a battery is the internal resistance. Therefore, the BT cell is represented by an ideal open circuit voltage source (V_{oc_BTcell} [V]) in series with the internal resistance (R_{int_BTcell} [Ohm]). As shown in
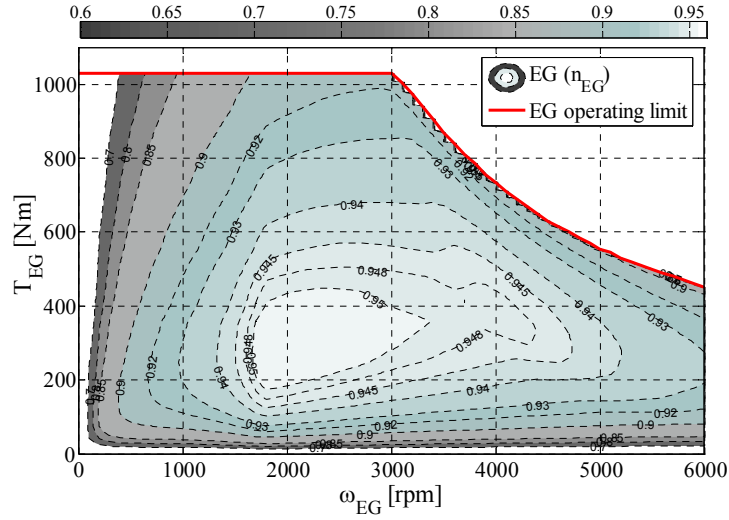
Figure 2.5: Electric generator efficiency map.

figure 2.6, both are nonlinear functions of the state-of-charge of the BT cell (SOC_{BTcell} [%]). These relationships have been obtained by experimental tests carried out on the BT cell [102] and implemented as look-up tables in the MATLAB/Simulink model of the vehicle.

(a) SOC_{BTcell} vs. V_{oc_BTcell}

(b) SOC_{BTcell} vs. R_{int_BTcell}
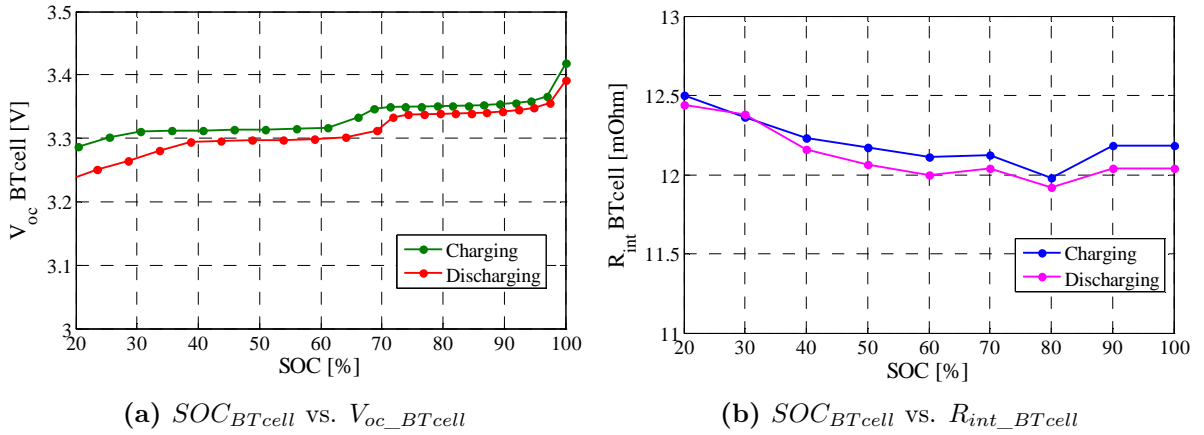
Figure 2.6: Relation between SOC and electrical parameters of the BT cell [102].

Assuming that a string contains n_{BT} BT cells in series and the BT pack groups m_{BT} strings in parallel (figure 2.7) [23]:

$$U_{oc\_BT} = V_{oc\_BTcell} \cdot n_{BT} \ [V] \tag{2.15}$$

$$R_{BT} = \frac{n_{BT} \cdot R_{int\_BTcell}}{m_{BT}} \ [Ohm] \tag{2.16}$$

being U_{oc_BT} [V] and R_{BT} [Ohm] the equivalent open circuit voltage and internal resistance for the BT pack.
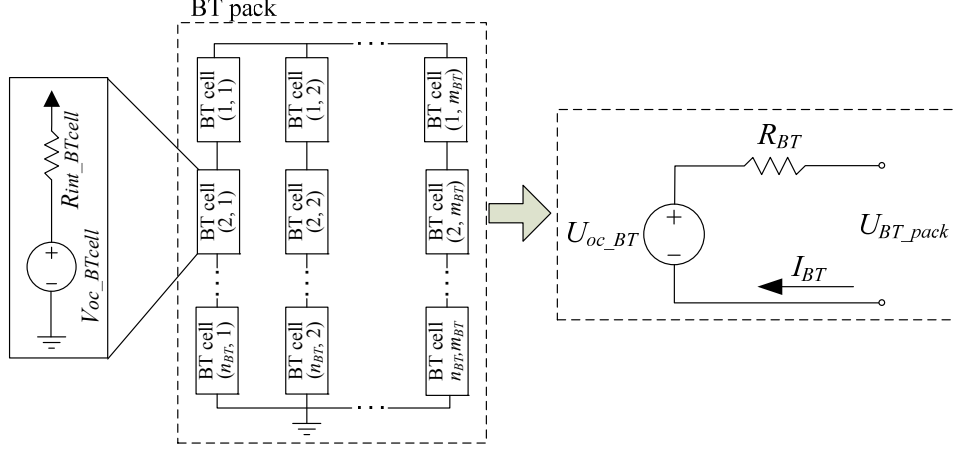
Figure 2.7: Battery pack configuration.

The input of the BT pack model is the power target (P_{BT} [kW]) injected/absorbed from/in the pack and defined by the EMS. The model output is the corresponding state-of-charge of the BT pack (SOC_{BT} [%]). The BT pack current at the discrete step k is calculated as follows:

$$I_{BT}(k) = \frac{U_{oc\_BT}(SOC_{BT}(k))}{2 \cdot R_{BT}(SOC_{BT}(k))} -$$

$$\frac{\sqrt{U_{oc\_BT}^2(SOC_{BT}(k)) - 4 \cdot R_{BT}(SOC_{BT}(k)) \cdot P_{BT}(k) \cdot 10^3 \cdot \eta_{conv}^{-sgn(P_{BT}(k))}}}{2 \cdot R_{BT}(SOC_{BT}(k))} \ [A]$$

(2.17)

SOC_{BT} [%] is defined as the ratio of the available electric charge that can be supplied by the BT pack ($Q_{BT}(k)$ [C]) and the nominal charge Q_{BT_0} [C] of the BT pack [103]:

$$SOC_{BT}(k) = \frac{Q_{BT}(k)}{Q_{BT\_0}} \cdot 100 \ [\%]$$

(2.18)

The state of charge is updated at each discrete step (with a time step of Δt [s]) as follows:

$$SOC_{BT}(k+1) = SOC_{BT}(k) - I_{BT}(k) \cdot \frac{\Delta t}{Q_{BT\_0}} \cdot 100 \ [\%]$$

(2.19)

In order to determine the weight of the BT pack ($mass_{BT}$ [kg]) the following equation is applied:

$$mass_{BT} = \frac{(V_{nom\_BTcell} \cdot n_{BT}) \cdot (C_{nom\_BTcell} \cdot m_{BT})}{10^3} \cdot \rho_{BT} \ [kg] \qquad (2.20)$$

being V_{nom_BTcell} [V] and C_{nom_BTcell} [Ah] the nominal voltage and capacity of the BT cell. ρ_{BT} $[\frac{kg}{kWh}]$ is the energy density of the BT cell technology.

2.2.7   Supercapacitor model

For the SC model a similar approach, that the one previously explained for the BT, has been applied. In this case, an equivalent circuit of a capacitor with a capacitance C_{SCcell} [F] in series with a resistance R_{int_SCcell} [Ohm] has been considered [62]. Assuming that a string contains n_{SC} SC cells in series and the SC pack groups m_{SC} strings in parallel (figure 2.7) [23]:

$$C_{SC} = \frac{m_{SC} \cdot C_{SCcell}}{n_{SC}} \ [F] \qquad (2.21)$$

$$R_{SC} = \frac{n_{SC} \cdot R_{int\_SCcell}}{m_{SC}} \ [Ohm] \qquad (2.22)$$

being C_{SC} [F] and R_{SC} [Ohm] the equivalent capacitance and internal resistance for the SC pack, respectively.
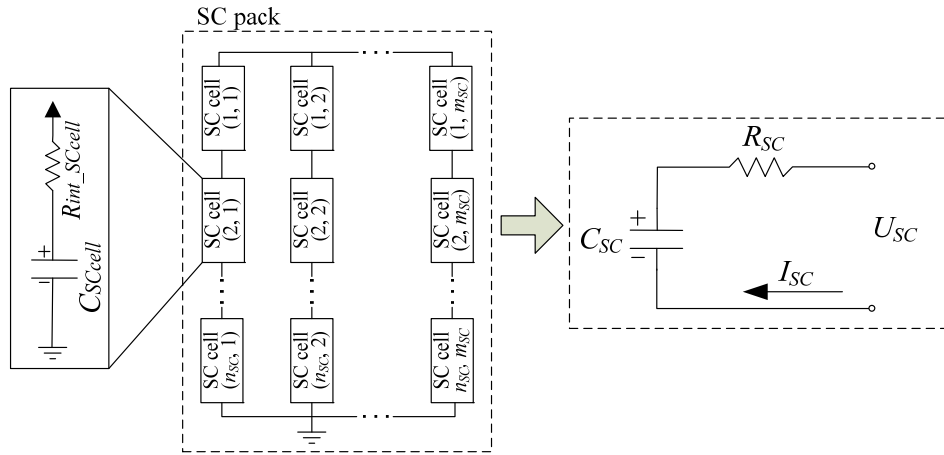
Figure 2.8: Supercapacitor pack configuration.

The input of the SC model is the power target P_{SC} [kW] injected/absorbed from/in the SC pack (obtained from the EMS). The model output is the SOC of the SC pack (SOC_{SC} [%]). The SC pack current at the discrete step k is calculated as follows [62]:

$$I_{SC}(k) = \frac{Q_{SC}(k)/C_{SC}}{2 \cdot R_{SC}} -$$

$$\frac{\sqrt{(Q_{SC}(k)/C_{SC})^2 - 4 \cdot R_{SC} \cdot P_{SC}(k)\dot{1}0^3 \cdot \eta_{conv}^{-sgn(P_{SC}(k))}}}{2 \cdot R_{SC}} \ [A]$$

(2.23)

where $Q_{SC}(k)$ [C] is the available charge stored in the SC pack related to the equivalent of the pack U_{SC} [V] as follows:

$$U_{SC}(k) = \frac{Q_{SC}(k)}{C_{SC}} \ [V]$$

(2.24)

The charge stored in the SC pack is updated by:

$$Q_{SC}(k+1) = Q_{SC}(k) - I_{SC}(k) \cdot \Delta t \ [C]$$

(2.25)

The energy stored in the SC pack can be defined as follows:

$$E_{SC}(k) = 0.5 \cdot C_{SC} \cdot U_{SC}^2(k) \ [J]$$

(2.26)

From the efficiency standpoint, the SC pack voltage $U_{SC}(k)$ [V] is not allowed to fall below half of the nominal voltage U_{SC_nom} [V], considering that at this point 75% of the energy stored in the SC pack has been released [23]. Finally, the SOC of the SC pack in terms of voltage can be defined as [39]:

$$SOC_{SC}(k) = \frac{U_{SC}(k)^2}{U_{SC\_nom}(k)^2} \cdot 100 \ [\%]$$

(2.27)

Therefore, with half of the nominal voltage, the minimum allowable SOC_{SC} will be 25%.

Similarly to the BT pack case, the weight of the SC pack ($mass_{SC}$ [kg]) is determined as follows:

$$mass_{SC} = \frac{1}{2 \cdot 3.6^6} \cdot C_{SC} \cdot (U_{SC\_nom} \cdot n_{SC})^2 \cdot \rho_{SC} \ [kg]$$

(2.28)

being ρ_{SC} $[\frac{kg}{kWh}]$ the energy density of the SC cell technology.

Table 2.1 summarizes the main parameters of the BT and SC cells considered as base to compose the packs in this thesis. It is noteworthy that, this BT cell has been selected due to the wide cycle ageing analysis made on it [102, 104], which allows a more accurate degradation and lifespan estimation on the BT pack. Furthermore, the max C-rate for charging and discharging has been limited up to 3.5, due to most of the experimental

tests related to the degradation of this BT cell have been made up to these values [104]. The SC cell parameters were obtained from the data-sheet of the manufacturer [105].

Table 2.1: Electrical parameters of BT and SC base cells.

BT (LFP/graphite 2.3Ah 26650-type [106])		SC (BCAP3000) [105]	
Nom. voltage	3.3V	Nom. voltage	2.7V
Nom. capacity	2.3Ah	Nom. capacitance	3000F
Int. resistance	$R_{int}(SOC_{BT})\ Ohm$	Int. resitance	0.29 $mOhm$
Max C-rate disch/ch.	3.5/3.5 $C - rate$		
Specific energy	108Wh/kg	Specific energy	6.0Wh/kg

2.2.8   Auxiliary loads

An average constant power consumption value for the auxiliary loads P_{aux} [kW] (fans, air conditioning, lights, etc.) is considered for the entire route. The value for the scenarios HET or HEB will be introduced in chapter 3 and chapter 4, respectively.

2.3   Economical model

This section describes the cost model applied for evaluating the economic feasibility of each solution. The cost functions consider both the HESS operation as well as the additional energy source depending on the vehicle (genset or catenary). It is worth mentioning that the proposed cost model considers the whole lifetime of the vehicle. Thus, it includes the initial investment and replacement costs (defined by the cycling operation) of the HESS.

2.3.1   Operating cost of the BT and SC pack

The total operating cost of the BT pack is defined as follows:

$$BT_{Tcost} = \frac{BT_{M\_y} + BT_{Ca\_y} + BT_{Re\_y}}{360} \left[\frac{euros}{day}\right] \tag{2.29}$$

being BT_{M_y} $\left[\frac{euros}{year}\right]$ an average value related to the maintenance cost of the BT pack. BT_{Ca_y} $\left[\frac{euros}{year}\right]$ is the annualized capital cost related to the initial investment for the BT pack calculated as follows:

$$BT_{Ca\_y} = (C_{kW\_dcdc} \cdot P_{dcdc\_BT} + C_{kWh\_BT} \cdot Ca_{BT}) \cdot CRF \left[\frac{euros}{year}\right] \tag{2.30}$$

where C_{kW_dcdc} $\left[\frac{euros}{kW}\right]$ is the referential cost of the DC/DC converter. P_{dcdc_BT} [kW] is the power of the DC/DC converter. C_{kWh_BT} $\left[\frac{euros}{kWh}\right]$ is the referential cost of the BT

technology (Li-ion technology for this scenario). Ca_{BT} is the capacity of the installed BT pack in kWh. CRF is the capital recovery factor, which allows annualizing the cost taking into account the lifetime of the whole system [16]:

$$CRF = \frac{I \cdot (1+T)^T}{(1+T)^T + 1} \left[\frac{1}{year} \right] \tag{2.31}$$

where I [%] and T [years] are the interest rate and the lifetime of the whole system (vehicle), respectively.

On the other hand, BT_{Re_y} $\left[\frac{euros}{year} \right]$ represents the annualized replacement cost (cycling cost) of the BT pack:

$$BT_{Re\_y} = \sum_{i=1}^{r\_BT} \left(\frac{C_{kWh\_BT} \cdot Ca_{BT} \cdot CRF}{(1+I)^{i \cdot Life_{BT}}} \right) \left[\frac{euros}{year} \right] \tag{2.32}$$

where

$$r\_BT = ceil \left(\frac{T}{Life_{BT}} - 1 \right) \tag{2.33}$$

being r_BT the number of BT pack replacements during the lifetime of the system T [years]. $ceil(x)$ is a mathematical function which returns the higher integer value of its argument x. $Life_{BT}$ [years] is the lifespan estimation for the BT pack.

The equations to calculate SC_{Tcost} $\left[\frac{euros}{day} \right]$ are the same that those given for the BT_{Tcost} case but the variables set on the SC pack context as follows:

$$SC_{Tcost} = \frac{SC_{M\_y} + SC_{Ca\_y} + SC_{Re\_y}}{360} \left[\frac{euros}{day} \right] \tag{2.34}$$

$$SC_{Ca\_y} = (C_{kW\_dcdc} \cdot P_{dcdc\_SC} + C_{kWh\_SC} \cdot Ca_{SC}) \cdot CRF \left[\frac{euros}{year} \right] \tag{2.35}$$

$$SC_{Re\_y} = \sum_{i=1}^{r\_SC} \left(\frac{C_{kWh\_SC} \cdot Ca_{SC} \cdot CRF}{(1+I)^{i \cdot Life_{SC}}} \right) \left[\frac{euros}{year} \right] \tag{2.36}$$

$$r\_SC = ceil \left(\frac{T}{Life_{SC}} - 1 \right) \tag{2.37}$$

2.3.2 Cost of the energy from the catenary

The total cost related to the energy absorbed from the catenary is defined by:

$$Cat_{Tcost} = \sum_{k=1}^{p} \left(\frac{P_{CAT}(k) \cdot C_{kWh\_g}}{3600} \right) \left[\frac{euros}{day} \right] \tag{2.38}$$

where p is the number of discrete steps in the daily profile. $P_{CAT}(k)$ [kW] is the power absorbed from the catenary at the discrete step k, and C_{kwh_g} $\left[\frac{euros}{kWh} \right]$ is the referential cost of the grid energy.

2.3.3 Cost of fuel consumption from ICE

Based on equation (2.13) the actual fuel mass flow is calculated and integrated to obtain the total fuel mass consumed to complete the chosen driving cycle. The total fuel consumption cost is calculated as follow:

$$Fuel_{Tcost} = \sum_{k=1}^{p} \left(\frac{mf_{ICE}(k) \cdot k_{cs} \cdot C_{L\_fuel}}{\rho_{fuel}} \right) \left[\frac{euros}{day} \right] \tag{2.39}$$

being ρ_{fuel} $\left[\frac{kg}{liter} \right]$ the volumetric density of the fuel, k_{cs} [-] the global factor to cold starts, and $C_{L\_fuel)}$ $\left[\frac{euros}{liter} \right]$ the referential cost of the liter of fuel (diesel).

2.4 ESS lifetime estimation models

As mentioned in the previous section, the economic model related to the HESS operation considers the BT and/or SC pack replacements during the vehicle lifetime. Thus, the aim of this section is to introduce the degradation principle and lifespan estimation of the ESS mainly focused on BTs since this storage technology shows shorter lifespan that comparing with EDLCs ones and a degradation highly dependent on its operating conditions [107].

This way, the main ageing factors will be introduced and two different lifetime estimation models will be presented. The first one based on Whöler curves and cycling counting method [11, 108, 109] and the second one a semi-empirical model combining experimental tests carried out on the BT cell and mathematical approximations presented in [102]. This ageing models will allow to carry out analysis of the influence in lifetime estimation accuracy on the ESS sizing, vehicle performance and operating cost which will be addressed later in chapter 5.

2.4.1 Cell degradation principle: Lithium-ion technology

Since their manufacture, BTs start to age and degrade. The ageing is reflected in a reduction of the cell capacity and an increase of the internal impedance. This implies that the BT cell over time and with the utilization cycles is not able to supply the same amount of energy or power compared to a new BT cell [20].

Two main types of cell ageing processes can be distinguished. On the one hand, the calendar ageing represents the gradual degradation occurring while the BT is stored. This means that the process is maintained although the BT is not in operation. The influence of this effect depends on the BT storage conditions, so it is highly dependent on the SOC and temperature. The recommended storage conditions for a Li-ion cell are around 15-20°C and 40-50% SOC [12]. Table 2.2 shows the capacity loss in a BT cell at different storage conditions.

Table 2.2: BT cell capacity according to storage time, temperature and SOC [12]

	Capacity percent after 1 year of storage in Li-ion cell	
Temperature (°C)	40% SOC (recommended SOC for storage)	100% SOC
0	98%	94%
25	96%	80%
40	85%	65%
60	75%	60% (after 3 months)

On the other hand, the cycling ageing expresses the degradation in the performance parameters of the BT during cycles at different conditions. The cell degradation is dependent on the depth-of-discharge of each cycle and the current magnitude, which can be expressed as the C-rate. Consequently, it is possible to reduce the cell degradation controlling these factors [21, 42]. Figure 2.9 represents the lifetime reduction when the DOD grows.

Several curves of the cell voltage versus the discharged capacity are represented in figure 2.10. It can be observed that the increase on the charge and discharge cycles causes the cell ageing, reducing the available capacity.

Similarly, figure 2.11 shows the increment of the internal resistance and the reduction of the cell capacity when the number of cycles increase.

2.4.2 ESS ageing models

It is well known that still today, battery lifespan is typically shorter than the lifespan of power electronic systems, and usually shorter than the investment period on a certain application. On the other hand, ESS implementation costs still suppose a significant percentage of the initial investment, and in cases where BT and/or SC packs replacements
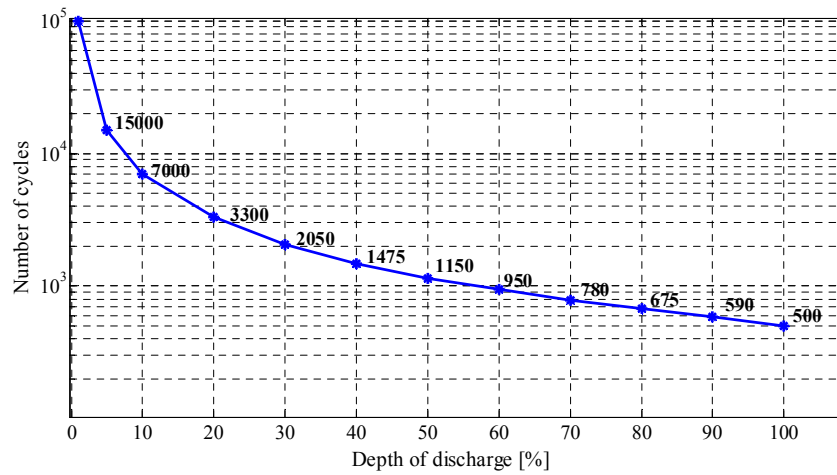
Figure 2.9: Life cycles according to DOD.
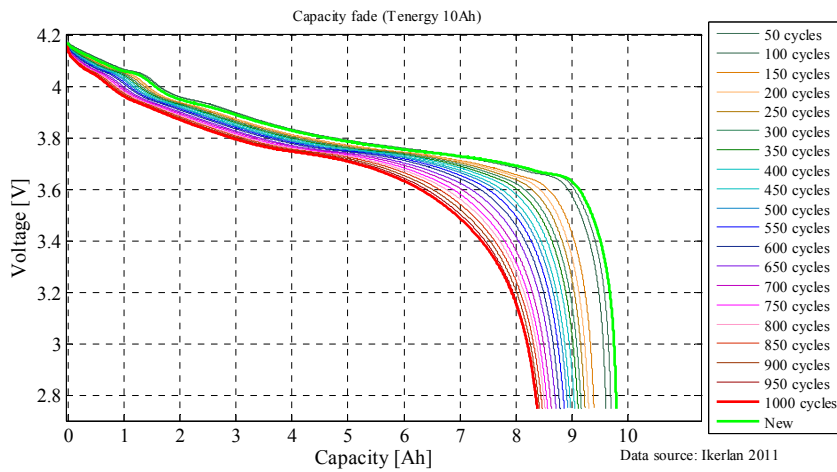
Figure 2.10: Capacity fade on a lithium-ion cell.
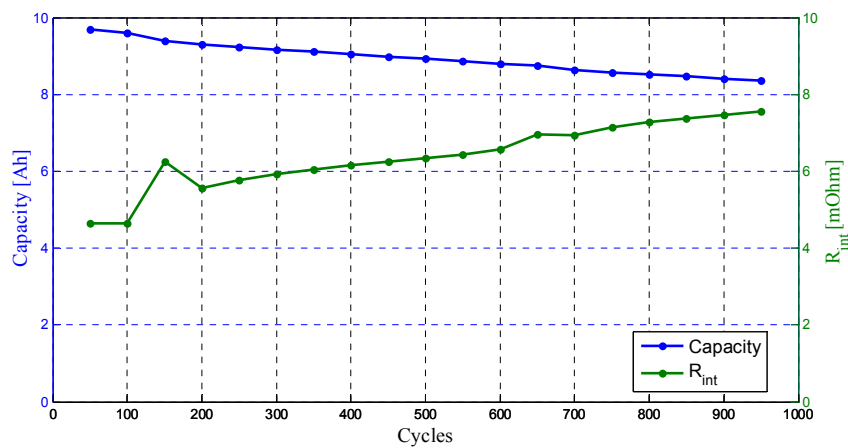
Figure 2.11: Increment on the internal resistance and capacity fade with ageing.

are required, also a significant part of the operating cost during vehicle lifetime.

Thereby, considering those two issues, the BT lifespan estimation included on mobility applications is one of the limiting factors when evaluating the economic feasibility of including BTs on a certain application. The uncertainly about the proper ESS sizing and operation increases when hybrid solutions are considered. Therefore, the lack on considering the lifespan estimation of the ESS or the sub-estimation of it may cause not only failures and early-degradations on the ESS but also increase on the operating and replacements costs that finally have to be assumed by the manufacturer or end-client.

Despite all this, most publications in literature rarely emphasize on ageing modeling when describing the ESS sizing. From the different ageing modeling approaches widely covered in literature [110] (see figure 2.12) most authors tend to the most simple solutions when analyzing BT sizing. This is due to three main reasons: 1) simpler ageing models imply lower computational costs, 2) there is lack of available data of the BT cell to be used (and obtaining such data supposes expensive and time-consuming experimental tests) and 3) properly sizing an ESS represents itself a big challenge, covering many aspects of the application and system performance, and the battery just represents a part of the whole system, usually not considered the main device of interest in the system. This way, the approach followed by different authors widely varies when it comes to the complexity of the ageing models considered.
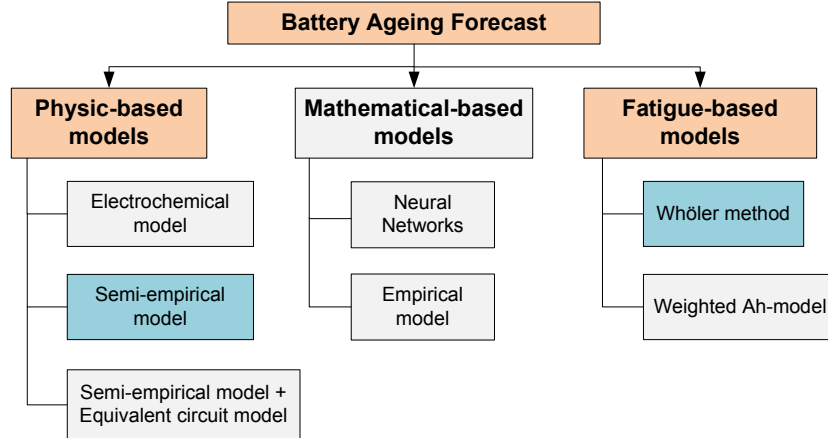
Figure 2.12: Ageing model classification [110].

In the current literature, several approaches have been followed to estimate the BT lifetime estimation. For instance in [111] the optimal sizing for a BT-based electric vehicle was evaluated without considering the effect of battery ageing and only selected the solution based on the minimum BT size (minimal costs). On the other hand, also pursuing a simple approach for BT ageing modeling, in [112] the authors presented a sizing method for residential ESS+PV system sizing, but in this case considering a calendar life model which evaluates BT degradation in function of the storage temperature from adjusted experimental data coupled with a linear cycle life model.

Some other authors have also considered fatigue methods based on the Rainflow cycle counting algorithm applied to Whöler curves of several battery chemistry and technologies. In [113] the optimal combination of BTs and SCs was evaluated in order to produce high-power and high-energy hybrid systems, modeling battery lifetime in function of the Whöler curve of a sample battery. In [114] it was analyzed how batteries could be controlled and how they should be sized to reduce the bill of the owner of any private electricity facility under Real-Time Pricing (RTP) tariffs. In [115], the Rainflow cycle counting algorithm was applied to estimate the lifetime of a BT bank (installed in a PV power plant) as part of an intelligent strategy for market participation by providing ancillary services to the main grid. Additionally, in [96] a cycle counting method was considered during optimization to determine the on-line adaptation of the BT operation to the desired trajectory.

Going a step further on battery ageing modeling, some authors like in [116] or [23] evaluate battery degradation via empirical models. In the latter, a thorough modeling approach is presented, from electric to ageing modeling, and even including a battery thermal model. Consequently, they evaluate the optimal sizing of a BT-SC hybrid system, and they model BT cell degradation considering four ageing factors: time, temperature, DOD, and discharge rate by a semi-empirical model previously proposed in [117].

Finally, other few authors such us [118] or [119] even introduce electrochemical models for BT lifetime prognosis on optimization problem formulations. However, the complexity and the high computational burden of electrochemical models usually requires simplifying the model for the system optimization simulation time required to be acceptable. This simplifications reduce model precision, and if no particular interest on BT component optimization is pursued, electrochemical model inclusion is normally avoided.

Heeding the different approaches observed in literature regarding BT degradation modeling for sizing and operation purposes, no clear conclusion has been obtained about the model accuracy required to obtain a reliable optimal BT sizing estimation. The direct conclusion is to consider that the higher the model precision, the more reliable battery sizing results will be. However, accurate ageing model development requires extensive experimental testing, and it is usually far from what the industry is willing to pay. Moreover, there is not a clear conclusion about how the error on battery lifetime estimation affects the final battery size on a certain application, and what economic implication such "non-optimal sizing" entails [19].

For this reason, from the different ageing models considered in figure 2.12, two main ageing models will be covered in this section, one based on *Whöler curves* and other based on *Semi-empirical* developments, which are deeply described below.

2.4.2.1 Lifespan estimation by *Whöler curve*-based method

The use of *Whöler curve*-based ageing models is typically done in literature, especially for sizing purposes or for economic calculations in applications where an ESS is integrated.

The modeling method was first introduced to Lead Acid BTs in 1983 by Facinelli [120] and lately expanded by Sauer and Wenzl [109]. The idea behind this model is quite simple, and mathematically expresses the number of events i_{evt} type that can occur during the lifetime of a BT cell until it reaches its end-of-life (EOL). In this case, i_{evt} represents a certain DOD, and hence the model evaluates the effect of the DOD on the BT degradation as follows:

$$LL_{i_{evt}} = \frac{NE_{i_{evt}}}{NE_{i_{evt}}^{max}} \tag{2.40}$$

being $NE_{i_{evt}}^{max}$ the maximum number of events i_{evt} type that the battery can withstand and $NE_{i_{evt}}$ the number of events accounted. Thereby, $LL_{i_{evt}}$ represents the lifetime lost caused by the occurrence of a certain number of i_{evt} events. Similarly for the whole range of events that could happen, *i.e.* for the whole range of DOD (from 0 to 100%), the total loss of lifetime is expressed according as follows:

$$LL = \sum LL_{i_{evt}} \tag{2.41}$$

Therefore, when the lifetime lost LL equals 1, it is considered that the cell has reached the EOL.

This method allows evaluating the corresponding loss of lifetime for a certain SOC profile, from which the number of events at each defined DOD range can be defined. Then, considering the period of time that such SOC profile represents, the total lifetime can be calculated as the inversion of LL, typically defined in years:

$$Lifetime = \frac{1}{LL} \tag{2.42}$$

In order to define the maximum number of events $NE_{i_{evt}}^{max}$ at each DOD that the cell can withstand, Whöler curves are used. Figure 2.13 depicts the Whöler curve experimentally obtained [104] for the BT cell considered in the framework of this thesis.

The main advantage of *Whöler curve*-based ageing models is that such curves are sometimes provided by BT manufacturers, and when this data is not available, related information can be usually found in literature. In addition, even when experimental tests are required to obtain such information, cycling a reduced number of cells at constant DOD conditions is enough to obtain such curves [19]. Besides, this kind of models suppose a very low computational burden, which is an important factor to be considered when an optimization process is carried out.

On the contrary, the main drawback from *Whöler curve*-based models lies in their partial consideration of the whole set of factors affecting battery degradation, as they only evaluate the effect of the DOD and the Ah (represented as number of cycles) that a battery can withstand before reaching EOL. The effect of other factors like the charg-
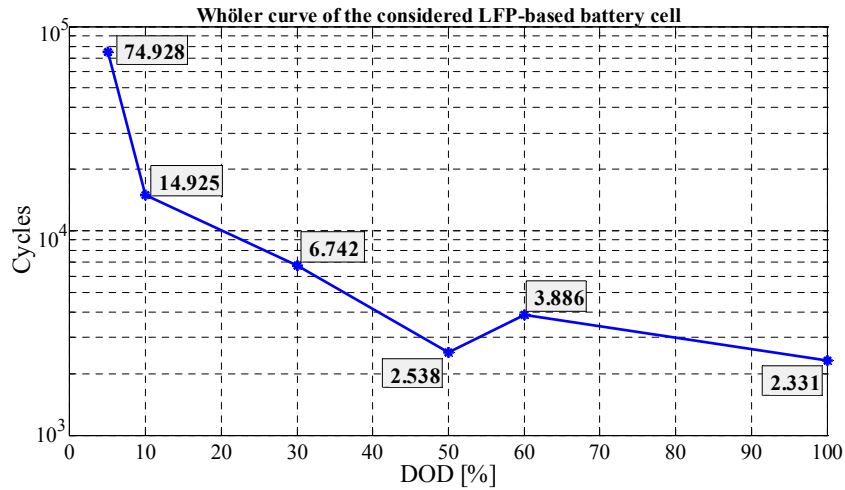
Figure 2.13: Whöler curve of the LFP/graphite 2.3Ah 26650-type cell [104].

ing/discharging speed (C-rate), temperature or even the effect of the calendar life are not taken into account. However, *Whöler curve*-based method can be implemented and considered as suitable solution especially when the fully developed ageing model (combining all the ageing factors) for a specific cell is unknown.

Therefore, in the scenarios proposed in this thesis some constraints related to the maximum charging/discharging rate (see table 2.1) have been considered in order to operate the BT cell between its safe ranges (avoiding high currents). This way, only the effect of cycling on the cell degradation can be considered.

As stated in section 2.3.1, the operating cost related to the SC pack also considers the pack replacements during vehicle lifetime. However, in literature for sizing and operation purposes, when the HESS includes a SC pack the lifespan estimation of it is disregarded. This mainly because the EDLCs technology is considered to have relatively very high number of charge/discharge cycles in their lifespan than compared with BT technologies. However, the SC ageing process can be influenced by the cycles and current rate during operation [11, 121]. Therefore, in order to take into account the influence of cycling in both BT and SC packs, the Whöler principle has been also applied for the SC case where a constant value of 10^5 cycles [105] has been considered for for $NE_{i_{evt}}^{max}$ in all the i_{evt} events [122].

2.4.2.2 Rainflow cycle counting algorithm

In order to determine the number of cycles at different DODs and apply the *Whöler curve*-based method, the Rainflow cycle counting algorithm has been considered [108]. The process carried out by the algorithm can be summarized as follows:

- The algorithm analyses the SOC profile beginning from the highest value and counting the discharging cycles from top to bottom. It analyzes the discharge curve until finding

the lowest SOC value following a continuously decreasing path. The algorithm restarts with the next highest SOC value and repeats the previous process until finding the next lowest value taking into account to not overlap the path defined previously. The process is repeated as many times as necessary until all the valleys in the SOC profile have been analyzed. Figure 2.14 shows as example this first process (red paths sequence).
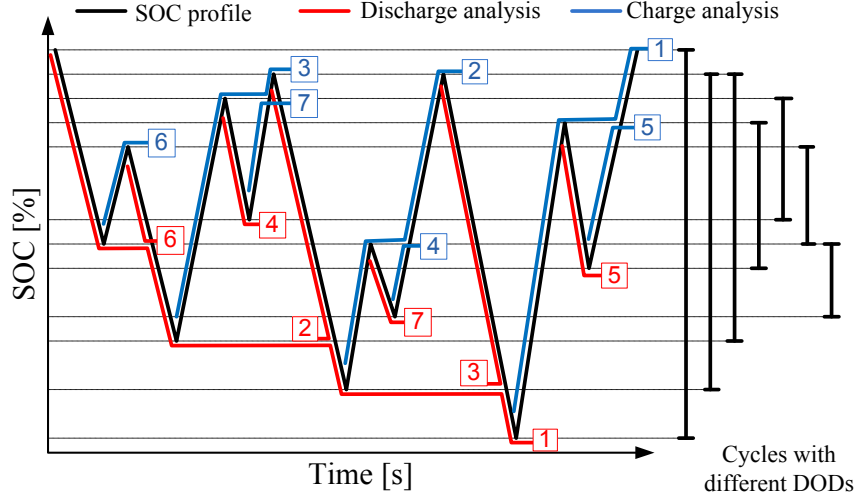
Figure 2.14: Discharging/Charging analysis [123].

- The second part of the algorithm corresponds to the charging analysis. It begins from the lowest SOC value and searches the highest one following a continuously increasing path. The process will be repeated until having analyzed all the peaks in the SOC profile (blue paths sequence on figure 2.14).

- Once finished these two processes, the next step is to gather the charging and discharging semi-cycles that fit in a same DOD range as shown in figure 2.14. The result are the complete cycles at different DOD ranges.

- Finally, the algorithm counts the specific complete cycles in each DOD range.

In order to update the SOH value during the lifetime (therefore the available capacity) of the BT pack an iterative process for the Rainflow algorithm has been implemented. Figure 2.15 illustrates the iterative principle where a time frame of n_d [days] has been considered to update the SOH value (assuming that during this period the SOH conditions will remain constant).

Therefore, at each iteration r the Rainflow algorithm is applied to calculate the remaining lifetime ($Life_{BT\_r}$) and interpolate the corresponding SOH (SOH_r) as follows [35, 123]:

$$Life_{BT\_r} = min\left[Life_{BT\_cal} \ , \ \frac{1}{\sum_{j=1}^{10}\left(\frac{N_{BT\_dj}}{LC_{BTj}}\right) \cdot 365}\right] \ [years] \ \ r \in \ [0...m] \qquad (2.43)$$
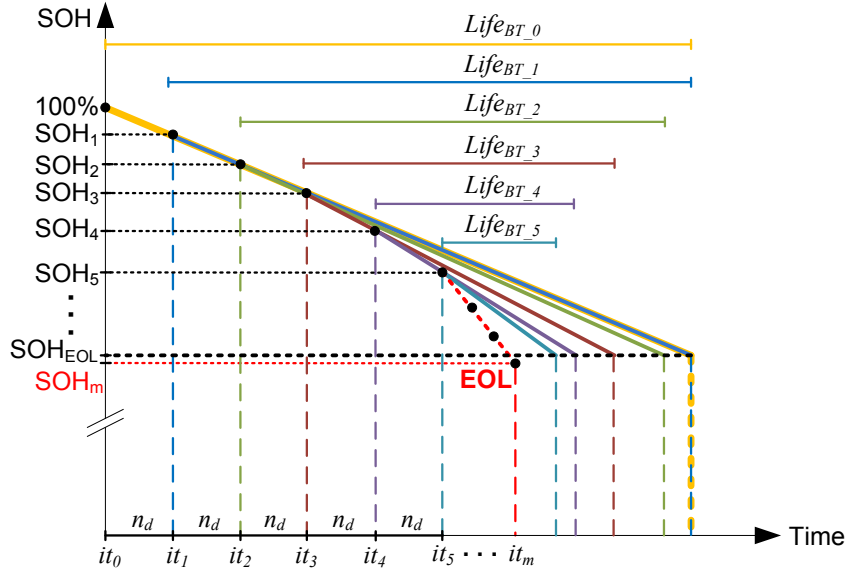
Figure 2.15: Iterative SOH update in Rainflow counting algorithm.

Table 2.3: Distribution of DOD ranges.

DOD_i	DOD_1	DOD_2	DOD_3	DOD_4	DOD_5
DOD range	]0 - 2]%	]2 - 15]%	]15 - 25]%	]25 - 35]%	]35 - 45]%
DOD_i	DOD_6	DOD_7	DOD_8	DOD_9	DOD_{10}
DOD range	]45 - 55]%	]55 - 65]%	]65 - 75]%	]75 - 85]%	]85 - 100]%

being r the iteration index. $Life_{BT\_cal}$ [years] is the floating life of the BT pack, which is the maximum lifespan if the BT pack remains in no operation conditions (calendar). m is the iteration index when the EOL has been reached. N_{BT_dj} is the number of cycles/day counted in each DOD range j (by Rainflow algorithm). LC_{BTj} is the specific amount of available life cycles at each DOD range j which is calculated by interpolating the middle point of the DOD range in the experimental test based curve depicted in figure 2.13. Hence, the $Life_{BT\_r}$ value will be the shortest lifespan one between the floating life and the lifetime in operation (cycling). The DOD ranges considered in this thesis are described in table 2.3.

Finally, the total lifetime of the BT pack is calculated by (2.44).

$$Life_{BT} = \frac{n_d \cdot m}{365} \ [years] \tag{2.44}$$

The equation for the SC lifetime estimation is the same as the one described for the BT case, but the variables set on the SC context as shown in (2.45). In this case, the value obtained for first iteration ($Life_{SC\_0}$) is adopted as lifetime estimation.

$$Life_{SC} = Life_{SC\_0} = min\left[Life_{SC\_cal} \,, \; \frac{1}{\sum_{j=1}^{10}\left(\frac{N_{SC\_dj}}{10^6}\right)\cdot 365} \right] \; [years] \qquad (2.45)$$

2.4.2.3 Lifespan estimation by *Semi-empirical* method

Previous research in IK4-IKERLAN led to the development of a thorough semi-empirical lifetime model for a LFP BT cell to evaluate the capacity fade over the time by superimposing the effect of calendar and cycle life degradations [102]. This model is considered a semi-empirical one since it is based on experimental tests carried out to the cell combined with mathematical approximations on the physical variables that are considered.

The calendar life model considered takes into account the capacity fade caused in steady situation of the cell, influenced by the storage time, cell temperature and the SOC at which the cell is stored [107]. The capacity loss due to calendar life Q_{loss_cal} is calculated as follows:

$$Q_{loss\_cal} = \alpha_1 \cdot e^{\beta_1 \cdot Temp^{-1}} \cdot \alpha_2 \cdot e^{\beta_2 \cdot SOC} \cdot t^{0.5} \; [\%] \qquad (2.46)$$

where $Temp$ [°C] and SOC are the ambient temperature and the state of charge at which the cell is stored, t is time elapsed on storage and α_1, α_2, β_1 and β_2 are fitting coefficients.

On the other hand, the cycle life model accounts for the capacity fade of the battery due to the operation conditions during charging and discharging [104]. In this case, the effect of the C-rate has been neglected (when operating under the conditions specified by the manufacturer) while the effect of the DOD and the Ah throughput have been considered.

Heeding to the characteristics of the cell shown in figure 2.16 and figure 2.17 (values obtained from experimental tests), it can be clearly seen that the base cell shows atypical performance features when it comes to the full equivalent cycles (FEC) that they can perform depending on the DOD at which are cycled.
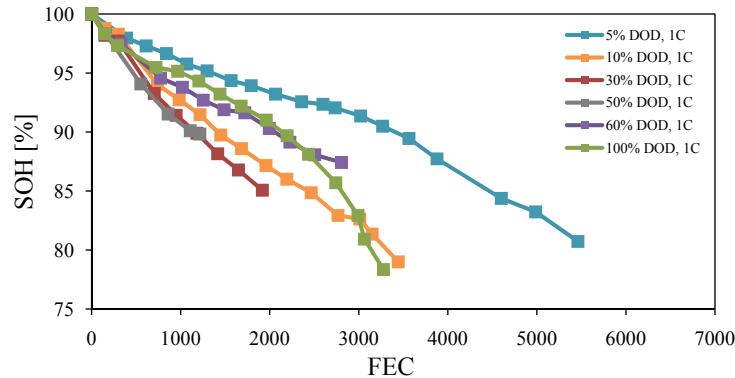
Figure 2.16: DOD vs. FEC curve considered for the cycle life model [104].
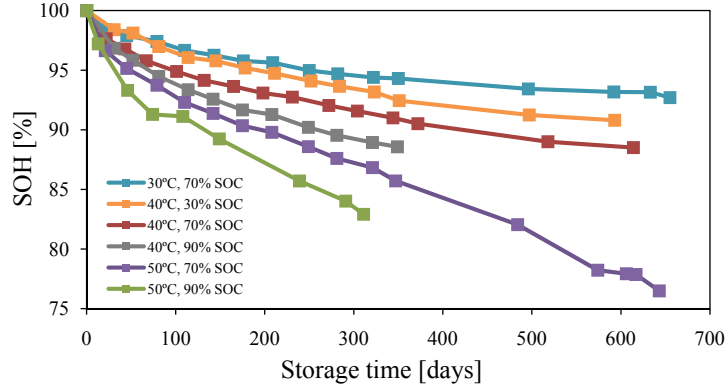
Figure 2.17: Storage conditions vs. time for the calendar model [104].

Therefore, the developed cycling model was split into two ranges [102], depending on the DOD vs. FEC curve shown in figure 2.16, as it can be seen in (2.47) and (2.48).

When $(10\% \leq DOD \leq 50\%)$:

$$Q_{loss\_cyc} = \left(\gamma_1 \cdot DOD^2 + \gamma_2 \cdot DOD + \gamma_3\right) \cdot Ah^{0.87} \ [\%] \tag{2.47}$$

When $(10\% > DOD > 50\%)$:

$$Q_{loss\_cyc} = \left(\alpha_3 \cdot e^{\beta_3 \cdot DOD} + \alpha_4 \cdot e^{\beta_4 \cdot DOD}\right) \cdot Ah^{0.65} \ [\%] \tag{2.48}$$

where Q_{loss_cyc} is the equivalent capacity fade caused by cycling, DOD and Ah represent the DOD at which the cycles are being performed and the Ah throughput (during the considered cycling period), respectively and γ_1, γ_2, γ_3, α_3, α_4, β_3 and β_4 are constant fitting coefficients.

Finally, the resultant total capacity loss Q_{loss} is calculated as follows [107]:

$$Q_{loss} = Q_{loss\_cal} + Q_{loss\_cyc} \ [\%] \tag{2.49}$$

The EOL was defined when Q_{loss} reaches the 10% and determined by experimental tests done to the BT cell [124]. The precision of this model has been thoroughly validated based on the methodology developed in IK4-IKERLAN and described in depth in [107] under different ageing conditions. For all the cases, the root-mean-square error (RMSE) prediction error calculated was below 1.4%.

2.5 Optimization by Genetic Algorithm

The Genetic Algorithm (GA) is a method for solving optimization problems based on natural selection, the process that drives biological evolution [125]. As mentioned in

section 1.5.2.1 the GA approach can be used as optimization solver instead of DP (or other methods based on cost-to-go or exhaustive search) when the addressed problem shows a complex structure with different optimization variables that interact among them for the system operation. Furthermore, since this is a stochastic method the approximation of the obtained solution to the optimal one will depend on how long the optimization is allowed to evolve.

The GA repeatedly modifies a population of individual solutions. At each step, the GA selects individuals at random from the current population to be parents and uses them to produce children trying to keep the best features for the next generation [89]. The structure of a GA has an iterative process throughout several phases [89, 125]:

Phase 1: a random initial population of *N* individuals (representing the search domain) is generated.

Phase 2: All the individuals are evaluated on a objective function *F* and ranked in ascending/descending.

Phase 3: fitness-based selection of best individuals. According to the evolutionary theory, the best individuals have the highest probability to join the next population.

Phase 4: Generation of new individuals. Phase 3 usually leads to a new set of individuals containing a higher number of "strong"solutions, whereas some of the weakest ones disappear. This intermediate set undergoes a renewal process consisting of three different steps:

- *Elite individuals* are the ones in the current generation with the best fitness values. These individuals automatically survive to the next generation.

- *Crossover individuals* are created by combining the vectors pair of parents.

- *Mutation individuals* are created by introducing random changes (or mutations) to a single parent.

Phases 2 through *Phase 4* are repeated as many times until the desired number of new generations is reached.

2.6 Multi-objective problem formulation

For most practical problems, related with complex systems containing several decision variables, the selection of an optimal solution is not an issue based on a single factor [23, 95]. Instead of that, it requires the analysis and weighing of different factors that have influence on the system's performance and which commonly are competitive and conflictive among them [125]. The resolution of these kind of problems is called multi-objective (MO) optimization where the optimal solution for a specific scenario is the one which fulfills each objective(s) at the desired value determined by the level of importance (or priority) assigned to the them while the other ones are penalized. The main advan-

tage of MO optimization is the possibility of evaluating the impact (or consequences) of the selected solution on the different objectives responding to a more practical conditions (*e.g.* efficiency, economic, operational) in a post-optimization analysis [126].

The mathematical description of a MO minimization problem is defined by [89]:

$$min \ F(X) = [f_1(X), f_2(X), ..., f_{m_{obj}}(X)] \quad X \in \Omega \tag{2.50}$$

subject to the constraints:

$$constraint_c > 0 \quad c = 1, 2, ..., n_{cstr} \tag{2.51}$$

where X is a vector of variables in a real N-dimensional space and Ω is the feasible solution space. There are m_{obj} objective functions and n_{cstr} constrains. There is no global optimal solution for all these objective functions. At each iteration, the population "evolves" toward a set of alternative solutions called non-dominated pareto-front optimal solutions. Each alternative optimal solution X^s has to satisfy for any feasible solution X simultaneously the following constraints [89, 123]:

$$\forall i \in \{1, 2, ..., m_{obj}\}, \ \ f_i(X^s) \le f_i(X) \tag{2.52}$$

$$\exists j \in \{1, 2, ..., m_{obj}\} \mid \ f_j(X^s) < f_j(X) \tag{2.53}$$

It means that there is no other feasible solution $X \in \Omega$ which is better with respect to all the objective functions than those involved in the set of alternative optimal solutions. Figure 2.18 illustrates the principle of MO optimization and pareto-front solutions for two objective functions.
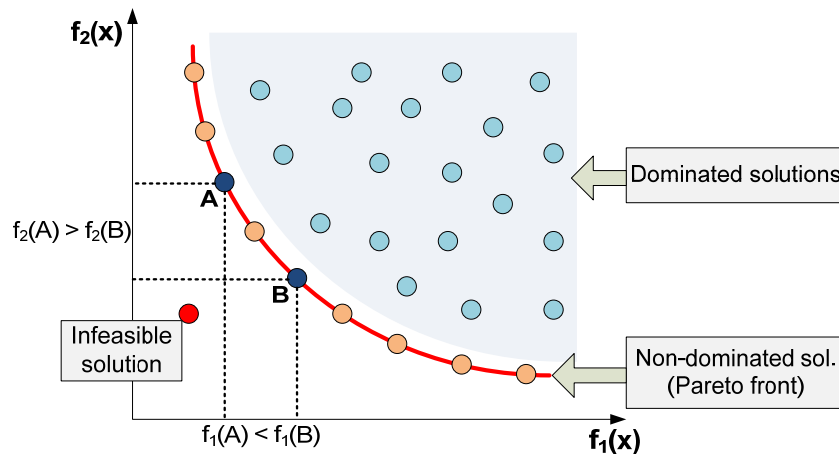
Figure 2.18: Representation of Pareto-front.

Considering the case studies proposed in this PhD thesis and the main elements in-

volved in their power-trains, three objective functions have been selected. The first two related with the daily operating cost of the HESS and the third one for the energy source depending on the case study (HET or HEB) as follows:

$$min \ OP_{Tcost} = [BT_{Tcost}, \ SC_{Tcost}, \ i_{Tcost}] \ \left[\frac{euros}{year} \right] \ \ i \in [Cat, \ Fuel] \tag{2.54}$$

where OP_{Tcost} is the total daily operating cost for the vehicle that has to be minimized.

2.7 Optimization methodology description

Taking into account the characteristics described in the previous section, it can be defined the analogy of the MO problem with the scenarios considered in this thesis. It means that a reduction on the energy absorbed from catenary (HET case) or fuel consumed during ICE operation (HEB case) results in a higher use of the ESS, hence an early degradation of it, and vice versa.

When a HESS is considered, the complexity to find the proper way to operate each single ESS is increased. As mention before, the BT pack is an important part of a hybrid power-train as alternative energy source and autonomy extender, where the lifetime and health of the cells will strongly depend on the operating behavior. On the other hand, despite the fact that for EDLCs a very long lifespan is considered, the proper operation of them (among suitable ranges of their electrical variables) will assure both health of the SC pack as well as the peak power regulation and energy harnessing during acceleration and regenerative braking phase, respectively.

If the factor of the HESS sizing is introduced, it can be noted that the EMS and the proper system's sizing are strongly related in order to find the suitable balance among the fulfillment of the application requirements, the ESS operating and health constraints as well as the economic objectives defined in each scenario. The economic issue becomes in an important decision factor to adopt a specific solution in more practical problems where the system has to show a competitive cost-benefit for both manufacturer and end-clients. This is the case of public transport vehicles where the agreement between manufacturer and owner can involve a long period of time (*e.g.* 10-15 years). On the one hand, during this period of time the manufacturer has to guarantee the correct vehicle operation (*e.g.* system's components maintenance or replacement). On the other hand, the purchase by the end-client is done at fleet level which implies several vehicles and a high investment. Therefore, it is clear that both technical and economic factors have to be evaluated to develop new solutions for HEVs.

In order to take into account the aforementioned factors, an optimization methodology is proposed as part of the contributions of this PhD thesis. Figure 2.19 depicts the flowchart of this methodology which has been defined in a generic way and will be characterized for each case study (HET, HEB) in chapters 3 and 4. The stages of the

methodology are detailed below [126].

1) The techno-economic characteristics and requirements of the scenario are defined. These characteristics will allow both to configure the power-train's elements (previously detailed in this chapter) and parameters of the EMS as well as to define different referential cost values in the economic model. On the other hand, the scenario's requirements are useful to determine the operating modes of the vehicle depending on the route profile or operating behavior needed (e.g. catenary-free zone, zero-emission zone, charging stations).

2) The GA is configured depending on the desired parameters: population size, number of generations, characteristics of selection, crossover and mutation. As defined in previous paragraphs, the aim of this methodology is to develop an integrated optimization of HESS sizing and energy management. Therefore, the individuals in the population will be characterized with the HESS sizing and energy/power targets for EMS (depending on the selected EMS).

3) In the technical requirements stage both BT and SC packs are configured (taking the values defined by individual i) based on the cells arrangement proposed in section 2.2.6 and 2.2.7, respectively. Then, the simulation of a complete daily route profile is carried out both to calculate the vehicle demand as well as the system's response based on the configured HESS and EMS. The ESS ageing analysis is done only in those cases when the system configuration and EMS fulfills the demanded power profile.

4) As stated in section 2.4.2 two ageing models were introduced and they will be evaluated in an iterative process to determine the SOH of the cell (updating the loss of capacity at each iteration) until reaching the EOL (SOH = 90% in this case). The loss of capacity will be updated in all the cells to obtain the available total capacity of the BT pack. This updated value will allow the assessment of the vehicle performance when the BT pack capacity decreases and the adaptation of the EMS to this behavior. Furthermore, the iterative process allows to assure that during all the time defined as lifespan estimation (independent of the selected ageing model) the HESS fulfills the vehicle demand (even when the cell has lost capacity). It is worth to mention that, in order to reduce the computational time, the operating profile for the BT pack will be extrapolated during 3 months (90 days) and then the next iteration will be evaluated.

5) The MO fitness function presented in (2.54) is evaluated by applying the economic model detailed in section 2.3 where whole vehicle lifetime is considered. For the individuals that do not fulfill the technical requirements of the applications a high cost is assigned to the objective functions in order to discard them.

6) As defined in section 2.5, steps 2-4 will be repeated until evaluating all the individuals in a generation and all the desired generations.

7) The optimization results are the set of alternative optimal solution. The selection of the suitable solution for the scenarios (HET or HEB) will be further explained in chapters 3 and 4, respectively.
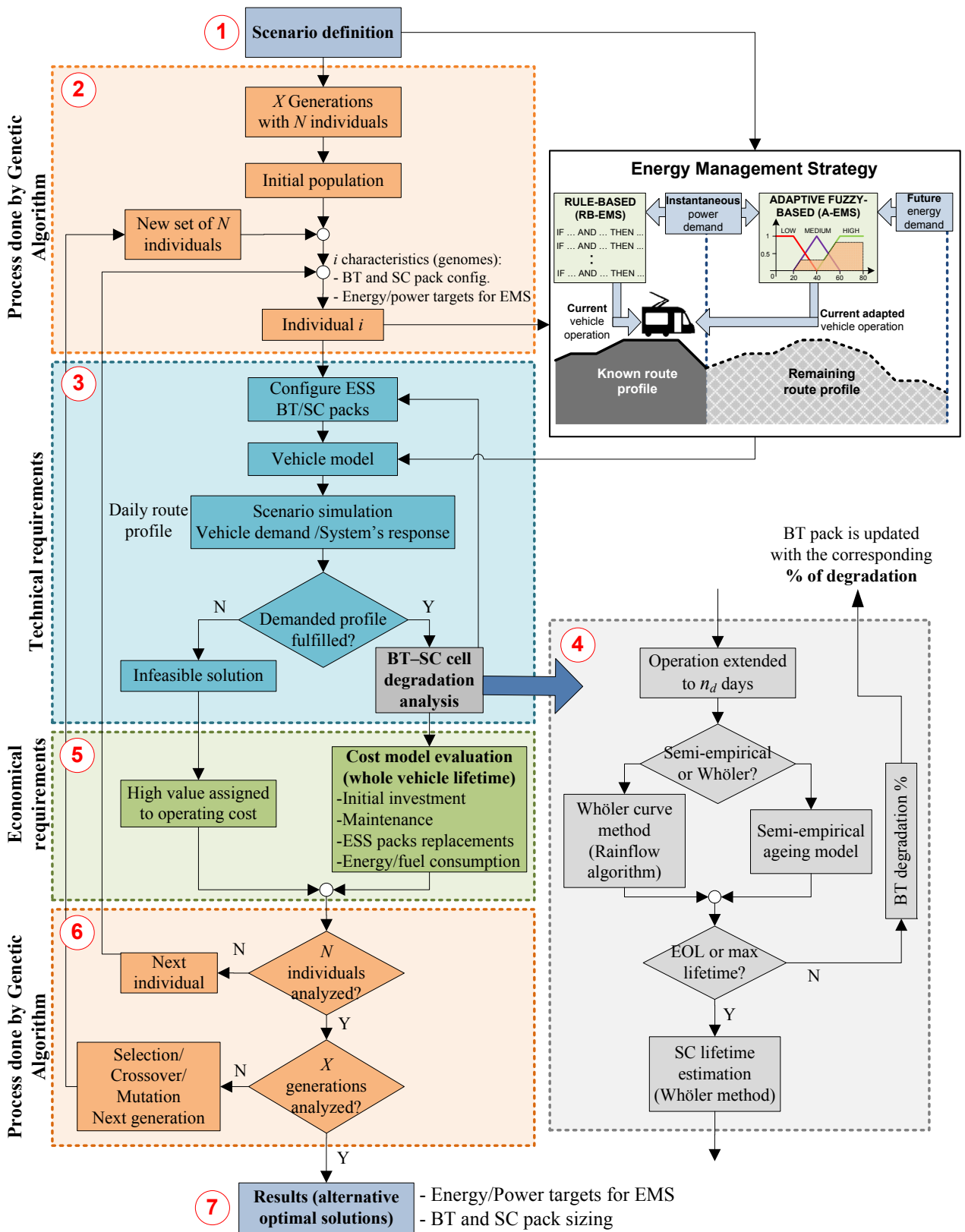
Figure 2.19: Optimization methodology for ESS sizing and vehicle operation.

2.8 Conclusions

In this second chapter the electrical and economic models for the HET and HEB scenarios have been presented. These models have been integrated in a simulation tool and serve as the basis of the present PhD work to evaluate either the performance of the developed EMS and the economic feasibility of the proposed solutions.

Firstly, the generic electrical models of the main elements involved in the power-train have been detailed. Considering that the study proposed in this thesis is focused on analyzing the power flow through the power-train's elements and the energetic conditions during vehicle operation, relatively basic electrical models were selected. These simplified models aim to reduce the computational effort mainly during the optimization process while allowing to be controlled by power targets coming from the EMS.

Secondly, cost models have been introduced to allow evaluating the economic performance during vehicle operation both in short term (daily operation) as well as in long term view (whole vehicle lifetime). The economic model for the HESS includes the replacement factor determined by the degradation behavior during operation. This allows defining the relation between the current HESS operation and the future need of replacements by translating it to economic terms that can be used to take decisions (in the design stage of the vehicle) about the proper HESS sizing which balance the technical requirement and desired economic profitability.

For long term analysis the lifespan estimation of the HESS is an important factor, therefore, in this chapter two ageing models have been introduced. On the one hand, the Whöler-curve based method which needs relatively few information about cell ageing (number of available cycles at different DODs) that can be provided for some cell manufacturers or obtained by experimental tests. On the other hand, a Semi-empirical ageing model (previously developed and validated in IK4-IKERLAN) and which requires more cell-dedicated experimental information and mathematical developments. The clear difference between them lies on the lifetime estimation accuracy where the semi-empirical model shows the best fitted degradation forecasting. However, other factors to take into account are the time needed for the models development and the cost linked to the experimental tests required for each one, where the Whöler based method can be seen as a better choice. Hence, the economic evaluation (considering different ageing models) is useful for the vehicle manufacturer to determine the suitable balance between investment cost during design stage (related to the ESS characterization) and the expected improvements (and resulting cost) on vehicle performance.

Finally, a methodology for the integrated optimization of HESS sizing and EMS has been proposed. Considering the available energy sources in the vehicle (BT and SC packs, genset or catenary) as well as the competitive and conflictive behavior among them when the optimal operation has to be selected, a MO problem has been proposed for both case studies (HET and HEB). The technical requirements evaluation is carried out, for

a daily route profile, with an iterative process that calculates the loss of capacity in the BT cells (due to their operation) and updates the available capacity of the BT packs at each iteration. This process shows two advantages: it will allow analyzing the behavior of the EMS when the available capacity of the BT pack is decreasing and; it does a prior selection of the admissible solutions guaranteeing that these fulfill the vehicle demand even when the BT pack is close to its EOL.

The optimization results is a set of alternative optimal solutions expressed in economic terms where each solution offers different HESS configurations and energy/power targets for the EMS. This is an advantage of the MO approach in the proposed methodology where the selection of the most suitable solution for a scenario can vary depending on the technical or economic priority desired for an objective while evaluating the impact of this choice on the other objectives and system's parameters.

3

Case study 1: Hybrid Electric Tramway

3.1   Case study 1: Hybrid Electric Tramway

In this chapter the energy management approach proposed in this PhD thesis will be introduced and applied on the Hybrid Electric Tramway (HET). In this scenario a real case study has been selected: Tramway of Seville (*Metro Centro*), which operates in zones with and without catenary and currently considers a single ESS based on Supercapacitors. Therefore, in the second section of this chapter the scenario and the configuration of the tramway's power-train are described and some technical data related to it are detailed.

In the third section of this chapter, the energy management approach for this scenario is described. Firstly, taking into account the current operation modes of the tramway, an improved Rule-based EMS (RB-EMS) is proposed in order to include the concept of HESS (by including the BT pack). Therefore, the current operation modes are maintained but the EMS will define the power demand split rate on the available sources (catenary, SC and BT pack) depending on the power and energy requirements and energetic conditions of the vehicle.

Then the adaptive EMS (A-EMS) approach based on fuzzy logic, which forms part of the contributions of this PhD thesis, is applied on the HET scenario. The A-EMS applies a sliding forward window which allows to estimate the future energy consumption in tramway operation. This way, the current targets of the available sources (BT and SC packs) are adapted either to fulfill the instantaneous traction power demand and as well as to take into account the future energy requirements, thus, improving the energy harnessing of the available on-board sources.

In the fourth section of this chapter, the MO problem proposed in chapter 2 (see section 2.6) is adapted to the HET case and the main constraints and techno-economic referential values are described.

In the fifth section, the optimization methodology proposed in chapter 2 is applied on both RB-EMS and A-EMS. At this point the current solution in the tramway of Seville (ESS based on supercapacitors) will be taken as base scenario to determine the techno-economic improvements that can be obtained with the HESS and optimized energy management approach proposed in this thesis. Furthermore, the scenario of unscheduled-stops operation will be introduced to evaluate the system behavior under these non-considered conditions in the most critical zone (catenary-free zone). The selected alternative optimal solutions and resulting vehicle performance from the considered approaches (RB-EMS and A-EMS) as well as the base scenario will be compared considering the technical, economic and energy efficiency factors. Finally the conclusions of this chapter will be presented.

3.2   Scenario overview

The scenario analyzed in this chapter is based on experimental data and driving cycle of the Tramway of Seville (figure 3.1) designed and developed in collaboration between

the traction equipment manufacturer CAF Power & Automation and IK4-IKERLAN Technology Research Center. The tramway is composed of bidirectional units made up of five articulated bodies resting on three boogies (the end ones are motor bogies and the intermediate one is a trailer bogie).

The tramway reaches a maximum speed of 50 km/h and has a maximum capacity of 275 passengers. The tramway traction system supplies the two bogies via its inverter box. Each box consists of two independent inverters that supply the traction motors (one per wheel). Each boogie has four traction motors. Each traction converter box has a rated power of 200 kW with supply voltage of 750 VDC from the catenary line (connected through the pantograph).

Figure 3.1: Tramway in the city center of Seville.

The energy and power requirements used as case study correspond to a section of the city route with several stops and a pedestrian zone with catenary-free operation (500 m) and speed limit of 15 km/h (in the catenary-free zone). Figure 3.2 shows the tramway speed and power demand (in the DC bus) profiles provided by the manufacturer (CAF P&A) which have been taken as starting point for the EMS design. This profile considers an average constant power consumption (during the entire route) of 40 kW due to auxiliary loads (fans, air conditioning, lights, etc). The shadowed sections correspond to the catenary-free zones.

Figure 3.3 depicts the power-train's architecture in the tramway. The black line elements represent the current configuration with an on-board SC-based ESS. Taking into account the aim proposed in this PhD thesis about considering HESS (combining BT and SC), in this scenario a BT pack will be included. Therefore, the red line elements represent the additional BT pack considered for the HESS solution.

As mention before, the current tramway solution has an ESS based on supercapacitors where two main control modes can be highlighted [72]:

-*Power control mode*: The DC/DC converters of the SC packs are controlled in power mode during the charging process (at a charging station) and during their operation as
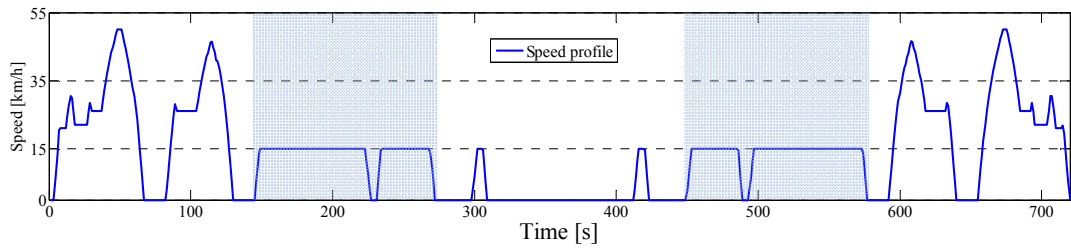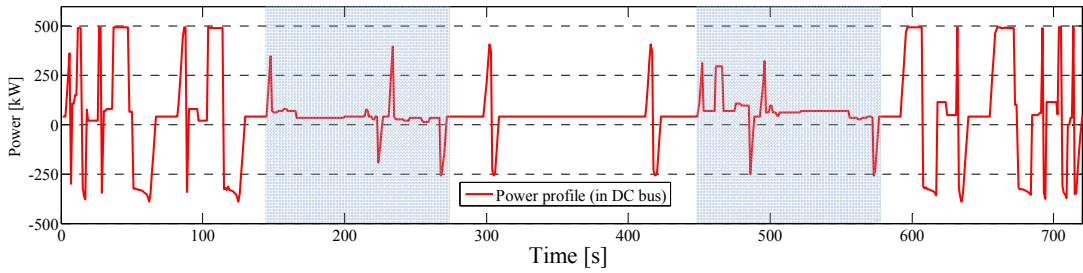
(a) Speed profile.

(b) Power profile.

Figure 3.2: Considered profiles for HET operation.
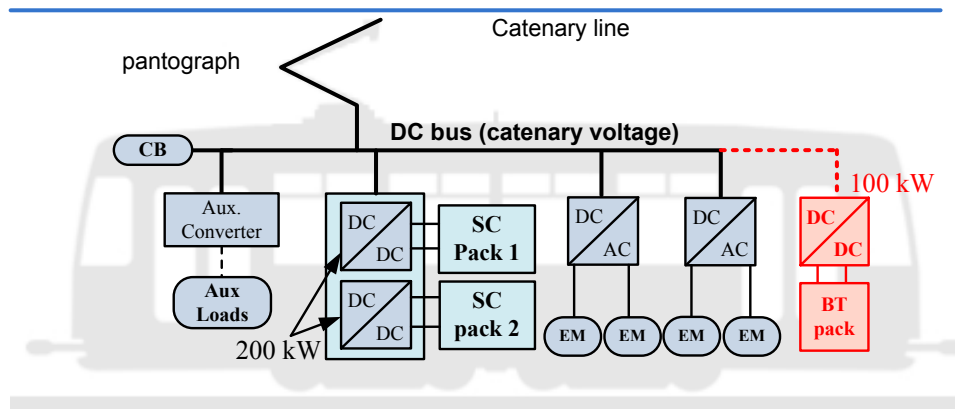
Figure 3.3: Block diagram of the power-train's architecture in the tramway.

catenary support device (smoothing catenary power peaks during traction periods). It is worth to mention that a charging station corresponds to a stop before entering to a catenary-free zone. In these cases the EMS defines the power target in the DC/DC converters (which is then transformed into a current target using the SC pack voltage). In these cases (charging process and traction within catenary zone) the catenary line is in charge of imposing the voltage in the DC bus and will react to the voltage drop variations to stabilize it (by injecting current to the DC bus).

-*Bus voltage control mode*: The DC/DC converters of the SC packs are controlled in voltage control mode during regenerative braking phase (within a zone with catenary) in order to stabilize the DC bus voltage and to maintain it into the appropriate range.

On the other hand, in catenary-free zone, the DC/DC converters of the SC packs are controlled in voltage control mode either in traction and regenerative braking phase cause these are the only energy source available for the vehicle operation. Therefore, the SC packs are in charge of regulating the DC bus voltage to allow the proper operation of the devices connected to it.

These modes have been used as basis to develop the improved EMS by including the BT pack operation which will be later explained in section3.3.

Table 3.1 summarizes the main technical characteristics related to the power-train's elements. As defined in section 2.2.6, the BT pack is composed of an arrangement of single cells in series (to compose a string) and several strings in parallel. Therefore, in the first case the aim is to increase the total voltage of the BT pack U_{BT} while in the second one total capacity (in kWh) is increased. However, in more practical applications the voltage of BT pack is imposed by the admissible operating range of the DC/DC converter located between the BT pack and the DC bus [26]. In other cases, when the BT pack is directly connected to the DC bus, this last will define the required voltage to the pack [42]. Considering this fact, in the HEB case the number of cells in series has been considered as constant, therefore, the sizing process will defined the number of branches in the BT pack (m_{BT}). Similarly, for the SC pack the same approach has been applied. During the BT and SC packs sizing the cells described in table 2.1 have been used as base ones to built up the packs.

Table 3.1: Technical characteristics of the HET.

	Characteristics	Description
General	Number of articulated bodies	5
	Number of bogies	3
Battery pack	Number of cells in series	160
	Maximum voltage	528 V
	DC/DC converter	100 kW / 0.95
Supercapacitor pack	Number of cells in series	178
	Maximum voltage	480.6 V
	DC/DC converter	2x200 kW / 0.95

3.3   Energy Management Strategies

In order to define the appropriate way to split the power demand from the tramway during operation either to fulfill the traction demand as well as to harness the energy recovered during regenerative braking phase, an EMS has to be developed. This EMS will be in charge of defining the proper power targets to the DC/DC converters of the BT and SC packs. In this chapter two EMS are proposed, on the one hand, a RB-EMS [123] (see section 3.3.1) which consider different operation modes depending on the route conditions (catenary zone, catenary-free zone and charging station).

On the other hand, a novel adaptive EMS based on fuzzy logic [35] is proposed as improvement over the common rule-based approach for the suitable management and operation of multiple on-board energy sources in road transport applications. This A-EMS approach (detailed in section 3.3.2) constitutes the main contribution of this PhD thesis that, together with the optimization methodology proposed in chapter 2, will define the optimal operation and sizing of a HESS (combining BT and SC) for applications in tramway vehicles.

This adaptive approach considers, in addition to the instantaneous conditions of the system (available energy in the HESS, power demand from the tramway), information about the future energy demand of the vehicle by applying a sliding forward window strategy. This strategy allows estimating the future energy consumed/absorbed from/in the BT and SC packs. This way, the operation targets for the BT and SC packs are adapted (update of the power split rate) to fully supply the instantaneous energy consumption but considering the future energy demand (increasing/decreasing the instantaneous consumption from the BT and/or SC pack). The aim is to increase the energy efficiency of the HESS with a proper harnessing of the on-board sources and the available energy from the vehicle (mainly in the regenerative braking phase). Figure 3.4 depicts the main concept adopted for the development of the EMSs.
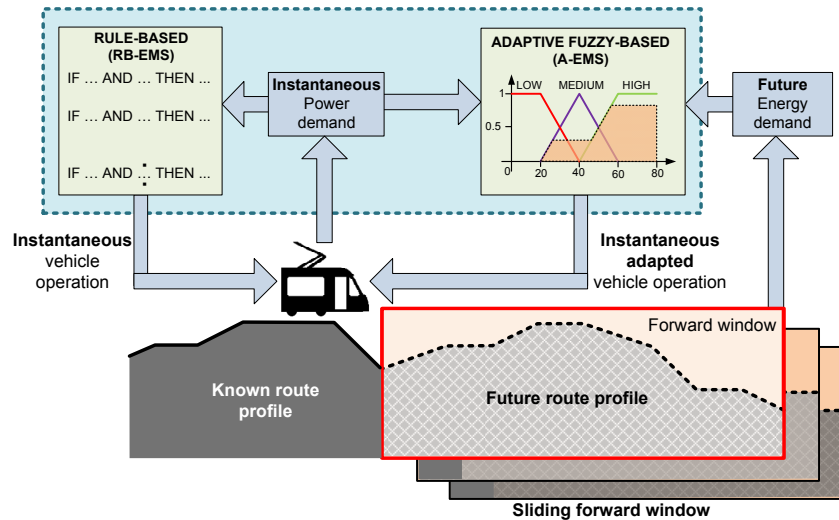
Figure 3.4: RB-EMS and A-EMS approaches for vehicle operation.

3.3.1 Rule-Based strategy

Based on the operation requirement previously introduced in section 3.2 about the operation of the tramway in zones with and without catenary and considering that two storage systems are working simultaneously all the time (BT, SC), different operation modes can be defined for the tramway operation [122, 123, 127]:

- *Energy charging mode (ECM)*

When the tramway is stopped at a charging station (before entering a catenary-free zone) the SC pack must be quickly charged using a power control strategy (by defining a power target P_{SC} [kW] to its DC/DC converter). The charging process of the SC pack is carried out when tramway is stopped at a constant power rate. The BT pack is not charged in this mode in order to avoid the high currents that may early degrade the BT cells. Considering that the tramway is into a zone with catenary, this will be in charge either of supplying the energy required by the auxiliary loads as well as to impose and maintain the voltage of the DC bus.

  - Catenary support mode (CSM)

While the tramway is running in a zone supplied by an overhead-line, the HESS plays a double role. On the one hand, the BT pack will provide energy supply assistance for traction (working with power targets within the recommended discharging rates based on the C-rate limitation, see table 2.1) or will be charged (in case of needed) taking energy from the catenary, while the SC pack will reduce the power peak during acceleration phases. On the other hand, during regenerative braking phase, the BT pack will store energy from breaking (working with power targets within the recommended charging rates based on the C-rate limitation, see table 2.1) with power peak regulation by the SC pack.

It is worth to mention that in CSM, the EMS provides power targets for the BT and SC pack operation. During traction power demand ($P_{DEM} \geqslant 0$) the catenary injects the remaining power that has not been provided by the HESS to fully supply the tramway power demand. In this case study it has been defined as condition that the energy will not be injected back to the catenery during the regenerative braking phase in order to avoid the voltage variations in the catenary line. In the regenerative braking phase ($P_{DEM} < 0$), the remaining energy that has not been absorbed in the HESS is absorbed by the crowbar (CB) resistance (P_{CB} [kW]) and dissipated as heat. As defined in section 3.2, during traction phase it has been assumed that the catenary will impose and regulate the voltage in the DC bus. Otherwise, during regenerative braking phase, the SC pack will be in charge of controlling the voltage in the DC bus (bus voltage control mode).

  - Autonomous mode (AM)

In this mode the tramway operates in a catenary-free zone and consequently, the HESS must fulfill the energy and power demand during the travel. In AM, the EMS only provides the power target for the BT pack operation (P_{BT} [kW]) in traction and regenerative phase. During traction ($P_{DEM} \geqslant 0$) the SC pack injects the remaining power to fully supply the tramway power demand. On the other hand, the SC pack absorbs the remaining power during regenerative phase ($P_{DEM} < 0$). In case of power surplus during the regenerative phase, it is absorbed in the crowbar resistance. With the aim of maintaining the same operation concept related to the SC-based tramway proposed in [72] (which has been assumed as case study for this chapter), it has been defined that the DC/DC converter of the SC pack will control the voltage of the DC bus (bus voltage control mode) either

in traction and regenerative braking phase.

The RB-EMS defines the power targets for the BT pack (P_{BT} [kW]) and SC pack (P_{SC} [kW]) as well as the power requested to the catenary (P_{CAT} [kW]) during the tramway operation depending on: the zone where the vehicle is running (operation modes), and the power demand (P_{DEM} [kW]) for traction ($P_{DEM} \geqslant 0$) or regenerative ($P_{DEM} < 0$) phase. Figure 3.5 depicts the hierarchical structure of the proposed RB-EMS.
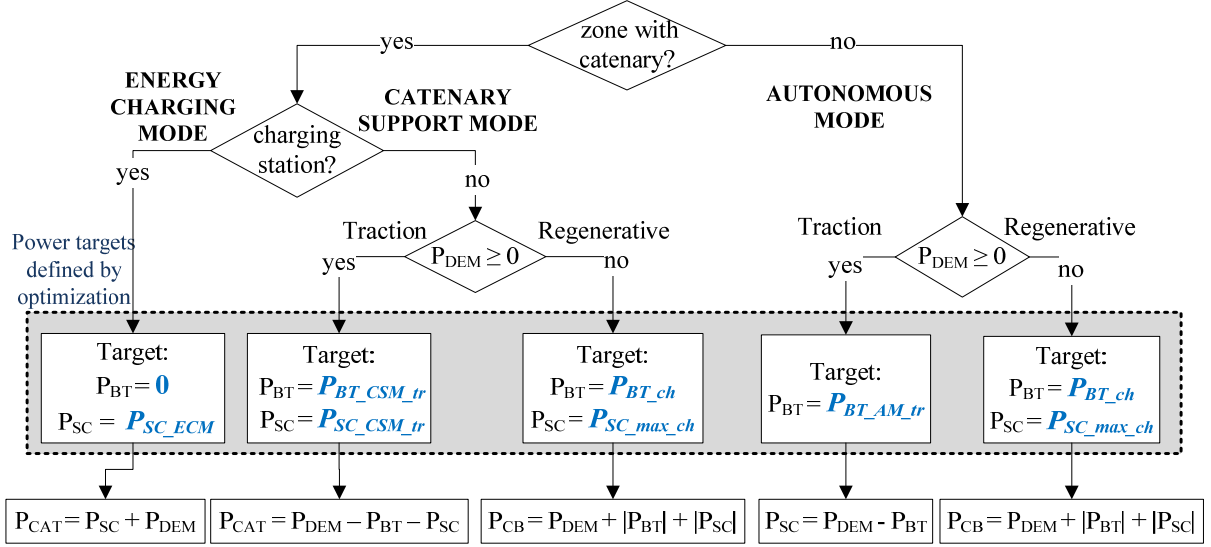
Figure 3.5: Hierarchical structure of the RB-EMS approach.

where P_{SC_ECM} [kW] is the power target for charging the SC pack in *ECM*. $P_{BT\_CSM\_tr}$ [kW] and $P_{SC\_CSM\_tr}$ [kW] are the power targets during traction in *CSM* for BT and SC packs, respectively. P_{BT_ch} [kW] and $P_{SC\_max\_ch}$ [kW] are the power targets used during regenerative braking phase in *CSM* for BT and SC packs. $P_{BT\_AM\_tr}$ [kW] and P_{BT_ch} [kW] are the power targets during traction and regenerative in *AM* for the BT pack. The aforementioned variables are related to the following constraints:

- For BT pack operation:

$$0 \leq P_{BT\_CSM\_tr} \leq P_{BT\_dch} \tag{3.1}$$

$$0 \leq P_{BT\_AM\_tr} \leq P_{BT\_max\_dch} \tag{3.2}$$

where $P_{BT\_max\_dch}$ [kW] ($P_{BT\_max\_dch} > P_{BT\_dch}$) is the maximum power target for discharging the BT pack (in this scenario the maximum power of the DC/DC converter linked to the BT pack, 100 [kW]). P_{BT_dch} [kW] and P_{BT_ch} [kW] are the power target limitations related to the C-rate for BT pack in discharging and charging calculated as follows:

$$P_{BT\_dch} = \frac{(V_{nom\_BTcell} \cdot n_{BT}) \cdot (I_{1C\_BTcell} \cdot C_{rate} \cdot m_{BT})}{10^3} \ [kW] \tag{3.3}$$

$$P_{BT\_ch} = -P_{BT\_dch} \ [kW] \tag{3.4}$$

being I_{1C_BTcell} [A] and C_{rate} the nominal current of the BT cell at 1C of discharge rate (2.3 A) and the C-rate limitation (3.5 C) detailed in table 2.1, respectively.

It is worth mentioning that, both P_{BT_dch} [kW] and P_{BT_ch} [kW] depend on the BT pack sizing. It means the cells arrangement in the BT pack (n_{BT} cells in series in a string and m_{BT} strings in parallel) as shown in section 2.2.6. Therefore, during the sizing process these power targets will be adapted to take advantage of the available power and energy in the defined BT pack.

- *For SC pack operation:*

$$0 \leq P_{SC\_ECM}, \ P_{SC\_CSM\_tr} \leq P_{SC\_max\_dch} \tag{3.5}$$

being $P_{SC\_max\_dch}$ [kW] and $P_{SC\_max\_ch}$ [kW] the maximum power target for discharging and charging the SC pack (in this scenario the maximum power of the DC/DC converter linked to the SC pack, 400 kW).

3.3.2 Adaptive fuzzy-based strategy

In a HET with multiple energy sources which includes a HESS where two storage systems are operating simultaneously all the time, the suitable power split among the available energy sources becomes in a complex problem. Indeed, there are several variables to take into account in order to defined the proper EMS performance: power demand for traction (P_{DEM} [kW]), state of charge of BT and SC pack (SOC_{BT} [%], SOC_{SC} [%]), future information about the energy consumption in BT and SC ($DeltaE_{BT}$ [kWh], $DeltaE_{SC}$ [kWh]), zones with and without catenary (Cat_{EN}) or charging stations (CH_{ST}). Besides it is important to take into account that the RB-EMSs, where predefined operating targets are considered, do not allow to operate the vehicle sources in their most efficiency and best performed rates (depending on the operating conditions) because of their fixed values during the whole route profile.

However, the fuzzy theory [80] can be highlighted as a noteworthy approach to deal with this kind of complex problem avoiding most of the mathematical stiffness during the modeling of the energy management problem. As described in section 1.5.1.2, the fuzzy approach allows to represent the main control variables and desired operation by means of more intuitive, practical and user-language oriented terms while obtaining a non-linear variable response depending on the operating conditions.

Therefore, with the aim of developing an adaptive EMS (A-EMS) able to consider

several inputs while reducing the complexity in the problem formulation for power split among the available energy sources (catenary, BT and SC packs), an EMS based on fuzzy logic has been proposed [35]. Figure 3.6 depicts the structure of the proposed fuzzy strategy which applies several sets of rules ($Rules_{SC1,2}$ and $Rules_{BT1,2}$) in order to define the power targets for the BT (P_{BT} [kW]) and SC (P_{SC} [kW]) pack operation.
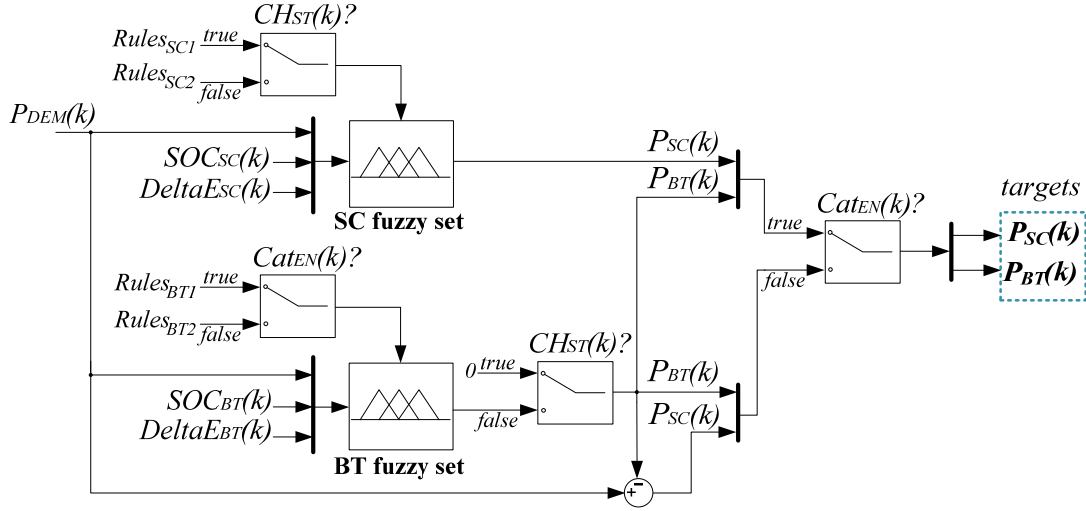
Figure 3.6: Proposed fuzzy approach for the A-EMS.

Section 3.3.2.1 describes the strategy to estimate the future energy consumption in the HESS by means of a sliding forward window. Section 3.3.2.2 describes the fuzzy sets and rules applied in the strategy.

3.3.2.1 Forward window calculation

The proposed forward window (FW) allows estimating the power split and the stored/-supplied energy between the BT and SC pack in the futures stages of the route. The FW is built based on information of the power demand profile. For the tramway case this profile is known in advance (based on the speed profile of the route) from the beginning of the journey (figure 3.2(a)), which allows calculating the FW_k related to each discrete step k.

In order to maintain the current management structure for the tramway operation, the same operation modes defined in section 3.3.1 have been applied during FW calculation. At a k discrete step, the window takes the power demand information within the n_{FW} forward steps from the power demand profile of the route (figure 3.2(b)). The strategy applied in the FW to estimate the stored/supplied energy in/from the BT and SC packs is depicted in figure 3.7 and it shows, with an example, the calculation of these estimated values. This strategy corresponds to the one previously introduced in section 3.3.1 which considers different power targets to estimate the stored/supplied energy depending if the tramway is running in a zone with catenary (CSM) or without catenary (AM).
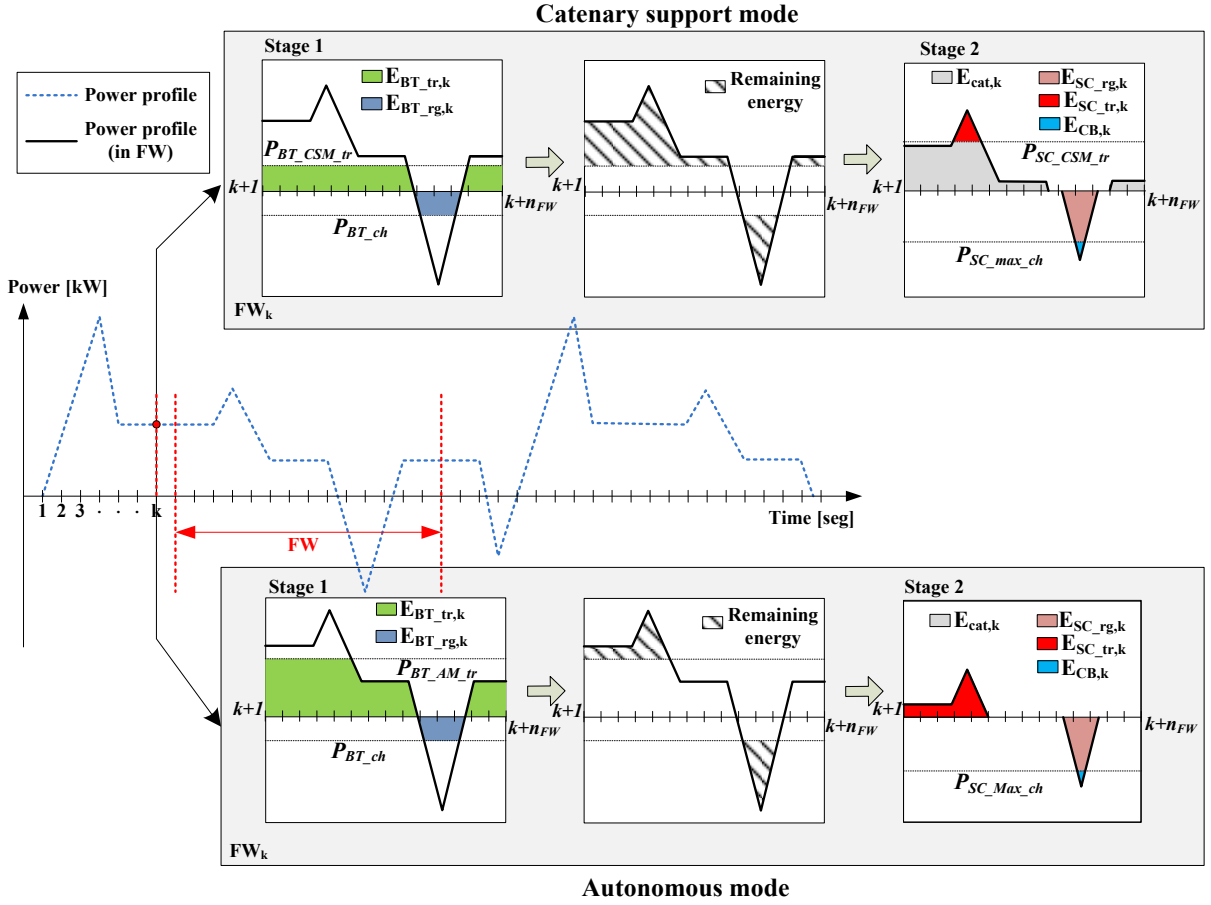
Figure 3.7: Forward window strategy for energy consumption estimation.

As shown in figure 3.7, the applied strategy follows a sequence to split the energy demand. In traction ($P_{DEM} \geqslant 0$) the sequence is: BT pack ($E_{BT\_tr,k}$ [kWh]), catenary ($E_{Cat,k}$ [kWh]) and SC pack ($E_{SC\_tr,k}$ [kWh]). In regenerative case ($P_{DEM} < 0$) the sequence is: BT pack ($E_{BT\_rg,k}$ [kWh]), SC pack ($E_{SC\_rg,k}$ [kWh]) and the surplus is dissipated by the crowbar resistance ($E_{CB,k}$ [kWh]).

Here, $E_{BT\_tr,k}$ [kWh] and $E_{BT\_rg,k}$ [kWh] represent the estimation of energy supplied or stored in the BT pack in FW_k, respectively. Similarly, $E_{SC\_tr,k}$ [kWh] and $E_{SC\_rg,k}$ [kWh] represent the estimation of energy supplied or stored in the SC pack, respectively. $E_{Cat,k}$ [kWh] and $E_{CB,k}$ [kWh] are the estimation of energy provided by the catenary and absorbed by the crowbar resistance, respectively.

In the *catenary support mode* (figure 3.7) the strategy calculates the stored/supplied energy in two stages:

- **Stage 1**: In traction case ($P_{DEM} \geqslant 0$), the strategy considers the power target $P_{BT\_CSM\_tr}$ [kW] (3.1). In regenerative case ($P_{DEM} < 0$), the power absorbed in the BT (P_{BT_ch} [kW]) is limited by the C-rate for charging the pack (maximum 3.5

C) as defined in (3.4).

- **Stage 2**: In traction case ($P_{DEM} \geqslant 0$), the energy demand that has not been satisfied yet is split between the SC pack and the catenary. The target $P_{SC\_CSM\_tr}$ [kW] has been defined order to reduce the power peak requested to the catenary. In regenerative case ($P_{DEM} < 0$), SC pack operates at $P_{SC\_max\_ch}$ [kW] which is the maximum power target for charging (in this scenario set at the maximum power of the DC/DC converter linked to the SC pack, 400 kW). The energy surplus will be absorbed by the crowbar system ($E_{CB,k}$ [kWh]).

In *autonomous mode* (figure 3.7), the same two stages have been defined (with different power targets):

- **Stage 1**: In traction case ($P_{DEM} \geqslant 0$), the power and energy demand have to be supplied only by the HESS. Therefore, the BT pack will operate at the power target $P_{BT\_AM\_tr}$ [kW] to provide as much energy as possible from the BT pack (3.2). In regenerative case ($P_{DEM} < 0$), it is applied the same power target (P_{BT_ch} [kW]) as in *catenary support mode* for charging the BT pack.

- **Stage 2**: In traction case ($P_{DEM} \geqslant 0$), the remaining energy is supplied by the SC pack. In regenerative case ($P_{DEM} < 0$), the same power target as in **Stage 2** of CSM is considered ($P_{SC\_max\_ch}$ [kW]). The aim is to minimize the lost energy in crowbar, considering that the tramway is running in a zone where the HESS has to fully supply the power/energy demand. For this reason, it results important storing as much energy as possible for traveling to the next zone with catenary and even to be able of overcoming unexpected events as unscheduled stops or delays in the catenary-free zone. As in CSM, the energy surplus will be absorbed by the crowbar system ($E_{CB,k}$ [kWh]).

This way, the energy variation in FW_k for the BT and SC packs at the discrete step k is calculated as follows:

$$DeltaE_{BT}(k) = E_{BT\_tr,k} - E_{BT\_rg,k} \ [kWh] \tag{3.6}$$

$$DeltaE_{SC}(k) = E_{SC\_tr,k} - E_{SC\_rg,k} \ [kWh] \tag{3.7}$$

Analyzing the dynamic of the power profile in the scenario proposed in this chapter, it can be noted that a "short time" FW could not include relevant information about the energy requested to the BT pack. Otherwise, a "long time" FW could include several variations in the dynamic related to the SC pack, hence; it would be difficult to interpret the value of $DeltaE_{SC}$ [kWh] by the linguistic terms. After several simulation tests a **FW**

size of 20 discrete steps has been defined. This way, the FW is slid and calculated for each discrete step k in the power demand profile.

As explained before, the power targets for the strategy are applied depending on the zone where the tramway is running (with or without catenary). For this reason, **the FW is resized when it is approaching to the end of a zone, avoiding the overlapping with the next zone (with other power targets to the BT and SC pack)**. In order to maintain the operation modes proposed in the previous section, in the *energy charging mode* the FW is not applied because in this stage only the SC pack is charged and the tramway is stopped. Figure 3.8 depicts the sliding and resizing window concept applied in the HET.
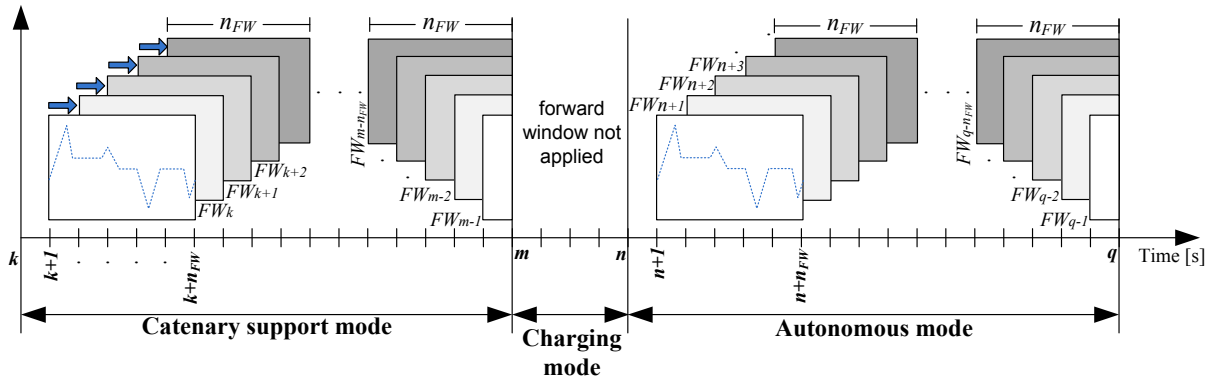
Figure 3.8: Sliding and resizing window concept.

The FWs are calculated previously using the power demand profile (figure 3.2(b)) to obtain the vectors $DeltaE_{BT}$ [kWh] and $DeltaE_{SC}$ [kWh]. However, during simulation the specific values for $DeltaE_{BT}(k)$ [kWh] and $DeltaE_{SC}(k)$ [kWh] have been obtained by interpolating the traveled distance (using look-up-tables). This is because during travel the tramway may have delays (due to unscheduled events), while the traveled distance will remain constant.

3.3.2.2 Description of the BT and SC Fuzzy sets

The fuzzy sets are based on the *Mamdani* Fuzzy Inference System (FIS) (see appendix A) [80]. The fuzzy sets define the power targets $P_{BT}(k)$ [kW] and $P_{SC}(k)$ [kW] for the BT and SC pack operation, respectively. It is worth to denote that the output of the **SC fuzzy set** is only considered when the tramway is running in a zone with catenary. Otherwise, in the catenary-free zone, the SC pack operates as power peak regulator (acceleration/braking) as explained in the strategy in the previous section (figure 3.7). The membership functions for each input/output in the FIS are depicted on figure 3.9. Triangular shapes have been defined with crossing in 0.5 in order to obtain symmetrical and smoothed transition among the membership functions.

The linguistic terms which represent the membership functions have been defined as

(a) HET power demand.

(b) SC power target.

(c) BT pack SOC.

(d) SC pack SOC.

(e) BT power target.

(f) Energy variation in BT and SC.
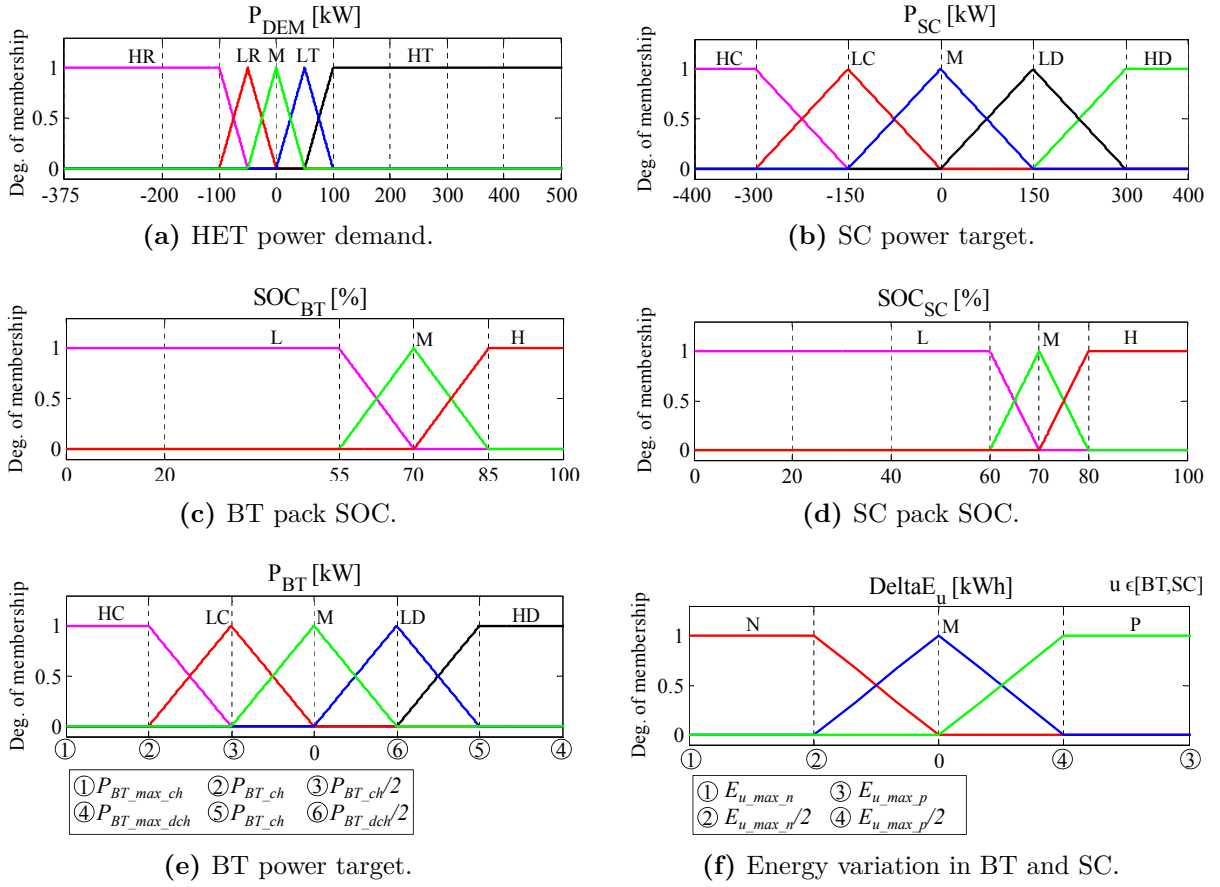
Figure 3.9: Membership functions applied on HET case study.

follows:

- P_{DEM}: (HR) High Regenerative; (LR) Low Regenerative; (M) Medium; (LT) Low Traction and (HT) High Traction.

- SOC_{SC},SOC_{BT}: (L) Low; (M) Medium and (H) High.

- $DeltaE_{SC}$, $DeltaE_{BT}$: (N) Negative; (M) Medium and (P) Positive.

- P_{SC}, P_{BT}: (HC) High Charging; (LC) Low Charging; (M) Medium; (LD) Low Discharging and (HD) High Discharging.

For the input P_{DEM} [kW] (figure 3.9(a)), the membership functions LT and LR have been selected around the average values 50 kW and -50 kW, respectively. The membership functions HT and HR have been defined for the maximum power peak during the acceleration and braking, respectively.

For the output P_{SC} [kW] (figure 3.9(b)), the LD and HD membership functions are intended to reduce the power peak requested to the catenary (maintaining the power peak

from catenary below 350 kW) during the tramway acceleration. On the other hand, LC and HC membership functions are intended to absorb as much energy as possible in the regenerative braking phase and avoiding losing it as heat in the crowbar (increasing the energy efficiency).

For the input SOC_{BT} [kW] (figure 3.9(c)), the membership function M has been defined between 55-85% to avoid deep discharges and to maintain enough energy stored in the BT pack in case of unscheduled events or delays during the travel (mainly in the catenary-free zone). Moreover, for the input SOC_{SC} [%] (figure 3.9(d)), the membership function M is narrower (60-80%) than the one in SOC_{BT} [%] since the energy stored in the SC pack is lower than in the BT pack and the power peaks in acceleration and/or braking have a greater impact on the SOC_{SC} [%].

For the output P_{BT} [kW] (figure 3.9(e)), the values of $P_{BT\_max\_dch}$ [kW] and $P_{BT\_max\_ch}$ [kW] are set according to the maximum peak power allowed in the DC/DC converter (see table 3.1). On the other hand, P_{BT_dch} [kW] and P_{BT_ch} [kW] are calculated in (3.3) and (3.4), respectively. As explained in section 3.3.2.1, these values are set once the sizing of the BT pack is configured. It allows obtaining the target for the BT pack taking advantage of the available power range, which varies depending on the pack sizing.

For the input $DeltaE_{BT}$ [kWh] (figure 3.9(f)), the membership function P denotes that the estimation (in the FW) of supplied energy is greater than the estimation of stored energy. The fuzzy EMS tries (by means of the defined rules) to reduce the instantaneous consumption from the BT pack to be prepared for a possible increase in the energy demand (related to the BT pack). The N membership function represents the opposite case, when the estimation of stored energy is greater than the estimation of supplied energy. In this case the fuzzy EMS aims to increase the instantaneous consumption from the BT pack. The M membership function allows to decide about charging (from regenerative braking or catenary) or discharging the BT pack considering the state of the other inputs (SOC_{BT} [%], P_{DEM} [kW], Cat_{EN}). The membership functions related to $DeltaE_{SC}$ [kWh] have similar meaning to the ones explained before but in the context of the SC pack operation. $E_{u\_max\_n}$ [kWh] and $E_{u\_max\_p}$ [kWh] represent, respectively, the maximum positive and negative value of energy variation reached in the vector $DeltaE_u$ [kWh] ($u \in [BT, SC]$) considering all the FWs for each discrete step k in the whole driving profile.

In figure 3.6 the input $Cat_{EN}(k)$ [kWh] allows to select which set of rules will be applied on the **BT fuzzy set**. If during the discrete step k the tramway is running in a zone with catenary the input $Cat_{EN}(k)$ [kWh] will have a true value, and $Rules_{BT1}$ will be applied. Otherwise in catenary-free zone $Cat_{EN}(k)$ will have a false value and $Rules_{BT2}$ will be considered.

Similar case for the input $CH_{ST}(k)$ to define the rules for the **SC fuzzy set**: if during the step k the tramway is at a charging station, $CH_{ST}(k)$ will have a true value, and $Rules_{SC1}$ will be applied. Otherwise $CH_{ST}(k)$ will have a false value and $Rules_{SC2}$ will

be considered. It is worth to mention that, in this scenario, a charging station is always a zone with catenary.

Table 3.2 and table 3.3 summarize the rules applied in the **SC fuzzy set** and **BT fuzzy set**, respectively. In this case the AND operator has been applied as logical connector through the elements in the antecedent part of the *If-Then* rules (see appendix A). This because all the possible combinations among the membership function from input variables have been analyzed and a specific fuzzy value has been given. Therefore, any simplifications in the rules or their combinations (to consider and OR operator) has been applied.

The values with "*" in table 3.2 represent the rules applied at a charging station ($Rules_{SC1}$), where only the SOC_{SC} [%] is considered. The values without "*" in table 3.2 correspond to the set $Rules_{SC2}$. The values without "*" in table 3.3 represent the rules defined for the zone with catenary ($Rules_{BT1}$). Finally, the values with "*" in table 3.3 correspond to the rules applied in the catenary-free zone ($Rules_{BT2}$). The defuzzification is carried out by the centroid method (see appendix A) [80].

Table 3.2: Rules applied on the **SC fuzzy set**.

$P_{DEM}(HR)$		$DeltaE_{SC}$		
		N	M	P
	L	HC	HC	HC
SOC_{SC} M		LC	HC	HC
	H	LC	LC	HC

$P_{DEM}(LR)$		$DeltaE_{SC}$		
		N	M	P
	L	HC	HC	HC
SOC_{SC} M		LC	LC	HC
	H	LC	LC	HC

$P_{DEM}(LT)$		$DeltaE_{SC}$		
		N	M	P
	L	LD	LD	LD
SOC_{SC} M		HD	LD	LD
	H	HD	HD	HD

$P_{DEM}(HT)$		$DeltaE_{SC}$		
		N	M	P
	L	LD	LD	LD
SOC_{SC} M		HD	LD	LD
	H	HD	HD	LD

$P_{DEM}(M)$		$DeltaE_{SC}$		
		N	M	P
	L	0	0	HC
SOC_{SC} M		0	0	HC
	P	0	0	0

$P_{DEM}(-)$		$DeltaE_{SC}$
		-
	L	HC*
SOC_{SC} M		HC*
	P	LC*

In the HET, the power balance equation that have to be satisfied at each discrete step k can be defined as follows:

$$P_{DEM}(k) = P_{BT}(k) + P_{SC}(k) + P_{CAT}(k) + P_{CB}(k) \; [kW] \qquad (3.8)$$

where $P_{CAT}(k)$ [kW] is the power absorbed from the catenary during traction ($P_{DEM}(k) \geqslant 0$) at the discrete step k. $P_{CB}(k)$ [kW] is the power absorbed in the crowbar system during

Table 3.3: Rules applied on the **BT fuzzy set**.

$P_{DEM}(HR)$		$DeltaE_{BT}$					
		N		M		P	
	L	HC	HC*	HC	HC*	HC	HC*
SOC_{BT}	M	LC	LC*	LC	LC*	HC	HC*
	H	0	LC*	LC	0*	LC	LC*

$P_{DEM}(LR)$		$DeltaE_{BT}$					
		N		M		P	
	L	HC	LC*	HC	LC*	HC	HC*
SOC_{BT}	M	LC	LC*	LC	LC*	HC	HC*
	H	0	0*	LC	0*	LC	LC*

$P_{DEM}(M)$		$DeltaE_{BT}$					
		N		M		P	
	L	HC	0*	HC	0*	HC	0*
SOC_{BT}	M	LC	0*	LC	0*	LC	0*
	H	0	0*	0	0*	LC	0*

$P_{DEM}(LT)$		$DeltaE_{BT}$					
		N		M		P	
	L	HC	HD*	HC	LD*	HC	LD*
SOC_{BT}	M	LC	HD*	LC	HD*	LC	LD*
	H	LD	HD*	0	HD*	0	HD*

$P_{DEM}(HT)$		$DeltaE_{BT}$					
		N		M		P	
	L	LC	HD*	LC	LD*	LC	LD*
SOC_{BT}	M	LD	HD*	0	HD*	0	HD*
	H	HD	HD*	LD	HD*	LD	HD*

regenerative braking phase ($P_{DEM}(k) < 0$).

3.4 Co-optimization of EMS and HESS sizing

The aim of this section is to describe the optimization approach to obtain the suitable operation for the HET by applying the methodology proposed in section 2.7. Therefore, the MO fitness function presented in (2.50) has to be adapted in the context of the HET scenario as follows:

$$min \ OP_{Tcost} = [BT_{Tcost}(X), \ SC_{Tcost}(X), \ Cat_{Tcost}(X)] \quad X \in \Omega \tag{3.9}$$

being X the vector containing the variables for the HET operation. $OP_{Tcost} \left[\frac{euros}{day}\right]$ rep-

resents the total operating cost of the vehicle as a result of the BT_{Tcost} $[\frac{euros}{day}]$, SC_{Tcost} $[\frac{euros}{day}]$ and Cat_{Tcost} $[\frac{euros}{day}]$ which are the cost models defined in section 2.3. Ω is the feasible solutions space.

Regarding the operation of the HESS, there are some constraints about the maximum and minimum allowable stored energy defined as follows:

$$SOC_{BT\_min} \leq SOC_{BT}(k) \leq SOC_{BT\_max} \tag{3.10}$$

$$SOC_{SC\_min} \leq SOC_{SC}(k) \leq SOC_{SC\_max} \tag{3.11}$$

and the constraints defined by the peak power limitations in the DC/DC converters:

$$P_{BT\_max\_ch} \leq P_{BT}(k) \leq P_{BT\_max\_dch} \tag{3.12}$$

$$P_{SC\_max\_ch} \leq P_{SC}(k) \leq P_{SC\_max\_dch} \tag{3.13}$$

For this scenario the SOC_{BT} [%] and SOC_{SC} [%] have been set to operate between 40-95% and 25-100%, respectively. These constraints are intended to maintain the enough energy needed to avoid the low efficiency conversion during the DC/DC converter operation.

Furthermore, the power targets for BT and SC packs are limited by the peak power of the DC/DC converters linked to them. Therefore, the P_{BT} [kW] and P_{SC} [kW] targets have been limited (in charging and discharging) to 100 [kW] and 400 [kW], respectively. Despite the fact that the current scenario in the tramway of Seville includes two DC/DC converters (peak power of 200 [kW] each) for the SC packs (see figure 3.3), for simulation purpose the power profile injected/absorbed from the SCs will be considered as a total value (peaks power of 400 [kW]).

Depending on the EMS (RB-EMS or A-EMS) applied during optimization process, different optimization variables have been considered:

On the one hand, **when the optimization is carried out based on the RB-EMS** (see section 3.3.1), the vector X with the optimization variables for the HET operation is defined as follows (considering operating targets and HESS sizing):

$$X = \begin{bmatrix} P_{SC\_ECM} \\ P_{BT\_CSM\_tr} \\ P_{SC\_CSM\_tr} \\ P_{BT\_AM\_tr} \\ m_{BT} \\ m_{SC} \end{bmatrix} \tag{3.14}$$

where the space of feasible solutions Ω is defined as follows:

$$\Omega = \begin{cases} -400 \leq P_{SC\_ECM} \leq 0 \; [kW] & \Rightarrow P_{SC\_ECM} \in \mathbb{Z} \\ 0 \leq P_{BT\_CSM\_tr} \leq 100 \; [kW] & \Rightarrow P_{BT\_CSM\_tr} \in \mathbb{Z} \\ 0 \leq P_{SC\_CSM\_tr} \leq 400 \; [kW] & \Rightarrow P_{SC\_CSM\_tr} \in \mathbb{Z} \\ 0 \leq P_{BT\_AM\_tr} \leq 100 \; [kW] & \Rightarrow P_{BT\_AM\_tr} \in \mathbb{Z} \\ 1 \leq m_{BT} \leq 25 \; [branches] & \Rightarrow m_{BT} \in \mathbb{Z} \\ 1 \leq m_{SC} \leq 10 \; [branches] & \Rightarrow m_{SC} \in \mathbb{Z} \end{cases} \tag{3.15}$$

On the other hand, when the optimization is carried out based on the A-EMS (see section 3.3.2) the following concept will be applied: from the set of alternative optimal solutions, in RB-EMS optimization previously mentioned in the last paragraph, **it will be selected the solution which offers the minimum total operating cost for the tramway and its operating targets will be used to configure the sliding forward window**. Therefore, in the A-EMS only the HESS sizing will be optimized. This way, the vector X with the optimization variables is defined as follows:

$$X = \begin{bmatrix} m_{BT} \\ m_{SC} \end{bmatrix} \tag{3.16}$$

where the space of feasible solutions Ω is defined as follows:

$$\Omega = \begin{cases} 1 \leq m_{BT} \leq 25 \; [branches] & \Rightarrow m_{BT} \in \mathbb{Z} \\ 1 \leq m_{SC} \leq 10 \; [branches] & \Rightarrow m_{SC} \in \mathbb{Z} \end{cases} \tag{3.17}$$

As mentioned previously in section 3.2, for the optimization of the HESS sizing, either in the BT pack and SC pack the number of cells connected in series have been maintained as constant. The sizing optimization will be done based on the number of branches in each ESS pack (following the electrical models proposed in section 2.2.6 and section 2.2.7).

Therefore in both aforementioned optimization cases (when RB-EMS or A-EMS are applied) the minimum allowable number of branches in parallel will be 1 both in the BT pack (1.21 [kWh]) and SC pack (0.54 [kWh]).

The referential costs and factors considered in the economic model (proposed in section 2.3) for the optimization process are summarized in table 3.4 [35, 123]. Besides, the assumed costs for the energy consumed from the catenary (C_{kwh_g} $[\frac{euros}{kWh}]$) are detailed in table 3.5 and have been obtained from the Spanish Electric grid web page for an average day [128].

Table 3.4: Assumed referential costs and factors in HET scenario [35].

Variable	Value	Units
P_{dcdc_BT}	100	kW
C_{kWh_BT}	500	euros/kWh
P_{dcdc_SC}	200x2	kW
C_{kWh_SC}	4000	euros/kWh
C_{kW_dcdc}	150	euros/kW
T	10	years
I	2.5	%
BT_{M_y}, SC_{M_y}	500	euros/year

Table 3.5: Cost of grid energy [128].

	Day hour [0-24 h]					
	]0-4]	]4-8]	]8-12]	]12-16]	]16-20]	]20-24]
E. cost (euros/kWh)	0.055	0.053	0.098	0.119	0.148	0.153

As described in section 2.4.2, in this PhD thesis two ESS ageing model have been proposed. During the optimization process carried out in this chapter the Whöler curve-based method (see section 2.4.2.1) for lifespan estimation has been applied. The Semi-empirical ageing model (see section 2.4.2.3) will be later applied in chapter 6 for purposes of comparison of optimization results. The optimization has been performed in MATLAB environment by means of the Genetic Algorithm toolbox [125] where the optimization parameters described in table 3.6 have been used to configure the optimization problem.

3.5   Optimization results

This section aims to present the optimization results from the process previously explained in section 3.4. The MO optimization result is a set of alternative solutions, where each solution offers different characteristics for the defined variables: in the HET scenario, the operating targets for EMS and HESS sizing in the RB-EMS optimization and the HESS sizing for the A-EMS optimization. The suitable solution for the tramway

Table 3.6: Parameters adopted for the GA optimization problem.

Parameter	Value
Population size	20x(Number of variables)
Individual selection	Tournament
Crossover fraction	0.8
Mutation rate	0.01
N° of generations	100

scenario can be based on the analysis of economic, technical and efficiency parameters. However, **in this thesis the selection of the suitable alternative optimal solution will be focused on minimizing the total operating cost of the vehicle** because this factor may be considered as highly important from the manufacturer and end-client point of view at the design stage of the vehicle for a particular scenario.

The optimization was carried out considering the speed profile depicted on figure 3.10(a) which represents a round trip travel. This profile has been repeated several times until completing a daily profile with 15 hours of operation. This 15 hours-profile has been analyzed in order to obtain a daily SOC profile and, this way, the cycles/day to apply the ageing model proposed in section 2.4.2.1. This scenario has been named as the Permanent Operation (PO) because is the profile on which the tramway will operate most of the time in normal conditions. Furthermore, at this point the concept of the Unscheduled Stop Operation (USO) profile (depicted on figure 3.10(b)) is introduced, which is explained later in section 3.5.1.
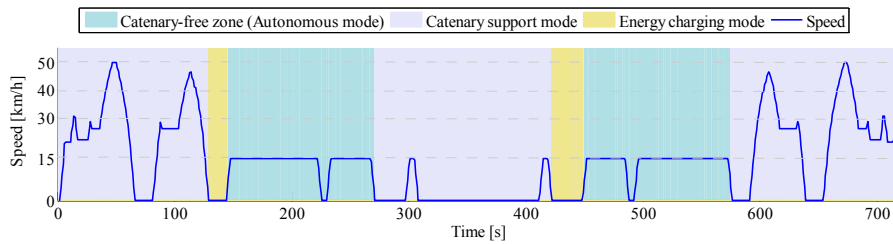
(a) Permament Operation (PO).
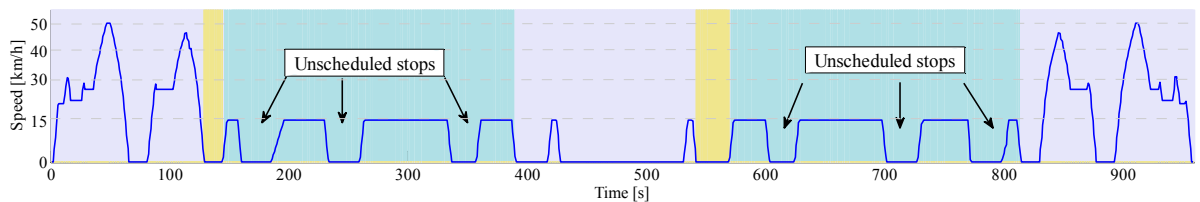
(b) Unscheduled-stops Operation (USO).

Figure 3.10: Considered speed profiles for optimization process.

Figure 3.11 depicts the evolution of the total daily operating cost for the tramway OP_{Tcost} $\left[\frac{euros}{day}\right]$ (3.9) depending on the BT and SC pack sizing for both RB-EMS and A-

EMS. The infeasible solutions correspond to those that, during the optimization, the GA algorithm discards because they do not fulfill the power/energy demand in the catenary-free zone. It is worth to denote that a higher cost represents a shorter lifespan of the BT and SC packs. Therefore, the BT and/or SC pack will require more replacements during the same lifetime of the tramway (*i.e.* 10 years). Furthermore, figure 3.11 depicts the different options of HESS sizing from the set of alternative optimal solutions (best three economical solutions which show the lowest daily operating costs for the tramway). Table 3.7 summarizes the HESS sizing results from the best three solutions depicted in figure 3.11.

(a) RB-EMS   **(b)** A-EMS
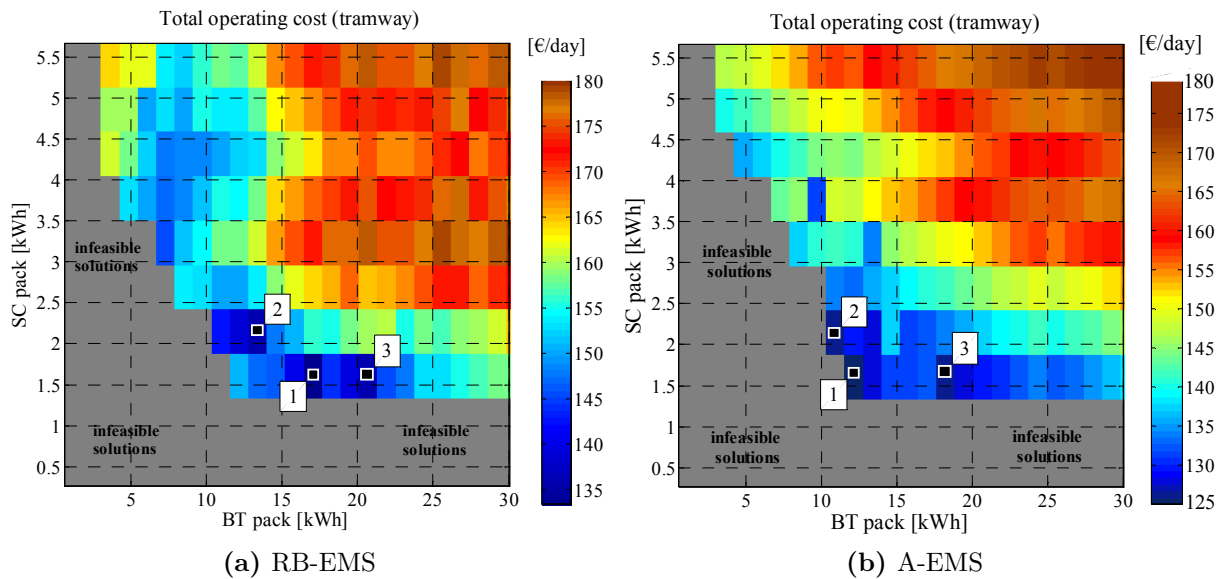
Figure 3.11: Optimal sizing results.

Table 3.7: ESS sizing results from the three best optimized solutions in RB-EMS and A-EMS.

Alternative optimal solution	HESS	**RB-EMS** Sizing [kWh]	**A-EMS** Sizing [kWh]
Solution 1	SC pack	1.62	1.62
	BT pack	16.91	12.10
Solution 2	SC pack	2.16	2.16
	BT pack	13.3	10.89
Solution 3	SC pack	1.62	1.62
	BT pack	21.70	18.15

The set of alternative optimal solutions have been ranked taking into account those with lowest daily operating cost for the tramway. Thus, figure 3.12 depicts the resulting operating costs for each objective in the MO problem for the best solutions from the optimization process on both EMS proposed (RB-EMS and A-EMS). As mention before, the aim of the approach proposed in this PhD thesis is to reduce the total daily operating

cost for the tramway. Therefore, in both cases (RB-EMS and A-EMS) the *solution 1* (which offers the minimum daily operating cost for the vehicle) has been selected as the suitable one for this scenario.

(a) RB-EMS   **(b)** A-EMS
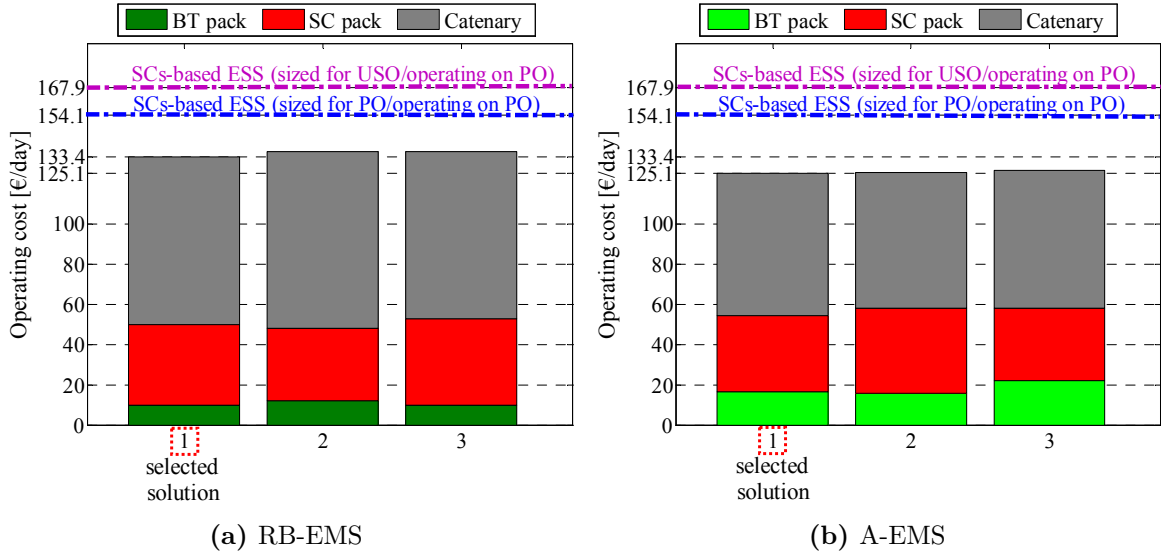
Figure 3.12: Set of alternative optimal solutions.

3.5.1   Operating cost and performance analysis

The aim of this section is to carry out the economic and performance assessment of the solutions selected as suitable ones from each optimization process (either in RB-EMS and A-EMS optimization *solution 1* have been selected, see figure 3.12). For this purpose, a comparison is done among the alternative optimal solution selected from the EMS proposed in this chapter (RB-EMS and A-EMS) with a base scenario (current SC-based ESS in the tramway of Seville). The comparison is focused on the economic factors and highlighting the cost reduction in the daily operating cost.

The base scenario is the current SC-based ESS. For this case, a simple RB-EMS has been applied: the targets for the SC packs operation have been defined either to fully supply the required power/energy in the catenary-free zone and to reduce the power peak requested to the catenary (when possible). Furthermore, the sizing of the SC pack (see table 3.8) was defined by calculating the energy demand in the catenary-free zone.

Thus, in this **base scenario** the first profile analyzed corresponds to the PO (figure 3.10(a)). By applying the economic model proposed in section 2.3 (without considering the operating cost for the BT pack) **the resulting daily operating cost is 154.1** $\left[\frac{euros}{day}\right]$ (blue dashed line on figure 3.12). This referential operating cost represents the one of a **tramway with SC-based ESS sized for PO and operating on PO (normal operation)**. The performance profile of the tramway with the SC-based ESS on PO is depicted on figure 3.13(a).
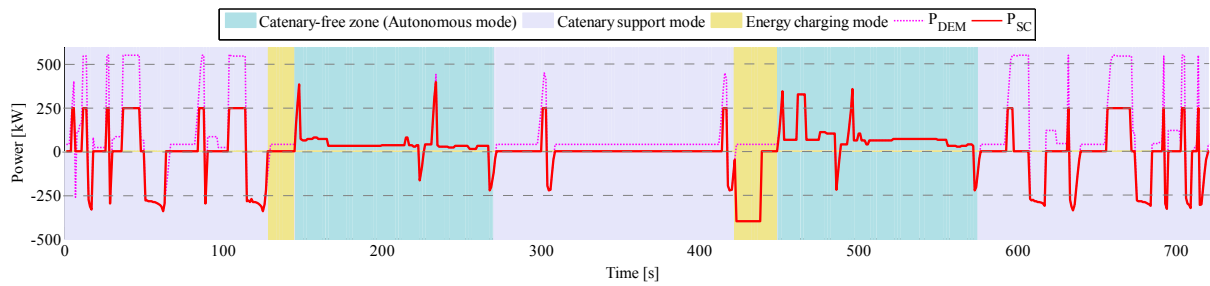
(a) Permanent Operation (PO).
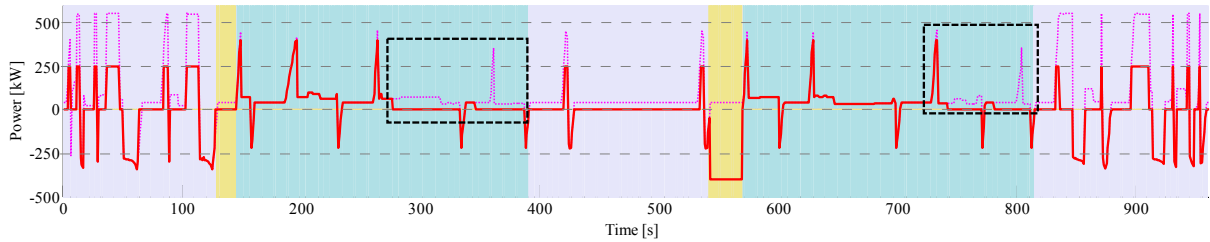
(b) Unscheduled-stops Operation (USO).

Figure 3.13: Tramway operation performance with the SC-based ESS.

The second speed profile analyzed is the USO (figure 3.10(b)). In this profile some unscheduled stops have been included in the catenary-free zone. It is worth to mention that, when these stops are included in the profile, the time span of the whole round trip travel (depicted on figure 3.10(a)) is increased (remaining constant the traveled distance). This profile is useful to evaluate the autonomy and behavior of the tramway in unscheduled events (*e.g.* pedestrians crossing, traffic lights, emergency situations) in the critical zone, where there is not catenary to supply energy. Figure 3.13(b) depicts the performance profile of the tramway with the SC-based ESS on USO scenario. Analyzing the behavior of the SC-based solution on USO, the ESS is not able to fully supply the energy demand in the catenary-free zone (black dashed rectangle on figure 3.13(b)). It means that, **in case of unscheduled events in the catenary-free zone the tramway could not reach the next section with catenary** (cause the limited energy stored in its ESS).

In this base scenario the provisional solution (if the concept of SC-based ESS has to be maintained) would be to increase the sizing of the SC pack (see table 3.8) until fulfilling the energy demand in the catenary-free zone under the USO scenario. Once, by applying the economic model (see section 2.3), this **new ESS sizing** (*resized SC-based*) **results in an operating cost of 167.9** $\left[\frac{euros}{day}\right]$ (pink dashed line on figure 3.12). It is worth to mention that, to obtain this operating cost the speed profile depicted on figure 3.10(a) has been applied. Thus, this value represents the daily operating cost for the **tramway with a SC-based ESS resized to be able of fulfilling the energy/power demand in USO but operating normally on the PO (simulation done with the PO profile)**.

On the one hand, by applying the parameters (power targets for the EMS and HESS sizing) from the optimal solution selected in the **RB-EMS optimization** (*solution 1*

100

depicted in figure 3.12(a)) **the minimum operating cost reached is 133.4** $\left[\frac{euros}{day}\right]$. It means that, **the RB-EMS approach allows reductions in the operating cost of around 13% and 20% from the base scenario (SC-based ESS) and the resized one (resized SC-based ESS), respectively**.

On the other hand, considering the **EMS proposed in this PhD thesis (adaptive fuzzy-based strategy)** with its optimal selected values (HESS sizing) **the resulting minimum operating cost is 125.1** $\left[\frac{euros}{day}\right]$ (*solution 1* depicted in figure 3.12(b)). **The simulation result with the novel A-EMS shows a reduction on the daily operating cost of 6.2% from the optimal RB-EMS solution selected** (see figure 3.14). Furthermore, comparing with the daily operating cost of the base scenario (SC-based), **the A-EMS approach allows a cost reduction (on PO) of 18.8%** (SC-based ESS sized for PO and operating on PO) **and 25.5%** (SC-based ESS sized for USO and operating on PO).
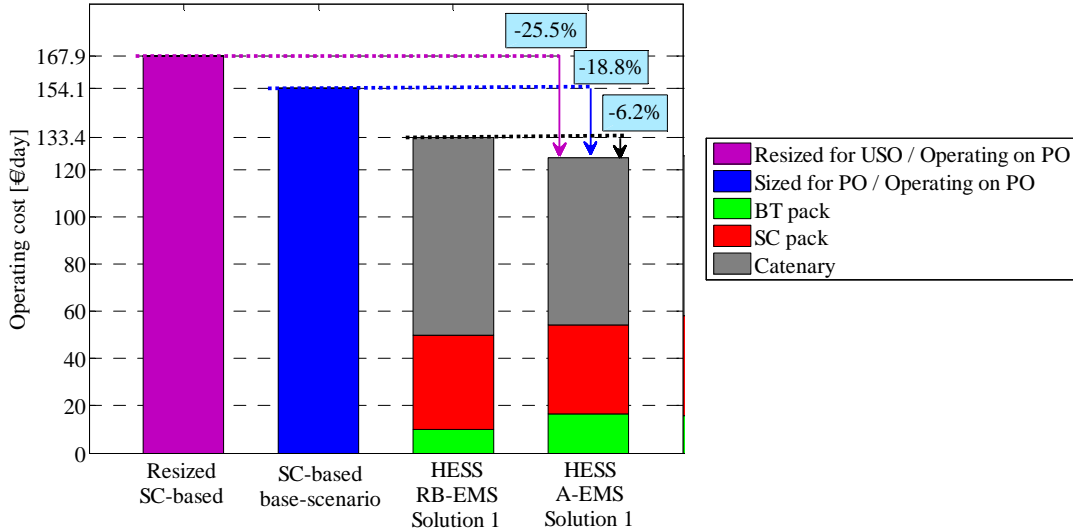
Figure 3.14: Operating cost reductions reached with the RB-EMS and A-EMS.

Table 3.8 summarizes the comparison of ESS sizing results for the HET case study in the scenarios analyzed in this section. Here, the most noteworthy result is that **the optimal BT pack sizing for the A-EMS shows a reduction of 28.4% from the BT pack sizing when RB-EMS was applied**. Despite the fact that operating cost related to the BT pack in the A-EMS is higher than comparing with the RB-EMS (see figure 3.14), the total operating cost for the tramway is lower, in this case, by reducing the energy consumption from catenary. It means that, **by applying the A-EMS, significant cost savings can be reached (-6.2%) from an already optimized RB-EMS approach and even allowing downsizing the BT pack**.

Figure 3.15 and figure 3.16 show the HET performance when the RB-EMS and A-EMS are applied on PO and USO, respectively. The HESS have been configured with

Table 3.8: ESS sizing comparison in the HET scenario.

HET Scenario	ESS	Sizing [kWh]	ESS sized for:	USO	Operating cost [euros/day]	Sizing increase/reduction from:		
						b.s.	r.b.s.	r.h.sol.
SC-based	SC pack	3.78	PO	**Not-fulfilled**	154.1	0% (b.s.)	-22.2%	+133.3%
	BT pack	-				-	-	-
Resized SC-based	SC pack	4.86	USO	Fulfilled	167.9	+28.6%	0% (r.b.s.)	+200.0%
	BT pack	-				-	-	-
HESS RB-EMS	SC pack	1.62	PO	Fulfilled	133.4	-57.1%	-66.7%	0% (r.h.sol.)
	BT pack	16.91				-	-	0% (r.h.sol.)
HESS A-EMS	SC pack	**1.62**	PO	Fulfilled	**125.1**	-57.1%	-66.7%	0%
	BT pack	**12.10**				-	-	**-28.4%**

b.s.: base scenario, r.b.s.:resized base scenario, r.h.sol.: reference hybrid solution

the results depicted in table 3.8, which correspond to the optimal sizing selected from the optimization process (minimum daily operating cost for the tramway) for each EMS. Figure 3.15(a) and figure 3.16(a) show de speed profiles where the HET operation has been evaluated.

Figure 3.15(b) and figure 3.16(b) depict the power absorbed from the catenary during the tramway operation in PO and USO. With both strategies the power peaks from catenary are shaved, this way, reducing the energy consumption and allowing the main grid stability. However, there is a clear difference between the RB-EMS and A-EMS about the power requested from catenary, where this last one shows the minimum consumption maintaining the power peaks most of the time below 350 [kW].

Figure 3.15(c)-(d) and figure 3.16(c)-(d) show the power profile during the BT and SC pack operation. It can be noted that, during the catenary support mode the BT pack provides energy assistance for traction and absorbs the remaining energy during the regenerative phase (fulfilling the C-rate constraints in charging and discharging). However, during the autonomous mode (catenary-free) the BT pack only provides energy for traction, while most of the regenerative energy is absorbed in the SC pack (storing energy to provide the power peaks during acceleration). In figure 3.16(c), during the last section with catenary ($k > 800[s]$) the BT pack does not provide energy for traction. The action aims to try charging the BT pack to the safe energy level (around 80%). The RB-EMS imposes defined power targets for each operating mode and zone where the tramway is running. Nevertheless, the main difference between RB-EMS and A-EMS is that with the last one is possible to get a variable output from the BT and SC pack in order to adapt their response to the energy and power needs.

Figure 3.15(e) shows the BT and SC SOC profiles, where SOC_{BT} [%] is maintained

around 80% and above 40%. This is considered the operation of the HESS in normal conditions (no unscheduled-stops during the route). However, in USO (figure 3.16(e)) the SOC_{BT} decreases below 60% due to the unscheduled-stops considered in the route (increasing the energy demand in the catenary-free zone). Both EMS try to recharge the BT pack up to the same energy level defined for PO (around 80%). However, the variable output for the BT pack operation from the fuzzy approach allows to compensate the extra energy consumption during the catenary-free zone while the fixed target from the RB-EMS will delay the return to that SOC condition. This way, showing the advantage of the adaptive behavior when not-considered events take place within the expected route profile.

3.5.2 Operating efficiency analysis

By calculating the energy absorbed in the HESS during regenerative braking phase in PO (based on the profile of power demand depicted in figure 3.15(b)), it is possible to estimate the system efficiency in terms of the harnessing of this energy during regenerative phase. This efficiency is defined as the ratio of the total energy absorbed in the HESS and the total available energy during the regenerative phase. Figure 3.17 depicts the efficiency analysis, where **the available energy to be absorbed during the regenerative phase is around 7 [kWh]**. It worth to mention that, **in case of a tramway without ESS this energy would be completely lost as heat in the crowbar resistance** (avoiding to inject this energy to the main grid through the pantograph). However, the proposed scenario needs at least one kind of ESS due to the catenary-free zone.

In the base scenario (current SC-based solution) the lost energy in crowbar is around 14% in both cases (SC-based and resized SC-based) **with an efficiency between 80.9-81.2%**.

Considering that the SC pack sizing in the HESS solution with the RB-EMS approach has a smaller capacity (see table 3.8) than comparing with the base scenarios (SC-based and resized SC-based), there exist energy (resulting from the regenerative power peaks) that cannot be fully absorbed in the SC pack. Therefore, **with the optimized RB-EMS approach, the lost energy in crowbar increases (up to 18.3%) reaching an efficiency of 77.8%**. Furthermore the non-adaptive approach of the RB-EMS defines several power targets for the BT and SC operation that do not consider the current/future energy consumption. Hence, these power targets do not allow harnessing of all the potential regenerative energy.

Finally, **the HESS solution (managed by the novel A-EMS proposed in this PhD thesis) shows the minimum value of lost energy (11.4%) with an efficiency around 84.4%**. This mainly because the A-EMS evaluates the current/future energy consumption allowing modifying the BT and/or SC power targets. These adaptive power targets allow increasing (if it were needed) the current consumption from the BT or SC

(a) Speed profile.

(b) Catenary power profile.

(c) BT pack power profile.

(d) SC pack power profile.

(e) SOC profiles for BT and SC packs.
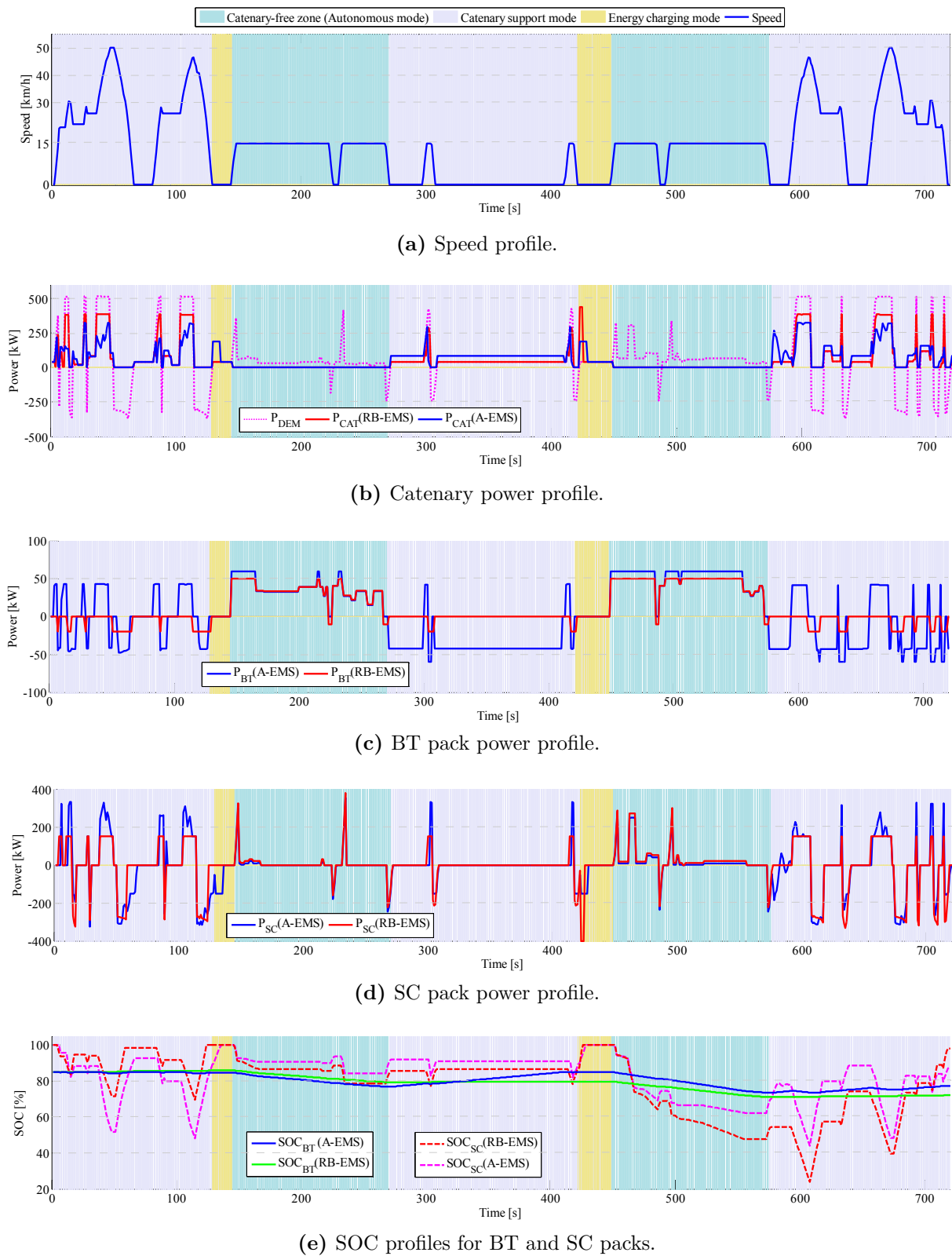
Figure 3.15: Tramway operating performance in Permanent Operation (PO).
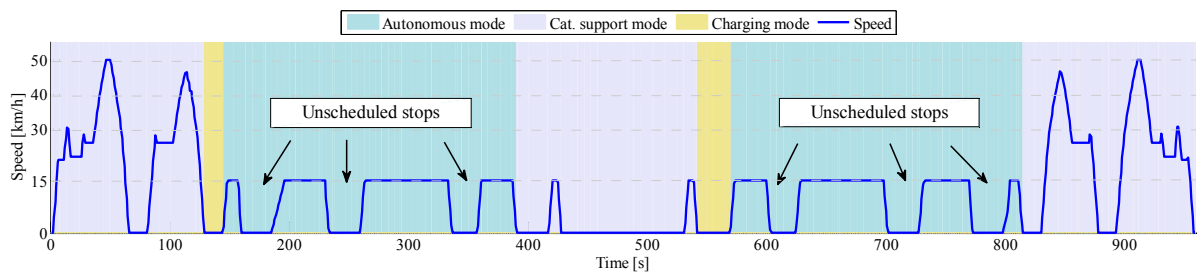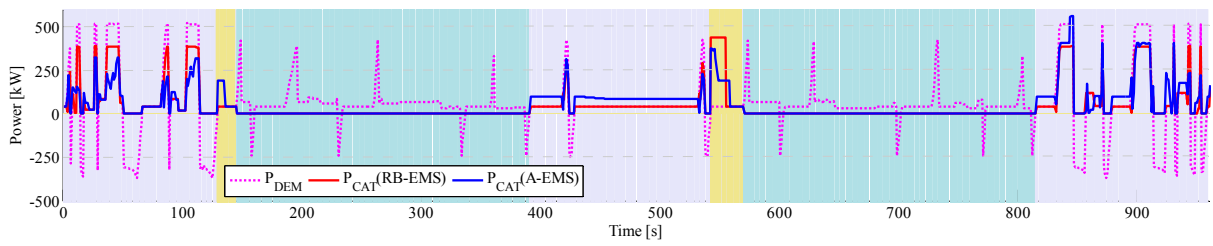
(a) Speed profile.

(b) Catenary power profile.
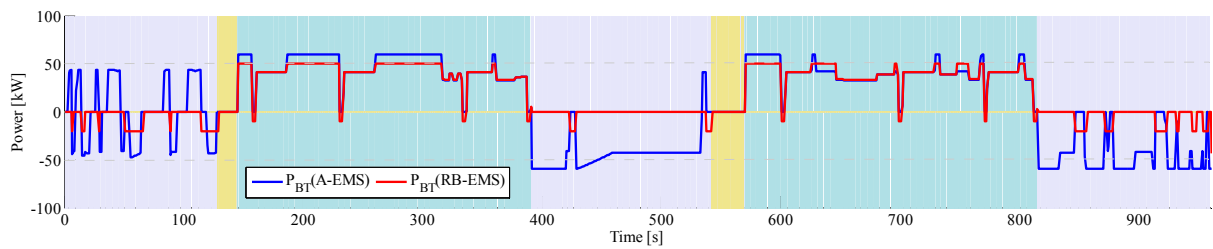
(c) BT pack power profile.
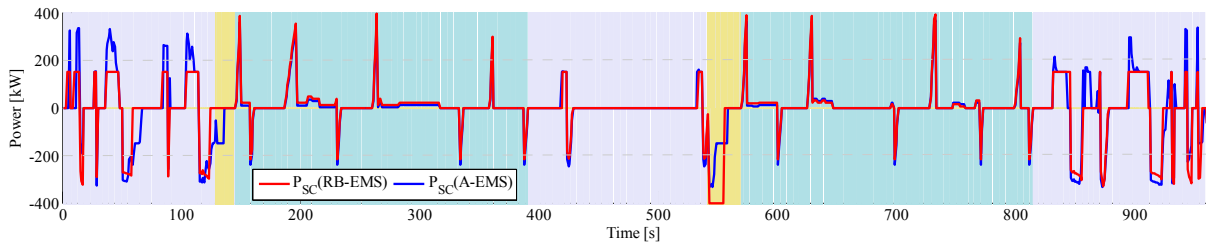
(d) SC pack power profile.
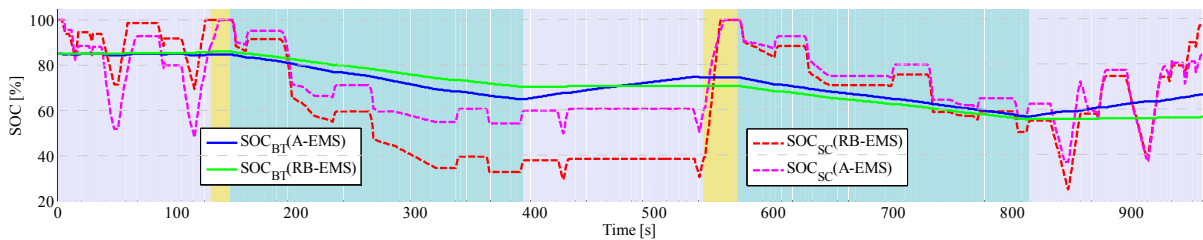
(e) SOC profiles for BT and SC packs.

Figure 3.16: Tramway operating performance in Unscheduled-stop Operation (USO).
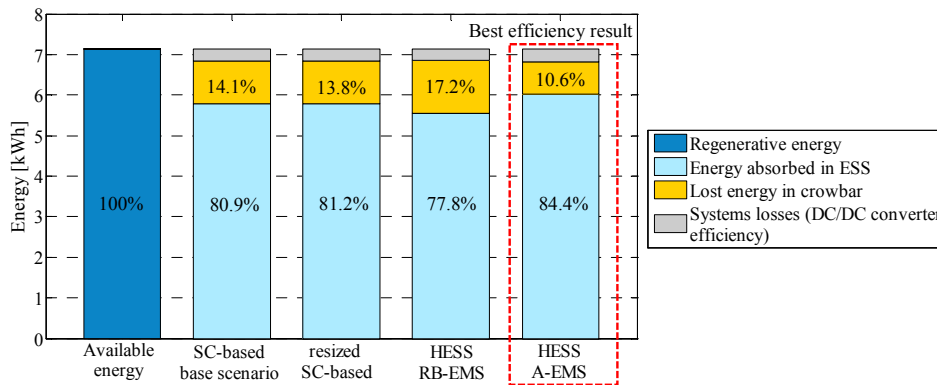
Figure 3.17: System efficiency analysis.

pack in order to take advantage of as much energy as possible during the regenerative phase in future driving stages. It is worth to note that in this analysis the average efficiency of the DC/DC converters (95%) has been considered (depicted as system losses on figure 3.17).

3.6 Conclusions

In this chapter two different energy management strategies applied on a hybrid electric tramway with HESS were presented. As case study a real application was selected corresponding to an urban route in the city center of Seville where the tramway operates in zones with and without catenary. Therefore, the vehicle requires to operate in catenary support mode (catenary+HESS) and autonomous mode (HESS). Additionally, an evaluation scenario was introduced (named as Unscheduled-stops operation) by including several non-considered stops within the catenary-free zone to assess the energetic behavior of the tramway when this kind of events occur in the autonomous zone.

On the one hand, a RB-EMS with different operation modes (depending on the zone where the tramway is running) was presented. The strategy considers different power targets to operate the HESS either during traction and regenerative braking phase which were set as optimization variables to obtain the optimal operation of the tramway.

On the other hand, the EMS approach proposed in this PhD thesis was introduced. It consists in an adaptive EMS (A-EMS) based on fuzzy logic, which applies a sliding forward window in order to adapt the instantaneous operation vehicle behavior (in this case the HESS operation) considering the current and future information about energy consumption. This energy management approach aims to fulfill the vehicle power demand while improving the energy harnessing of the on-board sources by means of the suitable and intelligent power split among the available sources (HESS and catenary). In this case, the fuzzy control will determine the power targets for the SC and BT packs operation in the catenary and catenary-free zones. Within the forward window (to estimate the future

energy consumption) the RB-EMS was applied.

The methodology previously proposed in chapter 2 for the co-optimization of EMS and HESS sizing was applied in both cases (RB-EMS and A-EMS). In the first case (RB-EMS) to optimize the targets for the power split strategy and the HESS sizing. In the second case (A-EMS) to optimize the HESS while the power targets for the strategy applied in the forward window were configured with the optimal values obtained in the RB-EMS optimization.

The optimization results from both energy management approaches (RB-EMS and A-EMS) were compared with the current solution of the tramway (ESS based on super-capacitors) in terms of daily operating cost reduction. Taking into account the assumed referential costs, both proposed strategies allow fulfilling the power and energy demand in the zones with and without catenary (even under unscheduled-stops in the catenary-free zone). However, the highest cost saving from the base scenario (SC-based sized for PO and operating on PO) was obtained with the A-EMS (around 18.8%) compared with the RB-EMS (around 13.4%). On the other hand, when the current SC-based scenario was resized to consider the possible unscheduled events in the catenary-free zone (SC-based sized for USO and operating on PO), the cost saving was even higher with the A-EMS (about 25.5%) than comparing with the RB-EMS approach (about 20.5%). It is worth to mention that, these cost savings were obtained by including the concept of HESS (which form part of the objectives proposed in this PhD thesis) instead of a single ESS.

Furthermore, comparing the cost saving between the proposed strategies, the A-EMS approach allows a cost reduction from the RB-EMS of around 6.2% even with a downsizing on the BT pack (-28.4%). This cost saving is reached due to the improvement approach for energy management proposed in this thesis on the A-EMS for a better harnessing of the energy and power split during operation.

Finally, the system efficiency was analyzed taking into account the energy harnessing during regenerative braking phase. The base scenarios (SC-based and resized SC-based) showed efficiencies between 80.9-81.2% with lost energy in crowbar (wasted as heat during braking) around 14%. The HESS with RB-EMS reached a lower efficiency around 77% with energy losses in crowbar of around 18%. The A-EMS reached an improvement in energy recovery, with an efficiency of 84.4% and minimum losses in crowbar around 10%. This is due to the forward energy analysis and the fuzzy approach to adapt the power targets during operation.

The chapter results highlight the HESS as the most suitable solution in terms of cost saving and energy efficiency. Moreover, for scenarios where the zone with autonomous operation increases (longer catenary-free distance) the use of batteries becomes essential in order to increase the energy autonomy of the tramway. Moreover, the EMS becomes in a key factor to assure the suitable harnessing of the on-board energy (fulfilling the operation requirements), minimizing the lost energy (increasing the energy efficiency)

while offering the minimum operating cost during the whole vehicle lifetime.

4

Case study 2: Hybrid Electric Bus

4.1 Case study 2: Hybrid Electric Bus

This chapter is dedicated to analyze the approach proposed in this PhD thesis on the Hybrid Electric Bus for urban applications as case study. Therefore, in the second section, the characteristics of the power-train architecture as well as some relevant technical information are introduced. Besides, the route characteristics of the selected scenario are described in order to analyze the operating requirements during hybrid and full-electric stages.

In the third section of this chapter a methodology for selecting the optimal operating points and most efficient operating curve in an ICE is fully described and applied for the genset selected in this scenario.

In the fourth section, the energy management approach for this case study is presented. Similarly to the case study of the HET, a rule-based EMS (RB-EMS) is firstly introduced. This strategy takes into account the scenario requirements, and it proposes both different energetic operating modes as well as a power split strategy to fulfill the vehicle power demand during hybrid and full-electric operation.

Then, the adaptive EMS (A-EMS) approach based on fuzzy logic, previously described for the HET case, is modified to be applied in the HEB scenario. In this case, the fuzzy sets and membership functions parameters are presented in a generic way in order to be configured depending on the HESS sizing and EMS' targets during the optimization process. The sliding forward window strategy of the A-EMS is built up based on the RB-EMS.

In the fifth section, the MO problem is adapted to the HEB case and the main constraints and techno-economic referential values are described.

Later, in the sixth section, an optimized base scenario is proposed by disregarding the HESS ageing and replacement factors while prioritizing only the fuel consumption reduction. Then, the optimization methodology proposed in chapter 2 is applied on the RB-EMS. The operating targets and HESS sizing from the set of alternative optimal solutions in the RB-EMS case are later used to configure either the parameters of the membership function in the fuzzy sets and the forward window strategy of the A-EMS. A comparison in terms of operating cost reduction, efficiency, fuel consumption and autonomy in full-electric operation is carried out in order to determine the improvements that can be reached with the approach proposed in this thesis (A-EMS and optimization methodology) over the base scenario and RB-EMS approach. Besides, the performance profile during vehicle operation with rule-based and adaptive fuzzy-based EMS are compared. Finally the conclusions of this chapter are presented.

4.2   Scenario overview

The scenario analyzed in this chapter is focused on a HEB with a series topology in its power-train. Figure 4.1 depicts the power-train configuration of the SHEB including the HESS [100]. The main propulsion element is the electric motor (EM) (operating as generator during regenerative braking phase) powered from the DC bus and mechanically connected to the vehicle transmission (T). The bus includes an energy storage system (ESS) based on: BT which provide high energy density as main energy storage unit, and SC with high power density, used to absorb/inject power peaks during the regenerative braking or acceleration, respectively. The genset includes an ICE + electric generator (EG) set. Additionally a crowbar system (CB) has been considered, in order to dissipate the surplus energy that has not been fully absorbed during regenerative braking phase.
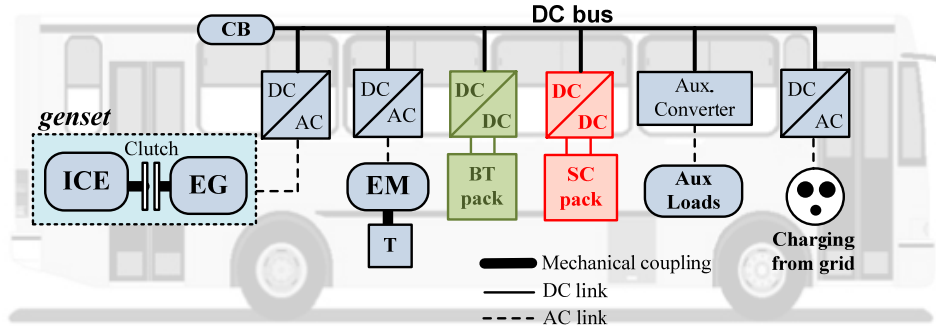
Figure 4.1: Series Hybrid Electric Bus power-train architecture.

Table 4.1 summarizes the main technical characteristics related to the power-train's elements. As defined for the HET case, the BT pack is composed of an arrangement of single cells in series (to compose a string) and several strings in parallel. Hence, in order to assure the needed voltage from the BT and SC packs side to allow the proper operation of their corresponding DC/DC converters, in the HEB case the number of cells in series (n_{BT} and n_{SC}) has been considered as constant, thus, the sizing process will define the number of branches in the BT and SC packs (m_{BT} and m_{SC}). Similarly as in the HET, in HEB case the BT and SC packs sizing will be carried out taking as base cells the ones previously introduced in table 2.1.

The HEB is able to operate in two different driving modes. The main characteristics of the operation in each mode can be briefly described as follows:

-*Hybrid driving mode*: In this mode both the genset as well as the HESS supply power during traction phase. The HESS plays a double role: energy supply assistance for traction (BT pack) with power peak regulation during acceleration (SC pack), and storing energy provided from genset for charging (BT pack) with power peak regulation during regenerative braking phase (SC pack). In this mode the ICE operates in its high efficiency zone (high power rates), and when there is not power requested to the genset (low power rates) the ICE is set at idle speed (low consumption), this way, avoiding the

Table 4.1: Technical characteristics of the HEB.

	Characteristics	Description
General	Dimensions (LxWxH)	12m x 2.55m x 3.4m
	Weight (empty)	12.5 tonnes
	Passengers capacity	95 pax
Internal combustion engine	Fuel	Diesel
	Maximum power output	160 kW
	Maximum torque	900 Nm
	Speed range	800 - 2600 rpm
Electric motor	Maximum power	196.5 kW
	Maximum torque	2100 Nm
	Speed range	0 - 6000 rpm
	AC/DC inverter	η_{inv}=0.95
Electric generator	Maximum power	190 kW
	Maximum torque	1000 Nm
	Speed range	0 - 6000 rpm
	AC/DC inverter	η_{inv}=0.95
Battery pack	Number of cells in series	181
	Maximum voltage	598 V
	DC/DC converter	75 kW / η_{conv}=0.95
Supercapacitor pack	Number of cells in series	144
	Maximum voltage	388 V
	DC/DC converter	150 kW / η_{conv}=0.95

continuous start/stop process of the genset system.

-*Full-electric driving mode*: During this mode the ICE is turned off (zero-emissions zone) and the HESS must fulfill the energy and power needs during the travel. Similarly as in *hybrid driving mode*, the BT pack will supply the energy for traction while the SC pack will do the power peak regulation during acceleration and regenerative and braking phases.

In order to validate the proposed energy management approach and the optimization methodology a driving cycle for an urban city route has been selected. The speed profile is depicted in figure 4.2 and corresponds to an urban route in the city of Zaragoza (Spain). Currently this route is operated by a tramway where a catenary-free operation in the city center area is considered. Therefore, taking into account that one of the aims in this chapter is to analyze the HEB behavior in both hybrid and full-electric operation, this route profile has been selected as case study where the catenary-free zone has been adopted as zero-emissions zone.

The route profile presents several stops (which have been also considered as zero-emissions zones), a maximum speed of 50 km/h, a traveling distance or around 27 km (round trip) while the full-electric operation zone has a driving section of around 2.4 km.

Figure 4.2: Driving cycle for HEB operation (single trip).
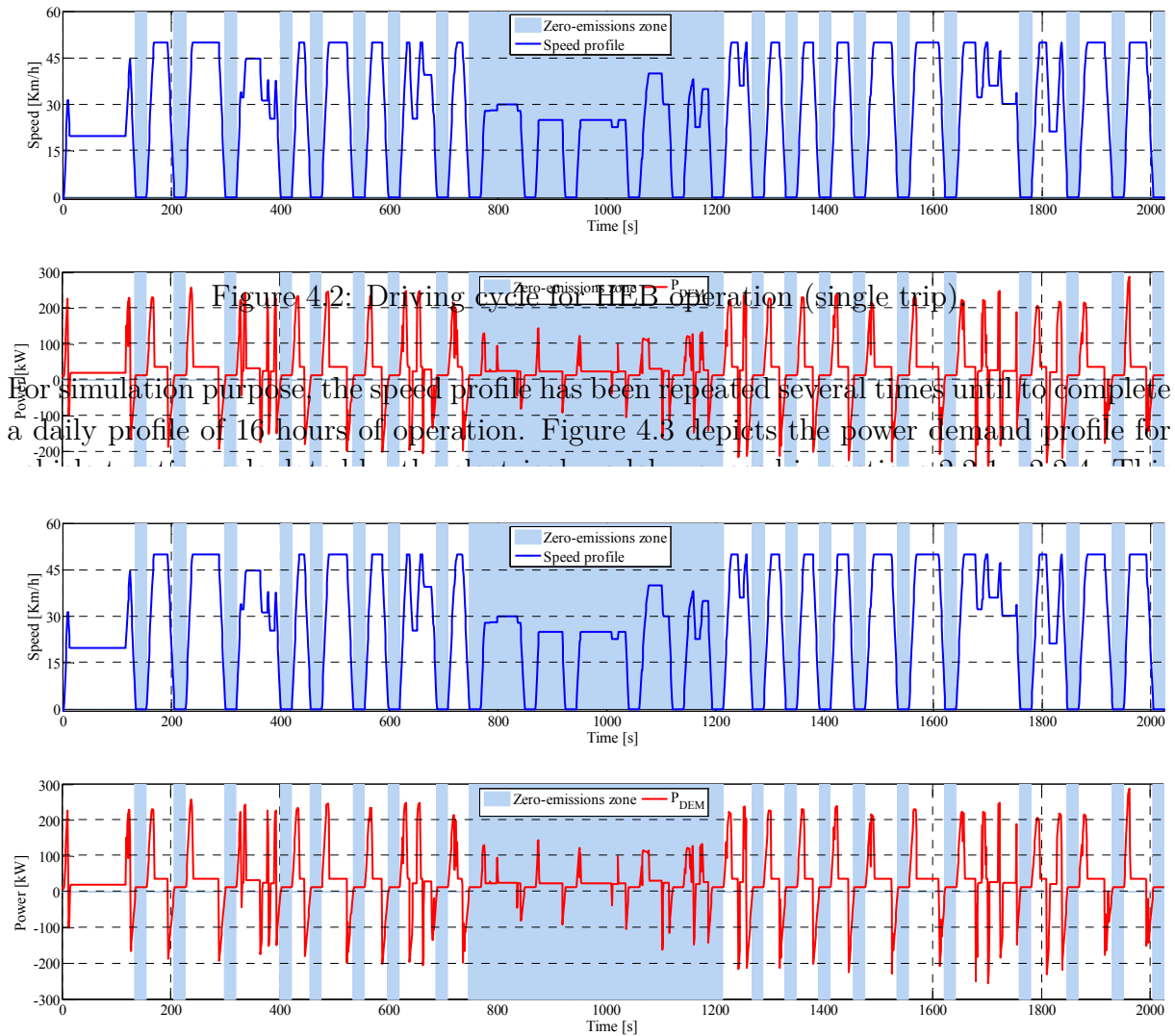
For simulation purpose, the speed profile has been repeated several times until to complete a daily profile of 16 hours of operation. Figure 4.3 depicts the power demand profile for

Figure 4.3: Power demand profile for HEB operation (single trip).

It is worth mentioning that, for the case study analyzed in this chapter, it has been only considered the recharging of the HESS at end station (after the round-trip travel). It means that, along the route, any intermediate recharging point has been considered. This way, during vehicle operation in the daily journey, the HESS will be recharged by the genset or regenerative braking. The process is later explained in section 4.4 devoted to the EMS description.

4.3 ICE map optimization

4.4 Energy Management Strategies

In this chapter two different EMSs are proposed, addressing the non-adaptive and adaptive approach. The first is a rule-based strategy (RB-EMS), detailed in section 4.4.1 [131], which allows the HEB operation in *hybrid* and *full-electric* driving mode. Here, several variables have been considered to define the proper operation of the vehicle and their optimal values will be defined optimized by applying the methodology proposed in section 2.7. Then adaptive EMS approach (based on fuzzy logic and sliding forward window) proposed as contribution of this PhD thesis and previously introduced in the HET case (see section 3.3.2) is modified and applied to the HEB case (see section 4.4.2). In this case the optimal results from RB-EMS optimization will be used as basis to define
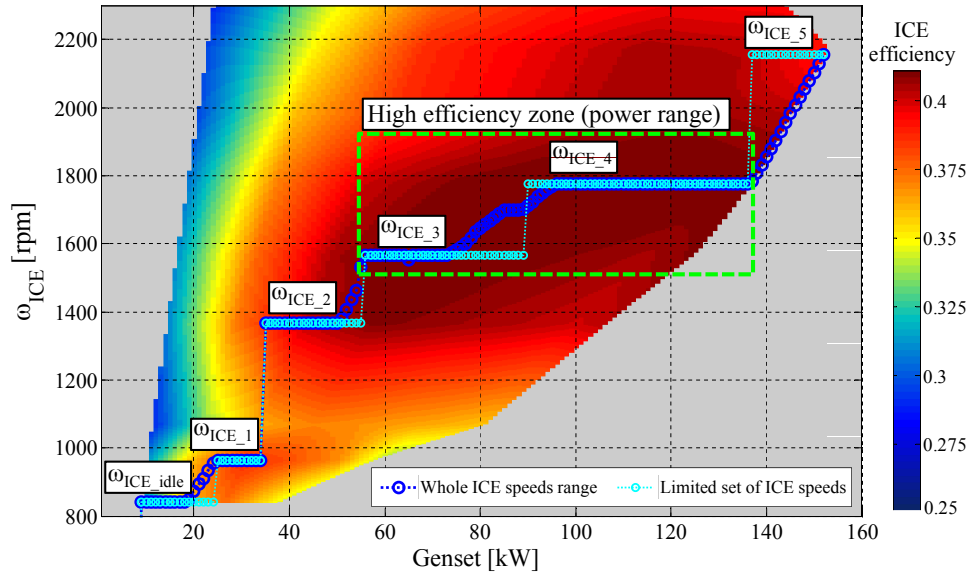
Figure 4.8: Optimal genset operating curve (power output vs. ICE speed).

the ranges of the membership functions in the fuzzy sets.

4.4.1 Rule-based strategy

In order to operate the vehicle under the different conditions explained previously (*hybrid* or *full-electric*) and also considering the available energy in the HESS, several operating modes have been defined. The performance of the RB-EMS depends on the driving mode [131]. Thus:

A. Hybrid driving mode

In this operation mode both genset as well as the HESS operate together. As depicted in figure 4.9 the *hybrid* driving mode is performed by comparing the SOC_{BT} [%] with two defined control levels (SOC_{u_ctrl} [%] and SOC_{l_ctrl} [%]) in order to define the *energetic operating mode* for the bus operation. Thus, within *hybrid* driving mode three different *energetic operating modes* have been defined: *Depleting mode* (DM), *Sustaining mode* (SM) and *Charging mode* (CM). In the first two modes either genset and BT pack operate with power targets by providing energy to supply the vehicle power demand. However, considering that in DM the available energy in the BT pack is higher than in SM, the power rate (of the BT pack) will be higher as well. On the other hand, during CM the BT pack does not supply energy and the genset aims either to fulfill the vehicle power demand and recharge the BT pack.

Therefore, taking into account the aforementioned characteristics for DM and SM, a strategy (figure 4.10) to split the power demand among the genset, BT and SC pack has been defined. The power split strategy considers two stages:
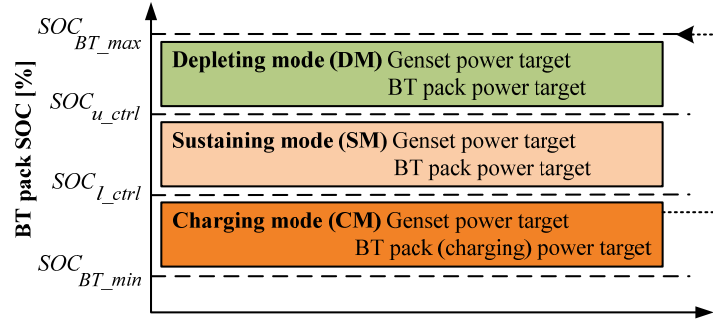
Figure 4.9: *Energy modes* during *hybrid driving mode* operation.

- **Stage 1**: In traction case ($P_{DEM}(k) \geq 0$), the genset power target ($P_{genset}(k)$ [kW]) considers the limits P_{genset_1} [kW] and P_{genset_2} [kW]. Hence, as shown in figure 4.10, the genset will provide the demanded power when it is within the power range $P_{genset\_1} \leq P_{DEM}(k) \leq P_{genset\_2}$.

  In regenerative case ($P_{DEM}(k) < 0$), the power absorbed in the BT (P_{BT_ch} [kW]) is calculated by the C-rate limitation for charging (maximum 3.5 C) as follows (modification of (3.4)):

$$P_{BT\_ch} = -\frac{(V_{nom\_BTcell} \cdot n_{BT}) \cdot (I_{1C\_BTcell} \cdot C_{rate} \cdot m_{BT}) \cdot p_{ch}}{10^3} \ [kW] \qquad (4.4)$$

  being p_{ch} the power split ratio for charging the BT pack ($p_{ch} \in \Re \ [0-1]$).

  E_{genset} [kWh] and E_{BT_rg} [kWh] (figure 4.10) are the energy provided by the genset and absorbed by the BT pack in this first stage, respectively.

- **Stage 2**: In traction case ($P_{DEM}(k) \geq 0$), the power demand that has not been satisfied yet is split between the BT and SC pack. The strategy considers the power target P_{BT_dch} [kW] related to the C-rate limitation for BT pack in discharging calculated as follows (modification of (3.3)):

$$P_{BT\_dch} = \frac{(V_{nom\_BTcell} \cdot n_{BT}) \cdot (I_{1C\_BTcell} \cdot C_{rate} \cdot m_{BT}) \cdot p_{dch}}{10^3} \ [kW] \qquad (4.5)$$

  where p_{dch} is the power split ratio for discharging the BT pack ($p_{dch} \in \Re \ [0-1]$) with different values defined for DM and SM (see section 4.6.2).

  SC pack is in charge of power peak regulation. E_{BT_tr} [kWh] and E_{SC_tr} [kWh] (figure 4.10) represent the energy provided by the BT and SC pack for traction.

  In regenerative case ($P_{DEM}(k) < 0$), $P_{SC\_max\_ch}$ [kW] is the maximum allowable power target for charging the SC pack (set at maximum power of the DC/DC converter linked to the SC pack, 150 [kW]). The energy surplus will be absorbed by the crowbar system (E_{CB} [kWh]). E_{SC_rg} [kWh] (figure 4.10) represents the energy

absorbed for the SC pack during regenerative phase. Both P_{BT_dch} [kW] and P_{BT_ch} [kW] depend on the BT pack sizing, it means the cells arrangement in the BT pack as shown in section 2.2.6.
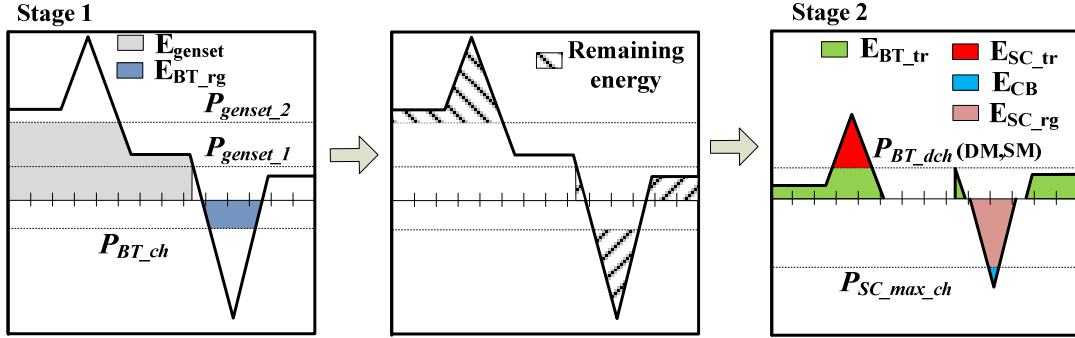
Figure 4.10: Power split strategy in *hybrid* driving mode (DM, SM).

As mentioned before, in *charging mode* ($SOC_{BT} < SOC_{l\_ctrl}$), the BT pack does not provide energy during traction ($P_{BT\_dch} = 0$). The genset will provide the traction power demand ($P_{genset\_1} \leq P_{DEM} \leq P_{genset\_2}$) and the power for charging the BT (P_{BT_ch} [kW]) until the BT pack is fully charged ($SOC_{BT} = SOC_{BT\_max}$) as follows:

$$P_{genset}(k) = P_{DEM}(k) + P_{BT\_ch} \ [kW] \tag{4.6}$$

Similarly as in DM and SM, during CM the SC pack is in charge of power peak regulation in traction and regenerative braking phase (see figure 4.11).
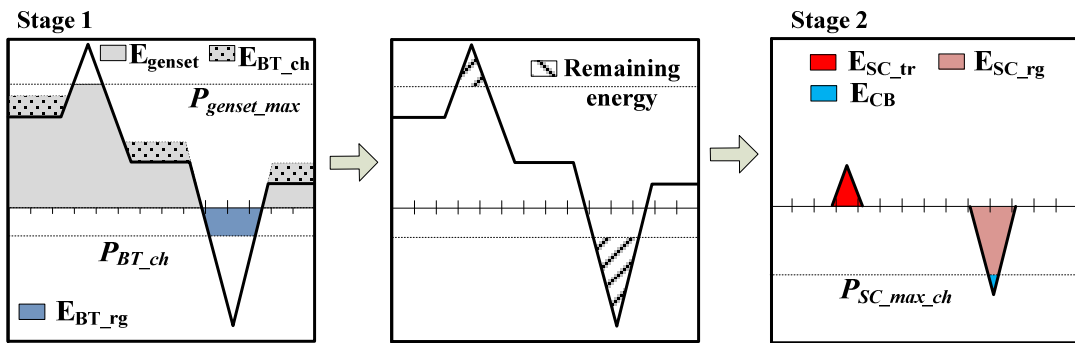
Figure 4.11: Power split strategy in *hybrid* driving mode (CM).

B. Full-electric driving mode

In *Full-electric* driving mode only the HESS operates to propel the vehicle while the genset is turned-off. In full-electric operation (figure 4.12) the same two stages (as in *hybrid* driving mode) have been considered (with different power targets):

- **Stage 1**: In traction case ($P_{DEM}(k) \geq 0$), the power target P_{BT_dch} [kW] (calculated by (4.5)) has been set at the maximum optimal power target for discharging ($p_{dch} = p_{dch\_AM}$) defined later by optimization. In regenerative case ($P_{DEM} < 0$), it is applied the same power target (P_{BT_ch} [kW]) as in **Stage 1** in *hybrid* driving mode.

- **Stage 2**: In traction case ($P_{DEM}(k) \geq 0$), the remaining energy is supplied by SC pack. In regenerative case ($P_{DEM}(k) < 0$), it is applied the same power target ($P_{SC\_max\_ch}$ [kW]) as in **Stage 2** in *hybrid* driving mode.
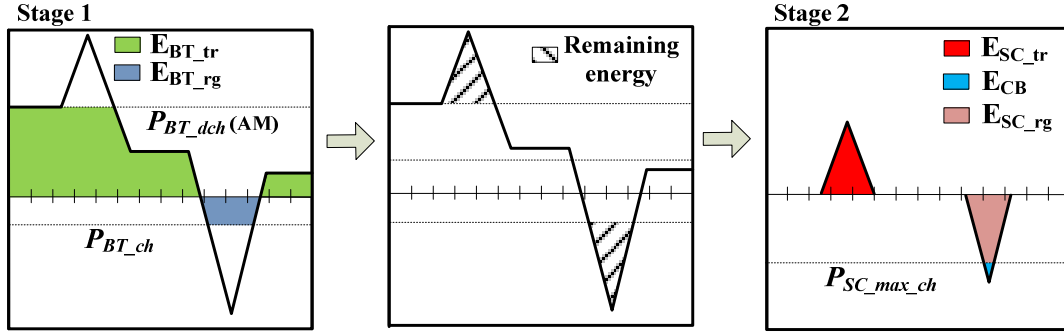
Figure 4.12: Power split strategy in full-electric driving mode.

As defined in both driving modes (*hybrid* and *full-electric*), the SC pack acts as power peaks regulator either during traction and regenerative braking phases. From the practical point of view, the genset and BT pack will operate by defining power targets to their corresponding drivers, while the SC pack will be in charge of maintaining the voltage in the DC bus in the appropriate range (DC bus voltage control mode). Therefore, in case of voltage drop, the DC/DC converter linked to the SC pack will inject current to the DC bus to increase and stabilize the voltage. Otherwise, in case of voltage rise, the action will be to absorb current to decrease the DC bus voltage. In both cases a fast response of the SC pack is needed in order to guarantee the stability of the DC link and proper operation of the devices connected to it.

4.4.2 Adaptive fuzzy-based strategy

As introduced in chapter 3, the adaptive approach proposed in this PhD thesis is intended to deal with the complexity about the suitable management of a system with multiple energy sources which operate simultaneously. The main idea is to adopt the philosophy of the fuzzy theory and the adaptive approach previously introduced and to translate it on the HEB case study. Therefore, the aim is to demonstrate that the EMS approach and optimization methodology can be applied on different transport scenarios where relevant improvements can be obtained from technical and economic points of view.

The HESS concept is maintained in both HET and HEB, therefore variables such as vehicle power demand (P_{DEM} [kW]), state of charge of BT and SC pack (SOC_{BT} [%],

SOC_{SC} [%]) and future information about the energy consumption in BT and SC packs ($DeltaE_{BT}$ [kWh], $DeltaE_{SC}$ [kWh]) will also be considered in this strategy. However, particular inputs as the *driving mode* (hybrid or electric) as well as the power supplied by the genset (P_{genset} [kW]) will be included. This last variable has notable interest since the fuel consumption and efficiency operation are directly related with it. Therefore, the fuzzy control structure depicted in figure 4.13 has been proposed in order to develop an adaptive strategy considering several inputs while reducing the complexity in the problem formulation for the power split among genset, BT and SC packs during the HEB operation.
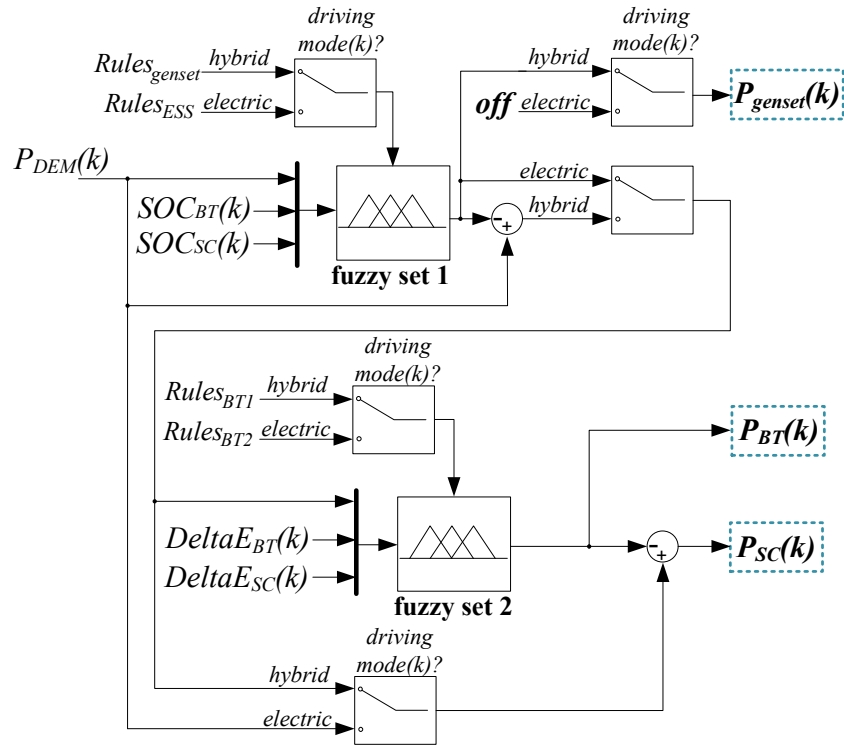
Figure 4.13: Proposed fuzzy approach for the adaptive EMS in the HEB case.

The strategy considers two fuzzy controls and several sets of rules ($Rules_{genset}$, $Rules_{ESS}$, $Rules_{BT1}$ and $Rules_{BT2}$) in order to define the operating power targets for genset (P_{genset} [kW]) as well as for the BT (P_{BT} [kW]) and SC (P_{SC} [kW]) packs. Section 4.4.2.1 describes the adaptation done on the strategy for sliding forward window calculation in the HEB case. Section 4.4.2.2 describes the fuzzy sets and rules applied in the strategy.

4.4.2.1   Forward window calculation

The FW is built based on information about the expected route profile as defined in the previous chapter [35]. In this case, the strategy applied in the FW to estimate the stored/supplied energy in/from the BT and SC packs is depicted on figure 4.14, and it corresponds to the strategy previously explained in section 4.4.1. At a k discrete step, the window FW_k takes n_{FW} forward steps. Thereby, depending on the driving conditions of

the step k (*hybrid* or *full-electric driving* mode) the corresponding strategy is applied in the FW. In *hybrid* mode, three FWs are solved in parallel for each *energetic operating mode* (DM, SM and CM) by applying the power targets defined in each one. The information from the FWs is stored in look-up-tables and the corresponding values for a k step during simulation are obtained based on the instantaneous *driving* and *energy* mode conditions.
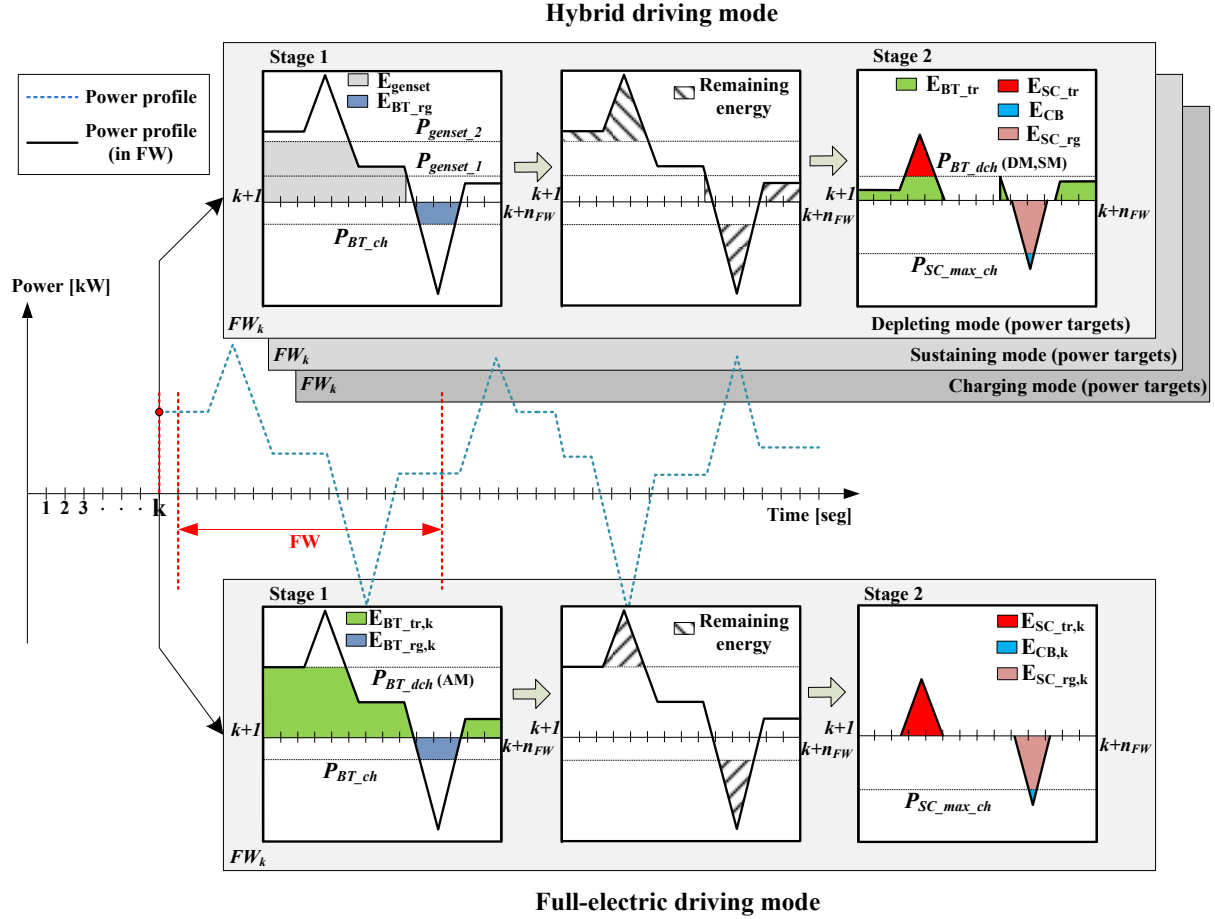
Figure 4.14: Forward window strategy for energy consumption estimation.

$E_{BT\_tr,k}$ [kWh] and $E_{BT\_rg,k}$ [kWh] represent the estimations of energy supplied and stored from the BT pack (in FW_k) and calculated at instant k, respectively. $E_{SC\_tr,k}$ [kWh] and $E_{SC\_rg,k}$ [kWh] have similar meaning in relation with the SC pack. The energy variations for the BT and SC pack are calculated by (3.6) and (3.7). $E_{genset,k}$ [kWh] represents the energy provided by the genset during its estimated operation within FW_k.

Based on an analysis done about the HEB operation and the RB-EMS proposed for this case, the sliding forward window will not be resized as in the HET case. As explained previously in the RB-EMS, the aim of the BT pack is to supply energy during the low power demands of the vehicle (hybrid driving mode) and to be the main energy source during the full-electric operation, therefore, the BT pack operates continuously in both driving modes. Thus, the overlapping of future energy information from different zones

results relevant to anticipate the instantaneous operation mainly considering that the alternative energy source to supply the vehicle power demand (taking into account that there are not intermediate recharging points along the route as in the HET case) will be the genset. For instance, in HET case during catenary zone, the energy provided by the catenary is always available and the consumption of it does not represent a factor as sensitive as the fuel consumption with its related emissions issues. Figure 4.15 depicts the sliding window concept.
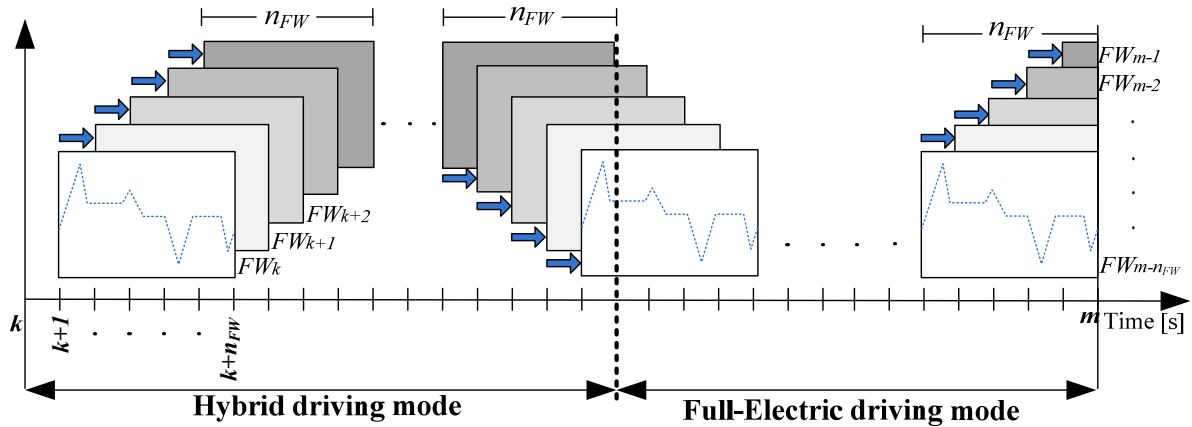
Figure 4.15: Sliding window concept applied on the HEB scenario.

Considering the energy and power behavior regarding the BT and SC pack, respectively, the FWs related to each one of the them will have a different size. Therefore, **for the BT case, a window size of 60 discrete steps has been selected while for the SC case a 20 discrete steps FW is considered**. The aim of applying a wider FW size for the BT pack is to be able of reacting to the energy variations ($DeltaE_{BT}$ [kWh]) that could appear on the future vehicle operation. On the other hand, the FW for the SC pack operation is shorter in order to response to the fast power dynamics in the short term as well as to be able of interpreting the meaning of the $DeltaE_{SC}$ [kWh] value and translating it to a linguistic term during the fuzzification process. Figure 4.16 depicts, as example, the $DeltaE_{BT}$ [kWh] and $DeltaE_{SC}$ [kWh] values calculated for each k discrete step. In the profiles depicted in figure 4.16, the values at each k discrete step represent the energy consumption estimation calculated into the FW, which is immediately ahead of the k step. In this case, three profiles of energy consumption estimation have been calculated in parallel (for DM, SM and CM). In figure 4.16 can be noted how the resulting vectors (red dashed lines that will be later assumed as input vectors in *fuzzy set 2*, see figure 4.13) adopt the corresponding value (overlapping the curve) depending on the *current driving mode* of the vehicle.
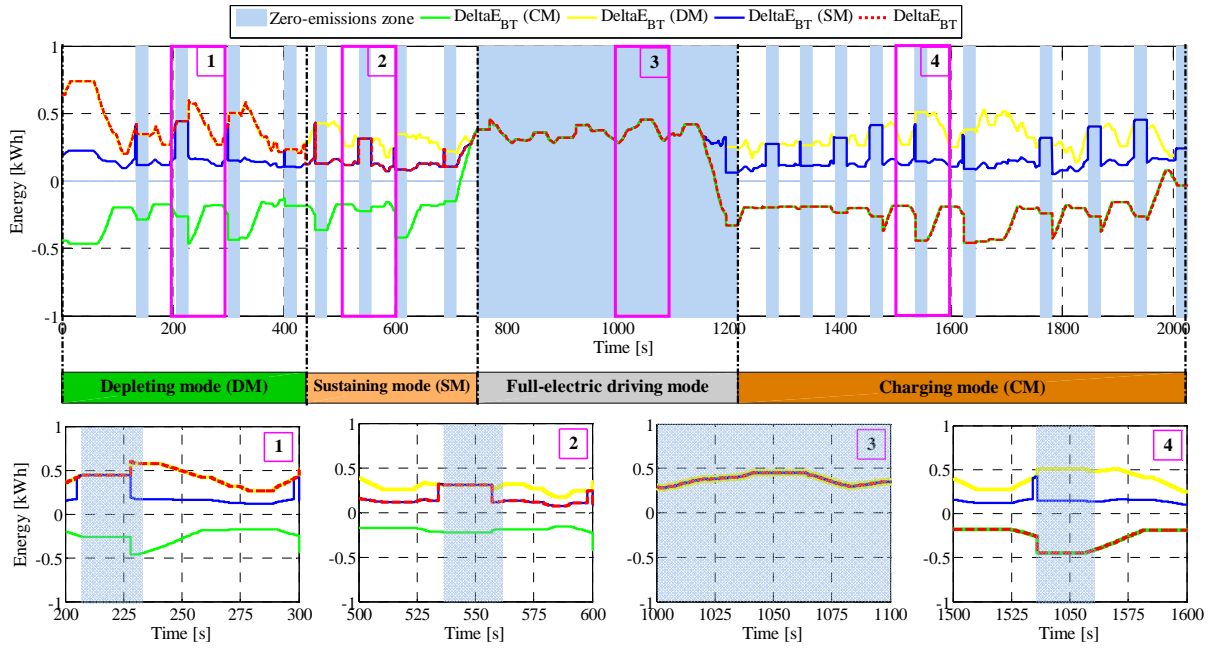
(a) $DeltaE_{BT}$ at each discrete step with a FW size of 60 discrete steps
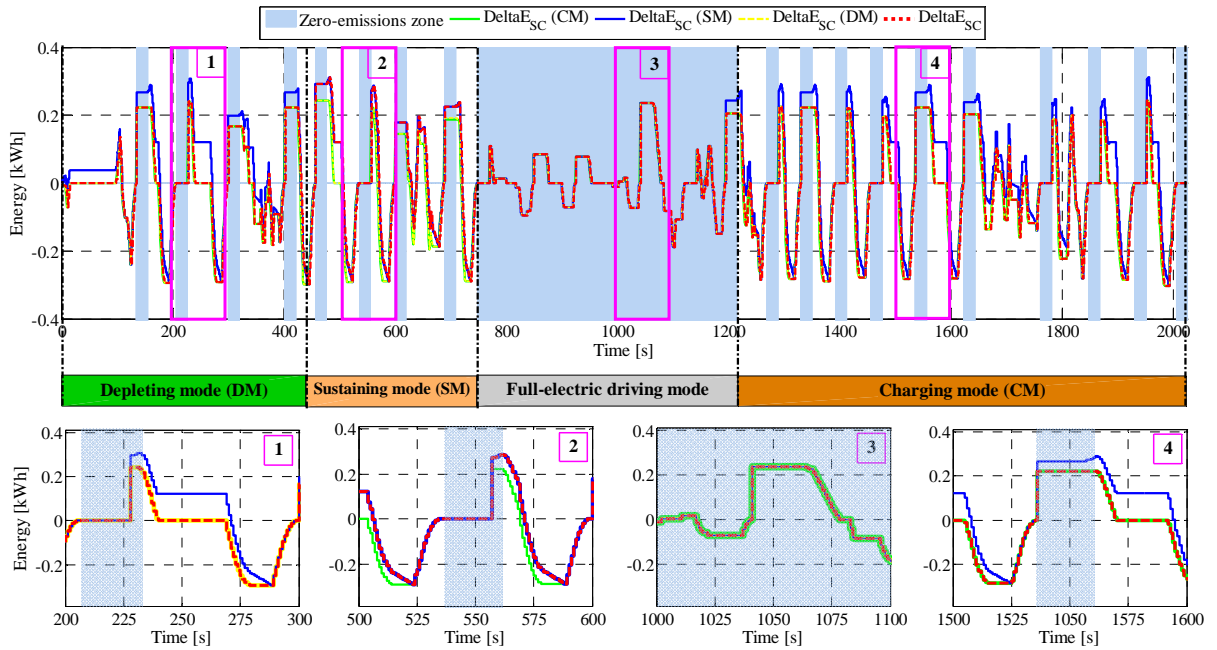
(b) $DeltaE_{SC}$ at each discrete step with a FW size of 20 discrete steps

Figure 4.16: Energy variation profiles calculated for each *driving* and *energy* mode.

4.4.2.2 Description of the fuzzy sets

The fuzzy sets are based on the *Mamdani* FIS (see appendix A) and define the power targets $P_{genset}(k)$ [kW] and $P_{BT}(k)$ [kW] for the genset and BT pack operation, respectively. Thus, taking into account the fuzzy sets defined in figure 4.13, the input/output

applied to them depending on the *driving* mode are depicted in figure 4.17.
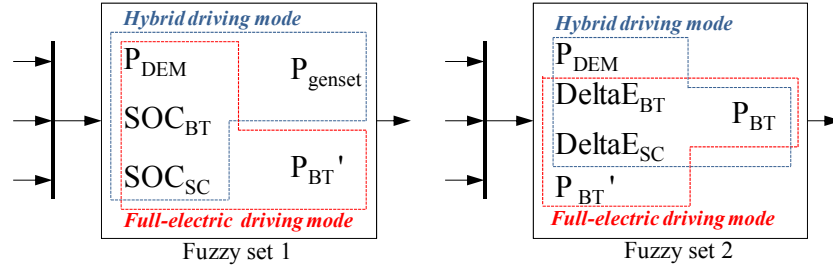
Figure 4.17: Input/output membership functions applied in the fuzzy sets.

Therefore, in case of *hybrid* operation (blue dashed line, figure 4.17), **fuzzy set 1** defines the power target $P_{genset}(k)$ [kW] and **fuzzy set 2** defines the power target $P_{BT}(k)$ [kW] depending on the energy consumption estimation in FW_k for the BT and SC pack ($DeltaE_{BT}(k)$ [kWh] and $DeltaE_{SC}(k)$ [kWh]). Otherwise, in case of *full-electric* operation (red dashed line, figure 4.17), **fuzzy set 1** defines the provisional power target for BT pack P'_{BT} [kW] and **fuzzy set 2** adapts this target depending on the energy consumption estimation in FW_k to obtain $P_{BT}(k)$ [kW]. It is worth to denote that, in both driving modes, the SC pack operates as power peak regulator (acceleration/braking).

The membership functions related to each input/output depicted in figure 4.13 are detailed in figure 4.18.

The linguistic terms for the membership functions have been defined as follows:

- P_{DEM}: (HR) High Regenerative; (LR) Low Regenerative; (M) Medium; (LT) Low Traction and (HT) High Traction.

- $DeltaE_u$ $u \in [BT, SC]$: (N) Negative; (M) Medium and (P) Positive.

- P_{genset}: (L) Low; (ML) Medium Low; (MH) Medium High and (H) High.

- SOC_{BT}, SOC_{SC}: (L) Low; (M) Medium and (H) High.

- P_{BT}, P'_{BT}: (HC) High Charging; (LC) Low Charging; (M) Medium; (LD) Low Discharging and (HD) High Discharging.

It is worth to denote that in the HEB model context, a positive value represents traction phase, while a negative one represents the regenerative braking phase. On the other hand, for the ESS a positive value is considered as discharging and a negative one as charging.

For the input P_{DEM} [kW] (figure 4.18(a)), the membership functions have been defined in a generic form. Thus, these functions can be configured depending on the dynamic of the vehicle power demand. P_{max_tr} [kW] and P_{max_rg} [kW] are the power peak demand

(a) HEB power demand.

(b) Energy variation in BT and SC.

(c) Genset power target.

(d) BT power target.

(e) BT pack SOC.

(f) SC pack SOC.
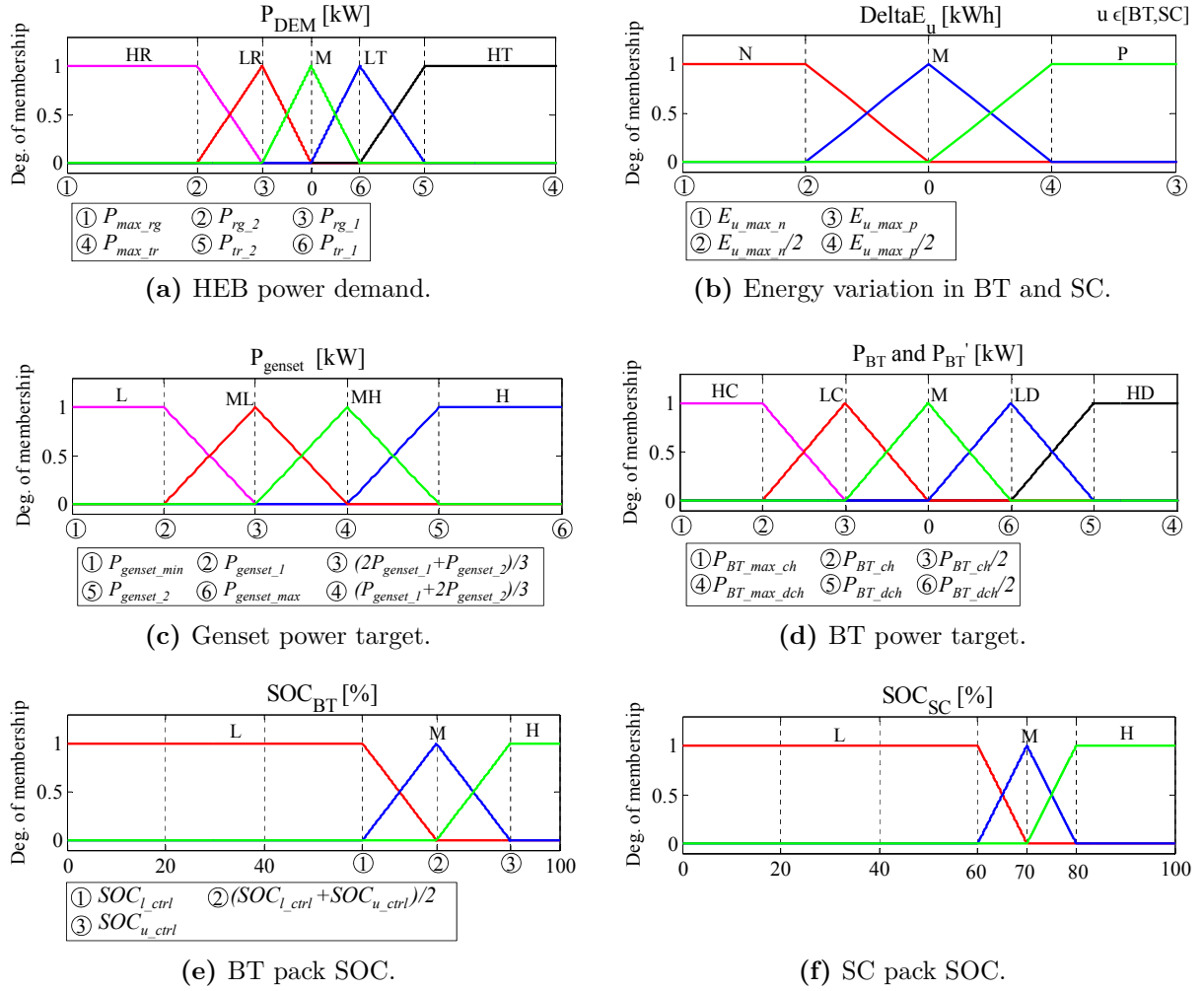
Figure 4.18: Membership functions applied on HEB case study.

during traction and regenerative phase, respectively. P_{tr_1} [kW] and P_{tr_2} [kW] are the average power values intended to include the low and medium-low power demands in traction case. P_{rg_1} [kW] and P_{rg_2} [kW] have similar meaning but during the regenerative braking context.

For the input $DeltaE_u$ [kWh] (figure 4.18(b)) used to describe the energy variation in the BT and SC cases, the membership function P ($DeltaE_u \geq 0$) denotes that the estimation (in FW_k) of supplied energy is greater than the estimation of stored energy. The A-EMS tries (by means of the fuzzy rules) to reduce the instantaneous consumption from the u pack ($u \in [BT, SC]$) to be prepared for a possible increase in the energy demand (related to the u pack). The N membership function represents the opposite case ($DeltaE_u < 0$), when the estimation of stored energy is greater than the estimation of supplied energy. In this case the A-EMS tries to increase the instantaneous consumption from the u pack to be prepared for absorbing the energy estimated in FW (avoiding losing it in the crowbar). As in the HET case, $E_{u\_max\_n}$ [kWh] and $E_{u\_max\_p}$ [kWh] represent,

127

respectively, the maximum positive and negative value of energy variation reached in the corresponding FW.

For the output P_{genset} [kW] (figure 4.18(c)), the membership functions consider the whole power operating range of the genset. Taking into account the optimal power range depicted on figure 4.8, the fuzzy rules are intended to maintain most of the time the genset operation around ML and MH (for high power peaks in case of the ESS is not able to fulfill them). The genset will operate in H for BT pack charging ($SOC_{BT} < SOC_{l\_ctrl}$) or when the SC pack is not able to fully supply the power peaks in acceleration. Otherwise, in regenerative phase ($P_{DEM} < 0$) (or when the BT pack is not able to supply energy) the genset will operate in L for low power demand, respectively.

For the variables P_{BT} [kW] and P'_{BT} [kW] (figure 4.18(d)), the values of $P_{BT\_max\_ch}$ [kW] and $P_{BT\_max\_dch}$ [kW] are set according to the maximum allowable peak power in the DC/DC converter in charging and discharging, respectively (see table 4.5). On the other hand, P_{BT_ch} [kW] and P_{BT_dch} [kW] correspond to the maximum power targets defined in (4.4) and (4.5), respectively. As explained in section 4.4.1, these values are set once the sizing of the BT pack is configured. It allows obtaining the target for the BT operation by considering its power rate (which varies depending on the pack sizing), this way, improving the harnessing the available power and energy stored in the BT pack.

For the input SOC_{BT} [%] (figure 4.18(e)), the membership function M has been defined based on the optimal values SOC_{l_ctrl} [%] and SOC_{u_ctrl} [%] to avoid deep discharges and to maintain enough energy stored in the BT pack in case of *full-electric* operation. On the other hand, for the input SOC_{SC} [%] (figure 4.18(f)), the membership function M considers the range 60-80% since the power peaks in acceleration and/or braking have a greater impact on the SOC_{SC} [%] due to the low energy stored in the SC pack. Therefore, the aim is to keep enough energy for power peak response while avoiding the depth discharge (low voltage from SC pack side) and allowing the proper operation of the DC/DC converter.

Following the input/output defined in figure 4.17, table 4.2, table 4.3 and table 4.4 summarize the rules applied on the **fuzzy set 1** and **fuzzy set 2**. Similarly as in HET case, here the AND operator has been defined as connector through the elements in the antecedent part of the *If-Then* rules (see appendix A). When the vehicle is in *hybrid* operation the values depicted without "*" are applied, otherwise (*full-electric* operation) the values with "*" are considered. For instance, in table 4.2, the inputs are P_{DEM} [kW], SOC_{BT} [%] and SOC_{SC} [%] and the outputs are P_{genset} [kW] in case of *hybrid* operation (values without "*") and P'_{BT} [kW] in case of *full-electric* operation (values with "*"). The defuzzification is carried out by means of the centroid method (see appendix A).

In the HEB, the power balance equation that has to be satisfied at each discrete step k can be defined as follows:

$$P_{DEM}(k) = P_{genset}(k) + P_{BT}(k) + P_{SC}(k) + P_{CB}(k) \; [kW] \tag{4.7}$$

Table 4.2: Rules applied on the **Fuzzy set 1**.

P_{DEM} (HR)		SOC_{SC}					
		L		M		H	
SOC_{BT}	L	L	LC*	L	HC*	L	HC*
	M	L	LC*	L	HC*	L	HC*
	H	L	0*	L	0*	L	LC*

P_{DEM} (LR)		SOC_{SC}					
		L		M		H	
SOC_{BT}	L	ML	LC*	ML	HC*	L	HC*
	M	L	LC*	L	LC*	L	HC*
	H	L	0*	L	0*	L	LC*

P_{DEM} (LT)		SOC_{SC}					
		L		M		H	
SOC_{BT}	L	ML	LD*	ML	LD*	ML	LD*
	M	ML	HD*	ML	HD*	ML	LD*
	H	ML	HD*	ML	HD*	L	HD*

P_{DEM} (HT)		SOC_{SC}					
		L		M		H	
SOC_{BT}	L	H	HD*	H	HD*	H	LD*
	M	MH	HD*	MH	HD*	MH	LD*
	H	MH	HD*	MH	HD*	ML	HD*

where $P_{CB}(k)$ [kW] would be the power absorbed in the crowbar system during regenerative braking phase ($P_{DEM}(k) < 0$).

4.5 Co-optimization of EMS and HESS sizing

As mention in chapter 2, the aim of the proposed approach in this thesis is to obtain the optimal vehicle operation (defined by the EMS) and the optimal HESS sizing in order to either fulfill the vehicle power demand and to offer an economically competitive solution by minimizing the operating cost of the vehicle. At this point it is worth mentioning that the optimization in the HEB will be carried out for the RB-EMS (optimization of the parameters for the EMS operation and HESS sizing, see section 4.4.1) and the alternative optimal targets obtained from this process will be used later to configure the fuzzy control and sliding forward window strategy proposed for the A-EMS (see section 4.4.2). Therefore, with the aim of applying the methodology proposed in section 2.7, the MO fitness function presented in (2.50) has to be adapted in the context of the HEB scenario as follows:

Table 4.3: Rules applied on the **Fuzzy set 2** (*Hybrid* driving mode).

P_{DEM} (HR)		$DeltaE_{SC}$		
		N	M	P
	N	L	L	L
$DeltaE_{BT}$	M	L	L	L
	P	L	L	L

P_{DEM} (LR)		$DeltaE_{SC}$		
		N	M	P
	N	ML	ML	L
$DeltaE_{BT}$	M	L	L	L
	P	L	L	L

P_{DEM} (LT)		$DeltaE_{SC}$		
		N	M	P
	N	ML	ML	ML
$DeltaE_{BT}$	M	ML	ML	ML
	P	ML	ML	L

P_{DEM} (HT)		$DeltaE_{SC}$		
		N	M	P
	N	H	H	H
$DeltaE_{BT}$	M	MH	MH	MH
	P	MH	MH	ML

Table 4.4: Rules applied on the **Fuzzy set 2** (*Full-electric* driving mode)

P'_{BT} (HC)		$DeltaE_{SC}$		
		N	M	P
	N	HC*	HC*	LC*
$DeltaE_{BT}$	M	HC*	HC*	LC*
	P	HC*	HC*	HC*

P'_{BT} (LC)		$DeltaE_{SC}$		
		N	M	P
	N	LC*	LC*	LC*
$DeltaE_{BT}$	M	HC*	LC*	LC*
	P	HC*	HC*	LC*

P'_{BT} (LD)		$DeltaE_{SC}$		
		N	M	P
	N	M*	M*	0*
$DeltaE_{BT}$	M	M*	M*	0*
	P	M*	M*	M*

P'_{BT} (HD)		$DeltaE_{SC}$		
		N	M	P
	N	HD*	HD*	HD*
$DeltaE_{BT}$	M	LD*	LD*	LD*
	P	LD*	LD*	LD*

$$min \ OP_{Tcost} = [BT_{Tcost}(X), \ SC_{Tcost}(X), \ Fuel_{Tcost}(X)] \quad X \in \Omega \tag{4.8}$$

being X the vector containing the variables for HEB operation. OP_{Tcost} $[\frac{euros}{day}]$ represents the total operating cost of the vehicle. BT_{Tcost} $[\frac{euros}{day}]$, SC_{Tcost} $[\frac{euros}{day}]$ and $Fuel_{Tcost}$ $[\frac{euros}{day}]$ are the cost models defined in section 2.3. Ω is the feasible solution space.

Similarly to the HET case, the operation of the HESS in the HEB have some constraints to maintain enough energy, defined as follows:

$$SOC_{BT\_min} \leq SOC_{BT}(k) \leq SOC_{BT\_max} \tag{4.9}$$

$$SOC_{SC\_min} \leq SOC_{SC}(k) \leq SOC_{SC\_max} \tag{4.10}$$

and the power constraints defined by the DC/DC converters and genset:

$$P_{BT\_max\_ch} \leq P_{BT}(k) \leq P_{BT\_max\_dch} \tag{4.11}$$

$$P_{SC\_max\_ch} \leq P_{SC}(k) \leq P_{SC\_max\_dch} \tag{4.12}$$

$$P_{genset\_min} \leq P_{genset}(k) \leq P_{genset\_max} \tag{4.13}$$

For this scenario the SOC_{BT} [%] and SOC_{SC} [%] have been limited to the same ranges as in the HET case (see section 3.4), being these [40-95]% and [25-100]%, respectively.

Furthermore, the power targets for BT and SC packs are limited by the peak power of the DC/DC converters linked to them. Therefore, the P_{BT} [kW] and P_{SC} [kW] targets have been limited (in charging and discharging) to 75 [kW] and 150 [kW], respectively (see table 4.1). P_{genset} [kW] is limited by the minimum (P_{genset_min} [kW]) and maximum (P_{genset_max} [kW]) power output of the genset which is its operating power range 0 - 155 [kW] (see figure 4.8).

The optimization variables corresponding to the EMS (previously explained for the RB-EMS, see section 4.4.1) as well as the HESS sizing are detailed in the following vector: where

$$X = \begin{bmatrix} SOC_{u\_ctrl} \\ SOC_{l\_ctrl} \\ P_{genset\_1} \\ P_{genset\_2} \\ p_{dch\_DM} \\ p_{dch\_SM} \\ p_{dch\_AM} \\ p_{ch\_CM} \\ m_{BT} \\ m_{SC} \end{bmatrix} \tag{4.14}$$

where the space of feasible solutions Ω is defined as follows:

$$\Omega = \begin{cases} 50 \leq SOC_{u\_ctrl} \leq 95 \; [\%] \quad \Rightarrow SOC_{u\_ctrl} \in \mathbb{Z} \\ 40 \leq SOC_{l\_ctrl} \leq 85 \; [\%] \quad \Rightarrow SOC_{l\_ctrl} \in \mathbb{Z} \\ 30 \leq P_{genset\_1} \leq 80 \; [kW] \quad \Rightarrow P_{genset\_1} \in \mathbb{Z} \\ 80 \leq P_{genset\_2} \leq 155 \; [kW] \quad \Rightarrow P_{genset\_2} \in \mathbb{Z} \\ 0 \leq p_{dch\_DM} \leq 1 \quad \Rightarrow p_{dch\_DM} \in \mathbb{R} \\ 0 \leq p_{dch\_SM} \leq 1 \quad \Rightarrow p_{dch\_SM} \in \mathbb{R} \\ 0 \leq p_{dch\_AM} \leq 1 \quad \Rightarrow p_{dch\_AM} \in \mathbb{R} \\ 0 \leq p_{ch\_CM} \leq 1 \quad \Rightarrow p_{ch\_CM} \in \mathbb{R} \\ 1 \leq m_{BT} \leq 25 \; [branches] \quad \Rightarrow m_{BT} \in \mathbb{Z} \\ 1 \leq m_{SC} \leq 10 \; [branches] \quad \Rightarrow m_{SC} \in \mathbb{Z} \end{cases} \tag{4.15}$$

Following the same concept adopted for the HESS optimization in the HET case study (keeping constant the number of cell connected in series either in the BT and SC pack), the minimum number of branches in the sizing process for the HEB will be 1. Thus, for the BT and SC pack the minimum allowable energy will be 1.37 [kWh] and 0.44 [kWh], respectively.

As detailed in section 2.3 the economic model considers different referential values and constant factors which are summarized in table 4.5.

Table 4.5: Assumed referential costs and factors in HEB scenario [131].

Variable	Value	Units
C_{kWh_BT}	500	euros/kWh
C_{kWh_SC}	4000	euros/kWh
C_{kW_dcdc}	150	euros/kW
T	10	years
I	2.5	%
BT_{M_y}, SC_{M_y}	500	euros/year
k_{cs}	1.15	-
C_{L_fuel}	1.339	euros/liter
ρ_{fuel}	0.832	kg/liter
H_l	43.5e3	kJ/kg

Finally, it is important to mention that during this optimization the Whöler curve-based method (see section 2.4.2.1) for lifespan estimation has been applied. Similarly as in the HET case, the optimization parameters described in table 3.6 have been considered to configure the optimization problem in the GA toolbox under MATLAB environment.

4.6 Optimization results

The aim of this section is to present the most relevant results from the optimization process previously explained in section 4.5. As explained in section 2.6, the MO optimization result is a set of alternative solutions, where each solution has different characteristics for the defined variables (in this scenario the power targets for the RB-EMS and HESS sizing). The selection of the most suitable solution for a specific scenario will be based on the analysis of the variable values and the impact of these ones on the system operation and on the defined fitness function. The suitable solution selection will also depend of an analysis on which objective (*e.g.* economic, technical, efficiency) has priority and what are the consequences of this operation on the other ones.

4.6.1 HEB base scenario

Firstly, in order to validate the improvements that can be obtained with the HESS solution discussed in this thesis and the energy management approach proposed in this chapter for the HEB, a base scenario (as in the case of the HET) will be proposed. Considering that currently in the evaluated scenario there is not an available HEB solution to establish a comparison, the base scenario will be intended to prioritize the minimization of fuel consumption. In this case, only the initial investment and maintenance costs for the HESS (BT and SC pack cost functions) will be consider. Therefore, the replacement costs (defined by the degradation approach of the HESS during its operation) will not be taken into account.

Hence, this optimization approach is intended to obtain the optimal vehicle performance that minimize the operating cost without considering the long term impact of this behavior on the HESS operation cost (mainly on the ageing and replacement process). In order to apply the aforementioned optimization scenario, (2.29) and (2.34) have to be rewritten to replace the functions BT_{Tcost} and SC_{Tcost} in (4.8) as follows:

$$BT'_{Tcost} = \frac{BT_{M\_y} + BT_{Ca\_y}}{360} \left[\frac{euros}{day} \right] \tag{4.16}$$

$$SC'_{Tcost} = \frac{SC_{M\_y} + SC_{Ca\_y}}{360} \left[\frac{euros}{day} \right] \tag{4.17}$$

Figure 4.19 collects the set of alternative optimal solutions obtained with this first optimization approach. In this case the solutions have been ranked in ascending order depending of the daily operating cost (OP_{Tcost}) taking the first five most economical solutions (see figure 4.19(a)). Figures 4.19(b)-(e) show the values of the optimization variables defined in the HEB scenario (see vector in (4.14)).

Figure 4.19(b)-(e) show the behavior of the main variables for the RB-EMS operation as well as the ESS sizing depending on the selected alternative optimal solution. Fig-

(a)

(b)

(c)

(d)

(e)
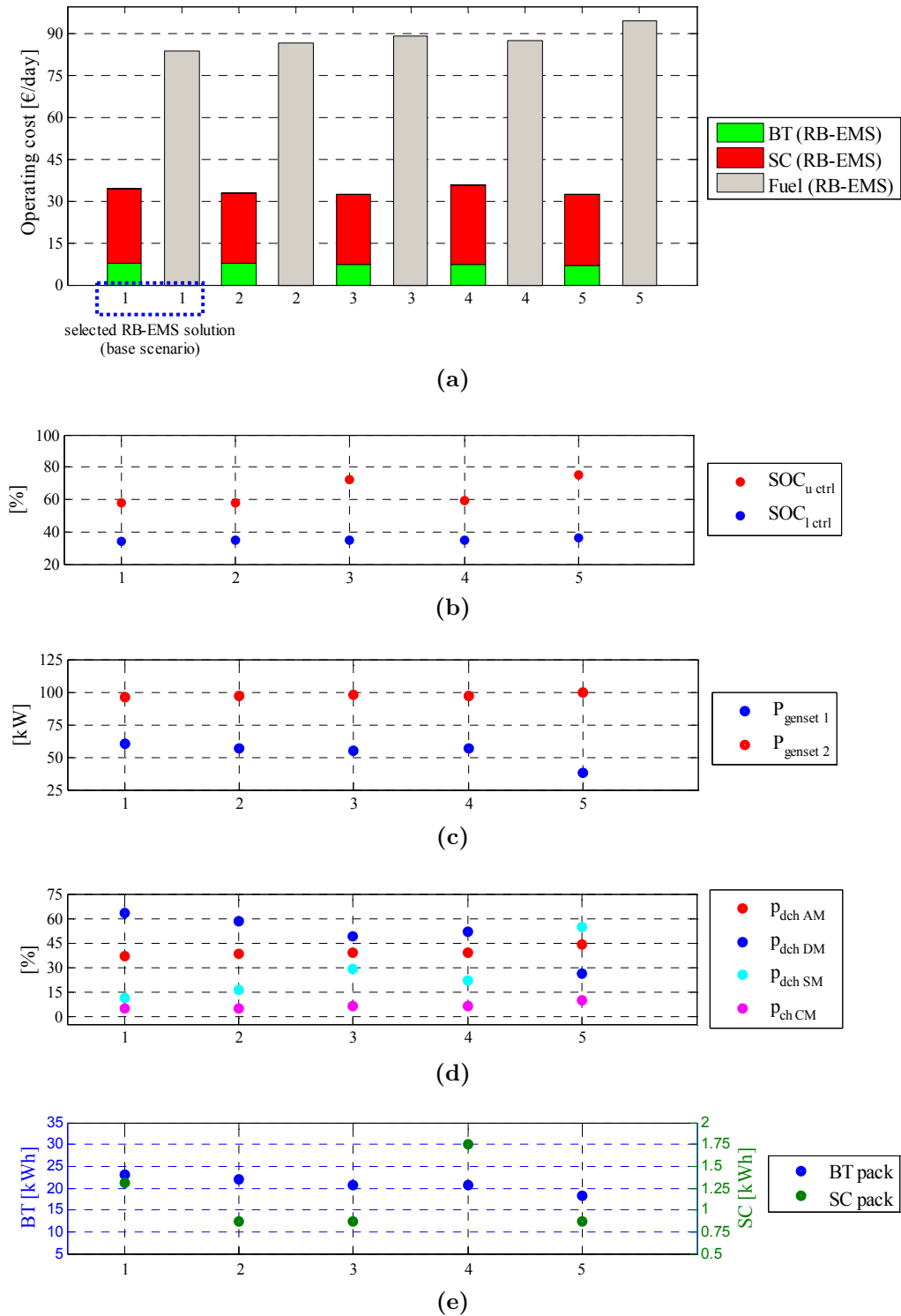
Figure 4.19: Alternative optimal solutions for the HEB base scenario (without considering HESS degradation factor).

ure 4.19(b) depicts the values to manage the SOC_{BT} and determine the corresponding *energetic operating mode*. Figure 4.19(c) shows the range for the genset operation, where

the speed and torque targets have been obtained from the optimal operating curve proposed in section 4.3 (see figure 4.8). Figure 4.19(d) depicts the percent of the nominal power that will be injected or absorbed from/to the BT pack. The BT power target during operation is determined by the C-rate limitation and the final arrangement of the cells in the pack (BT pack sizing), by calculating with (4.5)-(4.4).

It is important to mention that, to obtain the set of alternative optimal solutions depicted in figure 4.19 the same optimization methodology explained in section 2.7 has been applied. The only difference lies on the iterative degradation analysis that for this case has been avoided. Taking into account the economic factor as prior objective, the first alternative *solution 1* depicted in figure 4.19 (**which offers the minimum operating cost for the whole vehicle with minimum fuel consumption**) has been selected as the suitable one for the base scenario analysis.

It is clear that, the resulting daily operating cost from the solution selected in this base scenario will not be directly comparable with the ones that will be later obtained (see section 4.6.2) when the full economic model is applied (including the degradation approach). However, **the analysis with the base scenario will be focused on the optimization variables (EMS target and HESS sizing, see figure 4.19(b)-(d)) and how they will impact the vehicle operating cost (in the long term view) when the HESS degradation factor is considered**.

4.6.2   HEB improved scenario

Once a base scenario has been presented, this section is intended to collect the optimization results by applying the full economic model presented in section 2.6. Figure 4.20 collects the set of alternative optimal solutions obtained for the scenario proposed in this chapter. Figure 4.20(a) shows the daily operating cost of the vehicle composed of the partial costs for each analyzed factor (BT, SC and fuel costs) evaluated during operation. Mainly in the HESS, it is worth to denote that a higher cost represents a less lifetime of the BT and SC packs, and due to this fact, the BT and/or SC pack will have to be replaced more times in the same lifetime of the HEB (defined in 10 years for this scenario).

By applying the adaptive fuzzy-based approach proposed in section 4.4.2, it is possible to determine the operating cost for the same scenario using the improved A-EMS. In this case, the membership functions of the fuzzy strategy (see figure 4.18) have been configured with the values obtained in each alternative optimal solution from the RB-EMS optimization. The operating costs resulting from these re-evaluation based on the A-EMS are depicted in figure 4.20(a) with the corresponding cost reduction reached from the RB approach.

As mention before, when the suitable solution have to be selected from the set of alternative optimal solutions either technical and economic criteria can be applied. Table 4.6 summarizes the most relevant solutions mainly focused on economic and sizing factors in
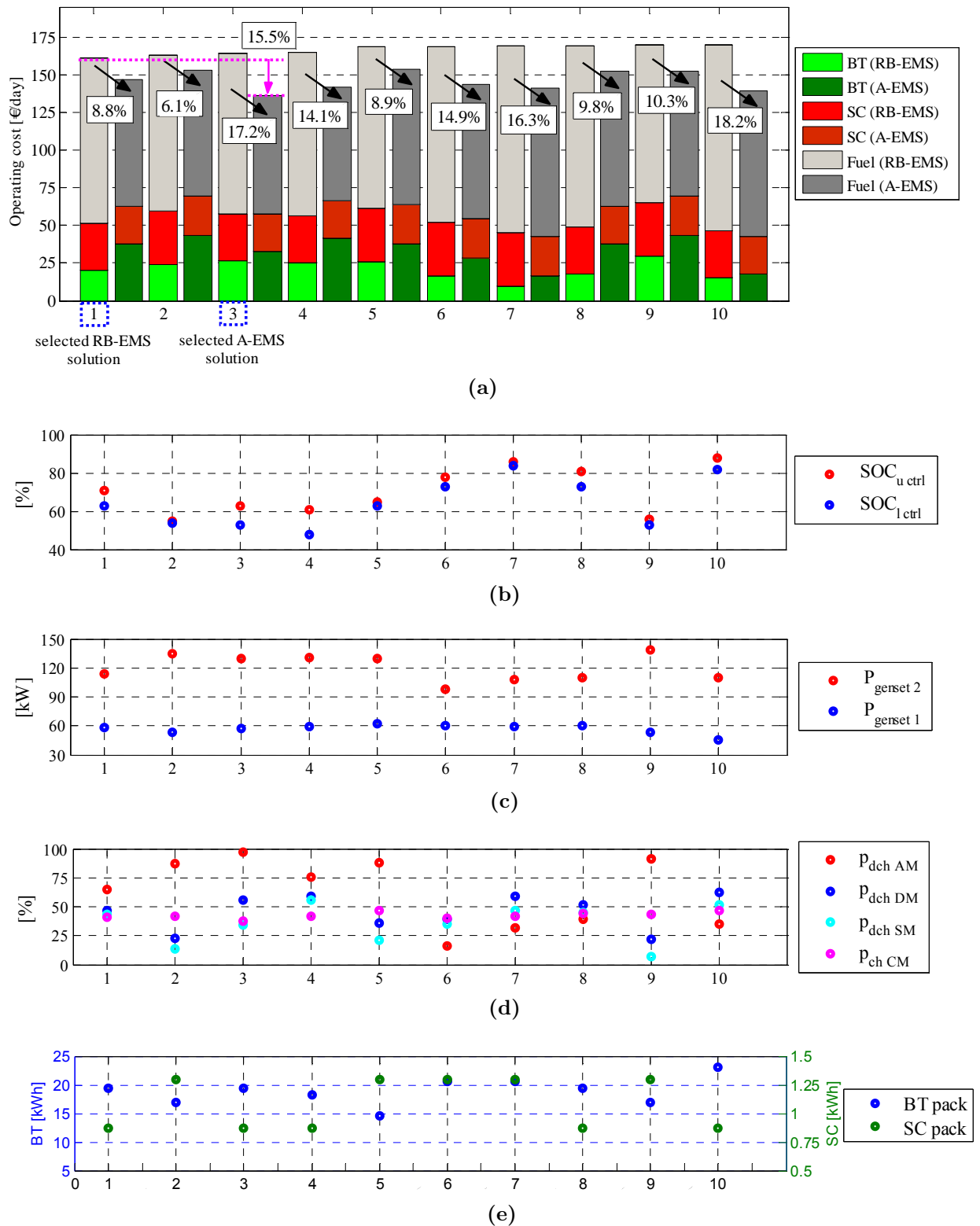
Figure 4.20: Alternative optimal solutions for the HEB scenario (considering HESS ageing and replacement factors).

case the priority in one of them is needed.

Table 4.6: Criteria for selecting a suitable solution.

| Criteria | RB-EMS | | | A-EMS | | |
| | (Solution - value) | HESS sizing [kWh] | | (Solution - value) | HESS sizing [kWh] | |
		BT	SC		BT	SC
Min. global operating cost	1 - 160.8 [$euros/day$]	19.4	0.87	3 - 135.9 [$euros/day$]	19.4	0.87
Min. BT operating cost	7 - 9.6 [$euros/day$]	20.6	1.3	7 - 16.6 [$euros/day$]	20.6	1.3
Min. SC operating cost	10 - 30.9 [$euros/day$]	23.1	0.87	3 - 24.8 [$euros/day$]	19.4	0.87
Min. fuel consumption	2 - 103.1 [$euros/day$]	17.0	1.3	4 - 75.7 [$euros/day$]	18.2	0.87
Smallest BT pack	5 - 14.6 [kWh]					
Smallest SC pack	1,3,4,8,10 - 0.87 [kWh]					

In order to fulfill the aim defined in this thesis about **minimizing the total oper-ating cost of the vehicle**, the alternative optimal solutions with the lowest total cost have been selected either in RB-EMS and A-EMS approach. In this case, **the *solution 1* from the RB-EMS optimization has been selected (160.8 [$\frac{euros}{day}$])**. Despite that *solution 1* with the A-EMS approach shows a cost reduction of around 8.8% from the RB-EMS, **the resulting cost in *solution 3* shows a saving of around 15.5% (135.9 [$\frac{euros}{day}$]), becoming in the selected choice for the A-EMS operation**. As it can be seen in figure 4.20(e), this operating cost reduction is reached only by the improvement on energy management obtained with the A-EMS because in both cases (*solution 1* and *solution 3*) the resulting HESS sizing is the same. However, the other solutions could be considered as feasible depending on the selection criteria (see table 4.6).

Taking the parameters values (EMS targets and HESS sizing, see figure 4.19(b)-(d)) of the alternative optimal *solution 1* from the base scenario presented in section 4.6.1, where the factor of the HESS ageing and their replacement were disregarded, it is possible to evaluate the impact of this operation on the long term view. In this case, these parameter values (assumed as optimal in the base scenario) have been used to configure the A-EMS. Then, the full economic model (this time taking into account the HESS ageing and replacement factors) has been applied. Figure 4.21(a) depicts this analysis where the resulting re-evaluated daily operating cost has been compared with the ones defined as optimal in this section, being these, *solution 1* and *solution 3* for RB-EMS and A-EMS, respectively (see figure 4.20).

In this case, **the re-evaluated solution (assumed as optimal when the factors of HESS ageing and replacements were disregarded) is 36% more expensive than comparing with the selected optimal one** (*solution 3*, see figure 4.20) **where either the proposed A-EMS and optimization methodology have been applied**. A similar analysis has been carried out with the fuel consumption (figure 4.21(b)) where the cost obtained with the selected alternative solution (*solution 3* with A-EMS, see fig-

(a) Daily operating cost.

(b) Fuel cost.
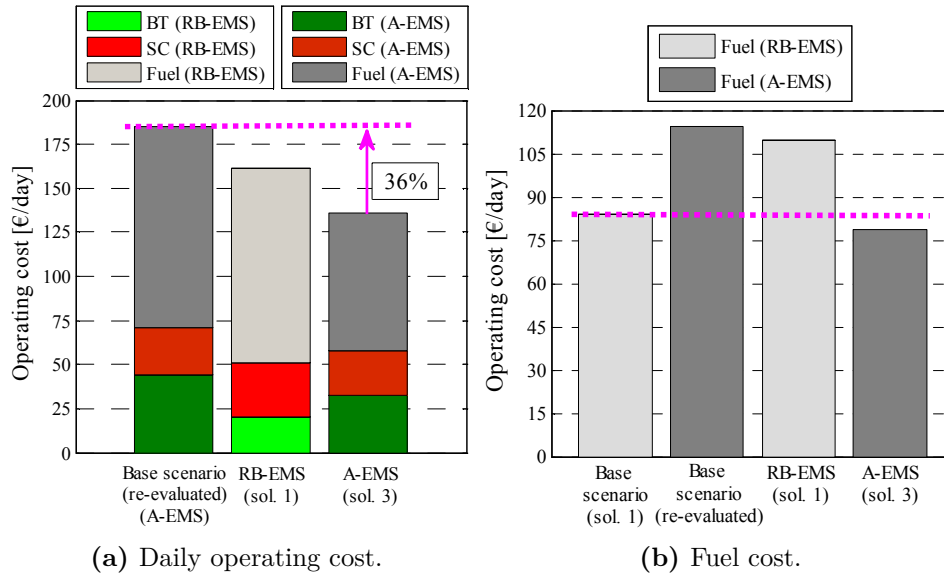
Figure 4.21: Comparative analysis with base scenario.

ure 4.20) is slightly lower than the one obtained in the base scenario (which prioritized the minimum fuel consumption, see figure 4.19). It means that, **with the proposed approach of this thesis (A-EMS and optimization methodology), it is possible to reach fuel consumption savings even lower than those when only the minimization of the fuel usage has been taken into account while still reducing the operating cost of the whole vehicle.**

On the one hand, the aim of this analysis from the base scenario has been to highlight the potential impact on the operating cost that may have to consider or not the factors of HESS ageing and evaluation on the long term scope during the design stage of the EMS and HESS sizing. On the other hand, it has been highlighted the economic improvements that can be obtained by applying the adaptive EMS together with the optimization methodology proposed in this PhD thesis.

Figure 4.22 and figure 4.23 depicts the operating performance of the HESS for a single trip (figure 4.2). In this case, the EMS and HESS sizing have been configured with the parameter values from the selected solutions (*solution 1* for RB-EMS and *solution 3* for A-EMS, see figure 4.20). In both EMS approaches the BT pack fulfills the low power demands avoiding to operate the ICE in its low efficiency zone (low power demand). Furthermore, the SC pack injects the power peaks during traction and absorbs most of the regenerative energy during braking. The BT pack is only charged from regenerative braking when the SC pack is not able to absorb energy, but fulfilling the power constraints to ensure the BT health.

However, there is clear differences of the adaptive approach from the non-adaptive one (pink circles on figure 4.22 and figure 4.23) that allow a better harnessing of the energy
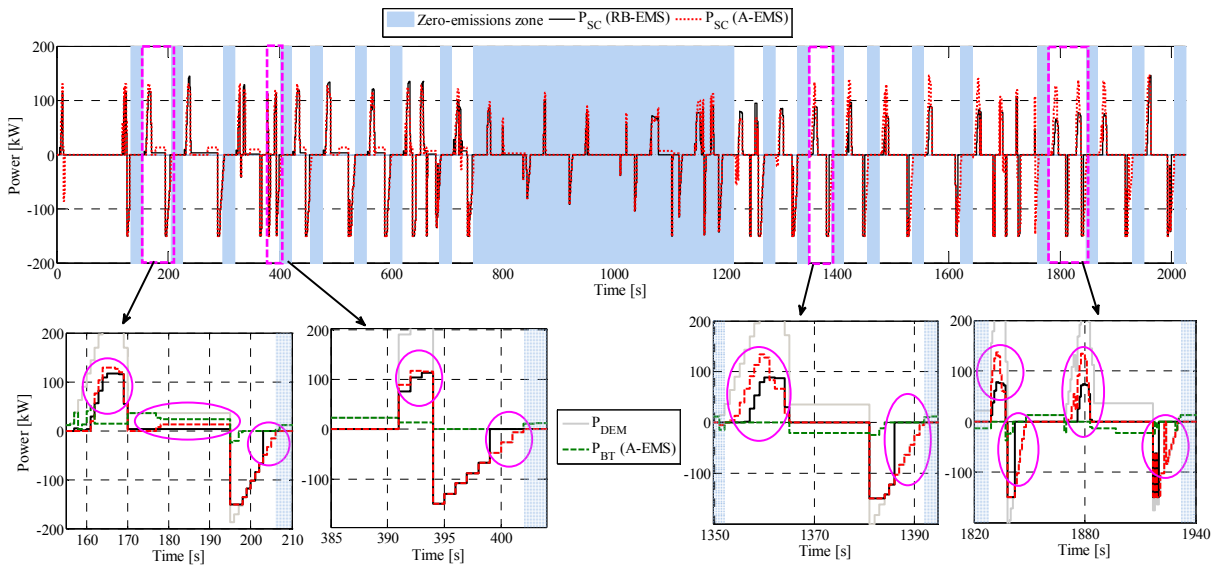
Figure 4.22: SC pack performance profile in HEB.
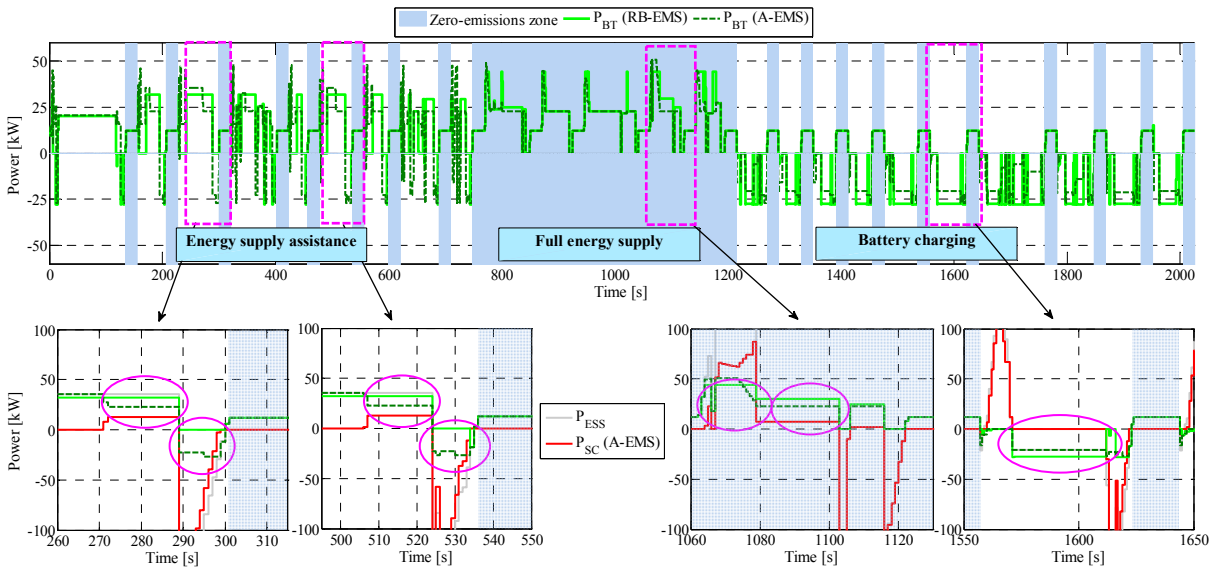
Figure 4.23: BT pack performance profile in HEB.

during traction and regenerative phase. As can be seen in figure 4.22 the adaptive approach allows increasing/decreasing the energy consumption from the SC pack depending on the future operating and energy demand conditions. This adaptive behavior allows to absorb most of the energy available during regenerative, that otherwise would be lost as heat in crowbar (as in some stages of the RB-EMS performance) while fulfilling the power and energy demand during traction. Similar adaptive behavior is shown in figure 4.23 for the BT pack operation comparing the RB-EMS with the A-EMS approach.

Figure 4.24 depicts the performance of the genset operation. As defined in the RB-

EMS, the genset will only operate at high power rates from vehicle power demand or during the BT recharging stage. It is worth mentioning that, the ICE is turning off (no fuel consumption) only in the zero-emission zones. During operation, if there is not power requested to the genset, the ICE is set at idle speed (low fuel consumption) avoiding the continuous start/stop issues of the system. Furthermore, Figure 4.24 shows the power demanded to the genset (grey dark zone), however, during the charging stage the genset demand is increased (instead of operating at low power demands) to recharge the BT pack. Thus, the vehicle could increase the autonomy for operating the whole daily journey without the need of stopping for plug-in recharging along the route.
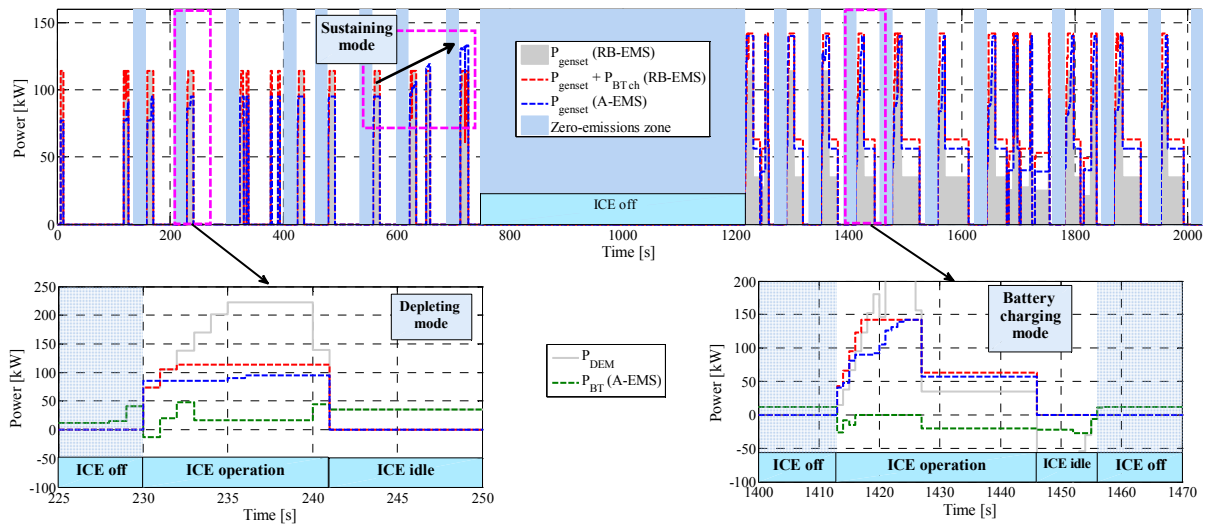
Figure 4.24: HEB performance: genset operation.

Figures 4.25-4.26 depict the daily SOC for the BT and SC packs with the optimal solution selected for RB-EMS and A-EMS.

By analyzing a complete day profile it is possible to determine (in terms of energy harnessing during braking phase) the energy efficiency of the vehicle. Thus, **the RB-EMS approach shows an efficiency of around 81.4%** (for the selected choice, *solution 1*) while **the adaptive strategy reaches the highest value around 94%** (in all the alternative optimal solutions). Table 4.7 summarizes the energy efficiency analysis done with both EMS approaches.

Finally, to determine the vehicle autonomy and average fuel consumption in *full-electric* and *hybrid* operation, respectively, the alternative solutions have been evaluated by using a sequence of several standardized **SORT 1** cycles (Figure 4.27). **The selected A-EMS solution (*solution 3*) shows an average fuel consumption reduction of around 16.1% from the RB-EMS choice (*solution 1*).** Nevertheless, **it is possible to reach a fuel saving up to 19% (from the RB-EMS choice) with *solution 4* when the A-EMS is applied**. On the other hand, the full-electric autonomy remains relatively similar by comparing the respective RB-EMS and A-EMS solutions with dis-
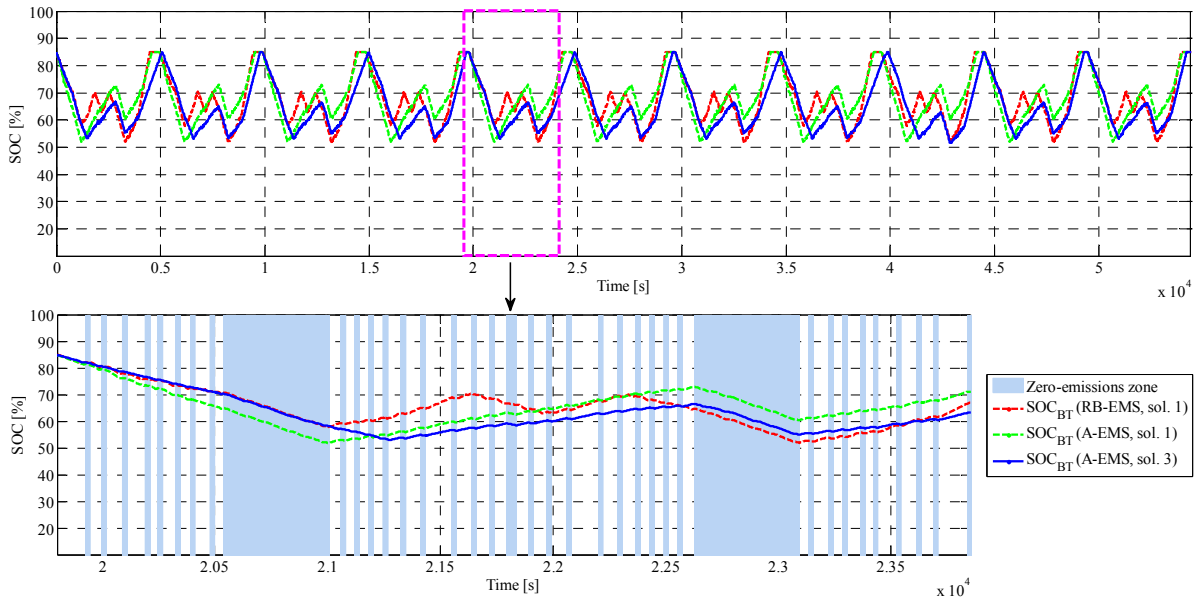
Figure 4.25: SOC_{BT} profiles during daily HEB operation.
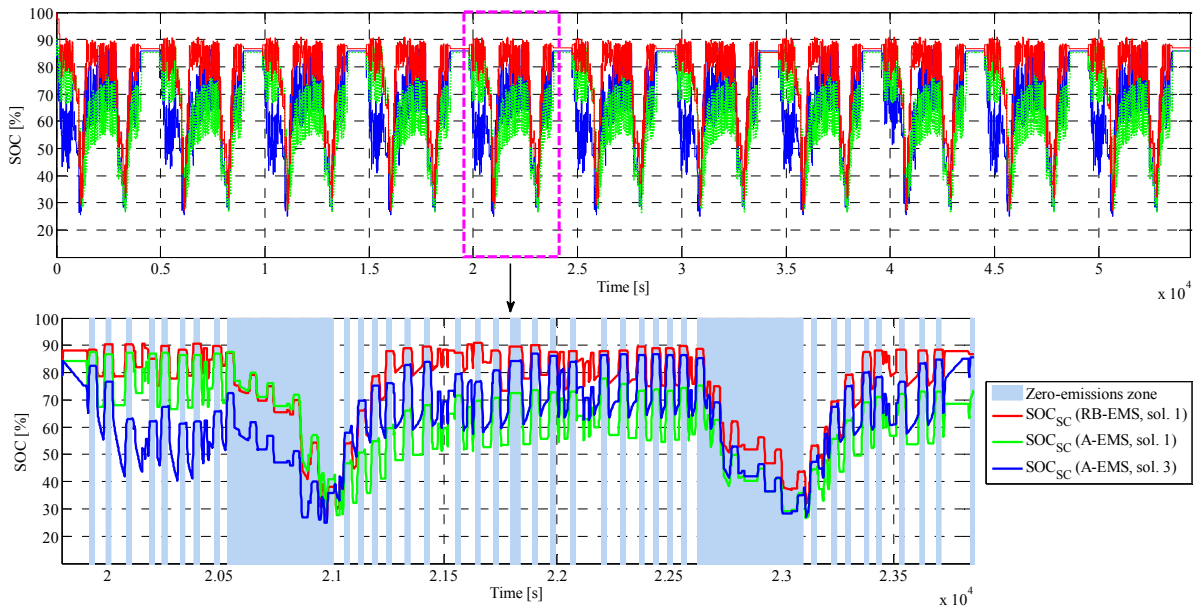
Figure 4.26: SOC_{SC} profiles during daily HEB operation.

tances between 8.2 up to 9.5 [km] and a slight increase of around 2% with the adaptive approach. Table 4.7 also includes the obtained results from fuel consumption and daily operating cost analysis, in this case, the values with "*" denote the solutions where the minimum values have been reached. Similarly, regarding the operating cost reduction, autonomy and efficiency analysis previously done, the values with "**" denote the solutions where the maximum values have been found.
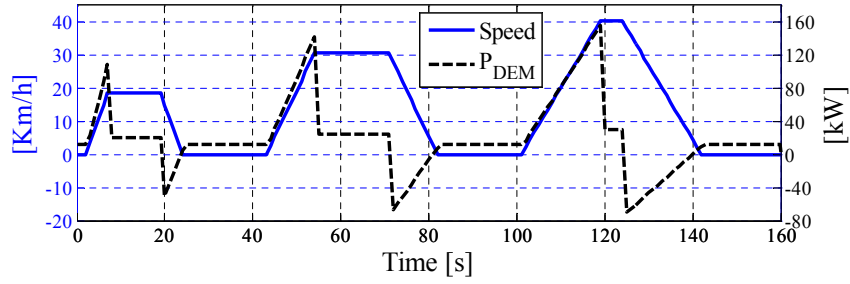
Figure 4.27: Standardized on-road test cycle (SORT 1).

Table 4.7: Fuel consumption and cost analysis.

Sol.	Avg. fuel consumption [liter/100km]			Full-electric dist. [km]		Regen. eff. [%] (kWh_{abs}/kWh_{reg})		Operating cost [euros/day]		
	RB	A	inc./red. of A from sol. 1_{RB}	RB	A	RB	A	RB	A	reducc. of A from sol. 1_{RB}
1	27.9	24.8	-11.1%	8.2	8.4	81.4	94.1	160.8*	146.6	-8.8%
2	26.6*	24.8	-11.1%	7.6	7.7	89.5	93.9	162.3	152.4	-5.0%
3	27.4	23.4	-16.1%	7.3	7.4	76.0	94.1	164.1	135.9*	-15.5%**
4	27.3	22.6*	-19%**	7.9	8.1	74.7	94.2	165.1	141.8	-11.8%
5	27.1	26.6	-4.7%	7.5	7.6	83.4	93.1	168.2	153.2	-4.7%
6	30.1	26.6	-4.7%	9.4	9.6	89.9	94.3	168.8	143.6	-10.6%
7	32.3	29.4	+5.4%	9.1	9.5	87.3	94.2	169.0	141.5	-12.1%
8	31.5	26.9	-3.6%	8.8	8.9	87.3	94.1	169.1	152.5	-5.1%
9	26.9	24.6	-11.8%	9.5**	9.7**	90.7**	93.6	169.6	152.1	-5.4%
10	33.6	28.7	+2.9%	8.9	9.2	84.6	94.8**	169.8	138.9	-13.6%

RB: RB-EMS, A: A-EMS, abs: absorbed, reg: regenerated, red: reduction, inc: increase, dist: distance, sol: solution

4.7 Conclusions

In this chapter the adaptive fuzzy-based EMS approach proposed in this PhD thesis, and previously applied on the HET scenario, was modified and applied on the HEB case study. Firsly, the application scenario was presented for an urban route including several stops and zero-emission zones, therefore, combining hybrid (genset+HESS) and full-electric (HESS) operation during the daily journey.

Furthermore, in this chapter an optimization methodology for selecting the most efficient point and optimal operating curve in an ICE was presented and applied on the genset of the HEB scenario. This methodology allows to consider the whole space of possible combinations of ICE rotational speed and torque to determine, by an exhaustive optimization, the operating points where the high efficiency is reached for each discrete power output in the available operating range of the genset (ICE+EG). Therefore, the optimal operating curve (on which the genset will operate) can be calculated off-line and then included as look-up-table in the on-board ICE controller to obtain the instantaneous

rotational speed and torque targets.

In this chapter two EMS approaches for the HEB with HESS were presented. On one hand, a RB-EMS with different operation modes depending on the operating conditions of the vehicle. The RB-EMS was developed in a generic way and some key parameters were highlighted to be included as variables in the optimization methodology proposed in this PhD thesis. On the other hand, in the A-EMS based on fuzzy-logic, the membership functions were built around generic values that later were configured with the optimal ones selected from the RB-EMS optimization. This way, the whole structure of the fuzzy sets in the A-EMS is modified depending on the EMS targets and HESS sizing to obtain a vehicle performance adapted to each set of analyzed variables and allowing a better harnessing of the available energy in the HESS.

In the optimization results analysis, firstly a base scenario was introduced. In this case an optimization, where the HESS degradation and replacement factors were disregarded, was carried out. The aim of this base scenario was to highlight the importance of considering either the HESS ageing and economic analysis with a long term view as well as to show the impact on the operating cost when these factors are disregarded. The simulation results showed that, when the optimal solution selected from the base scenario optimization (minimum daily operating cost with minimum fuel consumption) is re-evaluated including the avoided factors (HESS degradation and replacement costs) the daily operating cost is 36% more expensive than comparing with the optimal solution from the approach proposed in this thesis (A-EMS together with optimization methodology). It means that, even an optimized solution looking for the minimum fuel consumption (in the short term) will result more costly in the long term view for the vehicle operator or end-client. However, a more economical and still well performed solution can be obtained when the methodological optimization and improved EMS proposed in this PhD thesis are applied.

In case of RB-EMS and A-EMS optimization results, the alternative solutions were analyzed and compared in terms of minimum global operating cost, minimum cost for a specific objective, average fuel consumption and autonomy in full-electric operation. In both approaches (RB-EMS and A-EMS) the alternative optimal solutions which showed the minimum operating cost for the whole vehicle were selected.

Thus, the selected alternative optimal solution for A-EMS showed a daily operating cost reduction up to 15% (while maintaining the same HESS sizing) from the best value reached with the optimized RB-EMS approach. This shows an improvement in the harnessing of the on-board energy sources by reducing costs while using the same HESS sizing. Furthermore, the average fuel consumption was reduced up to 19% with the adaptive strategy (from the selected RB-EMS solution). These reductions were reached due to the improvement on the EMS for a better harnessing of the energy and power split during operation. Besides, the A-EMS allowed an improvement in energy harnessing during braking, with efficiencies around 94% than comparing with the RB-EMS approach

(efficiencies between 76 – 90.7%).

The results of this chapter reinforce the focus studied during this PhD thesis about the clear importance of the EMS and optimized selection of its operation (taking into account the sizing and ageing approach of the HESS) to assure the proper harnessing of the on-board energy (fulfilling the operation requirements) and the suitable vehicle performance while minimizing the operating cost during the whole vehicle lifetime.

5

Sensitive analysis on HET and HEB

5.1 Sensitive analysis on HET and HEB

This last chapter aims to evaluate the techno-economic impact that may have the ageing model (mainly focused on the batteries) considered as lifetime estimation method into the optimization methodology proposed in this PhD thesis. As mentioned in chapter 2, regarding the different types of ageing models available in the current literature, two different ones have been selected and described in section 2.4.2.1 (*Whöler curve*-based method) and section 2.4.2.3 (*Semi-empirical* method).

The basic idea in this analysis is to compare and quantify the techno-economic implications when a commonly used lifetime estimation method (*Whöler curve*-based) or a more accurate one (*Semi-empirical* method) are considered within the methodology for HESS sizing and EMS optimization proposed in this thesis. It means that, on the one hand, how the lifetime estimation affects the power targets for the EMS (modifying the optimization results) and the resulting optimal HESS sizing. On the other hand, how much the operating cost of the vehicle is increased/decreased depending on the lifetime estimator that is applied during the optimization and quantify the possible economic benefits of considering each one of them.

Throughout the several simulations and optimizations carried out either in chapter 3 (devoted to the HET case study) and chapter 4 (dedicated to the HEB case study) the *Whöler curve*-based method (together with *Rainflow cycle counting algorithm*) has been applied. This lifetime estimation method has been considered basically because the required information to configure it is relatively more simple to be obtained (comparing with more sophisticated semi-empirical methods). The process normally includes several cell tests at different DODs in order to obtain the life-cycles until the BT cell is considered exhausted. Due to the fact that the *Whöler curve*-based method does not need a dedicated mathematical modeling, the economic and time costs for its development can be considered lower than other Semi-empirical methods. Indeed, most of the cell manufacturers already present information regarding the available life cycles for the cell in their data-sheets [106, 132, 133].

Due to the aforementioned reasons, the *Whöler curve*-based method has become in a commonly used approach applied for ESS sizing purposes in HEVs [35, 96, 123] as well as in other kind of scenarios such us grid-connected storage [114], wind generation with storage [134] and Photo-voltaic power plants with BT storage [135]. Furthermore, the *Whöler curve*-based method is widely applied in the industrial sector by the vehicle manufacturers during the design stage of the vehicle in order to estimate the on-board energy needed and the replacement behavior during the lifetime of the vehicle.

It is worth to mention that, during the lifetime of the vehicle (HET or HEB), the end-client or the vehicle manufacturer (depending on the contractual conditions) are in charge of the maintenance and replacement of the ESS (and its electrical devices) to guarantee the correct operation of the vehicle. Hence, the suitable sizing and operation of the ESS

become in a key factor to assure the fulfillment of the operational conditions, avoiding the unscheduled maintenance and repairs which may affect both the estimated economic profits and the operational availability of the vehicle. Here, the lifetime estimation is a very useful tool which allows to organize the corresponding maintenances and replacement regarding the ESS.

The cost savings in the vehicle operating cost that can be reached when the lifetime estimation and ESS replacements are considered into the economic model during the optimization of sizing and EMS (as part of the methodology proposed in this PhD thesis, see section 2.7) have been widely presented and explained either for the HET and HEB scenarios. Along this thesis, it had been stated that the research project is focused on the development of an optimized and adaptive EMS, that together with a methodological optimization of the HESS sizing, are able to fulfill the technical requirements of the vehicle while assuring the minimization of total operating cost. Nevertheless, taking into account the importance of the ESS lifetime estimation factor into the economic model, it arises the need of evaluating and to quantify the economic deviation (from the expected cost savings) when a more-accurate lifetime estimation model is applied. It is understood for deviation the corresponding increase or decrease in the ESS lifetime which may have repercussions in the replacement behavior during the vehicle lifetime (increasing or decreasing the total operating cost for the end-client or vehicle operator).

Regarding the HESS, the *Whöler curve*-based method has been applied either for the BT as well SC pack lifetime estimation both in chapter 3 and chapter 4. Considering the relatively long life of the SC technology (determined by its quite high number of charging/discharging cycles) compared with the BT technology, it is clear that the sensitive storage system in a hybrid topology is this last one.

Based on the aforementioned reasons, a second method has been considered for the BT lifetime estimation (*Semi-empirical* method). As mentioned in chapter 2, this lifetime estimation method was previously developed and validated in IK4-IKERLAN for a specific LFP BT cell to evaluate the capacity fade over the time by superimposing the effect of calendar and cycle life degradations and reaching a very promising RMSE prediction error of around 1.4% [102]. Therefore, due to the high accuracy of this *Semi-empirical* model, it allows to establish a more realistic comparison level for the *Whöler curve*-based lifetime estimation.

Thus, in the second section of this chapter, the process defined for the techno-economic comparison of both aforementioned lifetime estimation methods is described. Then, in the third section, the simulation results for the HET case either from the *Whöler curve*-based as well as *Semi-empirical* based optimization are compared and the main economic and technical differences are highlighted. In the fourth section, a similar comparison approach is applied for the Hybrid Electric Bus case, highlighting the main obtained results. Finally, the conclusions regarding this chapter are presented.

5.2 Process for the techno-economic comparison of lifetime estimation models

As stated in chapter 2, one of the contributions of this PhD thesis is a methodology for the multi-objective optimization of HESS sizing and parameters for the EMS. As described in section 2.7, within the steps in which these methodology has been organized, it has been defined a *technical requirements* analysis (*Step 3*, see figure 2.19). This level of the methodology is in charge of simulating the vehicle operation (based on the vehicle electrical model and a set of parameters for the HESS sizing and EMS) an evaluating the technical fulfillment of the scenario requirements. After this, the operation profiles for the BT pack and SC pack are obtained and an ageing model (iterative process) is applied on each ESS.

This ageing model allows, on the one hand, to estimate the current SOH of the cell (in case of batteries) to update the corresponding loss of capacity on it and to re-calculate the available capacity of the ESS pack. On the other hand, it allows to estimate the lifetime of the ESS (BT pack and SC pack), which is an input for the economic model (see section 2.3). Based on this lifetime estimation is calculated the number of replacements needed of the BT and SC pack, which have direct impact on the operating cost of the system when the scope of the whole vehicle lifetime is considered.

5.2.1 Main steps for the *Whöler curve*-based and *Semi-empirical* based optimizations

Figure 5.1 illustrates the optimization process followed in the previous chapters 3- 4 for the HET and HEB case studies, respectively. In both chapters the lifetime estimation is obtained by means of the *Whöler curve*-based method and *Rainflow cycle counting algorithm* (see section 2.4.2.2) either for the BT and SC pack. The sets of alternative optimal solutions (HESS sizing and parameters for the EMS) have been presented and discussed in both aforementioned chapters. The results have been presented in economic terms in order to quantify the improvements that can be obtained by means of the novel adaptive EMS and optimization methodology proposed in this PhD thesis.

Figure 5.1 also illustrates the optimization process that is carried out in this chapter. In this case, the difference lies on the ageing model that is applied for lifetime estimation of the BT pack while the other stages of the process are the same as the ones considered for the *Whöler curve*-based optimization. At this point it is worth to mention that, to obtain the techno-economic results presented in this chapter only the A-EMS has been applied. This strategy as well as the potential improvements that can be reached when it is applied (in terms of operation performance, economical, efficiency) have been widely presented and discussed in the previous chapters.
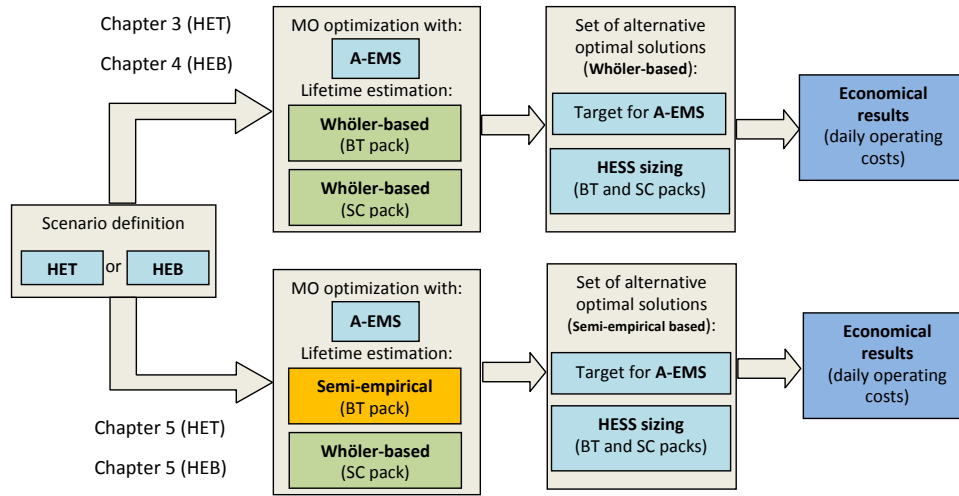
Figure 5.1: Methodological optimization followed in Chapters 3, 4 and 5.

5.2.2 Re-evaluation process of *Whöler curve*-based optimization results with *Semi-empirical* method

Figure 5.2 shows the **re-evaluation process** carried out to determine the economic impact of the lifetime (in the BT pack), therefore, the importance of the ageing model accuracy for the sizing and operation of a HEV. This re-evaluation process considers as input the set of alternative optimal solutions (parameters to configure the A-EMS and HESS sizing) obtained from the MO optimization when the *Whöler curve*-based method was applied as lifetime estimator.
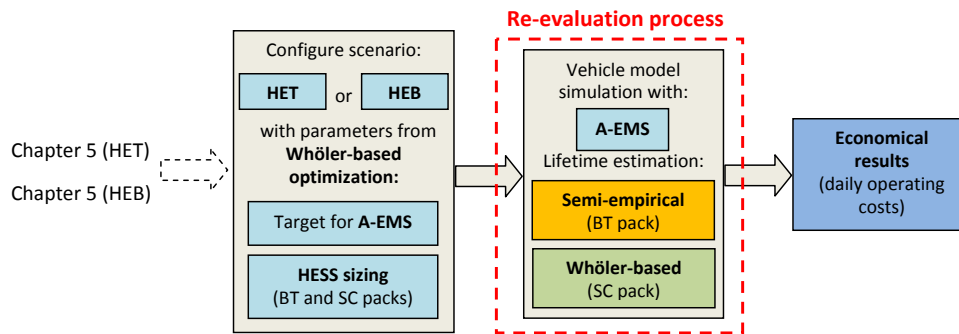
Figure 5.2: Proposed re-evaluation process for the lifetime estimation.

Then, the simulation model is applied but this time the *Semi-empirical* method is considered as lifetime estimator. As mention before, the lifetime estimation done by the *Semi-empirical* model will be assumed as the most realistic for the BT cell (which has been applied for composing the BT packs along the simulations carried out in this thesis). Therefore, the results obtained from this ageing model will be used as target for comparing the *Whöler curve*-based optimization. The economic results from this **re-evaluation process** aim to provide information about:

Assuming that the Semi-empirical ageing method is the most accurate one for the BT cell, what are the economic implications if the ESS is sized and operated considering the ageing and lifetime estimation based on a commonly used method (Whöler curve-based) but finally, along the lifetime of the vehicle, the ageing process (therefore the lifespan of the BT pack) follows a different behavior.

Furthermore, based on the optimization results when the *Semi-empirical* model is applied as lifetime estimator (Figure 5.2), it is possible to determine the gap between the "error" in the estimated cost savings (defined by the **re-evaluation process**) and the more-realistic economic improvements that can be obtained (with the *Semi-empirical* based optimization).

5.3 Techno-economic comparison (HET case)

In this section the main results from the previously explained optimization process (see figure 5.1) and re-evaluation process (see figure 5.2) are applied for the HET case study. As stated in section 5.2.1, the simulation results presented in this chapter consider only the A-EMS, therefore, for the HET the adaptive strategy proposed in section 3.3.2 has been applied.

5.3.1 Assessment of the *Whöler curve*-based optimization results

Figure 5.3(a) depicts the set of alternative optimal solutions obtained by means of the MO optimization proposed in section 3.4 (see figure 3.11(b)). The objective defined for the MO optimization was to minimize the total daily operating cost of the tramway. Thus, as discussed in chapter 3, the first alternative optimal solution (*solution 1*) was selected as suitable one for the HET scenario.

Furthermore, figure 5.3(b) illustrates the operating costs obtained after **re-evaluating** each alternative optimal solution depicted in figure 5.3(a) by means of the process explained in section 5.2.2. Comparing with the base scenario (SC-based tramway), a noticeable reduction in the expected cost savings is obtained. **The operating cost increase is significant mainly in the BT pack, which reduces the cost saving of the whole vehicle from 18.8% and 25.5% up to 7.7% and 15.3% in the two scenarios (*Permanent operation* and *Unscheduled stops operation*) proposed in chapter 3**, respectively.

Evaluating only the cost variation regarding the BT pack (figure 5.4), for the alternative optimal solution selected (*solution 1*) the operating cost is more than double of the expected one. It means that, the operation behavior defined as suitable for the BT pack (by means of the parameters to configure the A-EMS obtained from the *Whöler curve*-based optimization) with a long term analysis and comparing with a more realistic

(a) *Whöler curve*-based method   **(b)** *Semi-empirical* method (re-evaluated)
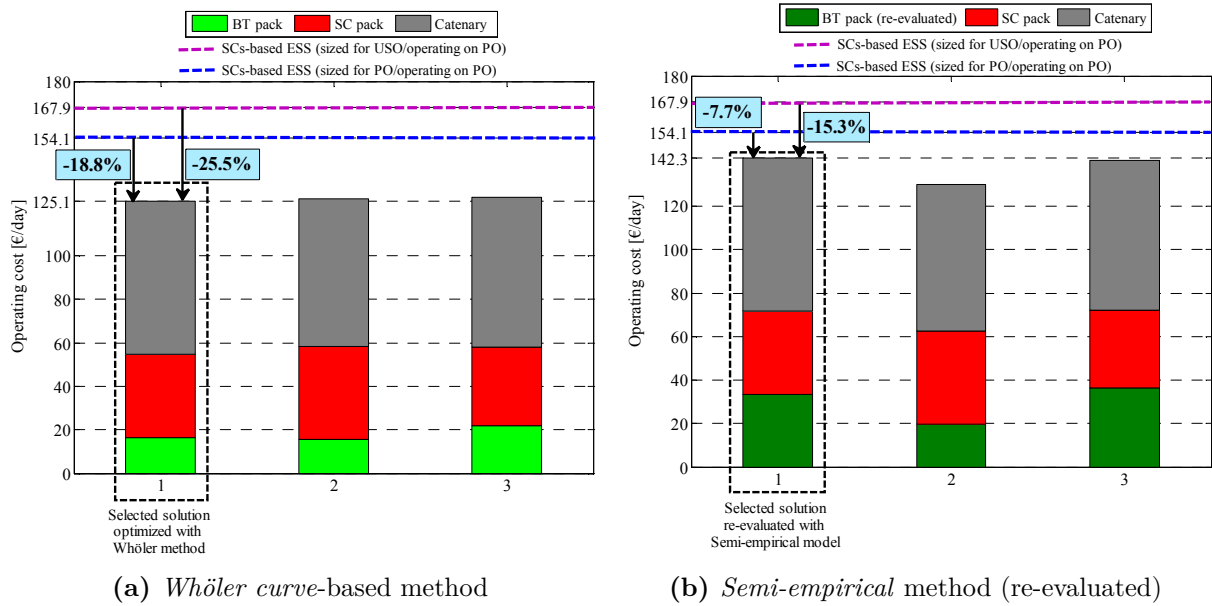
Figure 5.3: Alternative optimal solutions (applying *Whöler curve*-based lifetime estimation method) and re-evaluation applying *Semi-empirical* lifetime estimation method (HET).

ageing profile may result even more costly than other alternative optimal solutions (*e.g. solution 2*) that were disregarded in the first analysis. This cost increase reflects that the BT cell will degrade faster (less lifetime) and will force to a more number of replacements of the BT pack during the lifetime of the vehicle.
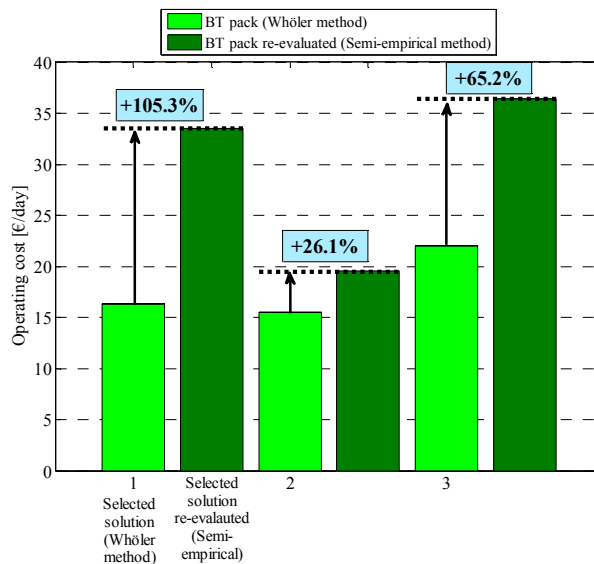
Figure 5.4: Re-evaluation of the BT pack operating cost (obtained with *Whöler curve*-based lifetime estimation method) with *Semi-empirical* lifetime estimation method (HET).

Despite this fact, **the cost increase in the BT pack operation is not constant for all the cases evaluated**. For instance, with *solution 2* the cost increase is just around 26% and with *solution 3* is 65% (while for *solution 1* was more than double). Therefore, this makes it difficult to estimate some kind of constant factor which may help to establish the gap (in economic or accuracy terms) between the *Whöler curve*-based method and *Semi-empirical* method for lifetime estimation.

Figure 5.5 shows the increase in the total operating cost of the tramway in each alternative optimal solution due to the **re-evaluation** of the BT pack ageing with the *Semi-empirical* method. From the expected operating cost, the updated ones show increases of 13.7%, 3.2% and 11.3% for the three alternative solutions (obtained with *Whöler curve*-based optimization), respectively.
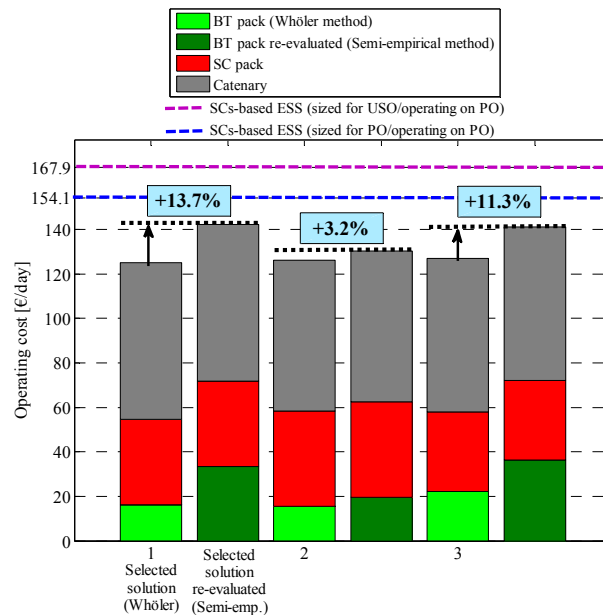
Figure 5.5: Update of the total operating cost (HET) with the re-evaluation applying *Semi-empirical* lifetime estimation method.

Figure 5.6(a) depicts the lifetime estimation done by the *Whöler curve*-based method for the BT pack as function of the HESS sizing (combining BT and SC) where the results are presented in *p.u.* with respect to the maximum lifetime [years] reached in the *Whöler curve*-based optimization. As mention in section 2.4.2.1, for the SC case the same principle of the *Whöler curve*-based method (combined with the *Rainflow cycle counting algorithm*) has been applied along the simulations carried out in chapters 3, 4 and 5. The estimation of lifespan for the SC pack is depicted in figure 5.6(b), similarly to figure 5.6(a), the resulting values are presented in *p.u.* with respect to the maximum lifetime [years] reached for the BT pack in the *Whöler curve*-based optimization. The unfeasible solutions are the ones that do not fulfill the energy/power requirements for the tramway operation, therefore, are discarded during the optimization process.

It is worth to mention that, **all the lifetime estimation plots presented in this chapter are depicted in *p.u.* values with respect to the maximum lifetime [years] reached in the *Whöler curve*-based optimization (figure 5.6(a))**.

(a) BT-pack   (b) SC-pack
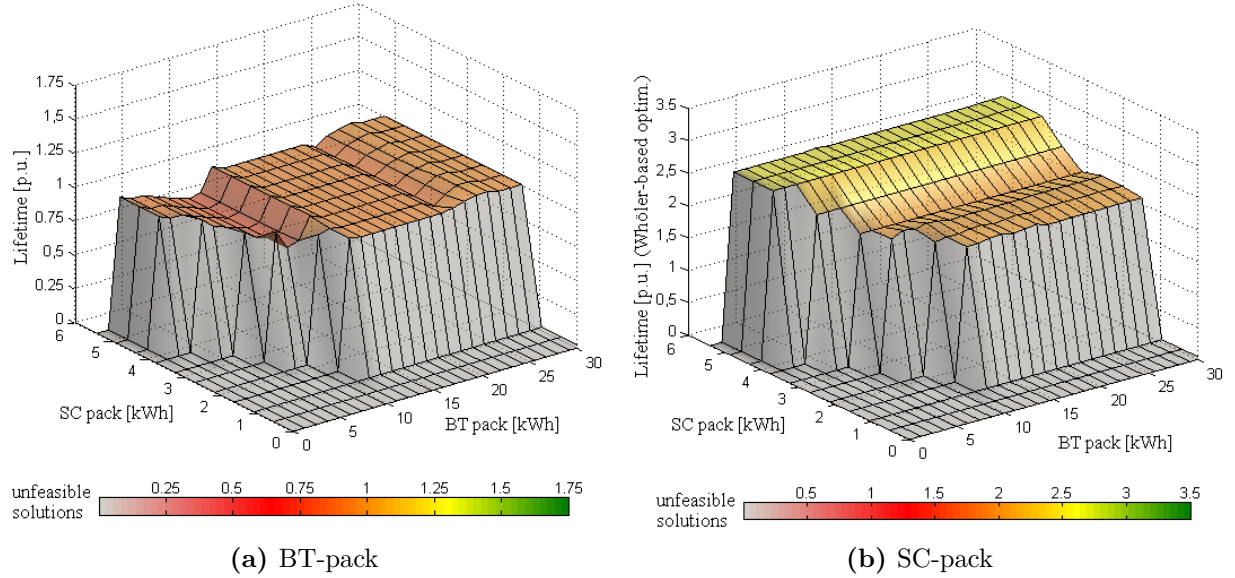
Figure 5.6: Lifetime estimation (*Whöler curve*-based optimization) depending on the HESS sizing (HET).

Figure 5.7 shows a similar analysis but in this case the lifetime estimation results are the ones obtained with the *Semi-empirical* method (by means of the **re-evaluation process** described in section 5.2.2). For the BT pack lifetime estimation (figure 5.7(a)), based on the operation behavior defined for the ESS by the A-EMS, there is a clear reduction in the lifespan for BT pack sizings below 15 [kWh] where the optimal selected solution is located (12.10 [kWh], see table 3.7). Due to this lifespan reduction the BT pack has to be replaced more times than the ones expected in the *Whöler curve*-based optimization, thus, increasing the total operating cost of the BT pack and vehicle (see figure 5.5).

Nevertheless, in figure 5.7(a), for BT pack sizings over 15 [kWh] the lifetime estimation increase with respect to the expected values when the *Whöler curve*-based method is applied (see figure 5.6(a)). Based on this analysis, it can be concluded that the gap between the *Whöler curve*-based method and *Semi-empirical* method not always can be assumed as *less lifetime* with respect to this second one. Depending on the operation condition (EMS) and HESS sizing, the *Whöler curve*-based method may underestimate the lifespan of the BT pack. With these results of underestimation the opposite case may occur: *the BT pack presents a longer lifetime reducing the need of replacements and showing ever more economic benefits than the expected ones (less total operating cost for the vehicle)*. However, the selected solution has to be supported not only by the factor of the BT pack lifetime, but also considering the whole system (power-train) in

(a) BT-pack

(b) SC-pack
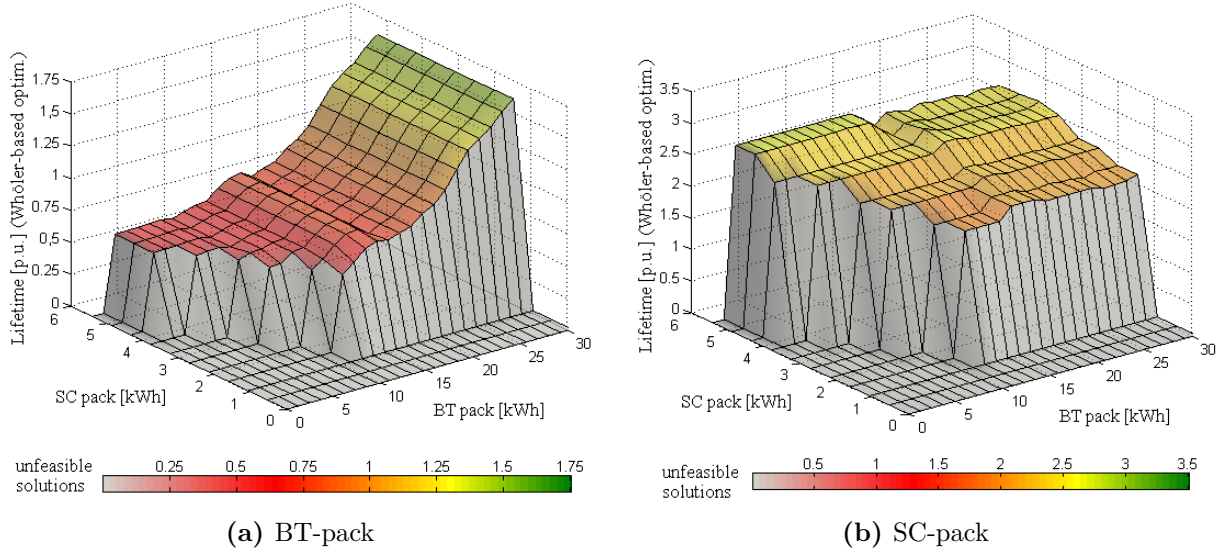
Figure 5.7: Lifetime estimation (re-evaluation of *Whöler curve*-based optimization results with *Semi-empirical* lifetime estimation method) depending on the HESS sizing (HET).

order to assure the lowest operating cost for the vehicle. Based on this argument lies the importance of the optimization methodology proposed as contribution of this PhD thesis.

Comparing the results presented in figure 5.6(b) and figure 5.7(b), the lifetime estimation done on the SC pack remains almost constant both with the *Whöler curve*-based method as well as during the **re-evaluation** with *Semi-empirical* method. Remarking that in both cases the lifetime estimation for the SC pack was done with the *Whöler curve*-based method and *Rainflow cycle counting algorithm*. Some sections of the plot in figure 5.7(b) presents slight variations compared with figure 5.6(b) mainly due to the ageing of the BT pack (modifying its available capacity) and possibly requiring more usage of power/energy from the SC pack. However, in both plots the values denote quite high lifespan estimations of around 2.5 - 2.8 times the lifespan of the BT pack (calculated with *Whöler curve*-based method, see figure 3.8(a)).

It has to be noted that, in the cases presented in figure 5.6 and figure 5.7 have been kept constant the parameters for the A-EMS (taken from the *solution 1* with *Whöler curve*-based optimization) whereas that the variation has been done in the HESS sizing (combining different BT and SC pack sizings).

5.3.2 Assessment of the *Semi-empirical* based optimization results

As depicted in figure 5.1, in the previous chapters the results have been obtained applying the optimization methodology proposed in this thesis (see section 2.7) and consider as lifetime estimator the *Whöler curve*-based method. The aim of this section is

to present the results applying the same optimization methodology but considering the *Semi-empirical* method for the lifetime estimation of the BT pack.

Figure 5.8 depicts the optimization results (set of alternative optimal solutions) ranked according to the total operating cost of the vehicle. In order to maintain the concept of the previous optimization analysis, the solution which shows the minimum total operating cost for the tramway (*solution 1*) has been selected as the suitable one for this scenario.
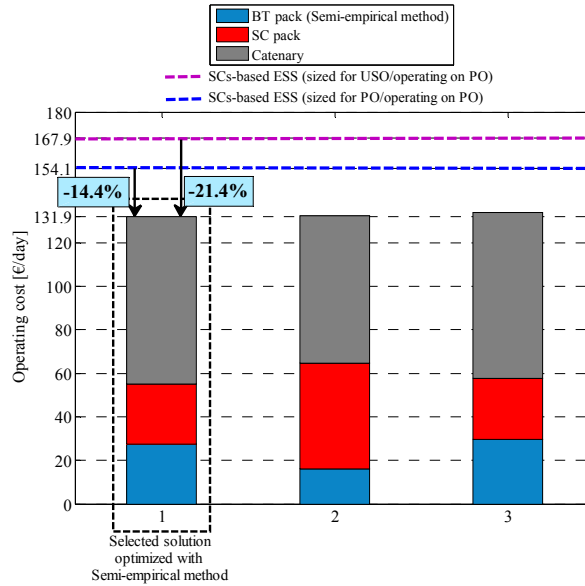
Figure 5.8: Alternative optimal solutions (applying *Semi-empirical* lifetime estimation method) for HET.

A similar lifetime analysis to the one described in the previous section (see figure 5.6 and figure 5.7) has been done for the *Semi-empirical* based optimization and it is depicted in figure 5.9. In this case the A-EMS has been configured with the parameters of the selected solution (*solution 1* from figure 5.8).

Taking into account the optimization variables defined in section 3.4 for the HET case, figure 5.10 summarizes the parameter values to configure the A-EMS (proposed in 3.3.2) as well as the optimal sizing for the HESS. On the one hand, the blue points denote those parameters and HESS sizing obtained by applying the MO optimization methodology for the *Whöler curve*-based case (analyzed in section 3.5 and further discussed in section 5.3.1). On the other hand, the red points depict the resulting parameters by applying the same methodology but considering the *Semi-empirical* method during the optimization process. Based on the optimization results presented in figure 5.10, it can be noted that, **the main modification of the *Semi-empirical* based optimization over the *Whöler curve*-based one lies on the variation of the targets for the EMS while the resulting HESS sizing remains constant.**

Figure 5.11 summarizes the results obtained in this section regarding the HET case.

(a) BT-pack

(b) SC-pack
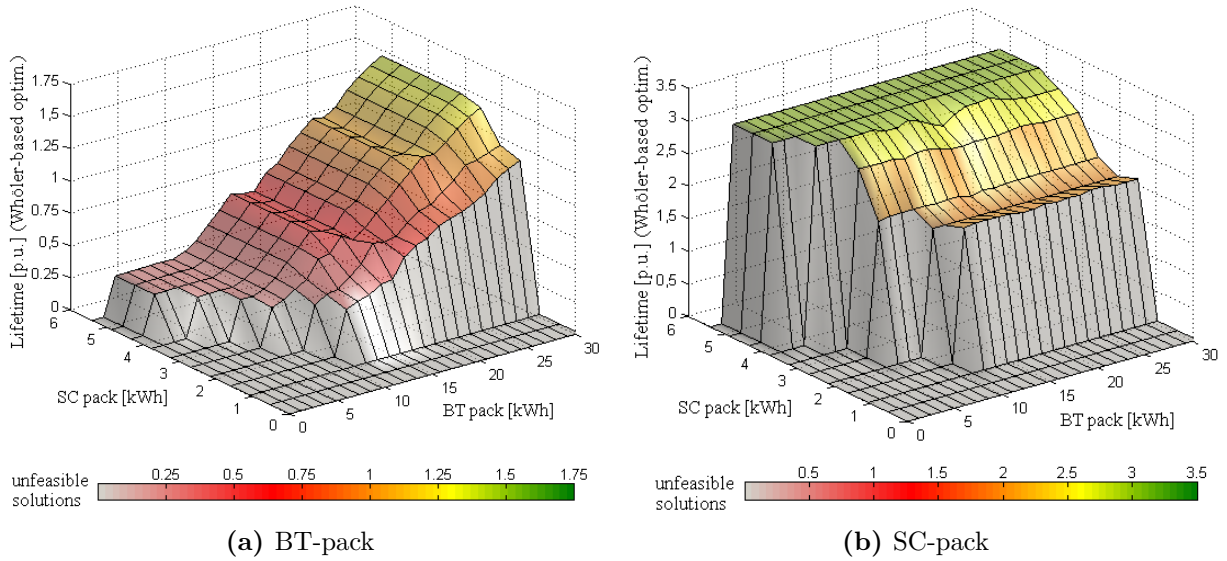
Figure 5.9: Lifetime estimation (*Semi-empirical* based optimization) depending on the HESS sizing (HET).

As defined in chapter 3, operating cost savings from 18.8% up to 25.5% (depending on the base scenario considers as target) were reached. Based on these results, the improvements on energy management (reflected in the economic results) have probed the effectiveness of the novel adaptive fuzzy-based EMS (proposed in this PhD thesis) for a better harnessing of the on-board energy sources while reducing the operating costs for the vehicle.

However, due to the **re-evaluation process** proposed in this chapter (considering a more accurate lifetime estimation method) these cost savings show a reduction reaching less values than the ones obtained previously (7.7% and 15.3% respectively). This reduction in the expected cost savings is useful to determine the importance of an accurate lifetime estimation for HESS sizing and EMS definition purposes. It can be said that, the results will be as prominent and realistic as accurate and realistic are the different parts of this methodology (in this case the lifetime estimation method).

In case of the optimization based on the *Semi-empirical* method, the cost savings increase again (see figure 5.11). Nevertheless, the obtained cost reductions are lower that the ones expected with the *Whöler curve*-based optimization **with values around 14.4% up to 21.4%**. The reason why the results from the *Semi-empirical* based optimization do not reach similar values that the ones obtained with *Whöler curve*-based method can be attributed that this last method (depending on the operating conditions) could overestimate the lifespan showing minimum economic values that, with a more realistic ageing method, cannot be reached. However, **the results from the optimization based on the *Semi-empirical* method still present noteworthy operating cost reductions (up to 21.4%) and reducing the gap from the re-evaluated solution in 7%**.
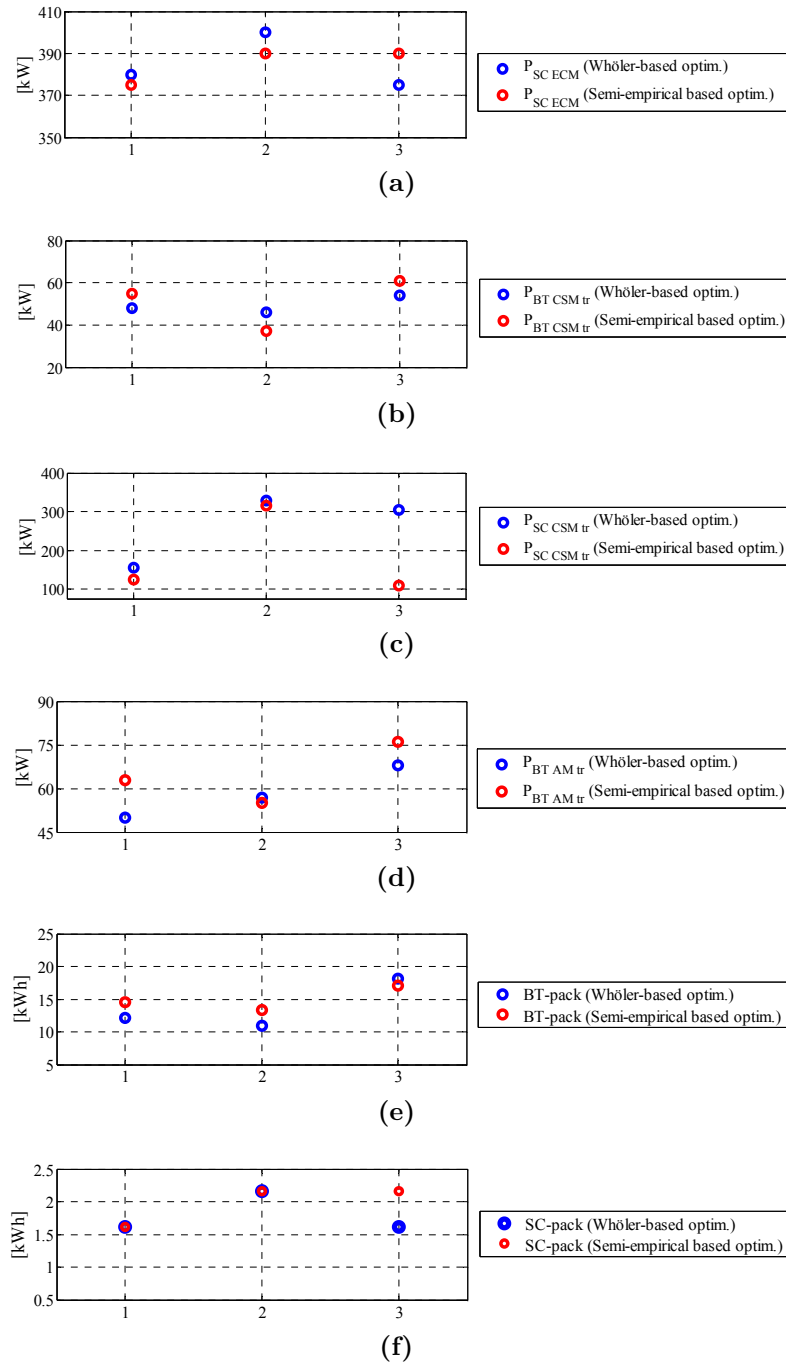
Figure 5.10: Alternative optimal solutions (A-EMS targets and HESS sizing) for the HET scenario.

Focusing on the selected solution in chapter 3 (*solution 1*), the economic "error" due to the lifetime estimation method applied corresponds to 13.7% (see figure 5.5). This percent represents around 17.1 $\left[\frac{euros}{day}\right]$ (considering the proposed economic model and referential costs assumed, see section 3.4). Extrapolating this referential value to the assumed lifetime of the vehicle (*i.e.* 10 years), it represents around

157
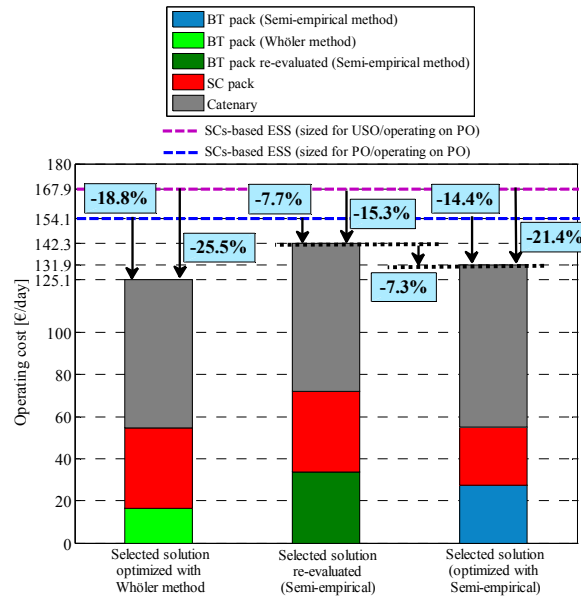
Figure 5.11: Summary of economic implications depending on the lifetime estimation method (HET).

61,560 [euros].

Therefore, this value may be compared to the referential cost regarding to the development (including experimental test on the cell, ageing model development and validation) of an *Semi-empirical* ageing model (or any other cell-dedicated method). This comparison may help to define if the economic "error" can be assumed by the vehicle manufacturer (or end-client) or it compensates (economically) the development of a more-accurate cell-dedicated ageing model considering the cost savings that can be reached with it (up to 21.4%).

5.4 Techno-economic comparison (HEB case)

For the HEB case, a similar process than the one previously described for the HET has been applied. The base results are the ones discussed in section 4.6.2 (considering the *Whöler curve*-based method in the optimization process) when the case study of the HEB was analyzed. In the same way, these results have been **re-evaluated** with the *Semi-empirical* method and a new optimization process has been carried out by using it as lifetime estimation method.

The set of plots corresponding to these aforementioned steps are depicted in Appendix B. In this chapter only the final results, depicted in figure 5.12, have been included.

In this case, in some alternative optimal solutions, the opposite case as the one presented for the HET (overestimation of lifespan with *Whöler curve*-based method) has been found. For the alternative optimal solution selected in the HEB case (*solution 3*, see

Figure 5.12: Summary of economic implications depending on the lifetime estimation method (HEB).

figure 4.20) **the expected cost saving (with *Whöler curve*-based optimization) was around 15.5% (from the RB-EMS operating cost)**.

When the **alternative optimal solutions were re-evaluated with *Semi-empirical* method** the cost savings increased even more in some of them (see figure B.4). For the selected solution (*solution 3*) **the cost saving increased in 2.9%** (up to 18% in the total operating cost, see figure B.2). This value represents a **decrease of around 11.2% in the operating cost of the BT pack** (see figure B.3). This allows to conclude that the lifetime estimation not always can be assumed as lower with *Whöler curve*-based method by comparing to *Semi-empirical* method.

When the Semi-empirical method was applied as lifetime estimator in the optimization process (see resulting parameters in figure B.9), the cost saving for the HEB operation is improved in 5.7% (see figure B.7).

In the context of vehicles manufacturers, for a real scenario there are more variables and factors that have to be considered to take a economic decision such as: business model of the company, volume of vehicle sales, contractual conditions with the vehicle operator or end-client, etc. It means that, the economic values and cost savings reached along this thesis will have different levels of representativeness depending on the scenario under analysis and the technical and economic conditions that define it. However, the presented results can help to identify the key factors that have to be taken into account to reach improved and efficient operation performance for the vehicle while ensuring the minimum operating cost for the whole system.

5.5   Conclusions

In this chapter a sensitivity analysis was done regarding the factor of the lifetime estimation mainly focused on the Batteries. The aim of this analysis was to highlight the importance, from the economic point of view, that may have the lifetime estimation accuracy (as part of the optimization methodology) and its impact on the sizing and operation of the HESS.

To evaluate this potential impact, two lifetime estimation models were considered. The first one, based on *Whöler curve*-based method and *Rainflow cycle counting algorithm*. This lifetime estimation method was applied, as part of the optimization methodology proposed in this thesis, along the optimization processes carried out in both previous chapters (devoted to the HET and HEB respectively). The second one, a *Semi-empirical* method developed and validated previously in IK4-IKERLAN for the BT cell considered as base one for sizing the BT pack.

A re-evaluation process was proposed considering as input the parameters (targets to configure the A-EMS and HESS sizing) from the alternative optimal solutions obtained during the optimization when the *Whöler curve*-method was considered as lifetime estimator. Then, the vehicle operation (based on the aforementioned parameters) was simulated but applying the *Semi-empirical* method to determine the economic gap derived from the error in the lifetime estimation.

For the HET case study, up to 25.5% of cost saving in the daily operation cost was expected with the *Whöler curve*-based optimization. However, this expected cost saving decreased up to 15.3% when the vehicle operation, based on the assumed optimal parameters (targets to configure the A-EMS and HESS sizing), was re-evaluated with the *Semi-empirical* method for BT lifetime estimation. Depending on the BT sizing and operation behavior the daily operating cost for the BT pack may increase from 26.1% up to 105.3% (due to the overestimation of lifetime done by the *Whöler curve*-based method). On the other hand, when the *Semi-empirical* method was considered as lifetime estimator into the optimization methodology, the cost savings reached total values up to 21.4%.

The process was repeated for the HEB case study, in this case (due to the underestimation of lifetime done by the *Whöler curve*-based method) the cost saving increased up to 18% (when expecting around 15.5%) in the re-evaluation process of the *Whöler curve*-based optimization results with *Semi-empirical* method. For the case of the *Semi-empirical* method based optimization, the cost saving increased in 5.7% (reaching a total reduction in operation cost of 21.2%)

The chapter's results do not affect the effectiveness of the adaptive fuzzy-based EMS proposed in this thesis, because in both optimization approaches (*Whöler curve*-based and *Semi-empirical* method based) noteworthy cost savings were obtained based on the improved operation performance. However, the chapter's results show how may impact the lifetime estimation accuracy as part of an optimization methodology and the possible

deviation from the expected economic profits when a less-accurate method is applied. Therefore it can be said that, the optimization results will be as prominent and realistic as accurate and realistic are the different parts that feed the proposed optimization methodology (in this case the lifetime estimation model).

From the optimal solution selected in the *Whöler curve*-based optimization (HET case), the economic "error" due to the wrong lifetime estimation for the BT pack represents around 13% of increase in the daily operating cost. Extrapolating this value to the whole lifetime of the vehicle, it represents around 61,560 [euros]. Nevertheless, in the HEB case the opposite case occurred, with a slight increase in the cost saving of about 2.9%. However, in the context of vehicles manufacturers, for a real scenario there are more variables that have to be considered to take a economic decision such as: business model of the company, volume of vehicle sales, contractual conditions with the vehicle operator or end-client, etc. Therefore, this economic "error" will have different levels of representativeness depending on technical and economic conditions against which it is compared.

6

Conclusions and future research lines

6.1   Conclusions

In this PhD thesis, the topic of the optimal sizing and energy management of HESS for transport applications has been studied. The scope of this thesis has been focused on the public transportation vehicles considering the technical, economic and environmental advantages that this kind of vehicles present for implementing on-board ESS in the challenge for developing more-efficient, best-performed and cost-competitive mobility solutions. In this scope, two main case studies has been addressed in this thesis: *Hybrid Electric Tramway* and *Hybrid Electric Bus.*

The most relevant lacks in the current state-of-art regarding the hybrid vehicles with HESS lie on: *the optimized energy management of the multiple energy sources on-board the vehicle* and the integration of it with *the proper HESS sizing* in order to ensure a *well performed and efficient system operation while taking into account the economic implications regarding operating the HESS under these conditions along the lifetime of the vehicle.*

Thus, this thesis has contributed by addressing both aforementioned issues:

On the one hand, **a novel adaptive EMS (based on fuzzy logic) to manage the power split in a hybrid vehicle with HESS (combining BT and SC)** has been developed. This A-EMS considers, in addition to the instantaneous conditions of the system (available energy in the HESS, vehicle power demand), information about the future energy demand of the vehicle by applying a sliding forward window strategy. This forward window allows estimating the future energy consumed/absorbed from/in the HESS and auxiliary energy source (catenary and genset for the HET and HEB, respectively). This way, **the BT and SC pack operation is adapted to fully supply the instantaneous energy consumption but considering the future energy demand (increasing/decreasing the instantaneous consumption from the BT and/or SC pack)**. The aim was to increase the energy efficiency of the system by a proper harnessing of the on-board sources and the available energy from the vehicle (mainly in the regenerative braking phase).

On the other hand, **a multi-objective methodology for the co-optimization of the sizing and operation of the HESS** (including the novel adaptive fuzzy-based EMS as a part of its optimization process) has been proposed. The multi-objective approach (solved by genetic algorithms) is **based on an economic model** in order to evaluate the influence of the sizing and operation of the HESS on the operating cost of the whole system with a long term view (whole vehicle lifetime). Therefore, either **initial investment and replacement costs of the HESS have been evaluated**. For determining the replacements of the BT and/or SC pack along the vehicle lifetime, **the ageing factor of the HESS has been estimated by means of two different lifetime estimation methods**. The first one, a *Whöler curve*-based method which takes into account mainly the ageing by cycling of the HESS. The second one, a *Semi-empirical* method widely

validated for the base BT cell adopted in this thesis.

Therefore, the main contribution of this PhD is *the development of an optimized and adaptive energy management strategy, which forms part of a methodology for the co-optimization of sizing and operation of a HESS, allowing an intelligent and more efficient operation of the hybrid system while assuring the minimum operating cost along the vehicle lifetime.*

In the **HET scenario**, a real case study was selected corresponding to an urban route in the city center of Seville where **the tramway operates in zones with and without catenary**. Two EMS were proposed: on the one hand, a RB-EMS with different operation modes (depending on the zone where the tramway is running) was presented. On the other hand, the adaptive fuzzy-based EMS proposed in this thesis was adapted for the HET case and the main variables to be taken into account for the energy management were detailed. The optimizations results from both energy management approaches (RB-EMS and A-EMS) were compared with the current solution of the tramway (SC-based ESS). From this base scenario, **the highest cost saving was obtained with the optimized A-EMS (around 18.8%) compared with the optimized RB-EMS (around 13.4%)**. When the current SC-based scenario was resized to consider the possibility of **unscheduled event in the catenary-free zone** (which would increase the energy consumption in the catenary-free zone), **the cost saving was even higher with the optimized A-EMS (about 25.5%)**. By comparing the two energy management approaches, **the A-EMS showed a cost reduction of about 6.2% from the optimized RB-EMS while allowing downsizing the BT pack (-28.4%)**. In terms of energy efficiency (during the regenerative braking phase) the base scenarios (SC-based and resized SC-based) showed efficiencies around 80% while **the optimized A-EMS showed an improvement in energy recovery, with an efficiency of 84.4% and minimum losses in crowbar**.

For the **HEB scenario**, the case study was focused on an urban route including several stops and zero-emission zones, therefore, **combining hybrid (genset+HESS) and full-electric (only HESS) operation**. Firstly, **an optimization methodology for selecting the most efficient operating points and optimal operating curve in an ICE was proposed**. Similarly as in the HET case, for the HEB two EMS were proposed. On the one hand, it has been defined a RB-EMS with different operation modes depending on the operating conditions of the vehicle (*hybrid* or *full-electric*). On the other hand, the A-EMS approach has been considered, where the membership functions were defined in a generic way in order to obtain a vehicle operation adapted to each set of analyzed variables (HESS sizing and EMS targets). The optimization results of **the A-EMS showed a daily operating cost reduction up to 15%** from the best cost saving reached with the optimized RB-EMS approach while keeping the same HESS sizing. Besides, **with the adaptive approach the average fuel consumption was reduced in 19%** (from the optimal RB-EMS solution). Furthermore, the **optimized**

A-EMS allowed an improvement in energy harnessing during braking, with an efficiency around 94% comparing with the optimized RB-EMS approach (efficiency up to 90.7%).

Finally, it was stated **the importance of the accuracy on the ESS lifetime estimation** (mainly focused on the BT ageing) **as part of the optimization methodology and its techno-economic impact on the selected solution**. To do so, the optimized results, from the *Whöler curve*-based optimization were re-evaluated with the *Semi-empirical* method (assumed as the most realistic lifetime forecasting for the BT cell selected in this thesis). **In the HET case**, due to this re-evaluation, **the cost saving decreased (from the expected 25.5%) up to 15.3%** denoting an overestimation on the BT lifespan. For **the HEB scenario** the opposite case was obtained (underestimation of the BT lifespan), this time, **after the re-evaluation the cost saving increased up to 18% (when expecting around 15.5%)**. These results showed how may impact economically the lifetime estimation accuracy and the possible deviation from the expected operating costs when a less-accurate method is applied. However, in both scenarios (HET and HEB) **when the most realistic ageing method (*Semi-empirical*) was applied as lifetime estimator** into the proposed optimization methodology, **the cost saving was improved, increasing in 7.3% and 5.7% in each scenario** respectively. Therefore this analysis showed that, the optimization results will be as prominent and realistic as accurate and realistic are the different parts that feed the proposed optimization methodology.

As a general conclusion, it can be stated that the work developed in this PhD thesis has contributed to the topic of the energy management in hybrid vehicles with HESS by providing improved strategies and a methodological optimization for selection the most appropriate HESS sizing and operation which allow an increase in the energy efficiency and cost savings of the vehicle.

6.2   Future research lines

From the work developed in this PhD study, the following future research lines have been identified:

- An **upscaling in the optimization methodology** by considering as variable **the location of the recharging points throughout the route** (overnight and/or opportunity fast-charging) and **including in the economic model the infrastructure costs** (transformers, electrical connections, availability for connecting to the main grid, etc.) needed for implementing these recharging points. The inclusion of these factors may allow addressing the topic of the techno-economic optimization at fleet level. In this case, the multi-objective approach would include the route requirements and possible recharging points which would allow finding the optimal location and recharging strategy in order to **guarantee the economic (minimum**

time for return-of-investment) and efficiency improvements regarding the vehicle and fleet level operation. Furthermore, this study may help to analyze the possible impact of the recharging infrastructure (and charging behavior) on the grid stability.

- The development of a **self-adaptive EMS based on on-line building of the ageing model for the HESS**. This improvement on the EMS would be focused on maximizing the lifetime of the HESS by including an **intelligent ageing algorithm able to estimate and build-up the degradation behavior of the ESS** taking into account the historical data and future operation forecasting. This way, **the EMS would be able of re-configuring its operational behavior in order to correct the possible deviation from the expected ageing profile**. Thus, preventive and corrective actions could be applied to reduce this deviation and to comply the expected lifespan and profitability that was defined by the manufacturer/vehicle-operator or end-client for the specific scenario at the design stage of it.

- **Intelligent remote manager (IRM) for energy management of a fleet of vehicles**. This improvement in the energy management of a fleet of vehicles will allow decentralizing the traditional approach about having the full energy management algorithm on-board the vehicle (mainly regarding the heavy computational routines such us optimization processes). Thus, **the complex and heavy computational calculations may be solved in a remote server while the local controllers on-board the vehicle only would do the minor calculus to operates in the best efficient way** (based on targets imposed by the IRM). This IRM would communicate with the vehicles in the fleet via the cloud, thus, being able to manage a big volume of data. Furthermore, the decentralized control and high computational capabilities of the IRM would allow to analyze the different scenarios where the vehicles are operating with a wider scope than it is possible to solve in the local energy manager of a single vehicle. This way, more economic and efficient ways to operate each vehicle could be found taking into account, on the one hand, **short-term factors such us charging behavior and unforeseen events on the route resulting in reconfiguration of the energy management behavior**. On the other hand, it could be analyzed **long-term factors such us ESS lifetime extension** (*e.g.* by replacing an aged BT pack from one vehicle and installing it in another one with a less-demanding route) and **periodic update optimizations** (updating the EMS parameters based on the current conditions of each vehicle in the fleet to maximize their economic and technical performance).

A

Fuzzy Logic principle

A.1 Introduction of Fuzzy Logic and Fuzzy Inference Process

This Appendix is intended to briefly describe the definition of fundamental concepts in fuzzy logic: including the meaning of *fuzzy set*, *membership function*, *fuzzy logical operation* and *If-Then rule*. This appendix also illustrates the fuzzy inference process and the features of *Mamdani-type fuzzy inference system*. Furthermore, specific procedures of Mamdani fuzzy inference are discussed in brief.

A.1.1 What is Fuzzy Logic?

In a wide sense, *Fuzzy Logic* is a form of soft computing method which operates with the imprecision of the real world. The opposite of the traditional, hard computing, soft computing exploits the tolerance for imprecision, uncertainty, and partial truth to achieve controllability, robustness, and low cost solutions (from the point of view of control design). In a more specific sense, Fuzzy Logic is an extension of multivalued logic which is aimed of approximated to the reasoning rather than the exact solution.

On the one hand, considering the traditional *Crisp Logic*, such as binary logic, the variables may only take values of true and false (represented by 1 and 0). On the other hand, the variables in *Fuzzy Logic* may have a truth value that ranges in degree between 0 and 1. Instead of describing absolute yes or no, the truth value, or membership in *Fuzzy Logic* explains a matter of degree. Therefore, 0 shows completely false, while 1 expresses completely true, and any value within the range indicates the degree of truth of the variable.

The main advantage that fuzzy reasoning offers is the ability to reply to a yes-no question with a not-quite-yes-or-no answer in the way like humans take decisions or offer different ranges of solutions for the same problem depending on the conditions and degree-of-knowledge of it.

A.1.2 Fuzzy set

In order to understand the concept of *Fuzzy set*, firstly the meaning of *classical set* has to be defined. Therefore, a *classical set* is a container that wholly includes or wholly excludes any given element. The *fuzzy set* is an extension of the *classical set*, which can contain elements with degree of membership between completely belonging to the set and completely not belonging to the set. Due to this reason a fuzzy set does not have a crisp (clearly defined boundary) and its fuzzy boundary is described by *membership functions* which range the *degree of membership* of elements from 0 to 1. Figure A.1 depicts a simple example showing the difference between classical and fuzzy set.

(a) Classical set.
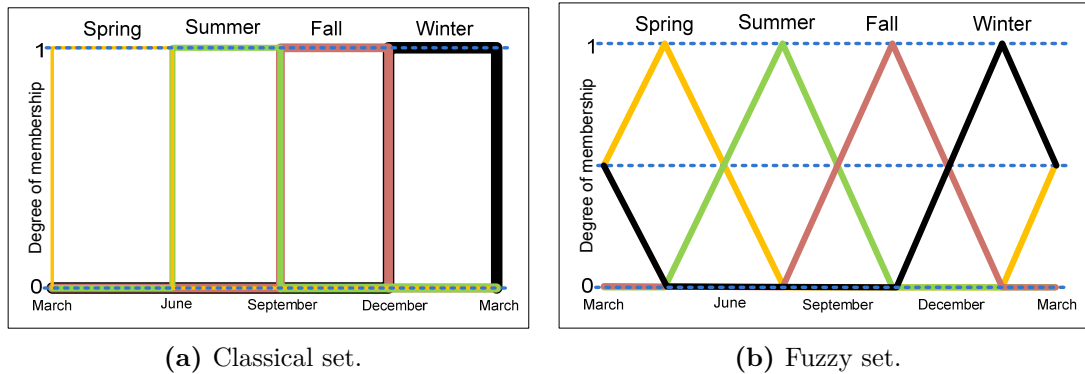
(b) Fuzzy set.

Figure A.1: Difference between classical set and fuzzy set.

A.1.3 Membership functions

A *membership function* is a curve that defines the feature of the fuzzy set by assigning to each element the corresponding membership value, or *degree of membership*. It maps each point in the input space to a membership value in the interval [0, 1]. Figure A.2 shows a general membership function curve. The horizontal axis represents an input variable x, and the vertical axis defines the corresponding membership value $\mu(x)$ of the input variable x. The *Support* of the membership function curve defines the range where the input variable will have a membership value different from zero. In figure A.2, $\mu(x) \neq 0$ when input x is at any value located between point a and point d. The *Core* of the membership function curve defines the range where the input x will have full degree of membership ($\mu(x) = 1$), in other words the arbitrary point within the interval $[b, c]$ completely belongs to a fuzzy set which is defined by this membership function.
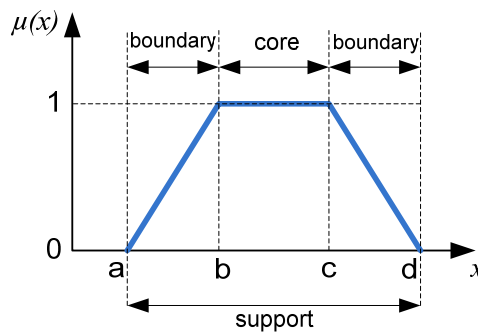
Figure A.2: Example of membership function.

In the current literature, there are five principle shapes of membership function (see figure A.3): Triangle, Trapezoidal, Gaussian, Generalized Bell, and Sigmoidal. However, different combinations of these basics shapes can be applied depending on the application and desired response from the fuzzy control. Independently of the shape, a single membership function is only able to define one fuzzy set. Normally, more than one membership

171

function are used to describe the behavior of a single input variable.

(a) Triangle.

(b) Trapezoidal.

(c) Gaussian.

(d) Generalized Bell.

(e) Sigmoidal (Z).

(f) Sigmoidal (S).
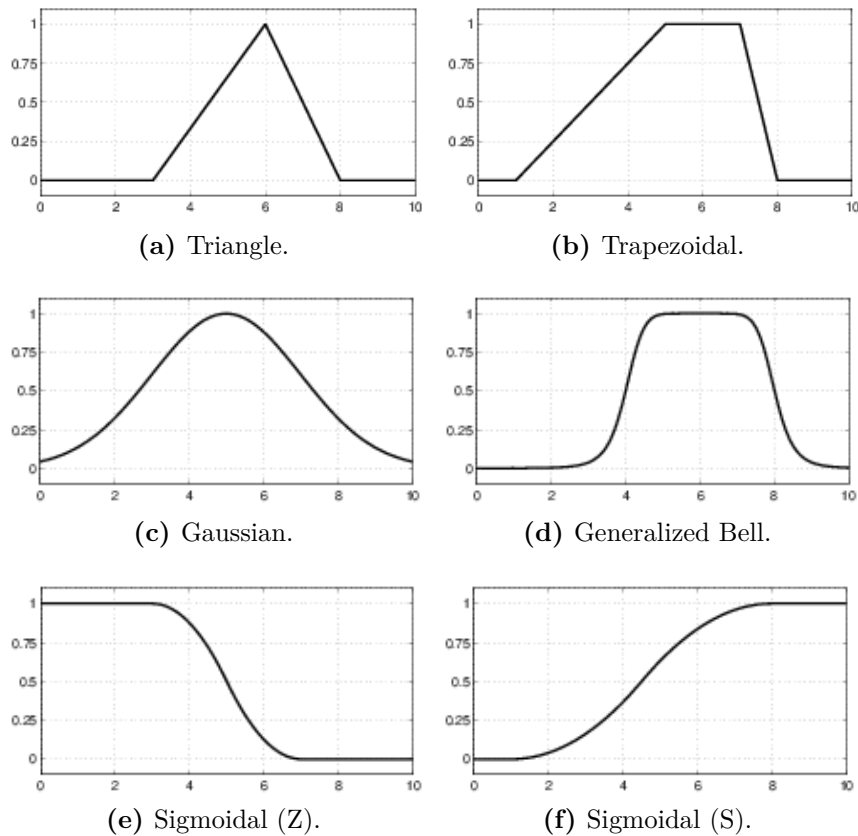
Figure A.3: Common membership function applied in fuzzy logic [80].

A.1.4   Logical operation

Taking into account that the standard binary logic is a special case of *fuzzy logic* where the membership values are always 1 (completely true) or 0 (completely false), fuzzy logic maintains the basic logical operations as the standard logical theory. Therefore, the logical operations used are: *AND*, *OR* and *NOT*. In the *fuzzy logic*, the logical operation *AND* is expressed by the function *min*, hence, statement *A AND B* is equal to $min(A, B)$. Similarly, logical *OR* is defined by function *max*, thus A OR B becomes equivalent to $max(A, B)$. And logical *NOT* makes operation *NOT A* becomes the operation $1 - A$. Figure A.4 depicts the logical operation adopted in *fuzzy logic*.

A.1.5   If-then rules

In fuzzy inference process, The evaluation of several *If-Then* rules in parallel defines how the input variables influence the output space to get the desired behavior. A single fuzzy *If-Then* rule follows the form:
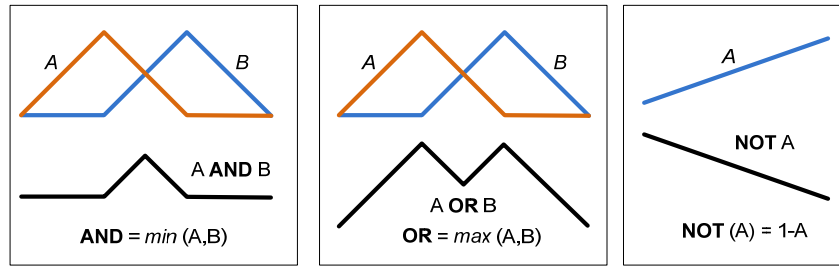
Figure A.4: Fuzzy logical operation.

if x is A, Then y is B

In the antecedent, the *If*-part is aimed to define the membership value of input variable x corresponding to fuzzy set *A*. While in the consequent, the *Then*-part assigns a crisp value back to the output variable y (measurable value). The reason why *If-Then* conditional statements are universally applicable is because both *A* and *B* are *linguistic values*, or adjectives in most cases, and this form of conditional statement works according to the human reasoning. For example, an appropriate If-Then rule might be "If P_{DEM} is *High* and SOC_{BT} is *Medium*, Then P_{BT} is *Low Discharge*".

A.2   Fuzzy Inference System

Fuzzy Inference System (FIS) is the process of transforming the given input variables to an output space by the deducing mechanism comprised by *If-Then* rules, *membership functions* and *fuzzy logical operations*. Generally, two types of fuzzy inference methods are the most common ones proposed in literature: *Mamdani* fuzzy inference, *Sugeno* fuzzy inference.

Independent on the method the process can be divided into two main stages. The first stage is the *fuzzification* of crisp values (from input variables) into degree-of-membership values according to appropriate fuzzy sets (membership functions). At this stage, either *Mamdani* and *Sugeno* FIS carry out the same process. However, the difference occur in the second stage when the results of all rules are integrated into a single precise value for output.

On the one hand, in *Mamdani* FIS (which is the most common used method) the consequent of *If-Then* rule is defined by another fuzzy set. The output fuzzy set of each rule will be reshaped by a matching number, and *defuzzification* is required after aggregating all of these reshaped fuzzy sets. On the other hand, in *Sugeno* FIS, the consequent of *If-Then* rule is explained by a polynomial function with respect to input variables where the output of each rule is a single number. Then a weighting mechanism is implemented to define the final crisp output. Although *Sugeno* FIS avoids the complex *defuzzification* process, the work of determining the polynomial coefficients becomes in a

more complex problem than defining the output fuzzy sets for *Mamdani.*

A.2.1   Mamdani FIS

In order to describe the *Mamdani* FIS a short example has been proposed to control de power output in a BT pack (P_{BT}) depending on two inputs: power demand from the vehicle (P_{DEM}) and BT SOC (SOC_{BT}). As shown in figure A.5 three rules have been defined to manage the behavior of the output variable P_{BT}.
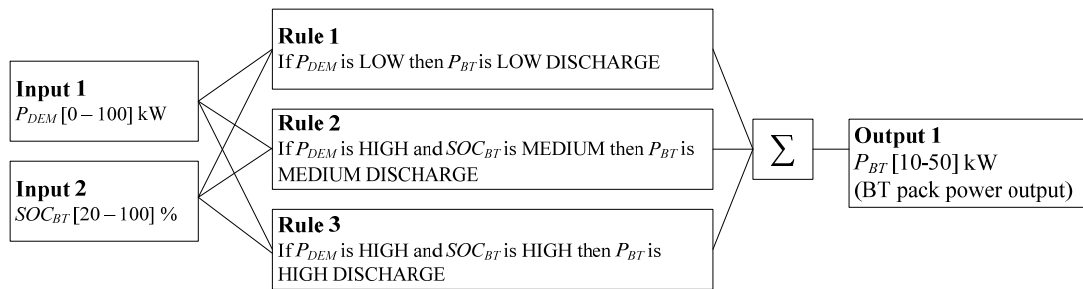
Figure A.5: Fuzzy logic example.

Mamdani FIS consists of five main steps:

1. Fuzzification of the input variables

The first step (depicted in figure A.6) is to transform the crisp numerical values from input variables into the equivalent degree-of-membership values of the appropriate fuzzy sets by the membership functions. From the practical point of view, the process consists in to intersect the the numerical input value with the corresponding membership function defined in the *If* part of rule, this way, identifying the corresponding degree-of-membership.
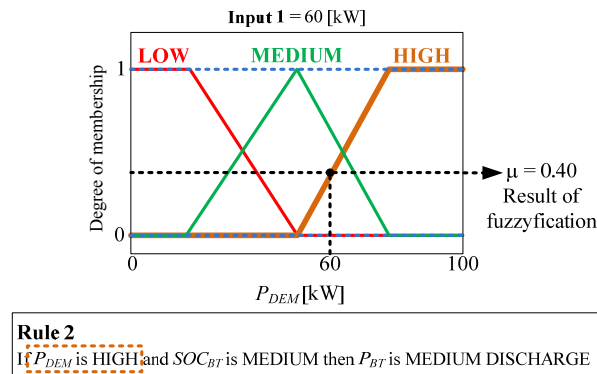
Figure A.6: Fuzzification of the **Input 1** value in the fuzzy set for variable P_{DEM} considering the membership function involved in the *If* part of **Rule 2**.

2. Apply Fuzzy operator

Commonly, when the FIS system contains more than one input variable, the antecedent of *If-Then* rule might be defined by more than one fuzzy set. Here the fuzzy operator (*AND*, *OR*) is used to combine the two membership values by applying the *min* or *max* concept. Figure A.7 depicts this procedure for **Rule 2** in the example proposed before in figure A.5.
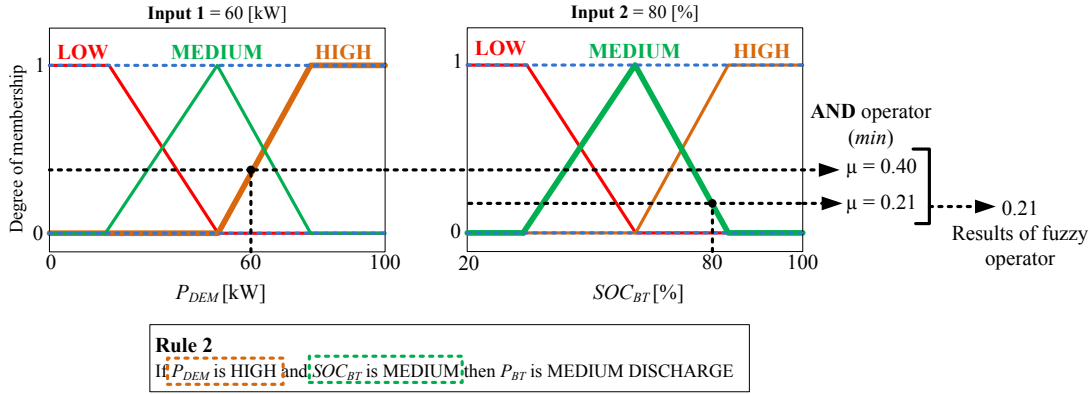
Figure A.7: Applying fuzzy operator considering **Input 1** and **Input 2** values and membership functions involved in the *If* part of **Rule 2**.

3. Apply Implication method

The consequent part of *If-Then* rule is another fuzzy linguistic set defined by an appropriate membership function. The aim of the *implication method* in *Then*-part is to reshape the fuzzy set of consequent part according to the result associated with the antecedent (figure A.8).
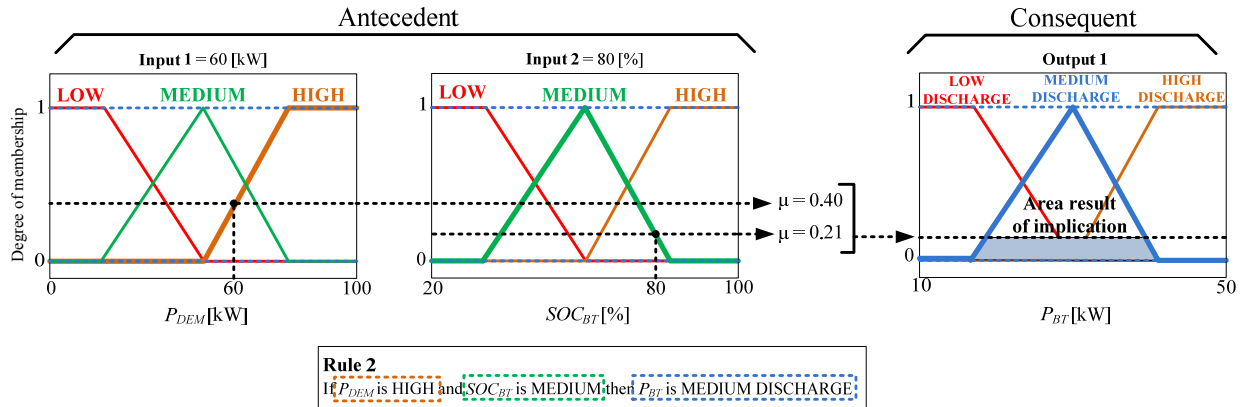
Figure A.8: Applying Implication method in the *Then* part of **Rule 2**.

4. Apply Aggregation method

Once all the *If-Then* rules have evaluated and the modified (reshaped) fuzzy set have generated, the *aggregation method* is implemented to combine these fuzzy sets (which represent the outputs of rules) into a single fuzzy set. The final combined fuzzy set is the

output of the *aggregation* process, and every output variable of the FIS will have a single matching combined fuzzy set for reference. Function *max, sum*, and *probabilistic OR* are the most common ones applied for aggregation operation. Figure A.9 depicts the full process carried out with *Mamdani* FIS and the result after applying the *max* aggregation method.

Figure A.9: Applying Aggregation method on whole fuzzy control.
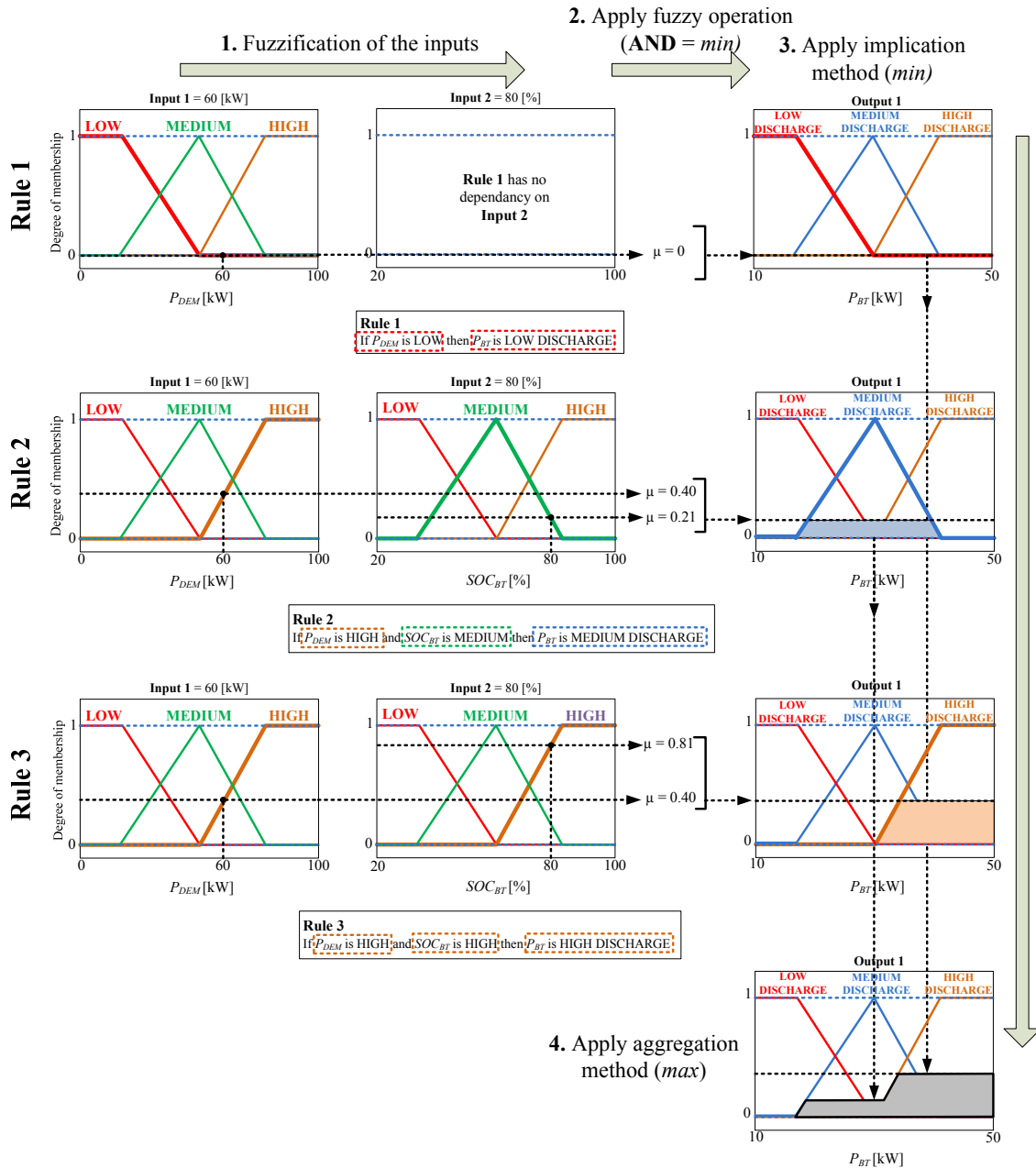
5. Defuzzification

The last step of fuzzy inference process is *defuzzification*, through which the combined fuzzy set from aggregation process will output a single scalar value. *Defuzzification* is

the opposite operation of *fuzzification*. Since in the first procedure the crisp values of input variables are fuzzified into degree-of-membership with respect to fuzzy sets, the last procedure extracts a precise value from the range of fuzzy set to the output variable. Among the different *defuzzification methods* that have been proposed in the literature, the Centroid Method (also called center of area or center of gravity, see figure A.10) is the most prevalent and physically appealing of all the defuzzification methods. It is given by the algebraic expression:

$$z_c = \frac{\int \mu_A(z) \cdot z dz}{\int \mu_A(z)} \tag{A.1}$$

where z is the output variable, and $\mu A(z)$ is the membership function of the aggregated fuzzy set A with respect to z.
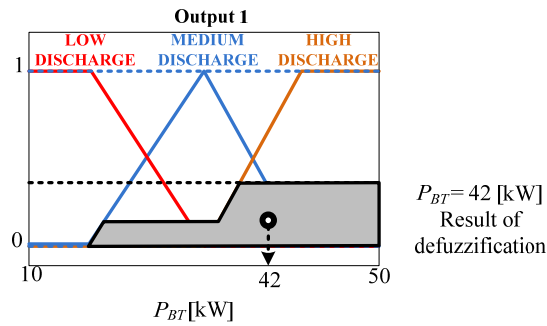
Figure A.10: Applying Centroid method for defuzzification.

B

Techno-economic comparison (Case study: HEB)
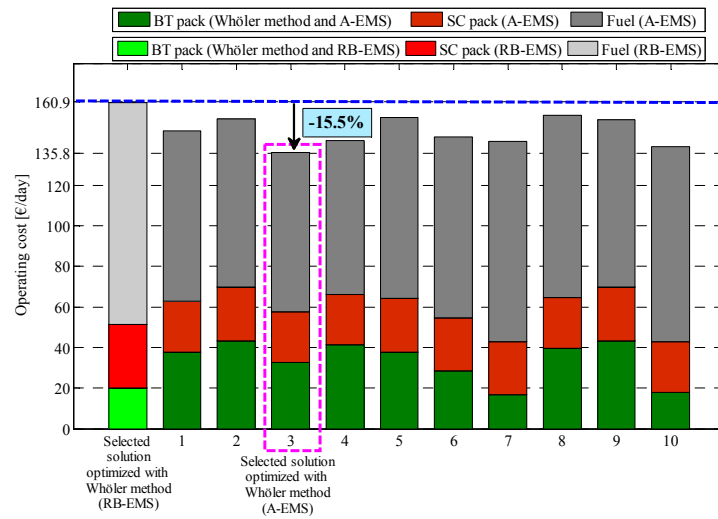
Figure B.1: Alternative optimal solutions applying *Whöler curve*-based lifetime estimation method (HEB).
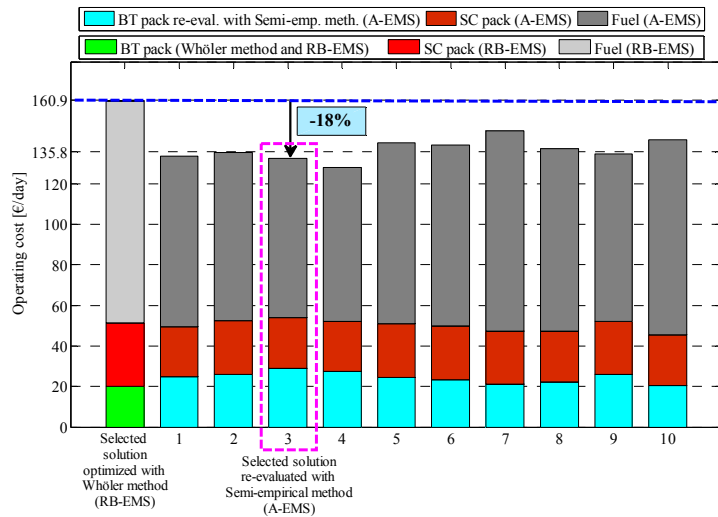
Figure B.2: Re-evaluation of alterntive optimal solutions (*Whöler curve*-based optimization) applying *Semi-empirical* lifetime estimation method (HEB).
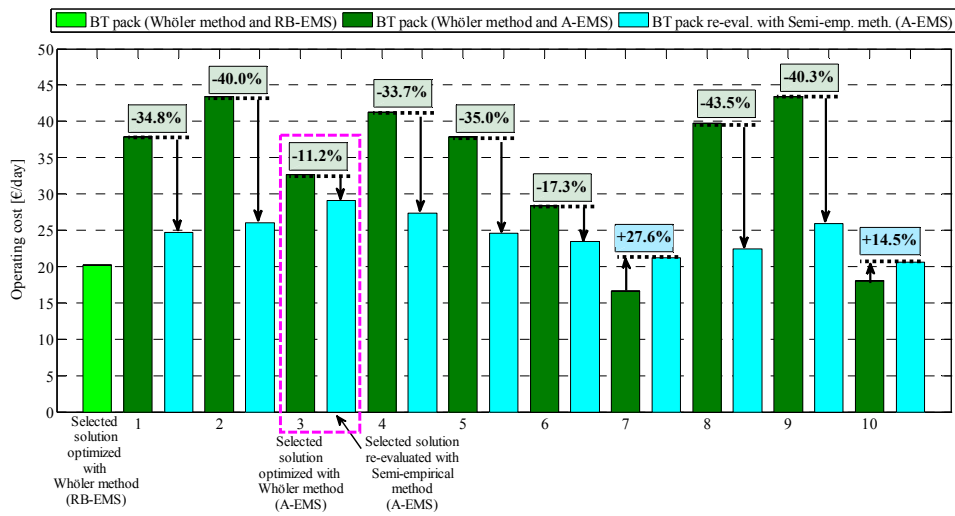
Figure B.3: Re-evaluation of the BT pack operating cost (obtained with *Whöler curve*-based lifetime estimation method) with *Semi-empirical* lifetime estimation method (HEB).
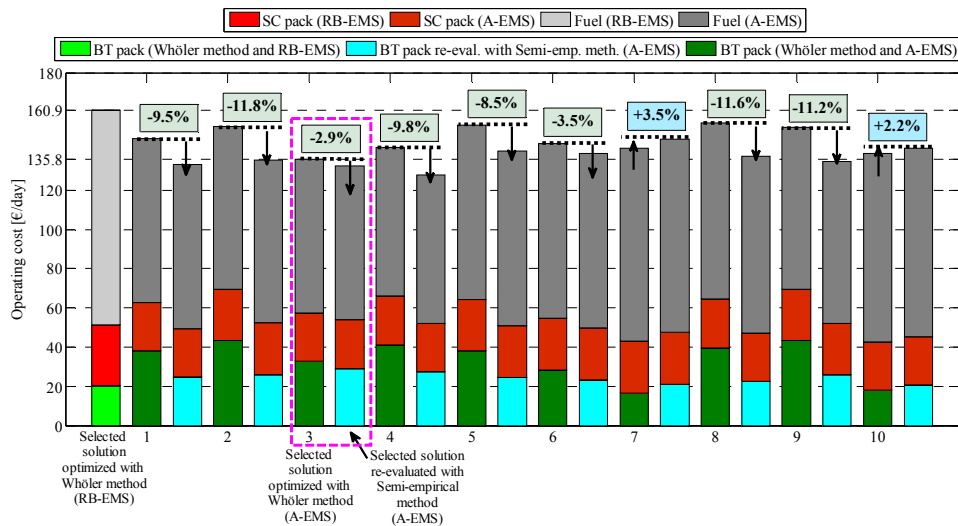
Figure B.4: Update of the total operating cost (HEB) with the re-evaluation applying *Semi-empirical* lifetime estimation method.

(a) BT-pack

(b) SC-pack

Figure B.5: Lifetime estimation (*Whöler curve*-based optimization) depending on the HESS sizing (HEB).

(a) BT-pack

(b) SC-pack
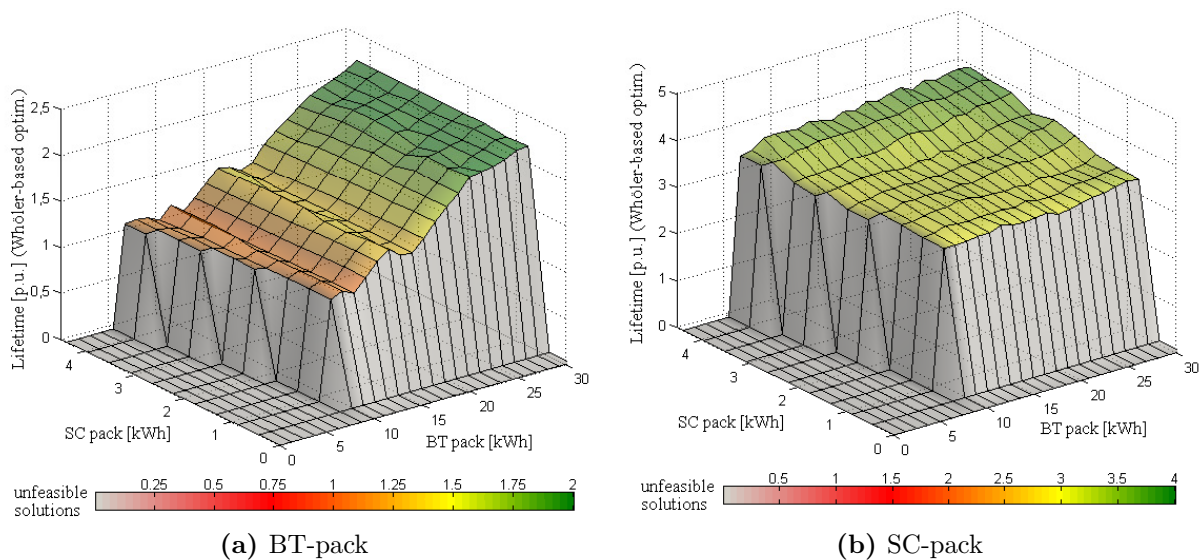
Figure B.6: Lifetime estimation (re-evaluation of *Whöler curve*-based optimization results with *Semi-empirical* lifetime estimation method) depending on the HESS sizing (HEB).
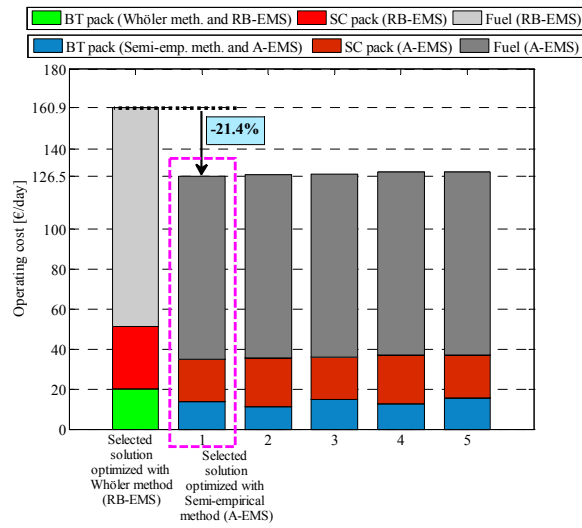
Figure B.7: Alternative optimal solutions (applying *Semi-empirical* lifetime estimation method) for HEB.

(a) BT-pack

(b) SC-pack
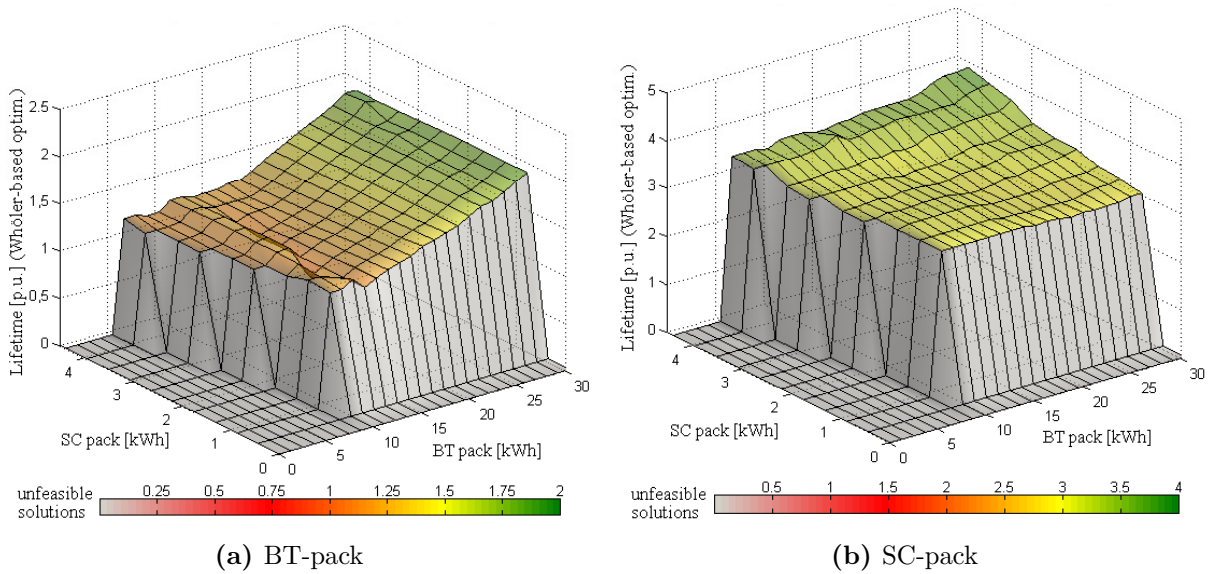
Figure B.8: Lifetime estimation (*Semi-empirical* based optimization) depending on the HESS sizing (HEB).

Figure B.9: Alternative optimal solutions (A-EMS targets and HESS sizing) for the HEB scenario.
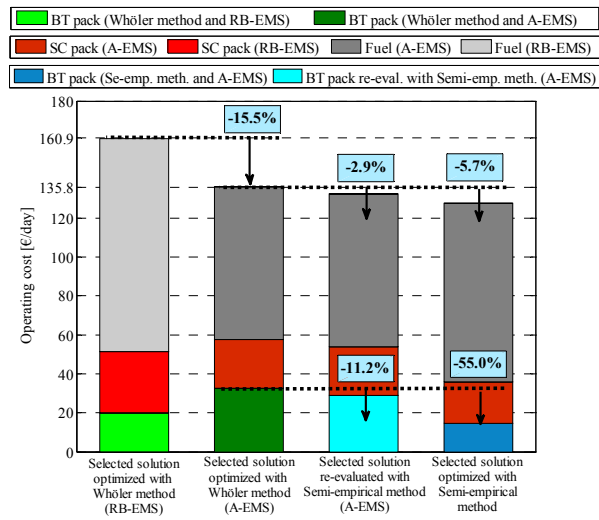
Figure B.10: Summary of economic implications depending on the lifetime estimation method (HEB).

Bibliography

[1] International Energy Agency. Energy and air pollution, world energy outlook. Technical report, IEA, 2016.

[2] International Energy Agency. Key world energy trends, excerpt from: World energy balances. Technical report, IEA, 2016.

[3] Clean Buses. Experiences with fuel and technology options. *www.clean-fleets.eu.*

[4] L. Kumar and S. Jain. Electric propulsion system for electric vehicular technology: A review. *Renewable and Sustainable Energy Reviews*, 29:924–940, 2014.

[5] Antti Lajunen and Timothy Lipman. Lifecycle cost assessment and carbon dioxide emissions of diesel, natural gas, hybrid electric, fuel cell hybrid and electric transit buses. *Energy*, 106:329–342, 2016.

[6] M.F. M. Sabri, K.A. Danapalasingam, and M.F. Rahmat. A review on hybrid electric vehicles architecture and energy management strategies. *Renewable and Sustainable Energy Reviews*, 53:1433–1442, 2016.

[7] International Energy Agency. Hybrid and electric vehicles, the electric drive commutes. Technical report, IEA, 2016.

[8] V. Fernão Pires, Enrique Romero-Cadaval, D. Vinnikov, I. Roasto, and J.F. Martins. Power converter interfaces for electrochemical energy storage systems – a review. *Energy Conversion and Management*, 86:453–475, 2014.

[9] Flavio Ciccarelli. *Energy management and control strategies for the use of supercapacitors storage technologies in urban railway traction systems*. PhD thesis, University of Naples "Federico II", Department of Electrical Engineering and Information Tecnologies, 2014.

[10] I. Prasad, P. Borza, V.I. Herrera, and A. Milo. Energy management of a hybrid energy storage system for e-bike application. In *Conférence Internationale en Sciences et Technologies Electriques au Maghreb (CISTEM), Marrakech, Morocco*, 2016.

[11] M. A. Tankari, G. Lefebvre, K. Bellache, M. B. Camara, and B. Dakyo. Supercapacitor lifetime estimation based on rainflow cycle counting method. In *Vehicle Power and Propulsion Conference (VPPC), 2015 IEEE*, pages 1–6, Oct 2015.

Bibliography

[12] Gustavo Pérez. *Advanced closed loop algorithms for state of charge and state of health estimation in li-ion batteries at wide operating conditions*. PhD thesis, Polytechnic High School, University of Mondragon, Spain, 2016.

[13] Siang Fui Tie and Chee Wei Tan. A review of energy sources and energy management system in electric vehicles. *Renewable and Sustainable Energy Reviews*, 20:82–102, 2013.

[14] S. Vazquez, S. M. Lukic, E. Galvan, L. G. Franquelo, and J. M. Carrasco. Energy storage systems for transport and grid applications. *IEEE Transactions on Industrial Electronics*, 57(12):3881–3895, Dec 2010.

[15] A. González-Gil, R. Palacin, and P. Batty. Sustainable urban rail systems: Strategies and technologies for optimal management of regenerative braking energy. *Journal on Energy Conversion and Management*, 75:374–388, 2013.

[16] B. Zakeri and S. Syri. Electrical energy storage systems: A comparative life cycle cost analysis. *Renewable and Sustainable Energy Reviews*, 42:569–596, 2015.

[17] X. Luo, J. Wang, M. Dooner, and Clarke J. Overview of current development in electrical energy storage technologies and the application potencial in power system operation. *Applied Energy*, 137:511–536, 2015.

[18] Guizhou Ren, Guoqing Ma, and Ning Cong. Review of electrical energy storage system for vehicular applications. *Renewable and Sustainable Energy Reviews*, 41:225–236, 2015.

[19] E. Martinez-Laserna, V.I. Herrera, E. Sarasketa-Zabala, A. Milo, and I. Villarreal. Techno economic impact of li-ion battery lifetime modelling on energy storage system sizing. In *Proceedings of Electric Vehicle Symposium and Exhibition EVS29, Montreal, Canada*, 2016.

[20] M. Masih-Tehrani, M.R. Ha'iri-Yazdi, V. Esfahanian, and A. Safaei. Optimum sizing and optimum energy management of a hybrid energy storage system for lithium battery life improvement. *Journal of Power Sources*, 244:2–10, 2013.

[21] J. Shen, S. Dusmez, and A. Khaligh. Optimization of sizing and battery cycle life in battery/ultracapacitor hybrid energy storage systems for electric vehicle applications. *IEEE Transactions on Industry Informatics*, 10:2112–2121, 2014.

[22] A. Nguyen, J. Lauber, and Dambrine M. Optimal control based algorithms for energy management of automotive power systems with battery/supercapacitor storage devices. *Energy Conversion and Management*, 87:410–420, 2014.

[23] Z. Song, J. Li, X. Han, L. Xu, L. Lu, and M. Ouyang. Multi-objective optimization of a semi-active battery/supercapacitor energy storage system for electric vehicles. *Applied Energy*, 153:212–224, 2014.

[24] J. Trovâo, P. Pereirinha, H. Jorge, and C. Henggeler-Antunes. A multi-level energy management system for multi-source electric vehicles - an integrated rule-based meta-heuristic approach. *Applied Energy*, 105:304–318, 2013.

[25] H. Yin, W. Zhou, M. Li, C. Ma, and C. Zhao. An adaptive fuzzy logic-based energy management strategy on battery/ultracapacitor hybrid electric vehicles. *IEEE Transactions on Transportation Electrification*, 2(3):300–311, Sept 2016.

[26] M. Meinert. New mobile energy storage system for rolling stock. In *Proceedings of 13th European Conference on Power Electronics and Applications EPE'09, Barcelona, Spain*, 2009.

[27] Via Libre. Avenio, la nueva plataforma tranviaria de siemens. *http://www.vialibreffe.com/pdf/6109SistemaSiemens.pdf*.

[28] U.S. Department of Transportation. Assessment of needs and research roadmaps for rechargeable energy storage system onboard electric drive buses. Technical report, U.S. Department of Transportation, 2010.

[29] Department of Management & Engineering. Compilation of field notes and empirical insights from: Uitp world congress & exhibition 2015. Technical report, Linköping University-Sweden, 2015.

[30] Ziyou Song, Heath Hofmann, Jianqiu Li, Xuebing Han, Xiaowu Zhang, and Minggao Ouyang. A comparison study of different semi-active hybrid energy storage system topologies for electric vehicles. *Journal of Power Sources*, 274:400–411, 2015.

[31] Shuo Zhang, Rui Xiong, and Fengchun Sun. Model predictive control for power management in a plug-in hybrid electric vehicle with a hybrid energy storage system. *Applied Energy*, pages 1654–1662, 2015.

[32] Ali Castaings, Walter Lhomme, Rochdi Trigui, and Alain Bouscayrol. Comparison of energy management strategies of a battery/supercapacitors system for electric vehicle under real-time constraints. *Applied Energy*, 163:190–200, 2016.

[33] Ziyou Song, Heath Hofmann, Jianqiu Li, Xuebing Han, and Minggao Ouyang. Optimization for a hybrid energy storage system in electric vehicles using dynamic programing approach. *Applied Energy*, 139:151–162, 2015.

[34] R. Castro, C. Pinto, R.E. Araújo, P. Melo, and D. Freitas. Optimal sizing and energy management of hybrid storage systems. In *Proceedings of 2012 IEEE Vehicle Power and Propulsion Conference, Seoul, Korea*, 2012.

Bibliography

[35] V.I. Herrera, A. Milo, H. Gaztañaga, I. Etxeberria-Otadui, I. Villarreal, and H. Camblong. Adaptive energy management strategy and optimal sizing applied on a battery-supercapacitor based tramway. *Applied Energy*, 169:831–845, 2016.

[36] L.M. Fernández, P. García, C. García, and F. Jurado. Hybrid electric system based on fuel cell and battery and integrating a single dc/dc converter for a tramway. *Energy Conversion and Management*, 52:2183–2192, 2011.

[37] C.Y. Li and G.P. Liu. Optimal fuzzy power control and management of fuel cell/-battery hybrid vehicles. *Journal of Power Sources*, 192:525–533, 2009.

[38] J.P. Torreglosa, F. Jurado, P. García, and L.M. Fernández. Application of cascade and fuzzy logic based control in a model of a fuel-cell hybrid tramway. *Engineering Applications of Artificial Intelligence*, 24:1–11, 2011.

[39] H. Aouzellag, K. Ghedamsi, and D. Aouzellag. Energy management and fault tolerant control strategies for fuel cell/ultra-capacitor hybrid electric vehicles to enhance autonomy, efficiency and life time of the fuel cell system. *International journal of Hydrogen Energy*, 40:7204–7213, 2015.

[40] M.C. Kisacikoglu, M. Uzunoglu, and M.S. Alam. Load sharing using fuzzy logic control in a fuel cell/ultracapacitor hybrid vehicle. *International Journal of Hydrogen Energy*, 34:1497–1507, 2008.

[41] D. Gao, Z. Jin, and Q. Lu. Energy management strategy based on fuzzy logic for a fuel cell hybrid bus. *Journal of Power Sources*, 185:311–317, 2008.

[42] X. Hu, L. Johannesson, N. Murgovski, and B. Egardt. Longevity-conscious dimensioning and power management of the hybrid energy storage system in a fuel cell hybrid electric bus. *Applied Energy*, 137:913–924, 2015.

[43] Qi Li, Weirong Chen, Yankun Li, Shukui Liu, and Jin Huang. Energy management strategy for fuel cell/battery/ultracapacitor hybrid vehicle based on fuzzy logic. *International Journal of Electrical Power & Energy Systems*, 43(1):514–525, 2012.

[44] P. García, L.M. Fernández, J.P. Torreglosa, and F. Jurado. Operation mode control of a hybrid power system based on fuel cell/battery/ultracapacitor for an electric tramway. *Computers and Electrical Engineering*, 39:1993–2004, 2013.

[45] Q. Li, W. Chen, Z. Liu, M. Li, and L. Ma. Development of energy management system based on a power sharing strategy for a fuel cell-battery-supercapacitor hybrid tramway. *Journal of Power Sources*, 279:267–280, 2015.

[46] J. Plomer and J. First. Flywheel energy storage retrofit system for hybrid and electric vehicles. In *Smart Cities Symposium Prague (SCSP), 2015*, pages 1–6, June 2015.

[47] H. Gao, Y.-J. Wu, and J.-J. Shen. Research on adaptive dual-mode switch control strategy for vehicle maglev flywheel battery. *Mathematical Problems in Engineering*, 2015, 2015.

[48] J.-K. Kuo and H.-K. Hsieh. Research of flywheel system energy harvesting technology for fuel cell hybrid vehicles. *Fuel Cells*, 13(6):1234–1241, 2013.

[49] G. D'Ovidio, C. Masciovecchio, and N. Rotondale. City bus powered by hydrogen fuel cell and flywheel energy storage system. In *Electric Vehicle Conference (IEVC), 2014 IEEE International*, pages 1–5, Dec 2014.

[50] C. S. Hearn, M. M. Flynn, M. C. Lewis, R. C. Thompson, B. T. Murphy, and R. G. Longoria. Low cost flywheel energy storage for a fuel cell powered transit bus. In *2007 IEEE Vehicle Power and Propulsion Conference*, pages 829–836, Sept 2007.

[51] F. Ciancetta, A. Ometto, A. Rotondale, N. Rotondale, G. D'Ovidio, and C. Masciovecchio. Analysis of flywheel-fuel cell system for mini electrical bus during an urban route. In *2016 International Symposium on Power Electronics, Electrical Drives, Automation and Motion (SPEEDAM)*, pages 1093–1098, June 2016.

[52] Kamil Çağatay Bayindir, Mehmet Ali Gözüküçük, and Ahmet Teke. A comprehensive overview of hybrid electric vehicle: Powertrain configurations, powertrain control techniques and electronic control units. *Energy Conversion and Management*, 52(2):1305–1313, 2011.

[53] Steve Caroll. Green fleet technology study for public transport. Technical report, CENEX Centre of Excellence for low Carbon and Fuel Cells Technologies, 2015.

[54] Brian Su-Ming Fan. *Multidisciplinary Optimization of Hybrid Electric Vehicles: Component Sizing and Power Management Logic*. PhD thesis, University of Waterloo, 2011.

[55] Zlatomir Živanović and Zoran Nikolić. The application of electric drive technologies in city buses. Technical report, University of Belgrade, 2012.

[56] Center for Advanced Automotive Technology. Hev levels. *http://autocaat.org/Technologies/HybridandBatteryElectricVehicles/HEVLevels*.

[57] A. González-Gil, R. Palacin, P. Batty, and J.P. Powell. A systems approach to reduce urban rail energy consumption. *Energy Conversion and Management*, 80:509–524, 2014.

[58] Maria Vittoria Corazza, Umberto Guida, Antonio Musso, and Michele Tozzi. A new generation of buses to support more sustainable urban transport policies: A path towards "greener" awareness among bus stakeholders in europe. *Research in Transportation Economics*, pages 20–29, 2016.

[59] Morteza Montazeri-Gh and Mehdi Mahmoodi-K. Optimized predictive energy management of plug-in hybrid electric vehicle based on traffic condition. *Journal of Cleaner Production*, 139:935–948, 2016.

[60] Liangfei Xu, Mingyin Hu, Jianqiu Li, and Minggao Ouyang. Comparison of energy management strategies for a range extended city bus. In *31st Chinese Control Conference, Hefei, China*, pages 6866–6871, Juny 2012.

[61] Philipp Elbert, hristopher Onder, and Hans-Jörg Gisler. Capacitors vs. batteries in a serial hybrid electric bus. *IFAC Proceedings Volumes*, 43(6th IFAC Symposium on Advances in Automotive Control):252–257, 2010.

[62] L. Guzzella and A. Sciarretta. *Vehicle Propulsion Systems: Introduction to Modeling and Optimization (3rd ed.)*. Springer, 2013.

[63] MAN Lions City. *http://www.bus.man.eu/de/en/city-buses/man-lions-city-hybrid /overview/Overview.html*.

[64] Mercedes Benz Citaro. *https://www.mercedes-benz.co.uk/content/unitedkingdom /alternativedrives/hybridtechnology.html*.

[65] ZeEUS eBus Report. An overview of electric buses in europe. *http://zeeus.eu/ uploads/publications/documents/zeeus-ebus-report-internet.pdf*.

[66] VOLVO 7900. *http://www.volvobuses.co.uk/en-gb/our-offering/buses/volvo-7900-hybrid/specifications.html*.

[67] Scania Citywide LE Hybrid. *https://www.scania.com/group/en/scania-delivers-51-hybrid-buses-to-madrid/*.

[68] Solaris Urbino Hybrid. *https://www.solarisbus.com/vehiclesgroup/hybrid*.

[69] IVECO Urbanway. *http://www.iveco.com/ivecobus/en-us/collections /technicalsheets/Documents/Urbanway.pdf*.

[70] BYD ebus. *http://www.byd.com/la/auto/ebus.html*.

[71] IRIZAR i2e. *http://www.irizar.com/autobuses-y-autocares/autobuses/irizar-i2e/*.

[72] L. Mir, I. Etxberria-Otadui, and I. Perez de Arenaza. A supercapacitor based light rail vehicle: System design and operating modes. In *Proceedings of ECCE 2009, San Jose, USA*, 2009.

[73] T. Ratniyomchai, S. Hillmansen, and P. Tricoli. Recent developments and applications of energy storage devices in electrified railways. *Electrical Systems in Transportation IET*, 4:9–20, 2014.

[74] MITRAC Energy Saver. *http://www.bombardier.com/content/dam/Websites /bombardiercom/supportingdocuments/BT/BombardierTransportECO4 /MITRACEnergySaverEN.pdf.*

[75] Sitras MES. *https://w3.usa.siemens.com/mobility/us/Documents/en/rail-solutions /railway-electrification/dc-traction-power-supply/sitras-mes-en.pdf.*

[76] CAF. Energy storage solutions for tramways. *http://www.caf.es/en/ecocaf/nuevas-soluciones/tranvia-acr.php.*

[77] Endika Bilbao. *Energy Management Strategies Based on Dynamic Programming for Applications with Energy Storing Capacity.* PhD thesis, School of Engineering, Laboratory of Industrial Electronics, EPFL Lausanne, Switzerland, 2013.

[78] M. Sorrentino, I. Arsie, R. Di Martino, and G. Rizzo. On the use of genetic algorithm to optimize the on-board energy management of a hybrid solar vehicle. *Oil and Gas Science and Technology*, 65(1):133–143, 2010.

[79] XM Wang, HW He, FC Sun, XK Sun, and HL Tang. Comparative study on different energy management strategies for plug-in hybrid electric vehicles. *ENERGIES*, 6(11):5656–5675, 2013.

[80] Mathworks. Fuzzy logic toolbox user's guide. *http://www.mathworks.com/help /pdfdoc/fuzzy/fuzzy.pdf.*

[81] A. Popov. *Genetic Algorithms for Optimization.* TU-Sofia, 2005.

[82] Javier Solano Martínez, Robert I. John, Daniel Hissel, and Marie-Cécile Péra. A survey-based type-2 fuzzy logic system for energy management in hybrid electrical vehicles. *Information Sciences*, 190:192–207, 2012.

[83] P. García, L.M. Fernández, J.P. Torreglosa, and F. Jurado. Control difuso de un tranvía híbrido propulsado por pila de combustible, batería y supercondensador. *Revista Iberoamericana de Automática e Informática Industrial RIAI*, 9:162–169, 2012.

[84] M. Bostanian, S.M. Barakati, B. Najjari, and D.M. Kalhori. Genetic-fuzzy control strategy for parallel hybrid electric vehicle. *International Journal of Automotive Engineering*, 3(3):482–495, 2013.

[85] Meng Dawei, Zhang Yu, Zhou Meilan, and Na Risha. Intelligent fuzzy energy management research for a uniaxial parallel hybrid electric vehicle. *Computers & Electrical Engineering*, pages 1–18, 2016.

[86] Z. Chen, X. Zhang, and C.H. Mi. Slide mode and fuzzy logic based powertrain controller for the energy management and battery lifetime extension of series hybrid electric vehicles. *Journal of Asian Electric Vehicles*, 8(2):1–8, 2010.

Bibliography

[87] Yaonan Wang, Qunming Yu, Huiqian Yang, M. Sorg, R. Stanislowski, C. Ament, and H. Selzer. Fuzzy prediction control strategy of ems with energy hybridization of high energy and high power. In *2005 International Conference on Electrical Machines and Systems*, volume 1, pages 843–848, Sept 2005.

[88] M. H. Hajimiri and F. R. Salmasi. A fuzzy energy management strategy for series hybrid electric vehicle with predictive control and durability extension of the battery. In *2006 IEEE Conference on Electric and Hybrid Vehicles*, pages 1–5, Dec 2006.

[89] L. Fang, S. Qin, G. Xu, T. Li, and K. Zhu. Simultaneous optimization for hybrid electric vehicle parameters based on multi-objective genetic algorithms. *Energies*, 4:532–544, 2011.

[90] Zeyu Chen, Rui Xiong, Chun Wang, and Jiayi Cao. An on-line predictive energy management strategy for plug-in hybrid electric vehicles to counter the uncertain prediction of the driving cycle. *Applied Energy*, 2016.

[91] Emilia Silvaş, Theo Hofman, and Maarten Steinbuch. Review of optimal design strategies for hybrid electric vehicles. *IFAC Proceedings Volumes*, 45(3rd IFAC Workshop on Engine and Powertrain Control, Simulation and Modeling):57–64, 2012.

[92] P. Elbert. *Noncasual and Casual Optimization Strategies for Hybrid Electric Vehicles, Ph.D. dissertation.* Institute for Dynamic Systems and Control, ETH Zurich, 2014.

[93] B. Adel, Y. Zhang, C. Ni, and J. Wei. Hybrid vehicle (city bus) optimal power management for fuel economy benchmarking. *Low Carbon Economy*, 2013.

[94] HW He, HL Tang, and XM Wang. Global optimal energy management strategy research for a plug-in series-parallel hybrid electric bus by using dynamic programming. *Matematical Problems in Engineering*, 2013.

[95] T. Knoke, C. Romaus, J. Bocker, A. Dell'Aere, and K. Witting. Energy management for an onboard storage system based on multi-objective optimization. In *Proceedings of 32nd Annual Conference IECON 2006, Paris, France*, 2009.

[96] Jihun Han, Youngjin Park, and Youn sik Park. A novel updating method of equivalent factor in ecms for prolonging the lifetime of battery in fuel cell hybrid electric vehicle. *IFAC Proceedings Volumes*, 45(30):227–232, 2012.

[97] J. P. Torreglosa, P. García, L. M. Fernández, and F. Jurado. Predictive control for the energy management of a fuel-cell x2013;supercapacitor tramway. *IEEE Transactions on Industrial Informatics*, 10(1):276–285, Feb 2014.

[98] Zeyu Chen, Rui Xiong, and Jiayi Cao. Particle swarm optimization-based optimal power management of plug-in hybrid electric vehicles considering uncertain driving conditions. *Energy*, 96:197–208, 2016.

[99] X. Qi, G. Wu, K. Boriboonsomsin, and M. J. Barth. Development and evaluation of an evolutionary algorithm-based online energy management system for plug-in hybrid electric vehicles. *IEEE Transactions on Intelligent Transportation Systems*, PP(99):1–11, 2016.

[100] V.I. Herrera, A. Saez-de Ibarra, H. Milo, A. Gaztañaga, and H Camblong. Optimal energy management of a hybrid electric bus with a battery-supercapacitor storage system using genetic algorithms. In *Proceedings of Electrical Systems for Aircraft, Railway, Ship Propulsion and Road Vehicles ESARS 2015, Aachen, Germany*, 2015.

[101] S.G. Li, S.M. Sharkh, F.C. Walsh, and C.N. Zhang. Energy and battery management of a plug-in series hybrid electric vehicle using fuzzy logic. *IEEE Transactions on Vehicular Technology*, 60:3571–3585, 2011.

[102] Elixabet Sarasketa-Zabala. *A novel approach for Li-ion battery selection and lifetime prediction*. PhD thesis, Ik4-Ikerlan, 2014.

[103] G. Pérez, M. Garmendia, J. Reynaud, J. Crego, and U. Viscarret. Enhanced closed loop state of charge estimator for lithium-ion batteries based on extended kalman filter. *Applied Energy*, 155:834–845, 2015.

[104] E. Sarasketa-Zabala, I. Gandiaga, E. Martinez-Laserna, L.M. Rodriguez-Martinez, and I. Villarreal. Cycle ageing analysis of a lifepo4/graphite cell with dynamic model validations: Towards realistic lifetime predictions. *Journal of Power Sources*, 275:573–587, 2015.

[105] MAXWELL. K2 series ultracapacitors. *http://www.maxwell.com/images/documents/K2SeriesDS1015370520141104.pdf*.

[106] A123. High power lithium ion anr26650m1a. *http://www.akukeskus.ee/anr26650m1adatasheetapril2009.pdf*, 2016.

[107] E. Sarasketa-Zabala, I. Gandiaga, L.M. Rodriguez-Martinez, and I. Villarreal. Calendar ageing analysis of a lifepo4/graphite cell with dynamic model validations: Towards realistic lifetime predictions. *Journal of Power Sources*, 272:45–57, 2014.

[108] R. Dufo. *Dimensionamiento y Control Optimo de Sistemas Híbridos Aplicando Algoritmos Evolutivos, Ph.D. dissertation*. Dept. Elect. Eng., Zaragoza Univ., 2007.

[109] D.U. Sauer and H. Wenzl. Comparison of different approaches for lifetime prediction of electrochemical systems - using lead-acid batteries as example. *Journal of Power Sources*, 176:534–546, 2008.

Bibliography

[110] Q Badey, G Cherouvrier, Y Reynier, J-m Duffault, and S Franger. Ageing forecast of lithium-ion batteries for electric and hybrid vehicles. *Current Topics in Electrochemistry*, 16, 2011.

[111] A Ostadi, M Kazerani, and Shih-Ken Chen. Optimal sizing of the Energy Storage System (ESS) in a Battery-Electric Vehicle, 2013.

[112] A Aichhorn, M Greenleaf, H Li, and J Zheng. A cost effective battery sizing strategy based on a detailed battery lifetime model and an economic energy management strategy, 2012.

[113] William Henson. Optimal battery/ultracapacitor storage combination. *Journal of Power Sources*, 179(1):417–423, Apr 2008.

[114] Rodolfo Dufo-López. Optimisation of size and control of grid-connected storage under real time electricity pricing conditions. *Applied Energy*, 140(0):395–408, February 2015.

[115] A. Saez-de Ibarra, A. Milo, H. Gaztañaga, V.I. Herrera, I. Etxeberria-Otadui, and A. Padrós. Intelligent photovoltaic power plants management strategy for market participation. In *Proceedings of Energy Conversion Congress and Exposition ECCE 2015, Montreal, Canada*, 2015.

[116] Raji Atia and Noboru Yamada. More accurate sizing of renewable energy sources under high levels of electric vehicle integration. *Renewable Energy*, 81:918–925, September 2015.

[117] John Wang, Ping Liu, Jocelyn Hicks-Garner, Elena Sherman, Souren Soukiazian, Mark Verbrugge, Harshad Tataria, James Musser, and Peter Finamore. Cycle-life model for graphite-LiFePO4 cells. *Journal of Power Sources*, 196(8):3942–3948, April 2011.

[118] Saeid Bashash, Scott J. Moura, Joel C. Forman, and Hosam K. Fathy. Plug-in hybrid electric vehicle charge pattern optimization for energy cost and battery longevity. *Journal of Power Sources*, 196(1):541–549, January 2011.

[119] Nansi Xue, Wenbo Du, Thomas A Greszler, Wei Shyy, and Joaquim R R A Martins. Design of a lithium-ion battery pack for PHEV using a hybrid optimization method. *Applied Energy*, 115(0):591–602, February 2014.

[120] W A Facinelli. *Modeling and Simulation of Lead-acid Batteries for Photovoltaic Systems*. University Microfilms, 1983.

[121] Thibaut Kovaltchouk, Bernard Multon, Hamid Ben Ahmed, Judicael Aubry, and Pascal Venet. Enhanced aging model for supercapacitors taking into account power

cycling: Application to the sizing of an energy storage system in a direct wave energy converte. *Ninth International Conference on Ecological Vehicles and Renewable Energies (EVER 2014)*, pages 1–9, March 2014.

[122] V.I. Herrera, H. Gaztañaga, A. Milo, I. Etxeberria-Otadui, and T. Nieva. Optimal operation mode control and sizing of a battery-supercapacitor based tramway. In *Proceedings of Vehicular Power and Propulsion Conference VPPC 2015, Montreal, Canada*, 2015.

[123] V.I. Herrera, H. Gaztañaga, A. Milo, A. Saez-de Ibarra, I. Etxeberria-Otadui, and T. Nieva. Optimal energy management and sizing of a battery-supercapacitor based light rail vehicle with multi-objective approach. *IEEE Transactions on Industry Applications*, pages 3367–3377, 2016.

[124] Realistic lifetime prediction approach for li-ion batteries. *Applied Energy*, 162:839–852, 2016.

[125] Mathworks. Global optimization toolbox user's guide. *http://uk.mathworks.com /help/pdfdoc/gads/gadstb.pdf*.

[126] V.I. Herrera, A. Milo, H. Gaztañaga, H. Camblong, and I. Isasa. *Energy Efficiency Management for Vehicles and Machines.*

[127] V.I. Herrera, H. H. Gaztañaga, A. Milo, A. Saez-de Ibarra, I. Etxeberria-Otadui, and T. Nieva. Optimal energy management of a battery-supercapacitor based light rail vehicle using genetic algorithms. In *Proceedings of Energy Conversion Congress and Exposition ECCE 2015, Montreal, Canada*, 2015.

[128] Spanish Electric Grid. Grid energy cost. *https://www.esios.ree.es/es/pvpc*.

[129] Zheng Chen, Bing Xia, Chenwen You, and Chunting Chris Mi. A novel energy management method for series plug-in hybrid electric vehicles. *Applied Energy*, 145:172–179, 2015.

[130] Morteza Montazeri-Gh and Mehdi Mahmoodi-k. Development a new power management strategy for power split hybrid electric vehicles. *Transportation Research Part D: Transport and Environment*, 37:79–96, 2015.

[131] V.I. Herrera, A. Milo, H. Gaztañaga, and H. Camblong. Multi-objective optimization of energy management and sizing for a hybrid bus with dual energy storage system. In *Proceedings of Vehicular Power and Propulsion Conference VPPC 2016, Hangzhou, China*, 2016.

[132] KOKAM. Slpb (superior lithium polymer battery). *http://www.e-transportation.eu /catalog/Kokam-SLPB526495-b.pdf*.

Bibliography

[133] Toshiba. Scib rechargable battery 20ah cell. *https://www.toshiba.com/tic/datafiles /SCiBBrochure2014Final.pdf*.

[134] D. Pavković, M. Hoić, J. Deur, and J. Petrić. Energy storage systems sizing study for a high-altitude wind energy application. *Energy*, 76:91–103, November 2014.

[135] A. Saez de Ibarra, V. I. Herrera, A. Milo, H. Gaztañaga, I. Etxeberria-Otadui, S. Bacha, and A. Padrós. Management strategy for market participation of photovoltaic power plants including storage systems. *IEEE Transactions on Industry Applications*, 52(5):4292–4303, Sept 2016.

List of Figures

202

List of Tables

Para empezar un gran proyecto, hace falta valentía.
Para terminar un gran proyecto, hace falta perseverancia.